University of Puerto Rico
Rio Piedras and Medical Science Campus
Department of Biology
Natural Science Dean and Biomedical Science Dean

Unraveling the role of RNA Binding Protein with Multiple Splicing (RBPMS) in ovarian cancer cells

Author: Robert J. Rabelo Fernández

A dissertation submitted in partial fulfillment of the requirements for the degree of Doctor in Philosophy for the Biology Intercampus Program of the University of Puerto Rico at Rio Piedras and University of Puerto Rico Medical Science Campus
17 January 2023

This Dissertation has been accepted by faculty of the
Biology Intercampus Doctoral Program
University of Puerto Rico
Rio Piedras Campus and Medical Science Campus

DOCTOR IN PHYLOSOPHY

In the Subject of Biology

Thesis Committee:

Pablo E. Vivas-Mejía, Ph.D., Advisor _____
Associate Professor, Department of Biochemistry,
School of Medicine, University of Puerto Rico,
Medical Science Campus, San Juan, Puerto Rico

Esther Peterson Peguero, Ph.D., co-Advisor _____
Associate Professor, Department of Biology,
College of Natural Science, University of Puerto Rico,
San Juan, Puerto Rico

José A. Rodríguez Martínez, Ph.D., _____
Associate Professor, Department of Biology,
College of Natural Science, University of Puerto Rico,
San Juan, Puerto Rico

José A. García Arrarás, Ph.D., _____
Professor, Department of Biology,
College of Natural Science, University of Puerto Rico,
San Juan, Puerto Rico

Bryan Ballif Ph.D., _____
Professor and Chair, Department of Biology,
College of Arts and Science, University of Vermont,
Vermont, USA.

"History will be kind to me; because I have the intend to write it."
Winston Churchill

"Science is fun. Science is curiosity. We all have natural curiosity. Science is the process of investigating. Its posing questions and coming up with a method. Its delving in."
Sally Ride

"Those who look for the laws of Nature as a support for their new works collaborate with the creator"
Antoni Gaudi

Dedication

I want to dedicate this dissertation, and all the hard work, effort, and sacrifice that made possible this research project, to who has always been there for me: *My God and my family*. My whole life is not enough to thank them for everything they do for me. *God* is my guide each day of my life. He blesses and supports me. He knows me better than anyone else. Thanks to *God*, all my achievements, challenges, and goals have become true. He allowed me to finish this stage of my professional carrier, to be part of this laboratory, and to be here. My Lord, thanks for giving me hope in the darkest moments. Thanks for putting angels on my path that have given me strength to continue; and for all the people around me who have made life so meaningful. Thank you for blessing me much more than I deserve. I give you all the honor and glory because I am just a simple human. You are my Lord, the one who helps me on every step of my life.

My family, the most wonderful blessing that *God* has given me, you are the columns of my life and all of who I am. My lovely Mami, my second mother and the best grandmother in the world; I thank you for all the prayers you have raised for me so I can achieve my goals. After you passed away, my life changed completely, as I went through my darkest moments. I miss you every single day. I hope I will meet with you at the end of my life and together praise our God with your "Virgencita". To Dr. Cristal Hernández Hernández, my love, I just want you to know how grateful I am for everything you do. You put so much thought and care into everything we do together. It makes me grateful that you're my fiancé. You're always ready to support me, and I can't thank you enough. "Coso" thanks for being a great support as my "official" manuscript reviewer. Thanks for all the time invested, for trusting me always, for your patience, love, motivation and for being my confidant.

Mamamía, you are my mother and my best friend. You always told me to persue my dreams no matter what. You have sacrificed a lot, and I hope that one day I would be able to pay you back. Thank you for being my counselor, my teacher, and my psychologist. You are the inspiration I need to move forward in my life. Thank you Papabelo! I feel honored to have such an amazing and supportive father like you. Thanks for both for your unconditional love and support. Titi and Papapiche, my aunt and uncle, thanks for all your support. Thanks for giving me all the love that a nephew can receive. Thank you for sharing what you have with me and for always being present in the most important moments of my life. Tio Tito, thank you for your unconditional love and support. My life without you would be incomplete.

Johanie, thanks for being my academic role model, the person who I admire and follow. You taught me that the hard work pays off. Javier, the best big brother that life could give me. Thanks for "alcaguetearme" all the crazy things that I wanted. Yomarie, my dear "Martirio", thanks for helping me persuade my dreams. I love you so much! Roberto, thank you for your support and for giving me the best energies and counseling possible.

Also, I need to mention the people who have given me the purest love: Joshvan, Joshua, Etienne, Aland and Alani. Thank you for making me smile in my saddest moments. Your hugs are the most comfort I have received in moments of frustration. They make me work hard and stronger every day to inherit a better future, a better country, and a better world. To my dear Godmothers, Dr. Carmen López y Dr. Rosaura Torres, thank you for being my angels. Thanks for being the best gift that God could put in my way. Thank you for all your support, your love and counseling. Also, thank you for teaching me the different cultures of the world and for being the best anti-stress therapy.

My whole life will not be enough to say thanks. I love you all!

Acknowledgements

I would like to acknowledge Dr. Pablo E. Vivas Mejia for allowing me to be part of his laboratory and the opportunity of working under his mentorship. I would always be grateful of having you as my mentor, not only in the lab, but also in many moments in my life. Thank you for your understanding, guidance, comprehension and mentoring in research during this journey. Thanks for being there and hearing me when I needed it. Thanks for everything; you always will be my research father. Thanks to my graduate committee. Dr. Esther Peterson Peguero, thank you for always having the doors of your office open for me. Thank you for your support, guidance, for gifting me a second research laboratory and the best cancer research partners: Xavier Bittman and Keyshla Rodríguez Martir. To Dr. José Rodríguez Martínez, Dr. José García Arrarás and Dr. Bryan Ballif, thanks for your inspiration, counseling, and guidance during this process. All of you have my respect and admiration. Thank you for giving me all the tools necessary and advice required to accomplish my goals. Thanks to Dr. Ricardo Papa, Dr. Alfredo Ghezzi, Dr. Carla Restrepo, Alonzo Ramírez, and Dr. José Agosto. I am very grateful to all of you since you marked my student life in many ways. Thanks for being such great role models.

To my laboratory mates: Dr. Jeyshka M. Reyes González, Dr. Eunice Lozada Delgado, Dr. Blanca I. Quiñonez Diaz, Dr. Nilmary Grafals Ruiz, Dr. Rohid Sharma and Dr. Annelys Sánchez you have all my respect and admiration. I wish you the best in your life. Dr. Ricardo Noriega Rivera, my science partner, thanks for making easier my adaptation process in the Medical Science Campus, for being like a brother in the laboratory, and for all the long conversations. Marienid Flores Colón, thanks for all the times that you made me laugh. “You are the best BTS Army Soldier, your legacy chance the laboratory”. Mariela Rivera, thanks for all your help during the RNA-Seq analysis. You are the best example of overcoming and dedication that I know. Both of

you girls are very noble and humanitarian. Victor Reyes Burgos thanks for your friendship. I really appreciate your help during the experiments. I bless you and wish an extraordinary life. To my Azerbaijani research mother, Fatma Valiyeva; Дорогая Фатима, Я всегда буду в долгу перед тобой. Спасибо за вашу помощь, за ваши консультации, ваши идеи, советы и дружбу. Благодаря вам этот тезис стал возможен. Я буду вечно благодарен. Спасибо, что стала моей русской мамой, за нагоняй и объятия. Нет слов, чтобы описать все, что вы сделали для меня. Я тебя люблю.

To the staff of the Biology Department, Mrs. Aidamarie Perez Burgos, thanks for giving more that you had to. Thanks for your help and support as the best administrative assistant in the UPR. You were always accessible to provide ideas and solve issues in the enrollment process. Thank you for your trust in me and for seeing my potential. I am part of the Biology Ph.D. program thanks to your advice. I also want to thank the staff of the Associated Deanship for Biomedical Science Graduate Program Julia Prado and Lisa Santos for kindly extending their help at various phases of my academic career. To the RISE program staff, Dr. Nestor Carballeira, Dr. Orestes Quesada, Julissa Morales and Grisselle I. Hernández, thanks you for your invaluable assistance during my academic travels and financial support (5R25GM061151-20). At last, I would like to acknowledge the proteomics facility core at the Comprehensive Cancer Center of the UPR, by the grant U54MD007600 from the National Institute on Minority Health and Health Disparities and by the PR- INBRE program Supported by an Institutional Development Award (IDeA) from the National Institute of General Medical Sciences of the National Institutes of Health under grant number “P20GM103475”. In addition, we thank the “Fundación Intellectus” for its financial contribution to this work.

Thank you all for believing in me!

Abstract

RNA-Binding Protein with Multiple Splicing (RBPMS) is member of a family of proteins that bind to nascent RNA transcripts and regulate their splicing, localization, and stability. Evidence indicates that RBPMS controls the activity of transcription factors associated with cell growth and proliferation, including AP-1 and Smads. Three major RBPMS protein splice variants (RBPMSA, RBPMSB, and RBPMSC) have been described in the literature. We previously reported that reduced RBPMS levels decreased the sensitivity of ovarian cancer cells to cisplatin treatment. However, little is known about the biological role of the RBPMS splice variants in ovarian cancer cells. We performed RT-PCR and Western blots and observed that both RBPMSA and RBPMSC are reduced at the mRNA and protein levels in cisplatin-resistant as compared with cisplatin-sensitive ovarian cancer cells. The mRNA and protein levels of RBPMSB were not detectable in any of the ovarian cancer cells tested. To better understand the biological role of each RBPMSA and RBPMSC, we transfected these two splice variants in the A2780CP20 and OVCAR3CIS cisplatin resistant ovarian cancer cells and performed cell proliferation, cell migration, and invasion assays. Compared with control clones, a significant reduction in the number of colonies, colony size, cell migration, and invasion were observed with RBPMSA and RBPMSC overexpressed cells. Moreover, A2780CP20-RBPMSA and A2780CP20-RBPMSC clones showed reduced senescence-associated β-galactosidase (β-Gal)-levels when compared with control clones. A2780CP20-RBPMSA clones were more sensitive to cisplatin treatment as compared with A2780CP20-RBPMSC clones. The A2780CP20-RBPMSA and A2780CP20-RBPMSC clones subcutaneously injected into athymic nude mice formed smaller tumors as compared with A2780CP20-EV control group. Additionally, immunohistochemical analysis showed lower proliferation (Ki67) and angiogenesis (CD31) staining in tissue sections of A2780CP20-RBPMSA

and A2780CP20-RBPMSC tumors compared with controls. In addition, Western blot analysis made with Immunoprecipitation (IP) samples suggested that Smad 2/3/4, c-Fos and c-Jun interact with RBPMS A and C splice variants when compared with A2780CP20-EV. Luciferase reporter assays identify RBPMS as miR-21-3p target gene. Real-time PCR confirmed that pri-mir-21 was significantly down-regulated in RBPMSA and RBPMSC when compared with control cell lines. RNAseq studies revealed many common RNA transcripts altered in A2780CP20-RBPMSA and A2780CP20-RBPMSC clones. Unique RNA transcripts deregulated by each RBPMS variant were also observed. Kaplan–Meier (KM) plotter database information identified clinically relevant RBPMSA and RBPMSC downstream effectors. Immunoprecipitation (IP) coupled to mass spectrometry (MS) revealed that RBPMSA and RBPMSC binds to proteins including the metastasis inhibition factor (NME1) and the immunoglobulin kappa locus (IGK). These studies suggest that increased levels of RBPMSA and RBPMSC reduce cell proliferation in ovarian cancer cells. However, only RBPMSA expression levels were associated with the sensitivity of ovarian cancer cells to cisplatin treatment. Also, our findings showed that RBPMS regulates the Smad-2,3,4/c-Fos/c-Jun/miR-21 pathway in ovarian cancer cells. Overall, our findings indicate that RBPMSA and RBPMSC acts as tumor suppressor gene in ovarian cancer cells.

Table of Contents

List of Figures and Tables

Pages

Chapter 1. Introduction

Chapter 3. Materials and Methods

Chapter 4. Results

List of Abbreviations

%	Percent
WHO	World Health Organization
EOCs	Epithelial ovarian cancer
BRCA1	Breast cancer gene 1
BRCA2	Breast cancer gene 2
KRAS	Kirsten rat sarcoma viral oncogene homolog
RAS	Rat sarcoma virus
G proteins	Guanine nucleotide-binding proteins regulatory proteins
TP53 or P53	Tumor protein 53
Ki-67	Nonhistone nuclear protein 67
ER	Estrogen receptors
PR	Progesterone receptors
g	Grams
M	Molar
mol	moles
cm^3	Cubic centimeter
° C	Degree celsius
log Kow	The log of the n-octanol/water partition coefficient
g/L	Grams per liter
FDA	Federal drugs administration
MDR1	Multidrug resistance mutation 1
ATPases	Enzymes that catalyze the decomposition of adenosine triphosphate

ATP7A/B	ATPase copper transporting alpha/beta
CTR1	High affinity copper uptake protein 1
SLCs	Solute-carrier genes
AQP2	Aquaporin 2
AQP9	Aquaporin 9
ATP	Adenosine 5′-triphosphate
DNA	Deoxyribonucleic acid
RNA	Ribonucleic acid
NER	Nucleotide excision repair
MMR	Mismatch repair systems
Phase S	Cell synthesizes a complete copy of the DNA
Phase G2	Gap 1 stage
ATM	Ataxia telangiectasia mutated
RAD3	Serine/threonine-protein kinase ATR
ATR	Ataxia telangiectasia related protein
CHEK1	Checkpoint kinase 1
CHEK2	Checkpoint kinase 2
MAPK	Mitogen-activated protein kinase
c-Jun	Jun oncogene AP-1 transcription factor subunit
GIST	Gastrointestinal stromal tumors
EGFR	Epidermal growth factor receptor
NSCLC	Non-small cell lung cancer
HER2	Human epidermal growth factor receptor 2

BCR	Breakpoint cluster region protein
ABL	Tyrosine-protein kinase ABL gene
CML	Chronic myelogenous leukemia
TKIs	Tyrosine kinase inhibitors
RTKs	Receptor tyrosine kinases
AKT	Protein kinase B
PI3K	Phosphatidylinositol 3-kinase
MET	MET proto-oncogene, receptor tyrosine kinase
RTK	Receptor tyrosine kinases
PTEN	Phosphatase and tensin homolog
MCT	Monocarboxylate transporter
MDR	Multidrug resistance protein
MRPs	Multidrug resistance associated proteins
PEPTs	Peptide transporters
NPTs	Na+ phosphate transporters
NBD	Nucleotide- binding domains
kDa	Kilodalton
Pgp	P-glycoprotein
YB-1	Y-box binding protein 1
NF-κB	Kappa-light-chain-enhancer of activated B cells
ERK	Serine/threonine protein kinase
Wnt	Wingless-Type
β	Beta

p38	Mitogen-activated protein kinase 38
miRNAs	MicroRNAs
JNK	c-Jun N-terminal kinases
3'-UTR	Three prime untranslated region
Raf	Raf-1 Proto-Oncogene, Serine/Threonine Kinase
Pim-1	Proviral integration site for moloney murine leukemia-1
GTPases	Enzymes that catalyze the hydrolysis of guanosine triphosphate
Rab5	RAB5, member RAS oncogene family
Rab4	RAB4, member RAS oncogene family
VEGF	Vascular endothelial growth factor
VEGFR	Vascular endothelial growth factor receptor
VEGFR1-3	Vascular endothelial growth factor receptor 1-3
IgG	Immunoglobulin G
VEGF-A	Vascular endothelial growth factor A
EGFR	Epidermal growth factor receptor
ErbB	Erythroblastic oncogene B
ErbB2	Erythroblastic oncogene B2
MEK	Mitogen-activated protein kinase
PDGFR-β	Platelet-derived growth factor receptor beta
mTOR	Mechanistic target of rapamycin kinase
IL8	Interleukin-8
RRM	RNA recognition motif

dsRNA	Double-stranded RNA
RBPs	RNA binding proteins
Zn^{2+}	Zinc (II) ion
ssRNA	Sense single-stranded RNA
Elav	Embryonic lethal abnormal vision
Sxl	Sex-lethal
Tra	T cell receptor alpha locus
Fog-1	Zinc finger protein, FOG family member 1
SRM	Spermidine synthase
Fos	Fos proto-oncogene, AP-1 transcription factor subunit
ETF1	Eukaryotic translation termination factor 1
Smad2	Smad family member 2
Smad3	Smad family member 3
TbetaR-1	Transforming growth factor-beta R-1
Pdlim5	PDZ and LIM domain 5
IL-1B	Interleukin-1beta
MOG-1	Myelin oligodendrocyte glycoprotein-1
MOG-4	Myelin oligodendrocyte glycoprotein-4
MOG-5	Myelin oligodendrocyte glycoprotein-5
RNP-4	Ribonucleoprotein rnp-4
MEC-8	RNA binding protein, mechanosensory abnormality-8
UNC-75	RNA binding protein, uncoordinated
EXC-7	RNA binding protein, excretory canal abnormal

Sam68	Src associated in mitosis 68
HUR	Human antigen R
FXR1	RNA-binding protein fragile-X mental retardation autosomal 1
BYSL	Bystin like
hnRNP1	Heterogeneous nuclear ribonucleoprotein A1
Rbm42b	RNA-binding motif protein 42
ESRP1	Epithelial splicing regulatory protein 1
CELF3	CUGBP Elav-like family member 3
RBM24	RNA-binding motif protein 24
IGF2BP2	Insulin like growth factor 2 MRNA binding protein 2
IGF2BP3	Insulin like growth factor 2 MRNA binding protein 3
MYC	MYC proto-oncogene, BHLH transcription factor
RBM38	RNA binding motif protein 38
CDKNIA	Cyclin dependent kinase inhibitor 1A
ZEB1	Zinc finger E-Box binding Homeobox 1
MM	Multiple myeloma
AML	Acute myeloid leukemia
DHCC	Dedifferentiated hepatocellular carcinoma
HCC	Hepatocellular carcinoma
CD44	Cell surface adhesion receptor 44
RBM38	RNA-binding motif protein 38
RBPMS2	RNA binding protein, MRNA processing factor 2
NMD	Mediated mRNA decay

NCBI	National Center for Biotechnology Information
3’UTR	Three prime untranslated region
NADH	Nicotinamide adenine dinucleotide
ETF1	Eukaryotic translation termination factor 1
BC	Blander cancer
RAI2	Retinoic acid induced 2
CRC	Colorectal cancer

Chapter 1. Introduction

1.1 *Ovarian cancer*

Cancer is one of the leading cause of death in the world, no matter the countries or income levels [1]. The forecast is not encouraging; the number of cancer cases and deaths is expected to grow rapidly as populations grow, age, and adopt lifestyle behaviors that increase cancer risk [1]. This is especially relevant in low and middle income countries where economic transformation is ongoing, which includes significant changes in the wide range of human movement and labor, cultural shifts in the roles of women, increased exposure to chemicals and access to international food markets. As a result, many lifestyle risk factors that are prevalent in high-income countries such as tobacco use, physical inactivity, excess body weight, and reproductive patterns, are also becoming common in low and middle income countries [1]. In 2022, the International Agency for Research on Cancer in collaboration with the World Health Organization (WHO) estimated 1,918,030 new cancer cases and 609,360 cancer deaths that are projected for the United States only [2].

Ovarian cancer is defined as uncontrolled growth of cells from one or more tissues that form the ovaries and fallopian tubes. These cells originate invagination, metaplasia and malignant transformation [3]. The ovaries are a pair of reproductive glands of the female reproductive system located on either side of the uterus, each about the size of a grape [4] (See Figure 1). They produce eggs that move through the fallopian tubes to enter the uterus, where they can be fertilized for reproduction. Also, the ovaries are the primary source of estrogen and progesterone, which are

hormones that are responsible for the health of the female reproductive system in premenopausal women [5].

Ovarian cancer is one of the 6 most common tumors in women and is the most common gynecological cause of death in western countries with a survival rate of 40% to 50% in the first 5 years following its diagnosis [6]. This is a global problem that is typically diagnosed at a late stage and has no effective screening strategy. Novoa et al. (2014) reported that ovarian cancer constitutes 4% of all cancers diagnosed in women, and there are 6.6 new cases per 100,000 women per year. Each year, 225,500 new ovarian cancer cases are diagnosed worldwide and are responsible for 140,200 cancer-specific deaths [7]. The American Cancer Society estimates that 19,880 women will receive a new diagnosis of ovarian cancer and 12,810 women will die from this disease in 2022 [8]. The incidence and survival rates depend by country, but the United Kingdom and Russia have the highest reported cases whereas China, the lowest rates [9]. In 2019, the American Cancer Society estimated that 233,565 women were living with ovarian cancer in the United States [10]. These proportions are based on the fact that the majority of patients are diagnosed in the advanced disease stage. The incidence and prevalence of ovarian cancer increases with age and is different between ethnic groups. For example, in 2019, ovarian cancer was more common among white women when compared with African American and Asian American women. On the other hand, Pacific Islanders have the lowest rate of incidence and mortality. The prognosis of ovarian cancer patients between 2012 to 2018 was 49.7% chance of survival in US, 5 years after completing chemotherapy treatment and using maintenance drugs [11]. Fortunately, reductions in incidence and improvements in treatment have been observed in the past decade. In the United States, the

ovarian cancer incidence rate declined from 15.9% to 9.1% between 1975 to 2020, and the mortality rate declined from 9.8% to 6.0% between 1975 to 2020 [11].

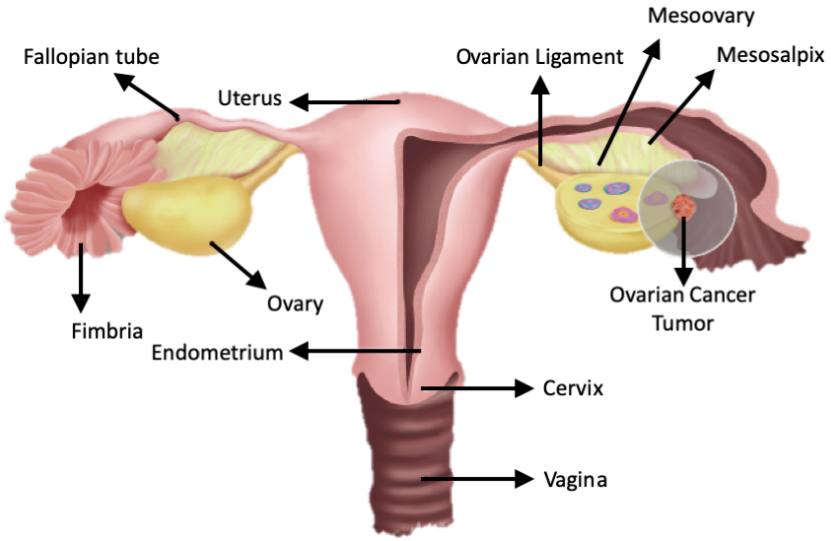

Figure 1: Anatomy of female reproductive system. The female reproductive system is divided in the internal and external genitalia. The internal organs are ovaries, fallopian tubes, and uterus. The vagina is attached to the uterus through the cervix, while the uterus is attached to the ovaries via the fallopian tubes. Ovaries produce gametes, called oocytes. In addition, the female reproductive system produces female sex hormones that maintain the reproductive cycle. Image modified from Karst et al. (2009) [12].

Ovarian cancer can be generated from one of four cell types: germ cells, sex-cord stromal, border cells, and epithelial cells [13]. Ovarian tumors associated with germ cells and sex cord stromal cells, constitute between 3% and 2%, respectively of the new diagnosis. On the other hand, epithelial ovarian cancer (EOCs) cells tumors arise in 90% of all new reported cases. Epithelial ovarian cancer are further subdivided into five histological types: high-grade serous, low grade serous, endometrioid, clear cell, and mucinous [4] (See Table 1). Each subtype has different cells of origin, molecular composition, risk factors, clinical features, and treatments. High grade serous tumors carcinomas, the most commonly diagnosed, are characterized by the involvement of both ovaries, aggressive behavior, late-stage diagnosis, and low survival rate. Accumulating evidence suggests its occurrence in 62% of cases and that it accounts for 80% of ovarian cancer deaths.

Low-grade tumors are slower growing, more genetically stable, and do not respond to chemotherapy as well as the faster growing and genomically unstable high-grade tumors [14].

Table 1: Principal histological types of ovarian epithelial tumors.

Histological Sub Type	Common Mutations	Response to Chemotherapy	Frequency	Cell of Origin	Prognosis
High Grade Serous	TP53, BRCA1, BRCA2 and CDK12 Deficiencies in homologous recombination (50% of tumors)	Initially good	~70%	Fallopian Tube Epithelium	Poor
Low Grade Serous	BRAF, KRAS, NRAS, and ERBB2 Tumor has genomic stability	Intermediate	~5%	Fallopian Tube Epithelium	Intermediate
Mucinous	KRAS and HER2 amplification	Poor	~5%	Unknown	Favorable
Endometrioid	PTEN, CTNNB1, PPP21 and MMR deficient Tumors has microsatellite instability	Good	~10%	Endometrium	Favorable
Clear cell	PIKECA, KRAS, PTEN, and ARID1A	Notorious Resistance	~5%	Endometrium	Intermediate

Mucinous tumors of the ovary represent a spectrum of neoplastic disorders, including benign mucinous cystadenoma, pseudomyxoma peritonei, mucinous tumors of low malignant potential (borderline), and invasive mucinous ovarian carcinoma. Mucinous tumors also represent a spectrum of malignant behavior and have benign, borderline, and invasive histologic variants. Among benign ovarian neoplasms, mucinous cystadenomas account for approximately 10% to 15% of all ovarian cancer cases [15]. These tumors are closely related to each other and are distinct from other histologic subtypes of epithelial ovarian neoplasms from a clinical, histologic, and molecular standpoint. Mucinous cystadenomas usually occur as a large, multiloculated cystic mass with mucus-containing fluid [16]. These tumors occur most commonly in women in their twenties to forties, but occurrences in adolescent, premenarchal girls, as well as postmenopausal patients have been documented [17]. In contrast to serous ovarian carcinomas, in which only 4% of patients

are Stage I at the time of diagnosis, 83% of mucinous ovarian cancers are Stage I at the time of diagnosis [18]. Thus, only 17% of patients with mucinous ovarian cancers are Stage II or higher. Some genetic mutations that are characteristic in mucinous ovarian cancers have been identified in mucinous ovarian cancers. For example, KRAS mutations occur within the RAS family of G proteins, which signal cell division; such mutations stimulate cell growth and are significantly increased in mucinous ovarian tumors, including mucinous cystadenomas, low malignant potential tumors, and invasive adenocarcinomas [19]. BRCA1 and BRCA2 mutations, genetic alterations in specific tumor suppressor genes that occur in many hereditary and some sporadic cases of breast and ovarian cancer, are not present in most cases of mucinous ovarian cancer. Among patients with known BRCA mutations, only 2% are of mucinous histology [20]. Mutations in the p53 tumor suppressor gene are less frequent in mucinous ovarian cancers than serous ovarian cancers; mutations in p53 have been found in almost 60% of serous tumors, but only in 16% of mucinous tumors [21]. Clear separation has also been seen in the gene expression profiling between serous and mucinous ovarian cancers [21]. These characteristics lead to specific biologic behavior and guide both clinical management and research efforts concerning patients with mucinous ovarian tumors.

In contrast, endometrioid clear cell cancer is an uncommon but notorious type of epithelial cancer disease because of its aggressive behavior. Endometrial clear cell cancer is rare and generally, it consists of <5% of all ovarian malignancies and its incidence of rate is in the range of 3.7%– 12.1% of all EOCs [22]. It can be defined as lesions that are characterized by clear cells growing in solid/tubular or grandular patterns, as well as hobnail cells lining tubules and cysts [23]. These features can exist alone or in combination. These tumors have a high incidence of

Stage I disease [24], frequently manifest as a large pelvic mass [25], rarely occur bilaterally, and are often associated with endometriosis [26], thromboembolic vascular complications, and hypercalcemia [27]. Tumors of this kind are the most common in women ages 50 to 70. Women with a family or personal history of colon or endometrial cancer have a higher risk. Moreover, women with endometriosis face a higher risk of developing this rare type of cancer. Most women with clear cell endometrial cancer are diagnosed after presenting post-menopausal bleeding. Many more women have endometriosis than those who are diagnosed with ovarian cancer, so having endometriosis should not cause undue concern [22].

Using cDNA microarray technology, Zorn et al. (2005) assessed the gene expression pattern of endometrioids, which are serous and clear cell cancers from the endometrium and ovary. Renal clear cell cancer was included for clear cell analysis. Endometrioid and serous cancers showed expression patterns that were unique to the organ of origin. Interestingly, the clear cell histologic type showed a remarkable similarity of gene expression patterns across the three organ sites, i.e. endometrium, ovaries, and kidneys [28]. Immunohistochemistry shows a high Ki-67 index, low immune reactivity for p53, and absence of estrogen receptor (ER) and progesterone receptor (PR). These can further help to distinguish clear cell cancer from endometrioid (usually ER/PR positive) and papillary serous endometrial cancers (high p53 immunoreactivity) [29]. This type of ovarian cancer is usually treated with a combination of chemotherapy and surgery. Additionally, hormonal therapies such as Letrozole or Anastrozole (aromatase inhibitors – drugs that block estrogen from being made) can be used [29]. Many researchers have studied the prognosis of patients with ovarian clear cell carcinomas, compared with that of patients with serous epithelial ovarian cancer. However, no clear agreement has been documented [30].

Ovarian cancer symptoms are not apparent in the early stages of the disease or may be confused with less serious, noncancerous conditions. Women are more likely to experience symptoms once the disease has spread beyond the ovaries. For that reason, most cases of ovarian cancer are not diagnosed until the disease has progressed to an advanced stage. Some of the symptoms of ovarian cancer include abdominal bloating, indigestion, nausea, changes in appetite, pressure in the pelvis or lower back, urinary urgency, constipation, changes in bowel habits, increased abdominal girth, tiredness, and changes in menstruation. Most of the current information on factors associated with ovarian cancer risks suggest that the strongest risk for ovarian cancer is a family history of breast or ovarian cancer [31]. Many other factors have been associated with increased risk of suffering ovarian cancer, such as menopausal hormone therapy, excess body weight, smoking, diet, and personal habits [32].

1.2 *Molecular mechanism of cisplatin action*

Cisplatin, cisplatinum, or *cis*-diamminedichloroplatinum, is a well-known chemotherapeutic drug. It has been used for treatment of numerous human cancers including bladder, head and neck, lung, ovarian, and testicular cancers [33]. Cisplatin has a molecular weight of 301.1 gm/mol, a density of 3.74 g/cm^3, a melting point of 270° C, a log K_{ow} of -2.19 and a water solubility of 2.53 g/L at 25° C. This compound was first synthesized by Peyrone in 1844 and its chemical structure was first elucidated by Alfred Werner in 1893. However, the compound did not warrant scientific research until the 1960's when the initial observations of Rosenberg [34] at Michigan State University, pointed out that certain electrolysis products of platinum mesh electrodes were capable of inhibiting cell division in *Escherichia coli.* The research endeavor

generated much interest in the possible use of these products in cancer chemotherapy. Among many chemotherapy drugs that are widely used for cancer, cisplatin is one of the most effective. It was the first FDA-approved platinum compound for cancer treatment in 1978 [35].

Although the precise mechanism of cisplatin's cellular uptake and efflux is still not fully understood, it is believed that once administrated, cisplatin enters the cells through passive diffusion across the cell membrane. Also, the activity of several membrane transporters of platinum compounds that are analogous to MDR1, including efflux ATPases (MRPs, ATP7A/B) and solute carrier importers (CTR1, the SLCs, AQP2, and AQP9), has been reported. MDR1 is an ATP-binding cassette transporter, known for years as P-glycoprotein [36]. The uptake of cisplatin is mediated by the copper transporter Ctr1 in yeast and mammals [37]. It has been further confirmed in human cells that cisplatin triggers rapid degradation of the copper membrane transporter CTR1, with diminished influx of cisplatin, resulting in resistance to the drug [38]. Genetic knockout of CTR1 results in cellular resistance to cisplatin in vivo. Cells with increased CTR1 expression exhibit increased platinum accumulation and in most instances, increased sensitivity to cisplatin.

Cisplatin is chemically inert; however, it is activated spontaneously once it enters the cell. In the cytoplasm, the chloride atoms in cisplatin are displaced by water molecules. This hydrolyzed product is a potent electrophile that can react with any nucleophile, including the sulfhydryl groups on proteins and nitrogen donor atoms on nucleic acids (deoxyribonucleic acid, DNA and ribonucleic acid, RNA) [39]. Cisplatin binds mainly to the N7 reactive center on purine residues and can cause a distortion in the structure of deoxyribonucleic acid (DNA), block cell division, arrest the cell cycle, and result in apoptotic cell death (See Figure 2). The 1,2- intrastrand crosslinks

of purine bases with cisplatin are the most notable among the changes in DNA. These include the 1,2-intrastrand d(GpG) adducts and 1,2-intrastrand d(ApG) adducts, which represent approximately 90% and 10% of adducts, respectively. 1,3-intrastrand d(GpXpG) adducts and others such as inter-strand crosslinks and nonfunctional adducts have been reported to contribute to cisplatin toxicity [40].

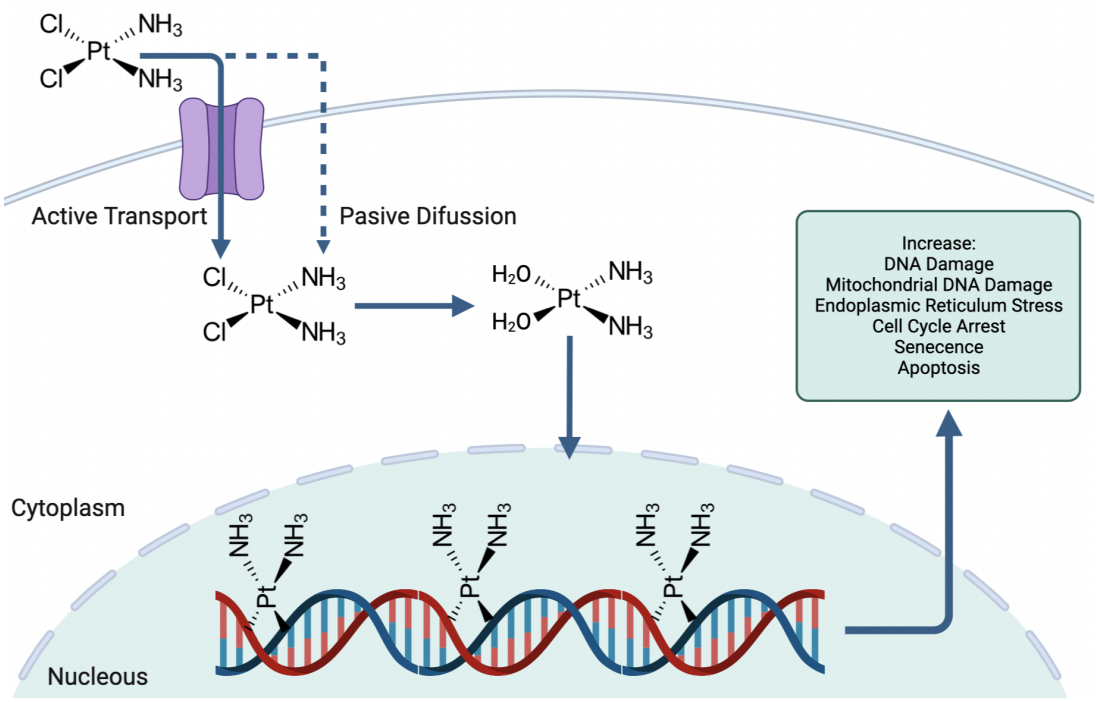

Figure 2: Cisplatin mechanisms of action. Through passive diffusion and active transport, cisplatin enters the cells in the cytoplasm and via a series of aquation reactions, it acquires the active form. The cisplatin hydrolyzed product reacts with the DNA, allowing the crosslinking with the urine bases which forms DNA adducts. These prevent the repair of the DNA, thus leading to DNA damage. They also induce programmed cell death within cancer cells. Image modified from Kelland et al. (2007) [35].

Distortion caused by cisplatin-induced lesions can be recognized by multiple repair pathways, including nucleotide excision repair (NER) and mismatch repair systems (MMR). Removal of cisplatin adducts occurs primarily through nucleotide excision repair, becoming one of the most important factors in cisplatin resistance. The mismatch repair system participates in

the recognition and resolution of cisplatin lesions [41]. When the extent of damage is limited, cisplatin adducts induce an arrest in the S and G2 phases of the cell cycle. These promote cytoprotective effects, such as repair mechanisms to re-establish DNA integrity and preventing potentially abortive or abnormal mitoses [42]. Conversely, if DNA damage is beyond repair, cells become committed to apoptosis.

The signaling cascade that bridges cisplatin DNA lesions involves the sequential activation of the ataxia telangiectasia mutated (ATM) and RAD3 related protein (ATR, a sensor of DNA damage) and checkpoint kinase 1 (CHEK1), the most prominent substrate and downstream effector of ATR. These, in turn, phosphorylate the tumor suppression protein p53 on serine 20, allowing for its stabilization [43]. Activated p53 exerts lethal functions via nuclear and cytoplasmic mechanisms that eventually lead to mitochondrial outer membrane permeabilization or increased signaling via death receptors, followed by cell death [44]. In response to cisplatin, CHEK1 has also been shown to activate various branches of the mitogen-activated protein kinase (MAPK) system, including those mediated by extracellular signal-regulated kinases, c-Jun N-terminal kinases and stress-activated protein kinases [45]. The relative contribution of these signaling modules to the cytotoxic effects of cisplatin is yet to be deciphered. Intriguingly, although ATM appears to participate in cisplatin-induced cell cycle arrest, but not cell death [46], its major downstream target, CHEK2, has been shown to convey lethal signals in response to cisplatin in an ATM-independent fashion [47].

Cisplatin chemotherapy is associated with multiple side effects that include hepatotoxic, nephrotoxic, cardiotoxic, neurotoxic and/or hematotoxic damage. Also, some patients may relapse

from cisplatin treatment with their cancers being refractory to the cisplatin regimen [39]. Hence, combination therapies of cisplatin with other drugs are common practices in the treatment of human cancers. Findings of several studies have proposed that other compounds, combined with cisplatin, constitute the best therapeutic approach to overcome drug resistance and reduce the undesirable side effects [47]. Together, , combinatorial strategies that target various cell survival pathways, , may offer the best chance for clinically meaningful treatment [33].

1.3 *Ovarian cancer and cisplatin resistance*

In the past decade, drugs that target vulnerabilities in human tumors have been clinically validated as effective cancer therapies. However, the relatively rapid acquisition of resistance to such treatments, observed in virtually all types of cancer, significantly limits their utility and remains a substantial challenge to the clinical management of advanced cancers. Therefore, cancer drug resistance continues to be a major impediment in medical oncology. Drug resistance arises prior to or as a result of cancer therapy. Currently, 90% of failures in chemotherapy during the invasion and metastasis of cancers are related to drug resistance. Based on tumor response to the initial therapy, cancer resistance can be broadly classified into two categories, primary and acquired [48, 49]. In both cases, the emergence of resistant cells could be due to, at least, two mechanisms.

While primary drug resistance exists prior to any given treatment, acquired resistance occurs after initial therapy. Unfortunately, in practice, most patients will likely develop resistance at a certain point of treatment. For example, according to O'Connor et al. (2011), approximately 20% of adults with acute lymphoblastic leukemia suffer from primary resistance to treatment [50].

In addition, Dingemans et al. (1998) recognized primary resistance in nearly 50% of all cancer patients in the 1990s [51]. A number of innate resistance factors are already known; Lippert et al. (2008) mention some that include members of the adenosine triphosphate (ATP)-binding cassette transporter gene family, gluthathione-dependent enzymes, topoisomerase, metallothioneins, O6-methylguanine-DNAmethyltransferase, thymidilate synthetase, dihydrofolate reductase, heat shock proteins, growth factors, factors associated with proliferation, apoptotic signaling and angiogenetic factors, as well as protooncogenes and suppressor genes. In general, innate resistance to targeted therapies may be due to activation or mutation of downstream signaling pathways or mutations in domains such as kinases, which do not allow access of the drugs to the ATP pocket [52].

Consequently, targeted therapies with single agent for tumors with multiple mutations, amplifications, and/or translocations could be highly effective at the beginning, but rarely curative. Along the same line, most cancers have a multiplicity of innate genetic alterations that contribute to their capacity to proliferate, become malignant, and invade tissue; therefore, the benefit of targeted therapies can be modest and transient [53]. Even if an initial response to targeted therapies is obtained, the vast majority of tumors subsequently become refractory and patients eventually succumb to the disease's progression. Examples include C-Kit mutations in gastrointestinal stromal tumors (GIST), epidermal growth factor receptor (EGFR) mutations in non-small cell lung cancer (NSCLC), HER2 amplification in breast cancer, and the BCR-ABL translocation in chronic myelogenous leukemia (CML). These mutations will explain the molecular mechanism of drug resistance already dilucidated in non-small cell lung cancer studies [54].

Patients with advanced NSCLC would normally be treated with Erlotinib and Gefitinib drugs, classified as EGFR tyrosine kinase inhibitors (TKIs). Unfortunately, despite an initial response, many patients develop resistance, resulting in a median time to progression for patients on EGFR-targeted therapies of approximately 12 months [55]. Resistance can be mediated through events acting at the level of the target EGFR itself, compensatory activation of other receptor tyrosine kinases (RTKs), or activation of downstream signaling pathways. Hence, a genetic mechanism responsible for its resistance is the acquisition of a secondary missense mutation, on EGFR T790M on exon 20. By affecting the 'gatekeeper' residue of the catalytic domain, an increased affinity of the mutant kinase for ATP occurs [56]. This finding is pertinent for the development of target therapy that is based on irreversible EGFR inhibitors, with the rationale that such binding would result in greater occupancy of the ATP binding site, thereby inhibiting T790M- mutated EGFR despite its enhanced ATP binding. Unfortunately, it has been shown that amplification of the T790M allele can cause acquired resistance even to an irreversible EGFR inhibitor [57].

The mechanism of mutational activation of other RTKs also appears to be a mechanism of resistance to EGFR TKIs. For example, it has been reported that HER2 kinase domain mutations confer resistance to EGFR TKIs by activating the AKT–PI3K signaling axis and uncoupling signaling from EGFR [46]. Also, in preclinical studies, KRAS mutation has been proposed as a primary resistance mechanism for EGFR TKIs. In addition, amplification of the gene encoding the MET RTK has been identified as an acquired resistance mechanism to EGFR TKIs in an EGFR-mutant NSCLC [58]. Engelman et al. (2007) suggests that cMET gene amplification in tumor cells can be clonally selected in the presence of EGFR inhibitors [58]. Activation of downstream signaling pathways that can uncouple EGFR from downstream signaling and confer resistance has

also been described; for example, the loss of the tumor suppressor PTEN leads to PI3K pathway activation. This study also revealed PTEN loss in primary NSCLC, suggesting that it may constitute an innate resistance mechanism [59].

Acquired resistance can be defined as the acquisition of stochastic alterations within cancer cells. In all cases, the surviving population of cells in the tumor is less likely to respond to any further therapy and will be responsible for the minimal residual disease and cancer relapse. The biochemical mechanisms associated with this kind of resistance are alterations to drug metabolism, increased drug efflux, decreased drug uptake, modification of the drug targets, specific protein modifications that are not driven by mutations, genetic rewiring, enhanced DNA repair, inactivation of apoptotic proteins, or activation of anti-apoptotic ones, the potential role of epigenetics, alternative RNA splicing, among others (See Figure 3). Nevertheless, such mechanisms play a significant role in the acquisition of resistance to cancer drugs, and while they remain poorly characterized thus far, evidence highlighting their importance is beginning to emerge [60]. Therefore, for this dissertation, I will explain the molecular mechanism of one of these mechanisms: the efflux pump.

Efflux pump mechanisms perform important physiological functions such as prevention of toxin absorption from the gastrointestinal tract, elimination of bile from the hepatocytes, effective functioning of the blood–brain barrier and placental barrier, and renal excretion of drugs. The problem of resistance to chemotherapeutic agents is perhaps one of the greatest challenges in clinical medicine [61]. Efflux pumps in eukaryotes are divided into five groups: Monocarboxylate transporter (MCT), Multidrug resistance protein (MDR, P-glycoprotein), Multidrug resistance-

associated proteins (MRPs), Peptide transporters (PEPTs), and Na+ phosphate transporters (NPTs). Its mechanism consists in the increased efflux of drugs from the intracellular compartment via energy-dependent efflux pumps. This mechanism is one of the main and best known mechanisms of resistance in cancer chemotherapy [62].

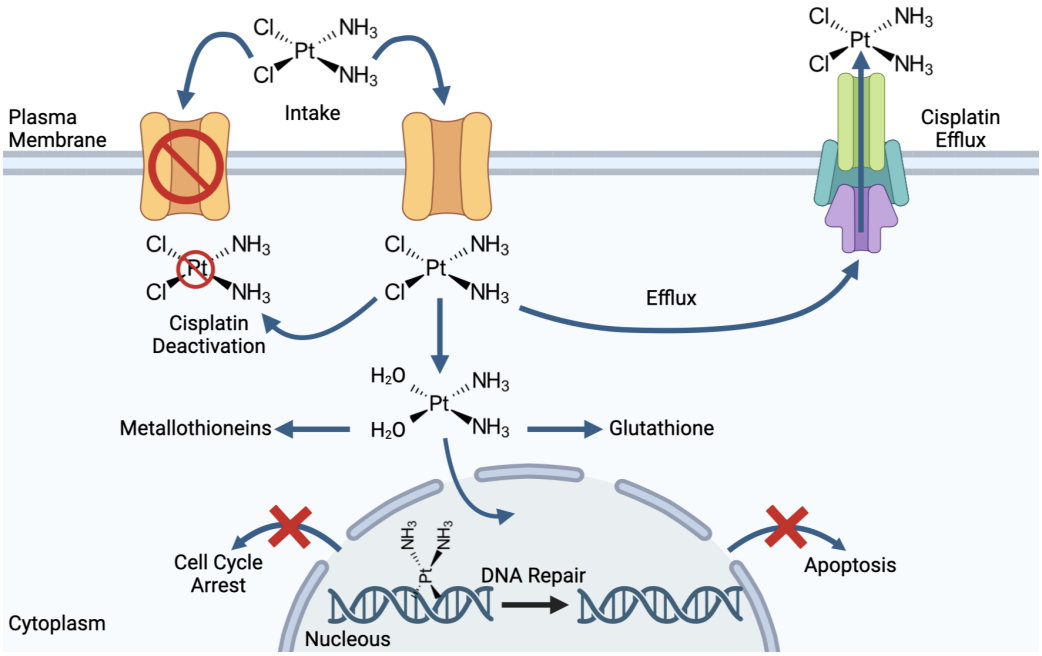

Figure 3: Cisplatin resistance mechanisms of action. Different mechanisms of cisplatin resistance have been identified in the past two decades. The postulated mechanism includes decrease in cisplatin uptake and increased efflux, increased detoxification by molecules such as sulfhydryl, increased inactivation of cisplatin, increased DNA repair, inactivation of cell death pathways and activation of cell survival pathways. Image modified from Kelland et al. (2007) [35].

Over 200 proteins involved in the transport of substrates across biological membranes are members of the ABC superfamily of proteins. A typical ABC transporter protein is consisted of four units [63]. Two are membrane-bound domains, both with six trans-membrane segments, and two are nucleotide- binding domains (NBD), which bind and hydrolyze ATP. Two sequence motifs located 100-200 amino acids apart in each NBD, designated as Walker A and Walker B, are conserved among all ABC transporter superfamily members. In addition, unique to ABC proteins, there is a third, highly conserved amino acid sequence (ALSGGQ) located between the Walker A

and B motifs, referred to as the ABC signature motif (C motif). The precise function of this sequence has been directly implicated in the recognition, binding, and hydrolysis of ATP [64].

The most common member of ABC transporter is the 170 kDa multidrug resistance protein MDR or P- glycoprotein (P-gp) encoded by ABCB1. P-glycoprotein includes 10-15 kDa of N-terminal glycosylation and the overexpression of these into the cancer cells contribute to chemotherapy resistance. The N-terminal contains 6 transmembrane domains, followed by a large cytoplasmic domain with an ATP-binding site. The second section of the molecule contains 6 transmembrane domains and an ATP-binding site that shows 65% of amino acid similarity with the first half of the polypeptide. Among the physiological functions of P-glycoprotein, are included the secretion of metabolites such as conjugated bilirubin which come out of the hepatocytes and turns into the bile. Also, it mediates the tubular secretion of cholesterol and uric acid, thereby protecting the proximal tubular epithelial cells from cellular injury. It is located on the luminal membrane of renal epithelial cells and actively secretes digoxin, cimetidine, and many other drugs. Moreover, the genetic absence of P-glycoprotein causes a decrease in the production of bilirubin which characterizes the Dubin–Johnson syndrome. This is why the regulation at transcriptional and post transcriptional level of this mechanism has been intensively studied [65].

A variety of transcriptional factors, such as p53, YB-1, and NF-κB, are involved in the direct regulation of P-gp by binding to promoter regions of the ABCB1 gene [66]. Many cell signaling pathways positively regulates P-gp; for instance, MAPK/ERK, PI3K/Akt, and Wnt/ β-catenin. Conversely, the p38 MAPK pathway has been implicated in negatively regulating the

expression of P-gp and c-Jun N-terminal kinase, which are involved in both positive regulation and negative regulation [67].

Also, microRNAs (miRNAs) are identified as players in regulating the expression of P-gp in both transcriptional and post-transcriptional levels. Some members of miRNAs, miR- 200c and miR-145, decrease the expression of P-gp: the first one, through JNK signaling pathway and the second one, by directly binding to the 3'-UTR of the ABCB1 gene. In contrast, miR-27a up-regulates the P-gp expression by suppressing the RAF kinase inhibitor protein [68]. This event occurs at the post-translational levelmainly by modification, degradation, and intracellular trafficking of P-gp. Pim-1 protects P-gp from ubiquitination and the subsequent degradation in proteasome. Small GTPases Rab5 down-regulates the endocytotic trafficking of P-gp and increases the functional P-gp level on the cell membrane while Small GTPases Rab4 down-regulates the exocytotic trafficking of P-gp from intracellular compartments to cell membrane, which decreases the functional P-gp level on cell membrane [69].

Therefore, considering the numerous mechanisms and individual variabilities of drug resistance in cancer cells, novel treatments must consider innate resistance before therapy is initiated. Acquired resistance should be repeatedly tested throughout the course of drug administration. Detection tests for close treatment surveillance would certainly reduce the number of therapy failures and protect patients from dangerous, futile, and costly treatment. Hence, available resistance tests should be improved to find the best treatment from the large cancer drug arsenal and replace standard chemotherapy practices with personalized treatments [70].

1.4 *Current models to study ovarian cancer*

Experimental models used in ovarian cancer research have evolved over the last few years. As a general concept, the ability of the experimental models to accurately recapitulate the complexity of human cancer represents a critical issue in preclinical studies for drug discovery. The high rate at which novel cancer therapeutics fail during clinical trials highlights the inadequate predictability of laboratory cancer models that are currently available for preclinical studies [71]. Accordingly, a model must be developed to understand the development and progression of the disease.

Despite improvements in ovarian cancer treatment over the last decades, ovarian cancer remains the most lethal gynecological cancer among women. Notably, after an initial effective response to the chemotherapeutic regimen, therapeutic resistance rises which leads to a patient's death. This scenario accentuates the urgent need to develop novel diagnostic and therapeutic strategies. Recently, several efforts to better understand the molecular bases of ovarian cancer, using integrated multiplatform molecular profiling, have revealed an intrinsic complexity and heterogeneity among ovarian cancers [72]. In addition, although the ovarian surface epithelium has been historically considered the primary site of origin of all (both benign and malignant) epithelial ovarian tumors, the origin of epithelial ovarian cancer is still being debated with an increasing consideration of extra-ovarian origin [71]. In particular, emerging evidences indicate the fallopian tube epithelium (FTE) and the endometrium as the origin sites of ovarian high grade serous carcinoma and endometrioid/clear cell carcinoma, respectively [71]. Therefore, this new conceptual framework has shifted the attention of ovarian cancer research to outside the ovary,

from the ovarian surface epithelium to the fallopian tube epithelium, thus reviving interest in refining *in vitro* and *in vivo* high grade serous carcinoma models (See Figure 3).

Cancer cell lines are the most commonly used models in cancer research and their use has undoubtedly ameliorated our understanding of cancer biology [73]. Short-term cultures derived from freshly isolated cells or tissues (designed primary culture) have many important applications since they can closely recapitulate the pathophysiological system. However, primary cell cultures have limiting characteristics, such as slow growth capacity and limited overall lifespan. Moreover, limitations of primary cell culture systems include loss of the endocrine, paracrine and neural regulators, gradients of nutrients, and other factors [74].

Generally, cancer cell lines possess the same spectrum of genetic aberrations as primary tumors. However, each cell line presents only a limited number of genetic aberrations, as each one represents the intertumoral heterogeneity that is observed among primary tumors [74, 75]. Therefore, it is of extreme importance to confirm that these immortalized cell lines accurately represent primary tumors with respect to original genomic alterations, as these alterations may result in molecular characteristics that predict responses (sensitivity vs resistance) to specific therapeutics [76]. Several methods have been described for the isolation and culture of primary epithelial ovarian cancer cells, derived from either fresh solid tumors or ascites fluid [77]. In general, epithelial ovarian cancer cells usually adhere and tend to reach confluence quickly when kept in culture for 2-3 months before going into senescence and be used for immediate experiments or cryostorage. However, cells derived from high grade serous carcinomas that have received recent chemotherapy show less growing efficiency and cell viability, *in vitro*. Thus, numerous

epithelial ovarian cancer cell lines have been established, but the histopathological origin of the most commonly used epithelial ovarian cell lines, namely A2780, CAOV3, IGROV1, OVCAR3 and SKOV3, remains unclear. Therefore, these epithelial ovarian cancer cell lines can be considered the most suitable models for preclinical studies of high-grade serous carcinoma [78].

On the other hand, animal models are valuable tools for studying the biology and genetics of human cancers, as well as for preclinical investigation of anti-cancer therapeutics and cancer prevention. Accumulating data from studies using those models have enabled us to gain insight into the genetic mechanisms underlying malignant transformation and cancer progression. Studies from animal models of cancer have been utilized for preclinical investigation of therapeutic efficacy and toxicity of chemicals and biologicals [79]. Significant advances have been made on the generation of animal models of cancer, which have become increasingly sophisticated by application of new technologies and integration of clinical information from patients [80]. Studies from the spontaneous and carcinogen induced models, genetically engineered mouse models, and xenograft models have led to the discovery of the molecular basis of tumor initiation, growth, and metastasis, as well as being utilized for anti-cancer drug discovery and testing. It is known that hens, some strains of mice, Wistar and Sprague Dawley rats, and macaques spontaneously develop ovarian tumors, thus making them adequate spontaneous and carcinogen models [81]. In any case, these models have a relatively late onset of tumor development and low incidence rate that make them ineffectual for in vivo studies. Since the late sixties, ovarian tumors have been induced in experimental animals by direct application of chemical carcinogens, although no chemical carcinogen has been consistently associated to EOC etiopathogenesis [82]. Interestingly, the initial lesions induced by these carcinogens, when analyzed, were ovarian surface epithelial proliferations

that were supporting the cancer origin from the ovarian surface epithelium. However, the induced carcinomas were composed of neoplastic cells resembling either endometrium or oviduct (that corresponds to the human fallopian tube epithelium in mice) and were organized either in glandular or papillary structures, similar to human endometrioid and ovarian serous carcinomas.

Another case is the genetically engineered model. Mice have been the traditional animal model for basic and preclinical studies of cancer, and other organisms (including zebrafish) play important and complimentary roles as models of cancer research. Genetically engineered mouse and zebrafish models of cancer have been generated by a variety of interventions, such as chemical or physical mutagenesis, viral infection, insertion of transgenes, homologous recombination, and the recently developed gene edition [83]. Genetically engineered mouse models for high grade serous carcinoma have been difficult to generate. Recently, the direct introduction of oncogenes and disruption of tumor suppressor genes into the oviduct have allowed the generation of mouse models that recapitulate the new pathogenetic model of high grade serous carcinoma, including the presence of lesions similar to serous tubal intraepithelial carcinoma, the putative precursor lesion [84]. There are numerous research studies regarding the generation of animal models of cancer and their pre-clinical applications. For example, Kim et al. (2012) developed an EOC mice model by the Dicer-PTEN double knockout. Other researchers have generated mouse models through the inactivation of BRCA 1/2, PTEN, and p53 in fallopian tube secretory cells, miming the molecular alterations commonly observed in human high grade serous carcinoma [83]. More recently, Sherman-Baust et al. (2014) reported a transgenic mouse model that develops high grade serous carcinoma from serous tubal intraepithelial carcinoma through the inactivation of both p53 and Rb pathways [84]. All these genetically modified mouse models provide new evidence

supporting the origin of high grade serous carcinoma from the fallopian tube in two possible manners (See Figure 4). Therefore, they certainly offer a unique opportunity for the investigation of high grade serous ovarian carcinogenesis and the exploration of new strategies for its early detection, prevention, and therapy. Nevertheless, the major limitations of these models are that they are labor-intensive, expensive, and time-consuming, and do not fully replicate the genetic and epigenetic complexity of a spontaneous high grade serous carcinoma [85].

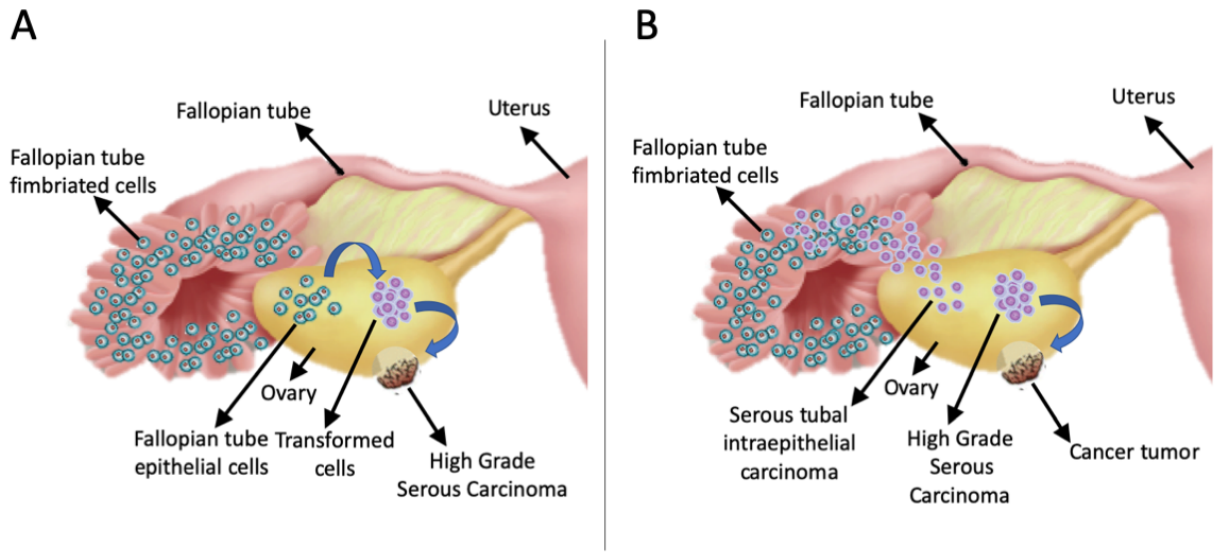

Figure 4: Fallopian tube origin of the high grade serous carcinoma. Studies indicate the fallopian tube epithelium and the endometrium as the place of ovarian high grade serous carcinoma origin. (A) Normal fallopian tube epithelial cells are entrapped in the ovary, favored by their anatomical proximity and physiological ovulation process. Entrapped fallopian tube epithelial cells undergo progressive neoplastic transformation inside the ovary through the accumulation of molecular alterations. (B) Fallopian tube epithelial cells of the fimbriated ends undergo initial neoplastic transformation, becoming serous tubal intraepithelial carcinoma. The ovarian microenvironment, rich in hormonal and inflammatory factors, drives the full neoplastic transformation to invasive high grade serous carcinoma. Image modified from Kuhn et al. (2015) [86].

Epithelial ovarian cancer cell line xenografts are the most utilized animal model in epithelial ovarian cancer research, providing a multifaceted tool to explore epithelial ovarian cancer biology and treatment [87]. Only selected epithelial ovarian cancer cell lines develop

tumors when injected into immunocompromised mice; the engrafted tumor usually acquires an indistinct undifferentiated morphology and displays complex genetic makeup, since it is usually derived from patients in advanced stage [88]. The epithelial ovarian cancer cell line xenograft models that are commonly used in ovarian cancer studies are obtained by intraperitoneal injection of the human cell lines A2780, OVCAR3, and SKOV3. Nevertheless, some preclinical studies, using epithelial ovarian cancer cell line xenografts, correctly predicted anticancer drug response and effectively contributed in guiding high grade serous ovarian cancer therapy [89]. Clinical trials with bevacizumab, a monoclonal antibody to human vascular endothelial growth factor, confirmed its efficacy in high grade serous ovarian cancer patients, both as a single agent and in combination with paclitaxel [90]. The advantages of cell line xenografts include the rapidity of tumor formation, easy predictability, reproducibility, synchronization, and the need of few mice in drug response studies.

Human xenografts are generated by engrafting a human tumor, either from a primary tumor or a cancer cell line, into immunodeficient mice. These include athymic nude mice that are deficient in T lymphocytes, lacking B and T lymphocytes, and have defects in adaptive and innate immunity due to the lack of mature lymphocytes and natural killer T cells. The three main routes of implantation for epithelial ovarian cancer xenografts are subcutaneous (ectopic), intraperitoneal, and intrabursal (orthotopic) [91]. Subcutaneous implantation facilitates manipulation and serial measurements, but it does not recapitulate clinical tumor progression, since rarely malignant ascites and peritoneal carcinomatosis develop [87]. Intrabursal implantation is the injection of cells into the bursal membrane that envelops the mouse ovary and oviduct. This implantation site reproduces the physiological environment in which high grade serous carcinoma can grow [88].

Therefore, intrabursal and intraperitoneal implantations are best in reproducing the clinical manifestations of human high grade serous carcinoma and recapitulating the early and late stage of the disease. This recently established application of patient tumor xenograft in cancer research is expected to help personalize treatments using chemo and targeted therapeutics [91].

Concisely, experimental cell lines and animal models are of pivotal importance to understand the natural history and pathogenetic steps that lead to a fully developed disease, identify potential therapeutic targets, and test novel therapeutics, either alone or in combination with standard therapies [92]. Currently, there is a lack of inbred laboratory animals that can develop high grade serous carcinoma. This is largely due to the limited understanding of the initiating factors that trigger this disease. Moreover, anatomical, physiological, and pathophysiological differences between animals and human female reproductive systems, including short lifespan, seasonal mouse reproduction, estrous cycle instead of menstrual cycle, and lack of menstruation, may hinder the development of a representative laboratory animal model [91]. In the opening era of personalized medicine, the optimal choice of experimental cell and animal models remain fundamental to broaden current knowledge of ovarian cancer.

1.5 *Therapeutic targets for ovarian cancer treatment*

Over the last 2 decades, chemotherapy along with platinum-based agents and taxanes have been the first-line agents to fight against ovarian cancer and other gynecological cancer malignancies. Major improvements in parameters associated with the disease's microenvironment, growth, angiogenesis, invasion, and metastasis will require the development of therapies that target multiple biological processes. The identification of specific pathways related to ovarian cancer progression has allowed for the discovery of a new class of molecularly targeted therapies. Such drugs interact with and inhibit molecules in these pathways to affect tumor growth, proliferation and subsequently, preventing cancer recurrence [52].

The Vascular Endothelial Growth Factor (VEGF) is an integral player in the process of angiogenesis, which is required for the survival, growth, and metastasis of cancer. The expression of VEGF and its receptors, especially VEGF Receptor-2, are involved in the malignant progression of ovarian cancer, as well as the formation of ascites. In consequence, many studies have focused on developing agents to target this signaling pathway, such as small molecule inhibitors and monoclonal antibodies to VEGF and VEGFR. For example, Bevacizumab (Avastin), a monoclonal antibody against VEGF, has shown clinical efficacy in Phase III trials for colorectal, lung and breast cancer, and is showing potential effectiveness in Phase II trials for ovarian cancer. As a monotherapy for patients with persistent/recurrent ovarian cancer or platinum resistant disease, Bevacizumab has a 16–21% response rate, with 52% of persistent/recurrent patients having stable disease [90]. Furthermore, ongoing trials are combining Bevacizumab with other chemotherapeutics. Garcia et al. (2008) study combined Bevacizumab with cyclophosphamide in

recurrent ovarian cancer patients achieved a 28% response rate with a 6-month progression-free survival rate of 57% [93].

Another VEGFR1-3 inhibitor in clinical trial is Cediranib, designed for patients with recurrent, platinum-sensitive disease. A Phase II trial by Hirte et al. (2015) revealed that 41% of patients with platinum-sensitive disease responded to monotherapy, while there was a 29% response rate in platinum-resistant patients [94]. Matulonis et al. (2009) also conducted a Phase II trial of Cediranib for recurrent EOC and cited a 17% partial response rate with 13% of patients having stable disease [95]. Another novel inhibitor of this pathway is the VEGF trap, a fusion protein comprised of the VEGFR1 and VEGFR2 extracellular domains that is fused to the Fc portion of human IgG. This agent is able to bind to VEGF-A and placental growth factor. A current Phase II trial performed by García et al. (2008) reported an 11% partial response rate in women with recurrent, platinum-resistant EOC [93].

Epidermal Growth factor receptor (EGFR) has been studied as a potential target for ovarian cancer treatment. EGFR is overexpressed in up to 70% of epithelia ovarian cancer [96]. Consequently, several inhibitors have been developed against this target. EGFR is a member of the ErbB family of receptor tyrosine kinases, which also includes ErbB2. When its ligand binds to these receptors, the tyrosine domains dimerize which leads to phosphorylation. This phosphorylation leads to the activation of multiple intracellular signaling pathways, such as the mitogen-activated protein kinase (MAPK) and the phosphatidylinositol 3- kinase (PI3K)-AKT pathways, which are involved in cell proliferation, growth, and survival [97].

An oral tyrosine kinase inhibitor EGFR Erlotinib was developed as a monotherapy in women with refractory, recurrent, EGFR positive epithelial ovarian cancer. There was a 6% response rate with 43% of patients having stabilized disease. This inhibitor has also been tested in combination with carboplatin and taxanes with positive results [98]. Another EGFR tyrosine kinase inhibitor in clinical trial is Gefitinib, which prevents the activation of EGFR as an ATP binding site competitor. Unfortunately, studies of this drug as a therapy and in combination with other drugs showed no significant clinical efficacy [99]. Another drug with similarly unremarkable results is Cetuximab. In a Phase II trial, Cetuximab was used in combination with carboplatin, in 28 women with recurrent platinum-sensitive ovarian and primary peritoneal carcinoma. The study reported that 32% had objective responses with an additional 8 patients having stable disease (Secord et al., 2008). Another trial combining cetuximab with carboplatin and paclitaxel evaluated 38 women and showed a progression-free survival of 39% at 18 months after treatment [100]. An evolutionarily conserved pathway that stimulates cell growth by producing metalloproteinases and facilitates drug resistance is MAPK (Raf/MEK/ERK). It is activated by receptor tyrosine kinases as well as other receptors for cytokines and integrins. Two isoforms b-Raf and c-Raf, have been associated with improved survival and poor prognosis, respectively, in ovarian cancer [101]. Oral kinase inhibitor, Sorafenib, targets the MAPK pathway as well as VEGFR1-3 and PDGFR-β tyrosine kinase. In a Phase II trial, it was combined and tested with gemcitabine. Han et al. (2009) showed a 4.7% partial response rate and 60.4% stable disease, as well as a 5.4 and 13.3 months progression for free and overall survival [102].

A Phase II trial is underway to determine the clinical efficacy of Temsirolimus, an inhibitor of mTOR, in recurrent ovarian cancer. The target pathway in this study is PI3K. This molecule has

been involved with functions related to cell growth, such as transcription, translation, protein degradation, and reorganization of the actin cytoskeleton. Also, PI3K mediates angiogenesis and vascular permeability through its effectors, AKT and mTOR [103].

The NFκB signaling pathway is a key player in the induction of inflammatory response and provides the link between inflammation and oncogenesis. In an ovarian cancer model, inhibition of NFκB by immunosuppressive agents resulted in decreased VEGF and IL8 expression, which correlated with decreased tumorigenicity, decreased vascularization, decreased formation of malignant ascites, and the prolonged survival of mice [104]. Mabuchi et al. (2004) reported that the NFκB inhibitor increased the therapeutic efficacy of cisplatin [105]. Additionally, Liu et al. (2006) revealed that the use of antioxidants that block paclitaxel induced NFκB activation leads to increased sensitivity to paclitaxel treatment and increased cell apoptosis [106]. Unfortunately, there are currently no NFκB inhibitors in clinical trials for ovarian cancer. However, these results indicate that targeting NFκB is an auspicious target, as it may show promise as an adjunct to the currently available regimens.

In summary, further research is necessary to elucidate the molecular mechanisms underlying epithelial ovarian cancer initiation, progression, and metastasis. Also, more research must be realized to identify novel biomarkers for the detection and diagnosis of ovarian cancer. Some of the challenges to address include the molecular heterogeneity between tumors, frequency of benign disease that reduces biomarker specificity for cancer, and low concentration of the potential biomarker in early stages. Advances in proteomic technologies that identify hundreds of

potential clinically relevant proteins represent a promising research area for the discovery of biomarkers and targets for ovarian cancer-specific therapeutics.

1.6 *RNA Binding Proteins (RBPs)*

Messenger RNAs are produced in the nucleus from the primary transcripts of protein-coding genes, pre-mRNAs, or heterogeneous nuclear RNAs by a series of processing reactions that typically include capping, pre-mRNA splicing, polyadenylation, mRNA localization, and translation. mRNAs are then transported to the cytoplasm, where the protein synthesis machinery is located, and their translation and stability are also subject to regulation [107]. These processes are mediated by numerous RNA-binding proteins (RBPs), non-coding RNA (LncRNA), and microRNA (miRNA). RBPs contain various structural motifs, such as RNA recognition motif (RRM), dsRNA binding domain, zinc finger, and others [108]. RNA-binding proteins are proteins that bind to the double or single stranded RNA in cells and participate in forming ribonucleoprotein complexes [109]. RBPs are cytoplasmic and nuclear proteins. They exhibit high specificity to their RNA targets by recognizing their sequences and structures [110]. The specific binding of RBPs allows them to distinguish their targets and regulate a variety of cellular functions via control of the generation, maturation, and lifespan of the RNA transcript. This interaction begins during transcription as some RBPs remain bound to RNA until degradation, whereas others only transiently bind to RNA to regulate RNA splicing, processing, transport, and localization [111].

Three classes of RNA-binding domains have been acknowledged. The first one, the RNA recognition motif (RRM), is a small protein domain of 75–85 amino acids that forms a four-

stranded β-sheet against the two α-helices. This recognition motif exerts its role in numerous cellular functions, especially in mRNA and rRNA processing, splicing, translation regulation, RNA export, and RNA stability [111]. Ten identifiable structures illustrate the intricacy of protein–RNA recognition of RRM, as it entails RNA–RNA, protein–protein, and protein–RNA interactions. All of RRMs' main protein surfaces' four- stranded β-sheet were found to interact with the RNA, which usually contacts two or three nucleotides in a specific manner. In addition, strong RNA binding affinity and specificity towards variation are achieved through an interaction between the inter-domain linker, the RNA, and between RRMs themselves. RRM's plasticity is the reason why it is the most abundant domain [112].

The second group is RBPs that contain a double strand RNA binding domain (dsRNA); it is a 70–75 amino-acid domain that plays a critical role in RNA processing, RNA localization, RNA interference, RNA editing, and translational repression [113]. The dsRNAs interact along the RNA duplex via both α-helices and β1-β2 loop. Moreover, all three dsRNA structures make contact with the sugar-phosphate backbone of the major groove and of one minor groove, which is mediated by the β1-β2 loop along with the N-terminus region of the alpha helix 2. This interaction is a unique adaptation of the shape of an RNA double helix, as it involves 2'- hydroxyls and phosphate oxygen. Despite the common structural features among dsRNAs, they exhibit distinct chemical frameworks which permit specificity for a variety for RNA structures, including stem-loops, internal loops, bulges, or helices containing mismatches [113].

Finally, the zinc finger domains are the most common DNA-binding domain within the eukaryotic genome. Zinc fingers exhibit ββα protein fold, in which a β-hairpin and a α-helix are

joined together via a Zn2+ ion [114]. Furthermore, the interaction between protein side-chains of the α-helix with the DNA bases in the major groove allows for DNA-sequence-specific recognition. Recent research efforts show that zinc fingers also have the ability to recognize RNA. In addition, CCHH zinc fingers were recently discovered to employ sequence-specific recognition of single-stranded RNA through an interaction between intermolecular hydrogen bonds; CCHH-type zinc fingers employ two methods of RNA binding [115]. Firstly, the zinc fingers exert non-specific interaction with the backbone of a double helix, whereas the second mode allows zinc fingers to specifically recognize the individual bases that bulge out. Differing from the CCHH-type, the CCCH-type zinc finger displays another mode of RNA binding, in which single-stranded RNA is identified in a sequence-specific manner. Overall, zinc fingers can directly recognize DNA via binding to a dsDNA sequence and RNA, via binding to a ssRNA sequence [112].

Since most mature RNA is exported from the nucleus relatively quickly, most RBPs in the nucleus exist as complexes of protein and pre-mRNA, called heterogeneous ribonucleoprotein particles. Eukaryotic cells encode diverse RBPs, approximately 500 genes, with unique RNA-binding activity and protein–protein interaction. During evolution, the diversity of RBPs greatly increase with the elevation in the number of introns. The diversity has enabled eukaryotic cells to utilize RNA exons in various arrangements, giving rise to a unique ribonucleoprotein (RNP) for each RNA. Although RBPs have a crucial role in post-transcriptional regulation in gene expression, relatively few RBPs have been studied systematically [116].

RBPs have been well studied in embryonic development. They control the transcriptional and post-transcriptional regulation of RNA, controlling the patterns of gene expression during

development [117]. RBPs are essential factors during germline and early embryonic development. Their specific function involves the development of somatic tissues, such as neurons, hypodermis, and muscles as well as providing timing cues for the developmental events [117]. Nevertheless, it is challenging to discover the mechanism behind RBPs' function in development, due to the difficulty in identifying their RNA targets because usually, most RBPs have multiple RNA targets [110]. However, it is indisputable that RBPs exert a critical control in regulating developmental pathways in a concerted manner. For example, Drosophila melanogaster, RNA-binding protein Elav, and Sxl encoding genes are critical in early sex determination and the maintenance of the somatic sexual state [118]. These genes regulate sex-specific splicing in Drosophila. Sxl produces a positive regulation of the feminizing gene Tra to produce a functional Tra mRNA in females. In other cases, RNA-binding proteins FOG-1, MOG-1/-4/-5, and RNP-4 regulate germline and somatic sex determination in C. elegans.

RBPs play a significant role and function in somatic development; they regulate tissue-specific alternative splicing of the mRNA targets. An example of these RBPs are MEC-8 and UNC-75, which contain RRM domains that localize regions of the hypodermis and nervous system, respectively [110]. Furthermore, another RRM-containing RBP, EXC-7, is localized in embryonic excretory canal cells and throughout the nervous system during somatic development in C. elegans.

In cancer, emerging RBPs are playing a crucial role in tumor progression and development [119]. The combination of their versatile RNA-binding domains with structural flexibility enables RBPs to control the metabolism of a large array of transcripts. Perturbations in RBP-RNA

networks' activity have been causally associated with cancer emergence, but the rational framework describing these contributions remains fragmented. Hundreds of RBPs are dysregulated across human cancers, impacting the expression and function of oncoproteins and tumor-suppressor proteins. Interestingly, most RBPs are predominantly downregulated in tumors related to normal tissues [109]. Several studies have provided immunohistochemical evidence that show how RBPs are abnormally expressed in cancer relative to adjacent normal tissues, and this expression correlates with patient prognosis [109]. It has been seen that many RBPs, including Sam68 [120], HuR [121], FXR1 [122] are differentially expressed in distinct cancer types. Some RBPs' change in expression is related to copy number variations; for example, gains in copy number of BYSL in colorectal cancer cells [121], ESRP1, CELF3 in breast cancer, RBM24 in liver cancer, and IGF2BP2, IGF2BP3 in lung cancer [123]. Hence, multiple in vitro studies have linked known cancer drivers to RBP dysregulation.

Particularly, the oncogenic transcription factor MYC upregulates the expression of heterogeneous nuclear ribonucleoprotein (hnRNP)A1 and hnRNPA2 in gliomas [124]. These hnRNPs promote the synthesis of the pyruvate kinase M isoform 2 (PKM2), which is involved in the glycolytic switch that underlies the Warburg effect. The PI3K/AKT/NF-kB signaling pathway activates the transcription of Hu-antigen R (HuR) in gastric cancer cells, enhancing cellular growth and resistance to apoptotic stresses [125]. The ZEB1 protein, an epithelial to the mesenchymal transition (EMT) specific transcription factor, directly represses the mRNA expression of the epithelial splicing regulatory protein 1 [126]. This event leads to the increased expression of a mesenchymal splice variant of the cell surface antigen CD44, thus inducing a more stemness and invasive phenotype in lung, breast, and pancreatic cancer cells [127]. The p53 tumor suppressor

protein induces the expression of RNA-binding motif protein 38 (RBM38) in cancer cell lines, which promotes G1 cell-cycle arrest by RBM 38 mediated stabilization of target mRNAs, such as cyclin-dependent kinase inhibitor 1A (CDKN1A)/p21 [128]. Several studies have related this change in the expression of RBPs to aberrant alternative splicing in cancer [129]. Therefore, understanding the function of RBPs in cancer cells will help in developing prognostic and response biomarkers, and in potentially unveiling new targets for the design of therapeutics.

1.7 *RNA Binding Protein with Multiple Splicing (RBPMS)*

The RBPMS gene is located on chromosome eight, position p12, and spans over 230 kb from 30,241,924 to 30,430,508 on the direct strand in the human genome. Previous studies show that this gene is expressed at high levels in the heart, breast, lung, kidney, ovary, stomach, muscle, liver, eye, adipose tissue, and ovary [130], [131-135]. RBPMS and its paralog RBPMS2 are expressed in several tissues and share 67% in amino acid composition with RBPMS isoform A, varying in their N- and C-terminal [130]. RBPMS and RBPMS2 can localize to the cytoplasm and nucleus, but aside from transcriptional co-regulation, most attention has been paid to cytoplasmic roles in mRNA stability [136], transport [137], and localization in cytoplasmic granules. Previous studies have shown that the expression of RBPMS2 in the intestine plays a role in motility disorders [138] and gastrointestinal tumors [139].

The RBPMS gene is also known as *HERMES*, *FLJ32971*, *LOC11030* or *sweyvyby*. It contains 30 distinct gt-ag introns, 9 probable alternative promotors, 3 non-overlapping alternative last exons, and 13 validated alternative polyadenylation sites. The mRNAs appear to differ by

truncation of the 5' end, truncation of the 3' end, presence or absence of 10 cassette exons, overlapping exons with different boundaries, splicing versus retention of 2 introns. The 232pb position of this gene is antisense to spliced gene, raising the possibility of regulated alternate expression.

At least 6 variants were isolated *in vivo*, despite being predicted targets of nonsense mediated mRNA decay (NMD) [140]. The gene has expressed multiple mRNA isoforms (5 according to uniport, 4 according to RefSeq, NCBI and at least 19 transcript variants according to AceView) resulting in multiple protein isoforms [140]. The RNA-binding protein with multiple splicing (RBPMS) is part of the RNA-binding proteins (RBPs) family. Each family is characterized for containing a single RNA recognition motif (RRM), corresponding to a protein domain of 80 amino acids. RRM domains are structurally diverse and bind to a multitude of sequence and structural motifs, such as the base and loop residues in stem–loop structures [141]. RRMs are present in proteins that regulate a variety of RNA processes, including pre-mRNA splicing, RNA transport, localization, translation, and stability. The RBPMS family is conserved in vertebrates and it is common to find RBPMS and RBPMS2 in the genome sequence from species that belong to this group. RBPMS and RBPMS2 are 70% identical to each other and have a single RRM domain that is responsible for both RNA binding and dimerization [142]. Its domain is flanked by 23 aminoacids in the N-terminal and 95 aminoacids in the C-terminal regions. The C terminal of RBPMS is unstructured and characterized by a high density of prolines without homology to other proteins [143].

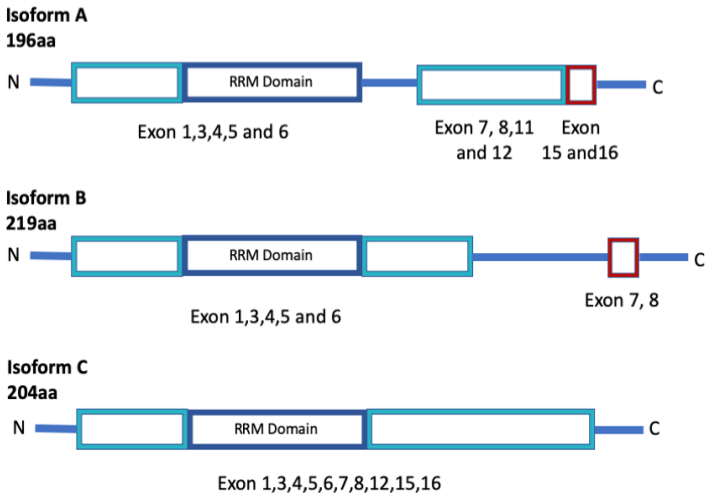

Figure 5: RBPMS isoforms A, B and C structural representation model.

RBPMS isoform A (GenBank accession numbers: NM_001008710) has a mass weight of 21,802 Da, encodes a protein of 196 aa, and has been chosen as the canonical sequence. Moreover, isoform C (GenBank accession numbers: NM_001008712) has a mass weight of 24,277 Da and its length is 219 aa. Isoforms A and B share the same N-terminal RRM domain. The C-terminus of RBPMS A and C, however, is different in both length and composition. For isoform C, the C-terminal is longer in comparison with RBPMS A. RBPMS isoform C lacks several exons and its 3'-terminal exon extends past a splice site that is used in isoform A. RBPMS isoform B (GenBank accession numbers: NM_001008711) has a mass weight of 22,416 Da, its length is 204 aa, and includes an alternate exon in the 3' end coding region of exon 7 and 8 which results in a frameshift and an early stop codon. The encoded isoform B has a longer and distinct C- terminus, compared to isoform A (See Figure 5). Isoform D isolates from *Mus musculus* differ from the canonical sequence between aminoacids 133 to 196. RBPMS isoform D mass weight is 15,794 Da and their length is 143 aa. Isoform E has a mass weight of 17,022 Da and their length is 152 aa. The isoforms messenger and protein sequence are shown with more detail in Appendix A and Appendix B.

According to Farrazi et al. (2014), RBPMS primarily bound with 3′ UTR, intronic, and coding sequences. The RBPMS RNA recognition element (RRE) consists of tandem CACs, separated by a spacer of ∼1-12nt. It is well known that RBPMS bound an (AC)9 dinucleotide repeat and (CAC)6 trinucleotide repeat RNA, that is responsible for both RNA binding and dimerization, but did not bind (CAU)6 nor (CU)9 [130]. Systematic deletion of AC study identifies four binding sites within the 3′ UTR of *NDUFA6* a NADH dehydrogenase (ubiquinone)*, ETF1* a class-1 polypeptide chain release factor, *SRM* that encodes a polycationic mediators of cell growth and differentiation, and *UBE2V1* that encodes Ubiquitin-conjugating E2 enzyme, a transcriptional activation of the human *FOS* proto-oncogene [133].

Furthermore, Farazi et al. (2014) suggests that RBPMS interacts with TGF-beta receptor type I (TbetaR-I). This increases phosphorylation of C-terminal SSXS regions in Smad2 and Smad3, and promotes the nuclear accumulation of the Smad's proteins. Those proteins are considered key mediators of transforming growth factor-beta (TGF-beta) signaling, and dysregulation of the pathway would be derived in uncontrolled cell proliferation and cancer [133].

Dysregulation of RBPMS family proteins has been reported in cancer [144] and chronic intestinal pseudo-obstruction [138]. In breast cancer, RBPMS inhibited c-Fos or Smad3 mediated AP-1 transactivation and the expression of AP-1 target genes. AP-1 regulated genes including vascular endothelial growth factor (VEGF) and cyclin D1 have beenare associated with cancer growth and progression. Mechanistically, RBPMS blocks the formation of the c-Fos/c-Jun or Smad3/c-Jun complex, as well as the recruitment of c-Fos or Smad3 to the promoters of AP-1 target genes [130]. Manipulation of RBPMS levels during embryogenesis suggested functions in

X. laevis oocyte maturation [145], heart and kidney development [134], and retinal ganglion cell development [137]. In *X. laevis*, RBPMS regulated cleavage of vegetal blastomeres in early embryogenesis [145, 146] and control mRNA processing [134] and the transport of mRNAs along the axon to the axon terminal of retinal ganglion cells [137]. RBPMS has been recently addressed as a master regulator of alternative splicing. It has been directly associated with numerous components of the actin cytoskeleton and focal adhesion machineries, an activity that is crucial for smooth muscle cells. RBPMS also regulates splicing of other splicing, post-transcriptional, and transcription regulators, one of which is the transcription factor, myocardin [134].

1.8 Biological roles of RNA Binding Protein with Multiple Splicing (RBPMS)

The RNA binding protein with multiple splicing (RBPMS) is a member of a family of proteins that bind to the nascent RNA and control their transcription, degradation, editing, translocation, translation, and splicing [147]. However, the functions of many more biological processes and their relevance to disease states are yet to be elucidated. Recently, studies explored the functions of RBPMS in vascular smooth muscle cell differentiation, aging, oogenesis, and retina ganglion cell [132], [148-151].

Vascular smooth muscle cells are important in the skeletal and cardiac muscle. The phenotypic plasticity of smooth muscle cells in healthy arteries is necessary in response to any injury or disease that commences a synthetically active, motile, and proliferative state [152]. Nakagaki-Silva et al. (2019) reported that RBPMS highly down-regulated phenotypic switching of smooth muscle cells from a contractile to a motile [153]. Moreover, RBPMS is responsible for

20% of the alternative splicing changes during this transition. RBPMS directly regulates alternative splicing of numerous components of the actin cytoskeleton and focal adhesion machineries, such as myocardin. The data presented by Nakagaki-Silva suggests that RBPMS has a critical role in vascular smooth muscle differentiation. Furthermore, RBPMS plays important roles in cardiac muscle and embryonic stem cells, where its expression is also a super-enhancer [153].

Peiheng Gan et al. (2022) showed that RBPMS deletion causes perinatal lethality in mice, due to congenital cardiovascular defects. They observed premature onset of cardiomyocyte binucleation and cell cycle arrest during mice development, after RBPMS was lost. Human cardiomyocytes with RBPMS gene deletion have a similar blockade to cytokinesis [154]. Data sequencing analysis revealed that RBPMS plays a role in RNA splicing involved in cytoskeletal signaling pathways. They concluded that RBPMS mediates the isoform switching of the heart-enriched LIM domain protein Pdlim5. The loss of RBPMS leads to the accumulation of Pdlim5 isoforms, disrupting cardiomyocyte cytokinesis [154].

RBPMS not only functions as a marker for cardiomyocyte differentiation processes, it also serves as a marker for retinal ganglion cells. In studies conducted by Ye, Linda et al. (2018) expression of the RBPMS gene was 2-fold higher when the pGL3-Basic vector they used was a negative control [155]. Within RGC-5 cells, 5-UTR structural differences allowed for 60-to-25-fold higher levels within promotor sequences in the -1603 to -1353 and -259 to -9 promotor regions in the RBPMS gene [155]. This made it possible to determine the effect of RGC cells and promotor

sequence regulation areas, relative to expression of the RBPMS gene. This was all allowed due to how the RGC cells serve to generate the marker function of RBPMS for these cells.

Additionally, information presented by Kwong et al. (2010) describing in situ hybridization with RBPMS antisense riboprobes postulated that RBPMS-positive cells were predominantly located in the ganglion cell layer, where they are co-localized with RGCs [132]. The latter was confirmed by using experimental RGC-deficient retinas, which showed that when RGC cells were not present, RBPMS was not present in the GCL as well. Interestingly, RBPMS expression was most noticeable in the cytoplasmic medium of these cells, given that the nuclear localization of these was too weak to assert a genuine presence [132]. This idea ties up with modern theories on cytoplasmic splicing, or the ability to give mRNA fragments resistance to the cytoplasmic medium for longer intervals until they reach a ribosome or the pertinent objective. RBPMS-positive cells also demonstrated staining near the perinuclear area of the cell, allowing for a possible association with the Golgi Complex. The importance of these conclusions is based on how RBPMS-positive cells expressed the gene in nearly 100% of the cell samples, which demonstrated the close association between RBPMS and RGC fuction [132].

Shanmugaapriya et al. (2016) examined how the RBPMS expression is altered during aging and whether RBPMS is regulated by the interleukin-1β (IL)-1β and TGF-β growth factor. This study characterized how the Smad signaling pathways regulate RBPMS expression. They used inhibitors for blocking the phosphorylation of Smad2/3 and Smad 1/5/8, through the use of inhibitors or inducing phosphorylation of Smad's via adenoviral vectors transfection [149]. Results showed that RBPMS expression increased when the phosphorylation of Smad2/3 was blocked or

when Smad1/5/8 signaling was activated. This suggested that reduced levels of pSmad2/3 or increased levels of pSmad1/5/8 directly regulate RBPMS expression. Also, this research team showed that significant reductions in the expression of RBPMS occur with aging in animal models, which contributes to the reduction of Smad2/3 signaling [149].

The reduced expression of the TGF-β signaling regulator RBPMS during aging suggests functional loss of factors that regulate TGF-β response. TGF-β responsiveness in signaling contributes to the development of osteoarthritis during aging, presenting a possible role for RBPMS in the development of the degenerative disease [149]. The negative relation between positive RBPMS cell signal and tissue damage demonstrates that cartilage damage affects RBPMS expression and has a negative effect on the phosphorylation of Smad2/3. Shanmugaapriya et al. (2016) showed that RBPMS, as well as the unphosphorylated and phosphorylated states of Smad2 and Smad3, has a potential role in maintaining normal articular cartilage [149]. However, more studies are necessary to prove whether RBPMS is a significant functional factor that is involved in the regulation of TGF-β responsiveness [149].

During oogenesis, a selected group of RNAs are localized and retained within the vegetal cortex at two different time periods [150]. The localization of these RNAs is a mechanism, by which cells control the protein synthesis at specific time periods in a particular space. In Xenopus laevis' vegetal region on the oocytes, the mRNA and RBPMS protein are localized in high amounts and decrease during maturation. The RBPMS protein is concentrated in a specific structure within the vegetal cortex, the germ plasm, where RBPMS protein co-localizes with different mRNAs. Aguero et al. (2016) explored the role of RBPMS in Xenopus laevis' stage I oocytes mitochondrial

cloud. One component of germinal granules in Drosophila melanogaster, Xenopus laevis, and Mus musculus is nanos, whose RNA product is essential for the preservation of the germline. Aguero et al. (2016) reported that the RBPMS protein is present throughout the cytoplasm and in the nucleus of stage I oocytes. Moreover, they confirmed that RBPMS co-localizes with nanos in the mitochondrial cloud, concentrating in the germ plasm within the germinal granules [150]. Song et al. (2007) results of the in vitro and in vivo assays suggest that RBPMS forms distinct particles and associates with nanos, but not with Vg1 or VegT RNA in the nucleus [156]. These findings propose that RBPMS binding might initiate a sorting pathway that terminates with nanos/RBPMS within the germinal granules. Moreover, Song and coauthors found that UGCAC repeats are essential for nanos RNA mitochondrial cloud localization and required for RBPMS binding to the mitochondrial cloud localization signal. The 34 amino acids in the RBPMS N-terminal, conserved region in human RBPMS isoforms, are required to form homodimers and bind the nanos 3′UTR region. In addition, Song et al. (2007) report that RBPMS binds the GGLE domain, which does not contain a UGCAC region, but does contain two binding sites for VM1 hnRNP I [156]. The association between RBPMS, hnRNP I, and nanos RNA remains unclear. However, in the absence of any RNAs, hnRNP I does not interact directly with the RBPMS protein, as suggested by these authors.

Other authors, such as Nijjar and Woodland (2013), identified four other proteins in stage VI oocytes that directly bind with RBPMS: *Xvelo* splice variant, *Xvelo*-full length, Rbm42b, and Rbm24b. Their findings indicate that RBPMS binding in the nucleus with Rbm42b (RNA binding protein) which localizes nanos RNA in late stage oocytes [157]. Therefore, Rbm42b could be one of the factors required for RBPMS nanos RNA binding. RBPMS localization with *Xvelo* in the

germ plasm is a significant finding. *Xvelo* is required for the formation of the mitochondrial cloud balbiani bodies and oocyte polarity. *Xvelo* had its homologue in zebrafish, called Bucky ball. Their analysis affirms that Rbm24b and *Xvelo* bind with each other in the cytoplasm, but not in the nucleus. Thus, *Xvelo* may join the RBPMS/nanos ribonucleoprotein complex after it exits the nucleus, which indicates the occurrence dynamic remodeling [157].

Song et al. (2007) explored the role of RBPMS targets (RNAs-encoding proteins) involved in meiotic maturation, early cleavage, and germline development. During meiotic maturation and early cleavage in Xenopus leavis, a group of maternal mRNAs, including RINGO/Spy and Mos, are regulated at the translational level [156]. The ectopic expression of RINGO/Spy or Mos causes the activation of meiotic maturation and cleavage arrests, which correlates with the loss of RBPMS phenotypes [156]. Accelerated maturation was observed when RBPMS antisense morpholino oligonucleotide was injected, stemming from RINGO/Spy mRNA. The RBPMS protein was present as an mRNP complex, containing RINGO/Spy, Mos, and Xcat2 mRNAs in vivo. RBPMS appears to negatively regulate RINGO/Spy and Mos RNAs that are involved in meiotic maturation and early cleavage, respectively [156].

As has been demonstrated, RBPMS is an important component of embryonic development. RBPMS has a critical role in the localization and expression of molecular signals that are involved in such development. Its function as a homodimer, in concert with other proteins, is crucial in different pathways that are carried out in the cell nucleus, as well as in the cytoplasm.

1.9 RBPMS dysregulation and cancer

Dysregulation of RBPMS family proteins has been reported in cancer [144] and chronic intestinal pseudo-obstruction [138]. The Human Protein Atlas pathology expression summary indicates that most cases of endometrial, ovarian, testicular, renal, and pancreatic cancers along with few cases of melanomas, cervical, breast, and lung cancers displayed moderate to strong nuclear staining, with additional cytoplasmic positivity.

This information can be corroborated by few studies that explored the relationship between RBPMS dysregulation and cancer. For example, in a breast cancer report, RBPMS inhibited c-Fos or Smad3 mediated AP-1 transactivation, and blocking the expression of AP-1 target genes. These transcription factors have been associated with cancer growth and progression, such as vascular endothelial growth factor (VEGF) and cyclin D1. The blocking formation of c-Fos/c-Jun or Smad3/c-Jun complex by RBPMS makes impossible the link of c-Fos or Smad3 to the promoters of AP-1 target genes [130].

The role of RBPMS has been explored by different authors in blood related malignancies, such as multiple myeloma (MM) and acute myeloid leukemia (AML). Gene expression profiling studies in patients with AML surprisingly identified RBPMS as one of the twenty genes that are most frequently published in AML expression studies [158]. RBPMS was identified as one of the ten most up-regulated genes associated with poor prognosis, and has not been previously described in AML. During the gene expression profiling analysis, RBPMS is positioned as a key insight into disease pathogenesis while exposing a potential diagnostic and prognostic marker and therapeutic

target for AML. Miller et al. (2010) reported that RBPMS is a direct and functionally relevant target of EZH2 in multiple myeloma (MM) [158]. The authors showed that RBPMS silencing confers resistance to Bortezomib (BTZ) in MM cells. Furthermore, restoration of RBPMS by miR-138 overexpression re-sensitizes the resistant cells to anti-myeloma drugs, such as BTZ and MG132 [158]. Rastgoo et al. (2018) demonstrated that miR-138 mimics a pharmacological inhibitor of EZH2. Delivery miR-138 in combination with a proteasome inhibitor BTZ, induces apoptosis and significant regression of tumor growth in assays that have mice xenograft models [159]. These results indicate that EZH2 regulates tumor cell proliferation by repression of tumor suppressor genes and RBPMS. It also remarks the importance of RBPMS in the drug resistance acquisition. In summary, Rastgoo et al. (2018) establishes the EZH2/miR-138 axis as a potential therapeutic target for MM [159]. Additionally, micro array analysis from dedifferentiated hepatocellular carcinoma (DHCC) and hepatocellular carcinoma (HCC) with chromosomal 13q region RBPMS loss, were among one of the six most significantly upregulated genes [144]. Drozdo et al. (2012) concluded that dedifferentiation of hepatocellular carcinoma is associated with upregulation of genes, such as RBPMS, which are involved in cell-cycle control and proliferation [160].

Growing evidence has revealed that RBPMS plays a critical role in the proliferation and invasion of bladder cancer (BC). Yang et al. (2021) performed an expression profile from qPCR in BC cell lines revealed that RBPMS was significantly downregulated in aggressive BC samples. However, upregulation of RBPMS suppresses BC proliferation and metastasis [161]. Yang et al. (2021) showed that miR-330-3p upregulation restored BC cancer cell proliferation, invasion, and migration, as well as silencing of RAI2. RAI2 silencing reversed miR-330-3p-induced cell growth,

invasion, and migration in vitro by directly targeting the miR-330-3p/ retinoic acid induced 2 (RAI2) axis [161]. Yang et al. (2021) concludes that RBPMS acts as a tumor suppressor and provides a potential biomarker and therapeutic target for BC.

Accumulating evidence supports a central role of RBPMS in ovarian cancer initiation, progression, and chemoresistance. Luciferase reporter assays identified RBPMS as a miR-21-3p target gene [162]. When RBPMS was silenced by siRNA, it exhibited a reduction of sensitivity in ovarian cancer cells towards platinum-based drugs, such as cisplatin. Also, significant decrease in RBMPS levels was observed between serous ovarian cancer patient and normal ovarian epithelium samples by immunohistochemical analyses [162]. Also, other micro RNAs (miRNAs) have been correlated with ovarian cancer recurrence prognosis, using bioinformatic tools. miRNAs, such as miR375 and miR141, are predominantly identified in literature as possible biomarkers and regulatory mechanisms during recurrent ovarian cancer [163]. The role of miR-21-3p in RBPMS regulation is also evident in colorectal cancer (CRC), one of the most prevalent malignancies in modern society, and a leading cause of cancer-related deaths [164]. Inhibition of miR-21-3p in CRC cells (Lovo, HT29, Colo320 and SW480 cells) resulted in the suppression of proliferation and induction of the cell cycle arrest, increasing the nuclear accumulation of Smad4 and reduced phosphorylation of ERK. Skawran et al. (2008) suggests that miR-21-3p inhibition suppresses cell biological functions depended on the cell cycle such as proliferation, thus inducing apoptosis by directly targeting RBPMS through the Smad4/ERK signaling pathway. Moreover, it suppresses cancer cell invasion as well as migration. In conclusion, all these studies assert that RBPMS dysregulation is an important factor in the development of cancer and a worse prognosis.

A recent publication from Rabelo et al. (2022) disclosed that reduced RBPMS levels increase the sensitivity of ovarian cancer cells to cisplatin treatment [147]. However, the role of RBPMS isoforms in cancer has not been explored sufficiently and as such, is not concretely understood. Some possible associations with the topic have been found in the literature but require more evidence. RBPMS could be an emergent and potent target for tumor progression suppression in the development of future cancers therapies.

Chapter 2. Significance, Specific Aims, Rationale, and Hypothesis

Cancer is one of the leading causes of death worldwide [1]. In 2018, the International Agency for Research on Cancer, in collaboration with the World Health Organization, reported between 2012 to 2017, 18.1 million new cases and 9.6 million deaths. Today, the total number of people in the world that live with a cancer diagnosis are estimated at 43.8 million. Ovarian cancer is one of the six most common cancers among women, and the most common cause of gynecological cancer-related deaths in western countries with a survival proportion of 40% to 50% in the first 5 years of diagnosis [10]. Depending on the type of ovarian cancer and how advanced it is, the standard medical care plans for patients can include cytoreductive surgery, combined with taxane and platinum based chemotherapy. Unfortunately, this disease is still the most aggressive and malignant type of gynecological cancer [165]. Although 60% to 80% of patients initially respond to the traditional treatment, only 10% to 30% of them, eventually recur and develop resistance to platinum-based chemotherapy [166]. Furthermore, a combination of cytotoxic agents (gemcitabine, pegylated liposomal doxorubicin and topotecan) and a second cycle of chemotherapy are recommended for these patients, but the long term efficacy of this treatment

need further investigation. Platinum-based chemotherapy, such as cisplatin, is one of the most currently used active anticancer agents, and the resistance patients develop to it is a major obstacle. As a result, the survival rate for patients with ovarian cancer has not improved over the past 20 years [167].

It is imperative to understand and identify molecules that are involved in platinum resistance/sensitivity-related mechanisms. Therefore, it is necessary to find a new strategy for the management of ovarian cancer in particular for patients that become resistance to chemotherapy. Recently, our laboratory published that the c-Jun transcriptional activation increased the expression of miR-21 in cisplatin resistance ovarian cancer cells [168]. Several other miRNAs have been seen associated with cisplatin resistance in ovarian cancer cells [159, 169]. They have been directly implicated with ovarian cancer initiation, progression, and cisplatin resistance. According to a recent study by Baez et al. (2016), the upregulation of miR-21-3p contributed to the cisplatin resistance of ovarian cancer cells. Three miR-21-3p target genes were identified, including RBPMS. Dysregulation of RBPMS family proteins has been reported in cancer [140] and such reports describe how RBPMS plays a central role in inhibiting the proliferation and migration of breast cancer cells by blocking the formation of c-Jun-c-Fos or c-Jun-Smad3-4 complexes [110].

The RBPMS gene is located on chromosome eight, position p12, and spans over 230 kb. Previous studies show that this gene is expressed at high level in heart, breast, lung, kidney, ovary, stomach, muscle, liver, eye, adipose, and ovary [131-135]. The RBPMS gene contains 30 distinct gt-ag introns, 9 probable alternative promotors, 3 non-overlapping alternative last exons, and 13

validated alternative polyadenylation sites. The gene expresses multiple mRNA in humans, resulting in three different products or isoforms [140]. The RNA-binding protein, with multiple splicing (RBPMS), binds to the nascent RNA transcripts and regulates their processing, including the pre- mRNA splicing and transport, localization, and stability of the RNA molecules. Alternative splicing results in multiple transcript variants encoding different RBPMS isoforms. RBPMSA, RBPMSB, and RBPMSC are the best described isoforms, according to the literature.

It is well known that RBPMS is bound to the basic leucine zipper domain of c-Fos that mediates the dimerization of AP-1 proteins 4 [130]. RBPMS inhibits c-Fos or Smad3-mediated AP-1 transactivation, and the expression of AP-1 target genes that are known to be the key regulators of cancer growth and progression, including vascular endothelial growth factor (VEGF) and cyclin D1. Mechanistically, RBPMS blocks the formation of the c-Fos/c-Jun or Smad3/c-Jun complex, as well as the recruitment of c-Fos or Smad3-4 to the promoters of AP-1 target genes. In cultured cells and a mouse xenograft model, RBPMS inhibited the growth and migration of cancer cells through c-Fos or Smad2/3/4 [130]. Fu et al. (2015) suggests that RBPMS is a critical repressor of AP-1 signaling [130]. Hence, RBPMS-related molecules may be a useful strategy for cancer treatment. Presently, little is known about the biological function of RBPMS in ovarian cancer and less is known about the specific isoform associated with cisplatin resistance. The following specific aims are expected to address this knowledge gap:

Specific Aim 1: To determine whether the decreased expression of RBPMS isoforms promotes the cisplatin resistance of ovarian cancer cells.

Rationale: Preliminary data was obtained by using RT-PCR and western blot analysis, which identified that cisplatin resistance (A2780CP20 and OVCAR3CIS) cells express low levels of RBPMSA, RBPMSC mRNA, and protein levels, in comparison with the cisplatin sensitive (A2780 and OVCAR3) cells. However, the specific RBPMS isoform that is responsible for cisplatin resistance in ovarian cancer cells is yet to be studied.

Hypothesis: Increased levels of RBPMS isoform A will increase the sensitivity of ovarian cancer cells to cisplatin treatment.

Approach: Cell proliferation was assessed by clonogenicity assay and cell growth curve, cell migration, and cell invasion by wound healing assay and transwell chamber assay. Moreover, the dose response to cisplatin was assessed by viability assay. A2780CP20-RBPMSA and A2780CP20-RBPMSC was implanted by overexpressing clones in the right flank of the nude mice. After cell implantation, tumor growth was recorded three times per week with a vernier caliper. After twenty-seven days, the mice were euthanized. Mice weight, tumor size, and number of nudes were recorded. The tumors were then collected to perform immunohistochemical studies against the KI67 proliferation marker and CD31 vascular endothelial cells marker.

Specific Aim 2: To determine the RBPMS isoform that represses AP-1 (c-Fos and c-Jun) dependent gene regulation in ovarian cancer cells.

Rationale: Fu et al. (2015) showed that in breast cancer, each RBPMS isoform interacts differently with an AP-1 member (c-Fos and c-Jun). Particularly, the RNA-recognition motif (RRM) and C-

terminus of the RBPMS isoforms RBPMS-A and RBPMS-C. However, the specific AP-1 member interacting with RBPMS in cisplatin resistant ovarian cancer cells has not been determined.

Hypothesis: RBPMS A represses AP-1 (c-Fos and c-Jun-) dependent gene regulation in cisplatin resistance, in ovarian cancer cells.

Approach: Immunoprecipitation was performed using DDK agarose beats and western blots analysis to determine whether RBPMS binds to AP1 proteins members and Smad's proteins. RNAseq studies were realized to identify common and specific RBPMSA and RBPMSC downstream effectors. Also, to explore the effect of RBPMS isoforms expression in pre-mir-21 transcription, RT-PCR was performed with specific primers against pre-mir-21 and siRNA experiments to validate the results.

Specific Aim 3: To identify RBPMS associated proteins in ovarian cancer cells.

Rationale: Reports evidence that RBPMS bounds other proteins (beside c-Jun and Smad's) to regulate gene expression. However, the proteins that bound to RBPMS isoforms during cisplatin resistance in ovarian cancer cells have not been identified.

Hypothesis: Each RBPMS isoform binds to its own group of proteins that is involved in the cell growth, proliferation, and survival of ovarian cancer cells.

Approach: Liquid chromatography was realized with tandem mass spectrometry in the immunoprecipitation sample that was extracted from protein lysates. These were obtained from RBPMSA, RBPMSC and A2780CP20-EV clones to identify the proteins that bind to each RBPMS isoform. Western blots analysis was done in immunoprecipitation samples, extracted from protein lysates, to validate the proteomic data. Also, the KM plotter database (https://kmplot.com, accessed on January 21, 2021) was explored to uncover its clinical relevance in the overall survival (OS) and progression-free survival (PFS) of the disease.

Chapter 3. Materials and Methods

3.1 Cell lines and Culture Conditions

The human ovarian epithelial cancer cells A2780 and A2780CIS cells were purchased from the European Collection of Cell Cultures (ECACC, Porton Down, Salisbury, UK), and the OVCAR3 cells from the American Type Culture Collection (ATCC, Manassas, VA, USA). The A2780CP20 cells were provided by Dr. Anil K. Sood (MD Anderson Cancer Center, Houston, TX, USA) and have been described elsewhere [168, 170]. The OVCAR3CIS cells were generated by exposing OVCAR3 to increasing concentrations of cisplatin (CIS; Sigma-Aldrich, St. Louis, MO, USA), as previously described [171]. The IC50 values and molecular characterization of these cells (A2780, A2780CP20, A2780CIS, OVCAR3, and OVCAR3CIS) have been published previously [172-174]. For propagation, A2780, A2780CP20, and A2780CIS were maintained in a RPMI-1640 medium (Thermo Scientific, Logan, UT, USA), supplemented with 10% fetal bovine serum (FBS) (Thermo Scientific, Logan, UT, USA) and 0.1% antibiotic/antimycotic solution

(Thermo Scientific, Logan, UT, USA). The OVCAR3, and OVCAR3CIS cell lines were maintained and propagated in RPMI-1640 (GE Healthcare Life Sciences, Logan, UT, USA; supplemented with insulin (0.01 mg/mL; Sigma-Aldrich, St. Louis, MO, USA; OVCAR3, OVCAR3CIS) supplemented with 10% FBS, and 0.1% antibiotic/antimycotic solution. All cells were maintained at 37 °C in 5% CO2 and 95% air. Cell lines were screened for mycoplasma, using the LookOut® Mycoplasma PCR detection kit as described by the manufacturer (Sigma-Aldrich, St. Louis, MO, USA), and authenticated by Promega (Madison, WI, USA) and ATCC using Short Tandem Repeat (STR) analysis. All in vitro assays were performed at a 70–85% cell density.

3.2 Western blot analysis

Cells were detached with Trypsin (0.25%) at 37°C, washed with Phosphate Buffer Saline (PBS), harvested, and stored at -80°C until processed. Cells were lysed with ice-cold lysis buffer and incubated on ice for 30 min. Whole cell lysates were centrifuged, supernatants were collected, and protein concentration was determined using Bio-Rad Protein Reagents (Bio-Rad, Hercules, CA). In all cases, protein lysates (50 μg) were separated by SDS-PAGE (12% Acrylamide), blotted onto nitrocellulose membranes, and probed with the appropriate dilution (1:1000) of primary antibody (Sigma, St. Louis, MO; Cat number AV3476). The membranes were rinsed and then incubated with mouse or rabbit IgG horseradish peroxidase (HRP)-linked secondary antibodies (Cell Signaling, 1:5000 dilution). Bound antibodies were detected using enhanced chemiluminescence (GE Healthcare, Logan, UT, USA) followed by autoradiography in a FluorChemTM 8900 (Alpha Innotech Corporation, San Leandro, CA). The signal intensity of each band was quantified using Image Lab software (BioRad, Hercules, CA, USA).

3.3 RNA Isolation, cDNA Synthesis, and RT-PCR

For the RT-PCR experiment, total RNA was isolated using the GenElute Mammalian Total RNA Miniprep kit from Sigma Aldrich (Cat #RTN350). RNA was converted into complementary DNA (cDNA) with the Sigma-Aldrich Enhanced Avian RT first strand synthesis kit (Cat #STR1-1KT). In brief, total RNA (1 μg), 500 mM dNTP, 2.5 mM random nanomers, and nuclease-free water were mixed for a total volume of 10 mL. The mixture was centrifuged and heated at 70°C for 10 minutes. After this period, 1 mL of enhanced avian RT, 2 mL 10X buffer, 1 mL RNase inhibitor, and nuclease-free water were mixed into each sample. Samples were incubated at 25°C for 15 minutes, followed by incubation at 45°C for 50 minutes to allow the conversion reaction. The RT-PCR reaction included 12.5 μl Master Mix (JumpStartTM REDTaq Ready Mix), 1.0 μl forward Primer (10 μM), 1.0 μl Reverse Primer (10 μM), 4.0 μl cDNA, and 6.5 μl RNase free dH2O. The PCR cycling conditions were one cycle of initial denaturation for 10 min at 95°C; 40 cycles of denaturation for 15 sec at 95°C; annealing for 30 sec at 60°C; and extension for 30 sec at 72°C. β-actin was used as an endogenous control. The next primer sequences were used: for RBPMSA forward, 5'- TTCACTGCATGCCCAGATGC-3′, and reverse, 5′-TTCAGCAGAACTGACGGGAC-3′; RBPMSB forward, 5′CCCAGCTCTGTGAAGGTCAG-3′, and reverse, 5′-GCACTATCAGGAGACGGAGC-3′; RBPMSC forward, 5′-ACACACCTGTCTTTTGTCC ACT-3′, and reverse, 5′-TGCTGGTCTGCAGTAGGTTG-3′; total RBPMS (RBPMST): forward, 5′-CTGTACCCAGCGGAGTTAGC-3′, and reverse, 5′-GTGAAGCGGGATAGGTGAAA-3′; and β-actin forward, 5′-GAACCCTAAGGCCAAC-3′, and reverse, 5′-TGTCACGCACGATTTCC- 3'. The next primer sequences were used: for pri-miR-21

experiment: forward, 5′-CATTGTGGGTTTTGAAAAGGT-3′, and reverse, 5′-CCACGACTAGAGGCTGACTTAGA-3′. The PCR products were separated in 3% tris-borate-ethylenediaminetetraacetic acid (TBE) agarose gel (1% EtBr). Bands were imaged using a gel imager (Gel Doc XR+, Bio Rad).

3.4 Stable transfection for RBPMS expression

A2780CP20 cells were seeded in 6 well plates at a concentration of 3.5 x 104 cells/mL and incubated at 37°C, 5% CO_2. The next day, pTPC (V123)-RBPMSA (1.0 μg), pTPC (V123)-RBPMSC or an Empty Vector (1.0 μg) pTCP (V123) (transOMIC Technologies, Huntsville, AL) (See figure: 6) were transfected into the cells using MegaTran 1.0 transfection reagent (1:1 v/v) (OriGene, Rockville, MD). Twenty-four hours later, the culture media was replaced by RPMI-containing puromycin (2.2 mg/mL). The pTCP plasmid contains a puromycin resistance cassette, which was used for mammalian cell clone selection and maintenance. Individual clones were picked up and grown in independent flasks. RBPMS expression levels in each clone were measured by western blot analysis. These RBPMS overexpressing cells are referred to as A2780CP20-RBPMSA and A2780CP20-RBPMSC clones.

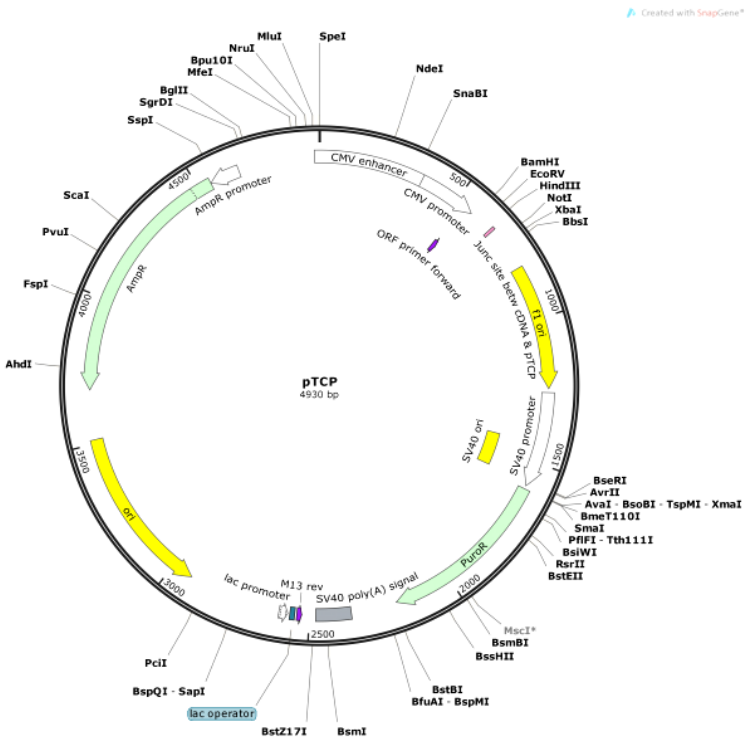

Figure 6. pTPC map vector. Mammalian cell vector with a puromycin resistance marker, for expressing a cDNA from the CMV promoter.

3.5 Colony formation, cell growth curve and cell viability assays

Cell proliferation was assessed by colony formation assays. One thousand cells of each: A2780CP20-RBPMSA, A2780CP20-RBPMSC or A2780CP20-Empty Vector (A2780CP20-EV) clones were seeded in 10-cm Petri dishes (2.0 x 10^4 cells/mL). Seven to ten days later, colonies were stained with 0.5% crystal violet in methanol. Colonies of more than 50 cells were counted in five random fields (10X), using the Nikon Eclipse TS100 micro-scope (Nikon, Minato, Tokyo, Japan). The percentage of colonies was calculated, relative to the number of colonies in the A2780CP20-EV plate, which was considered as 100%. For cell viability, cells (3.5 x 10^4 cells/mL) were seeded into 96-well plates and 24 hours later, exposed to different concentrations of cisplatin (0.1 µg/ml, 1.0 µg/ml, 10 µg/ml, 25 µg/ml, 50 µg/ml, 100 µg/ml) and incubated for 72 hours

(Sigma-Aldrich, St. Louis, MO, USA). After this period of time, the medium was removed and 100 µl of Alamar blue (Invitrogen) dye was added. The optical density (OD) values were obtained spectrophotometrically in a plate reader (BioRad, Hercules, CA, USA) after a maximum of 4 hr of dye incubation. In all cases, percentages of cell viability were obtained after blank OD subtraction, taking the untreated cells values as a normalization control. For cell growth, curve cells (2.0 x 104 cells/mL) were seeded in 10-cm Petri dishes and incubated for 24 hours at 37°C. Cells were detached with Trypsin (0.25%) at 37°C, stained with 0.5% trypan blue solution, and counted in triplicates in 24-hour intervals for 96 hours after plating with a hemocytometer. The effect of RBPMS A and C in cell growth, in combination with cisplatin, was assessed with clonogenic assays. Cells (5.0×10^3) were plated in a six well plate, and twenty-four hours later, cisplatin (2µM, final concentration) was added to the cells. Twenty-four hours after, cells were detached and 2.0×10^4 cells/mL was seeded onto 10-cm Petri dishes containing RPMI-1640 medium (10% FBS, 0.1% antibiotic/antimycotic solution), and incubated at 37 °C. Seven to ten days later, colonies were stained with 0.5% crystal violet in methanol. Colonies with more than 50 cells were counted in five random fields (10X), using the Nikon Eclipse TS100 microscope (Nikon, Minato, Tokyo, Japan). The percentage of colonies was calculated relative to the number of colonies in the A2780CP20-EV plate, which was considered as 100%.

3.6 Migration and Invasion Assays

Cell migration was measured with the wound healing assay and cell invasion by the matrigel transwell method, as previously described [147, 175]. For invasion assay, cells (3.5 x 10^4 cells/mL) were seeded into 6-well plates. The next day, Matrigel (BD Biosciences, San Jose, CA, USA) in serum-free medium was added onto the upper chambers of 24 transwell plates and incubated at 37 °C for polymerization. Clones and controls cells were collected and resuspended in serum-free medium, and re-seeded onto the Matrigel-coated chamber. Medium containing 10% FBS was added to the lower part of the wells and plates were incubated for 48 hours at 37 °C. Then, the medium was removed, and cells that had invaded through the Matrigel were fixed and stained using the Protocol Hema 3 Stain Set (Fisher Scientific, Kalamazoo, MI, USA). The invading cells were counted at 20X using an Olympus 1X71 microscope equipped with a digital camera (Olympus DP26). The cell invasion percentages were calculated by assuming the A2780CP20-EV values in terms of 100% cell invasion. For the wound healing assay, cells were seeded into 6-well plates and scraped with 200 µl pipette tips. The plates were washed with PBS to remove detached cells and then, incubated with the proper growth media for 24 hours. Cell migration was observed under a phase contrast microscope at 20X magnification at 0, 12 and 24 hours post-induction of injury. Migrated cells in the clean area in each of the five random fields were measured and quantified, using Nikon Eclipse Ts2R microscope with the Nikon DS-Qi2 camera and subsequently, analyzed with the NIS-Element Microscope Software.

3.7 Mice Experiments

Female BALB/c nude mice (4-6 weeks of age) were purchased from Taconic Biosciences (Rensselaer, NY, USA). Cells (2.0×106 cells/200 μL in PBS/Matrigel mixture) were subcutaneously injected into the right dorsal flank. The tumor growth was monitored with a Vernier caliper, three times per week. Tumor volumes were calculated using the following formula: volume = (L × W × H) × 0.5, where L is the length (longest diameter), W is the weight (thickness), and H is the height (shorter diameter). The size and weight of the tumors, as well as number of nodules, were recorded. Animal handling and research protocols were approved by the Institutional Animal Care and Use Committee (IACUC) of the University of Puerto Rico, Medical Sciences Campus on 25 January 2022 (protocol number: A870110).

3.8 Immunohistochemistry

Pieces of tumors, collected from mice experiments, were fixed on paraffin blocks and sectioned (5μm thick). The slides were then deparaffinized, rehydrated, and immersed in distilled water with 3% hydrogen peroxidase to suppress endogenous peroxidase activity. Antigen retrieval of tissue sections was performed by microwave treatment in an antigen unmasking solution (Vector Laboratories, Inc, Burlingame, CA) for 15 minutes. Sections were incubated with RBPMS antibody, proliferation antibody Ki67, or anti-VEGF antibody CD31 (Abcam, Cambridge, MA) at a dilution of 1:100, 1:500 and 1:100 respectively; in Dako antibody diluent (Dako North America Inc, Carpinteria, CA), overnight at 4°C. Subsequently, the Envision peroxidase-labeled polymer (goat anti-mouse; Dako North America Inc, Carpinteria, CA) was applied to the sections and

signals were developed with diaminobenzidine (DAB) chromogen. Three slides per mice were analyzed. Images from five microscopic fields per slide were taken using an Olympus 1X71 microscope equipped with a digital camera (Olympus DP26). The immunoreactivity was estimated and compared using Student's t-test for comparing two groups, and by ANOVA for multiple group comparisons. P-values of <0.05 were considered statistically significant.

3.9 Senescence-Associated β-Galactosidase Activity

Senescence was measured with the beta-galactosidase (β-Gal) Detection Kit from Abcam (catalog #AB176721). The fluorescein di-β-D-galactopyranoside (FDG) substrate kit generates a fluorescent product that can be measured. In brief, cells were collected, lysed with protein lysis buffer, and diluted for a final protein concentration of 1 µg/mL. The protein samples were incubated with FDG for four hours. After incubation, a stop buffer was added, and fluorescence was quantified in a Thermo Scientific Varioskan Flash spectral reader machine at 490 nm excitation and 525 nm emission. β-Gal levels of each sample were calculated with respect to the β-galactosidase standard curve prepared for each experiment. To assess the senescence associated β-galactosidase staining, 30,000 cells of each cell type (A2780-CP20, A2780CP20-EV, A2780CP20-RBPMSA (clones 7 and 8) and A2780CP20-RBPMSC (clones 3.3 and 3.10) per well in a 6-well plate, were seeded. Twenty-four hours later, the β-galactosidase staining was assessed using a senescence detection kit (Ab65351, Abcam, Cambridge, MA, USA), following the manufacturer's recommendations. Cell images were taken at 20X with an Olympus 1X71 microscope.

3.10 RNA Sequencing Library Preparation, Data Processing, and Statistics

For RNA sequencing library preparation, total RNA was extracted from cell pellets using the Qiagen RNeasy Kit (Cat #74004). The RNA quality was verified sing Agilent RNA TapeStation, and 1 ug of high-quality RNA was used for polyA mRNA enrichment (RIN > 9.7). The NEBNext polyA mRNA magnetic isolation module (NEB #E7490) was used for purification of the polyA mRNAs, according to the manufacturer's protocol. The isolated mRNA was then fragmented into ~200 bp fragments and further purified for the library preparation. cDNA preparation and adaptor ligation were performed, according to the manufacturer's protocol. The resulted DNA was amplified for eight PCR cycles. The final library was purified using NEBnext sample purification beads, and quality control was performed using Agilent HS-DNA Tapestation analysis. The samples were multiplexed for a final concentration of 5nM and sequenced on the IlluminaNovaseq platform. Files containing RNA sequencing reads were adapted and quality-trimmed, using Trim-Galore-0.6.0. Bowtie2 (version 2.2.9) was used to remove contaminating reads from ribosomal RNA and transfer RNA [176, 177]. The trimmed and contamination-filtered reads were mapped to the hg38 genome (GENCODE Release 31) using STAR aligner version 2.5.2a, and a count matrix was obtained using the "Gene Counts" option [178]. The DESeq2 (version 1.28.1) package was used to perform a differential expression analysis, using R version 4.0.1 [179]. The Ensembl IDs were converted to gene symbols and names, using the org.Hs.eg.db package (version 3.11.4). Significance was set at an FDR-adjusted p-value < 0.05 and fold change $\geq |2.0|$.

3.11 RNA Seq validation by SYBR-Green Based qRT-PCR

A custom-made 384-well plate containing pre-designed forward and reverse primers was purchased from Bio-Rad (Hercules, CA, USA). Total RNA was isolated from A2780CP20-EV, RBPMSA, and RBPMSC overexpressing clones, using the GenElute Mammalian Total RNA Mini Kit (Millipore-Sigma, St. Louis, MO, USA) following the manufacturer's instructions. RNA was reverse transcribed with the iScript Reverse Transcription Supermix for RT-qPCR from Bio-Rad. SYBR Green-based qPCR was performed using the SsoAdvanced™ Universal SYBR® Green Supermix (Bio-Rad) and a CFX384 Touch Real-Time PCR detection system. Fold-changes and cycle threshold (Ct) values were calculated by the instrument's internal software relative to A2780CP20-EV samples, and normalized to β-actin along with controls for gDNA, PCR reaction, RT reaction, and RNA quality.

3.12 Immunoprecipitation (IP) studies

IP was performed, as previously described [180]. Cells were collected, lysed in lysis buffer (50 mM Na-Hepes (pH 7.5), 150 mM NaCl, 1 mM EdTA), and disrupted by pipetting for 5 min. 40 µL of cleared supernatant was mixed with 15 µL anti-FLAG M2 affinity gel (Sigma-Aldrich), and incubated with gentle rotation at 4 °C for two hours. After supernatant removal, beads were washed out twice with wash 1 buffer (50 mM Na-Hepes, pH 7.5, 150 mM NaCl, 1 mM EDTA, 0.5% Triton X-100, 6% Glycerol, 0.5 mM DTT, 1 mM PMSF) and once with wash 2 buffer (50 mM Na-Hepes, pH 7.5, 150 mM NaCl, 1 mM EDTA, 6% Glycerol, 1 mM PMSF). Then, proteins were eluted with 200 µL flag elution buffer (25 mM Na-Hepes, pH 7.5, 100 mM

NaCl, 0.2 mg/mL 3× FLAG peptide; Sigma Aldrich). Eluent was analyzed by western blot to confirm the RBPMS co-immunoprecipitation. The samples were analyzed by mass spectrometry (San Juan, PR, USA).

3.13 Mass Spectroscopy (Proteomics), Data Processing, and Statistics

Sample Preparation for LC-MS/MS: Protein extracts (50 µg) of the IPs were mixed with 2X sample buffer (95% Laemli/5% β-mercaptoethanol) and heated at 70°C for 10 minutes, followed by SDS-PAGE. The gels were Coomassie-stained, and proteome bands were cut out. Gel pieces were distained by incubation with 50 mM ammonium bicarbonate/50% Acetonitrile solution at 37°C for 2 hrs. Afterwards, samples were reduced with Dithiothreitol (25 mM DTT in 50 mM Ammonium Bicarbonate) at 55°C, alkylated with Iodoacetamide (10 mM IAA in 50 mM Ammonium Bicarbonate) at room temperature in the dark, and digested with Trypsin (Promega) overnight at 37°C. Trypsin/Protein ratio used for optimal digestion was 1:50. The next day, digested peptides were extracted out of the gel pieces, using a mixture of 50% acetonitrile / 2.5% formic acid in water. Extracts were reconstituted for MS analysis, using 0.1 % formic acid in water (Buffer A) and a small portion was transferred to a special sample vial for injection into the instrument.

LC-MS/MS Analysis Easy-nLC1200 (Thermo Fisher Scientific): For peptide separation, a PicoChip H354 REPROSIL-Pur C18-AQ 3 µm 120 A (75 µm x 105 mm) chromatographic column was used. The separation was achieved using a gradient of 0.1% of formic acid in 80% acetonitrile (Buffer B) from 5% to 95% twice, in a total time frame of 69 minutes. Flow rate was set at 300 nl/min with a maximum pressure of 300 bar, and the injection volume was of 2 µL per sample. Q-

Exactive Plus (Thermo Fisher Scientific) was operated in positive polarity mode and data-dependent mode. The full scan/MS1 was measured over the range of 400 to 1600 m/z. The MS2 was configured to select the 10 most intense ions for fragmentation (resolution 17,500; AGC target 1e5). A dynamic exclusion parameter was set for 15 seconds.

Database analysis: The raw data was analyzed using Proteome Discoverer (PD) software version 2.5. The files were searched with a Human (Homo sapiens Tax ID=9606) database, downloaded through the software's protein center, last updated on July 30, 2021. A dynamic modification for oxidation +15.995 Da (M) and a static modification carbamidomethyl +57.021 Da (C) generated by the alkylation during processing were included in the parameters for the search.

3.14 Clustering and Network Analysis

To determine the functional networks and pathways associated with the differentially abundant transcripts, IPA (Ingenuity Systems, Qiagen, Redwood City, CA, USA) was performed. The cutoff for considering significance in the genes and proteins in the IPA CORE analysis, was based on a fold change $\geq |2.0|$ and p-value ≤ 0.05; the human was considered as the model organism for annotations [181]. Network and canonical pathway enrichment analyses were performed using Metascape a Gene Annotation & Analysis Resource, filtering for all tissues, cell lines, and human species [182].

3.15 Kaplan-Meyer (KM) Survival Analysis

KM survival analysis was performed using publicly available gene chip and RNA-Seq datasets in the KM plotter database (www.kmplot.com) [183]. For each gene symbol, a probe ID was selected, and the ovarian cancer patients were categorized into high- and low-expression groups, based on the RNA expression median values of the dataset. For genes with multiple probes, the best probe was selected. All available datasets were used for survival analysis. KM survival plots for OS and PFS were generated with their respective hazard ratios (HRs), confidence intervals (CIs), and p-values (log-rank). p-values < 0.05 were considered statistically significant.

3.16 Small interference RNA (siRNA) transfection

To silence human RBPMS (NM_001008710) two siRNAs targeting the sequences: 5′-GGGCTATGAGGGTTGTGTT-3′, and 5′-AAGAGAAACCCTCATAGCC-3′ were used (Sigma-Aldrich Cat# SASI_Hs01_00024546 and SASI_Hs01_00024547). A non-silencing siRNA (NC-siRNA) was used as the negative control (Sigma-Aldrich). In brief, A2780CP20-RBPMSA, A2780CP20-RBPMSC, A2780CP20-RBPMS-EV (3.5×10^4 cells/mL) were seeded in petri dishes. Twenty-four hours later, 200 nM of siRNA (final concentration) were mixed with using MegaTran 1.0 transfection reagent (1:1 v/v) (OriGene, Rockville, MD) at 1:2 ratio (siRNA:transfection reagent) in Opti-MEM I growth medium. The mix was incubated for 15 minutes at room temperature and added to the cells. Cells were collected after 24 hours and RBPMS expression levels in each clone were measured by western blot analysis.

3.17 Statistical analysis

All experiments were performed in triplicates and analyzed using GraphPad Prism 7 (GraphPad Software, La Jolla, CA, USA). Statistical differences were determined using a 2-tailed, unpaired Student's t-test, and one-way and two-way ANOVA tests were performed as per the requirement of the analysis * $p \leq 0.05$, ** $p \leq 0.01$, *** $p \leq 0.001$, **** $p \leq 0.0001$. p-value of less than 0.05 was considered statistically significant.

Chapter 4. Results

4.1 RBPMSA and RBPMSC protein levels are reduced in cisplatin resistance ovarian cancer cell lines

To assess the protein and mRNA levels of RBPMS splice variants, Western blots and real-time PCR was performed. The protein levels of RBPMSA and RBPMC levels were negligible in the cisplatin-resistant ovarian cancer cell lines (A2780CP20, A2780CIS, and OVCAR3CIS), when compared with their cisplatin-sensitive counterparts (A2780 and OVCAR3) (Figure 7A). The half maximal inhibitory concentration (IC50) values of these cells to cisplatin have been published [174]. Densitometric analysis of the band intensities confirmed the observation (Figures 7B and 7C). RT-PCR results showed that mRNA levels of RBPMSA and RBPMSC were also significantly lower in cisplatin resistant ovarian cancer cells, as compared with cisplatin-sensitive ovarian cancer cells (Figures 7D and 7E). Also, densitometric analyses of the PCR bands in the agarose gels confirmed the findings (Figures 7F and 7G). RBPMSA and RBPMSC levels in cisplatin-resistant ovarian cancer cells are reduced not only at protein level, but also at the transcriptional level. Levels of RBPMSB were not detected in cisplatin-sensitive ovarian cancer cells lines at the

mRNA and protein levels. Therefore, the focus was narrowed to the RBPMSA and RBPMSC splice variants.

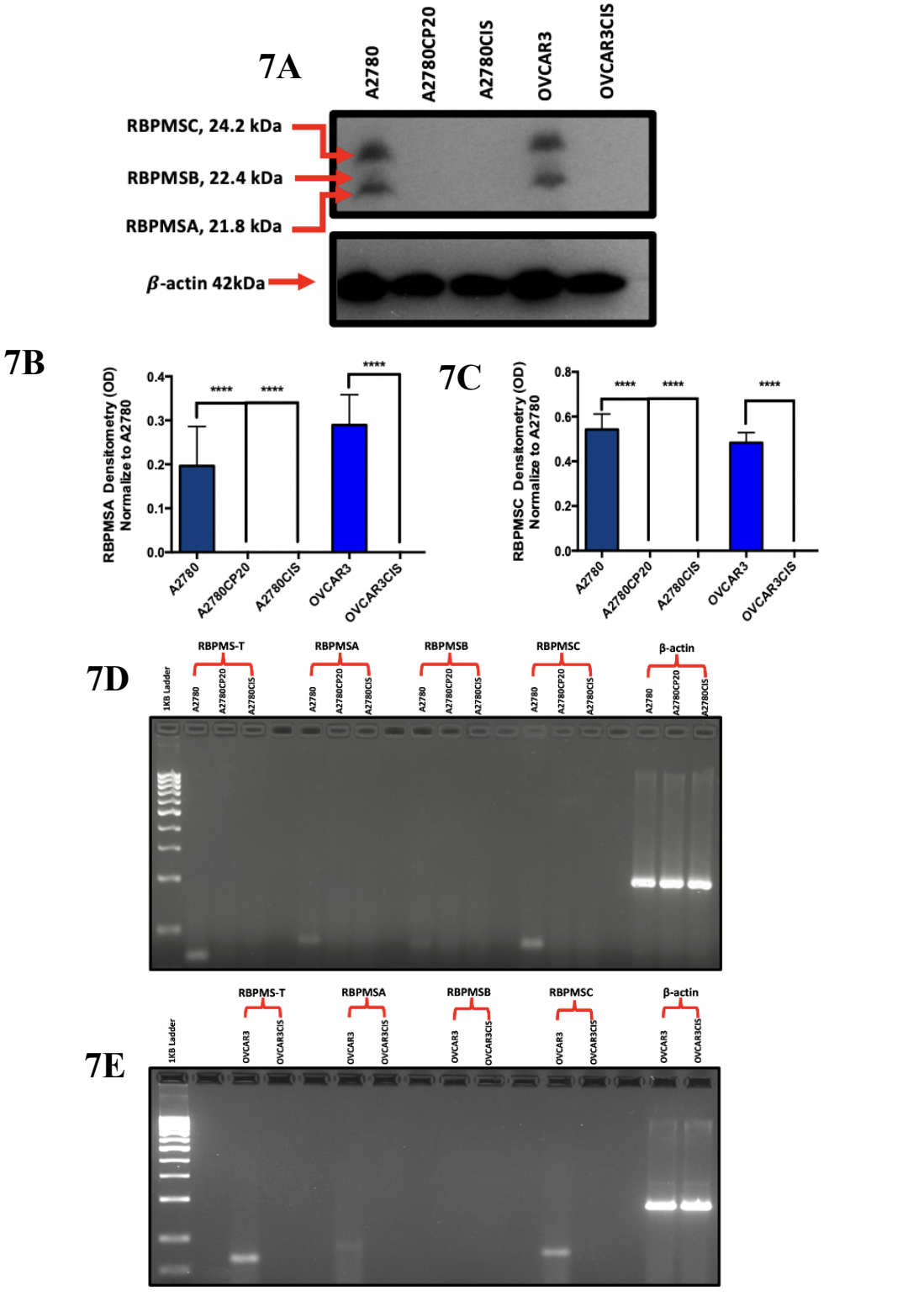

7F

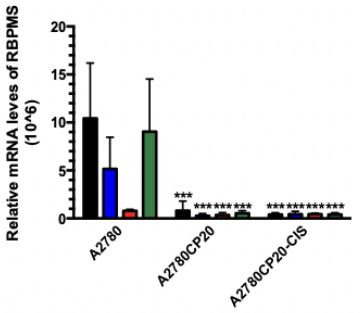
Relative mRNA leves of RBPMS (10^6)
Total
Isoform A
Isoform B
Isoform C
A2780
A2780CP20
A2780CP20-CIS

7G

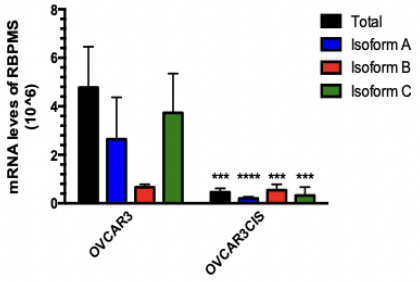
mRNA leves of RBPMS (10^6)
Total
Isoform A
Isoform B
Isoform C
OVCAR3
OVCAR3CIS

7H

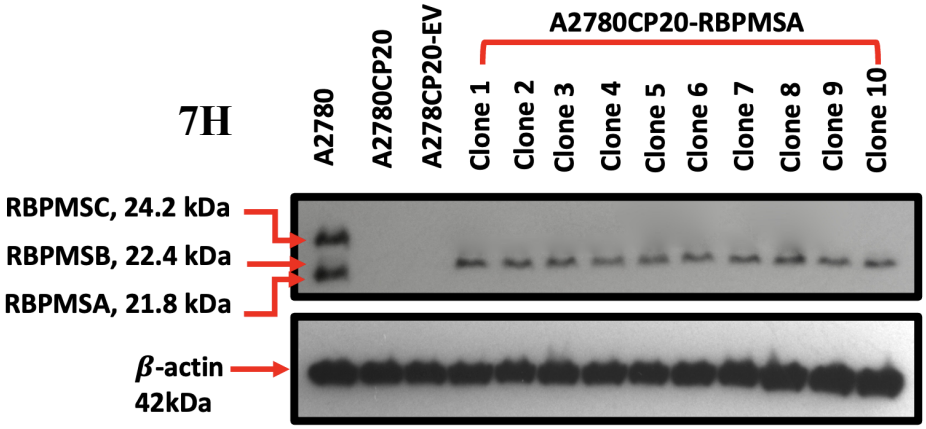
A2780-RBPMSA
A2780
A2780CP20
A278CP20-EV
Clone 1
Clone 2
Clone 3
Clone 4
Clone 5
Clone 6
Clone 7
Clone 8
Clone 9
Clone 10
RBPMSC, 24.2 kDa
RBPMSB, 22.4 kDa
RBPMSA, 21.8 kDa
β-actin
42kDa

7I

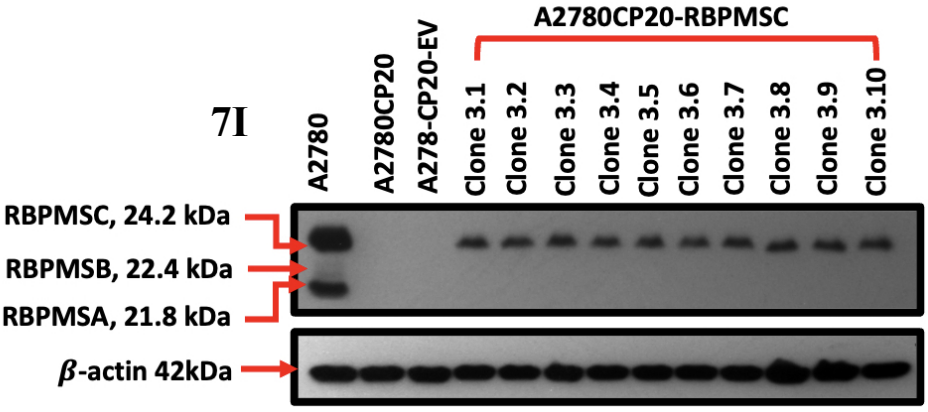
A2780CP20-RBPMSC
A2780
A2780CP20
A278-CP20-EV
Clone 3.1
Clone 3.2
Clone 3.3
Clone 3.4
Clone 3.5
Clone 3.6
Clone 3.7
Clone 3.8
Clone 3.9
Clone 3.10
RBPMSC, 24.2 kDa
RBPMSB, 22.4 kDa
RBPMSA, 21.8 kDa
β-actin 42kDa

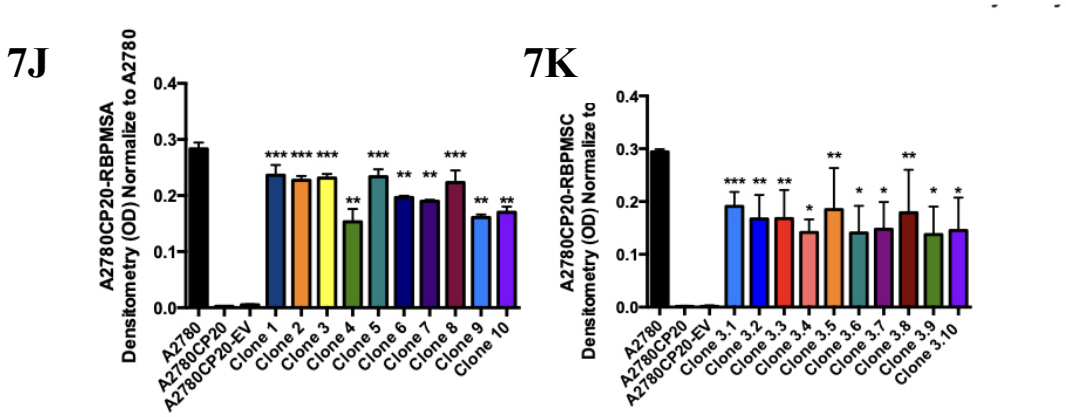

Figure 7. Protein and mRNA levels of RBPMS splice variants in ovarian cancer cell lines and stable transfected clones. (A) Western blot analysis was performed with 50 µg protein extracts and β-actin was used as a loading control. **(B and C)** Densitometry analysis of band intensities, shown in Figure 7A. **(D and E)** RT-PCR was performed, starting with 100 ng of total RNA. DNA products were separated in 2% agarose gel electrophoresis and the gel was stained with Ethidium bromide. **(F and G)** Densitometry analysis of band in-tensities, shown in Figures 7D and 7E. Fold changes at the protein and mRNA levels were calculated relative to the cisplatin sensitive cell pairs. Bars: averages ± SEM of three in-dependent experiments. **(H and I)** Western Blot images obtained with 50 µg of proteins, extracted of RBPMS and RBPMSC overexpression clones. **(J and K)** Densitometry analysis of band intensities, shown in Figures 7H and 7I. Fold changes in protein levels were calculated relative to the A2780CP20-EV clones. * $p < 0.05$, ** $p < 0.01$, *** $p < 0.001$, **** $p < 0.0001$.

4.2 Ectopic expression of RBPMSA and RBPMSC decreased cell growth and proliferation of cisplatin resistant ovarian cancer cells

Since RBPMSA and RBPMSC were dramatically reduced in cisplatin resistant ovarian cancer cells in contrast to cisplatin sensitive cells, the biological consequences of overexpressing each RBPMSA and RBPMSC in A2780CP20 and OVCAR3CIS cells was studied. A2780CP20 cells were stable transfected and OVCAR3CIS were transiently transfected with RBPMSA or RBPMSC plasmids. Figures 7H and 7I are Western blots that show the protein levels of A2780CP20-RBPMSA (21.8 kDa) or A2780CP20-RBPMSC (24.2 kDa) clones. Figure 7J and 7K are densitometric analyses of the Western blot images' band intensities. In the clonogenic assays, a significant reduction was observed in the number of colonies formed by cells that overexpressed

RBPMSA or RBPMSC (***p<0.001 and ****p <0.0001, respectively), compared with A2780CP20-EV clones (Figures 8A and 8B). Moreover, the size of the colonies (Figures 8C and 8D) formed by A2780CP20-RBPMSA or A2780CP20-RBPMSC overexpressing clones were significantly smaller when compared with A2780CP20-EV clones (****p<0.0001 and **p<0.01, respectively). Figure 8E is a Western blot, showing the overexpression of each RBPMS isoform in OVCAR3CIS. The bands close to 21.8 kDa correspond to RBPMSA, and the band close to 24.2 kDa corresponds to OVCAR3CIS-RBPMSC. These increases in molecular weight are due to the additional 12 aminoacids of a DDK-Tag sequence. Overexpression of RBPMSA and RBPMSC in OVCAR3CIS resulted in a significant reduction in the number of colonies, and the colony sizes compared with OVCAR3CIS-EV clones (***p<0.001 ****p<0.0001) (Figure 8F and 8G). The effect of RBPMSA and RBPMSC overexpression on cell growth rates was also tested. Figure 8H shows that both A2780CP20-RBPMSA and A2780CP20-RBPMSC grew slower than the A2780CP20-EV clones. Together, these results suggest that increased levels of RBPMSA and RBPMSC reduce cell proliferation in cisplatin resistant ovarian cancer cells.

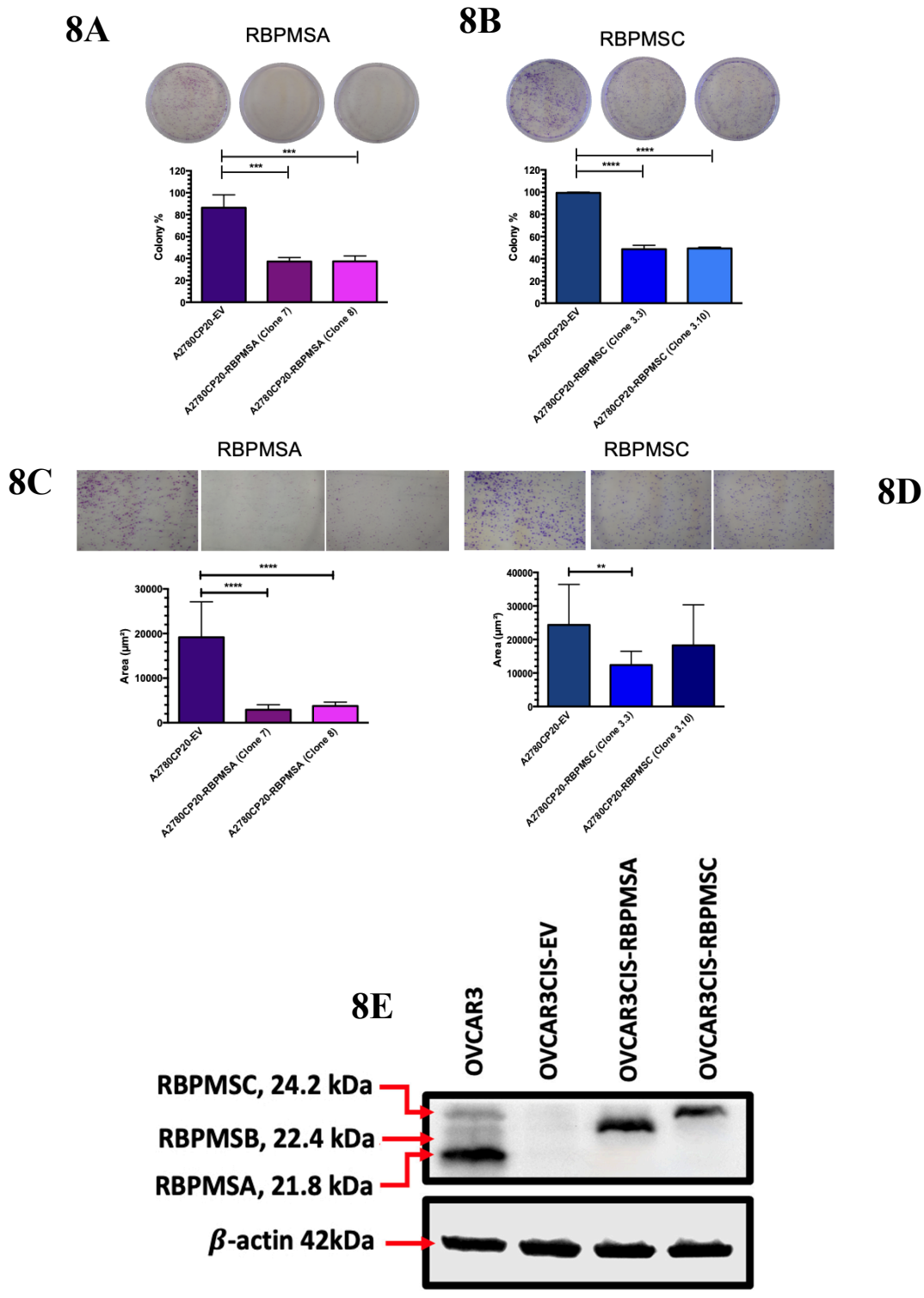
8A
RBPMSA
***
***
Colony %
A2780CP20-EV
A2780CP20-RBPMSA (Clone 7)
A2780CP20-RBPMSA (Clone 8)
8B
RBPMSC
****
****
Colony %
A2780CP20-EV
A2780CP20-RBPMSC (Clone 3.3)
A2780CP20-RBPMSC (Clone 3.10)
8C
RBPMSA
****
****
Area (µm²)
A2780CP20-EV
A2780CP20-RBPMSA (Clone 7)
A2780CP20-RBPMSA (Clone 8)
RBPMSC
8D
**
Area (µm²)
A2780CP20-EV
A2780CP20-RBPMSC (Clone 3.3)
A2780CP20-RBPMSC (Clone 3.10)
8E
OVCAR3
OVCAR3CIS-EV
OVCAR3CIS-RBPMSA
OVCAR3CIS-RBPMSC
RBPMSC, 24.2 kDa
RBPMSB, 22.4 kDa
RBPMSA, 21.8 kDa
β-actin 42kDa

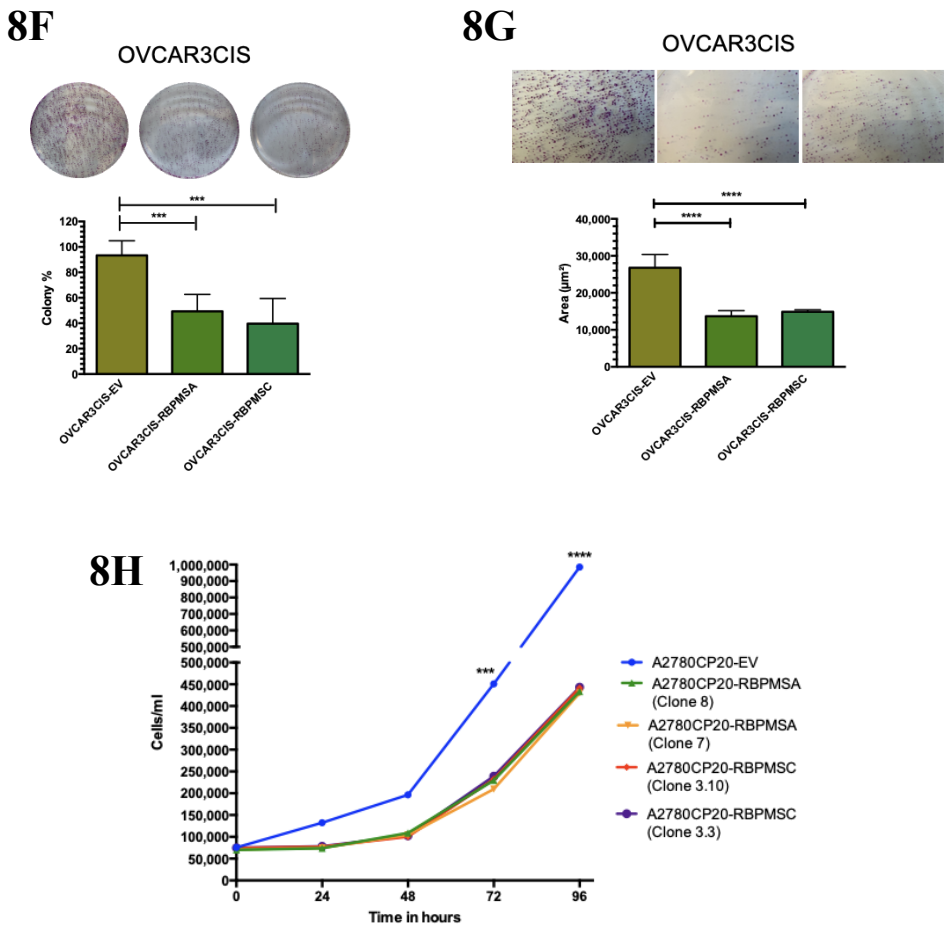

Figure 8. Effect of RBPMSA and RBPMSC overexpression in cell growth, proliferation, invasion, and migration. (A and B) Colony formation assay. Percentages of clonogenicity were calculated relative to A2780CP20-EV cells. **(C and D)** Colony Size. Percentages of size measures were calculated relative to A2780CP20-EV cells. **(E)** OVCAR3CIS were transiently transfected with RBPMSA, RBPMSC, or an empty vector. A concentration of 50 µg of protein extracts was used to perform Western blots, and β-actin was used as a loading control. The increases in molecular weight of the RBPMSA and RBPMSC bands correspond to the additional 12 amino acids of the DDK-Tag sequence. **(F)** Colony formation assay. Percentages of clonogenicity were calculated relative to OVCAR3CIS-EV cells. **(G)** Colony Size. Percentages of size measures were calculated relative to OVCAR3CIS-EV cells. **(H)** Cell growth curves cells (2.0×10^4 cells/mL) were seeded in a 10 cm Petri, detached with Trypsin (0.25%) at 37 °C, stained with 0.5% trypan blue solution, and counted in triplicates every 24 h for 96 h after plating using a hemocytometer.

4.3 RBPMSA overexpression increased the sensitivity of ovarian cancer cells to cisplatin treatment

The next aim was to determine whether the overexpression of RBPMSA or RBPMSC splice variants increased the sensitivity of ovarian cancer cells to cisplatin treatment. A2780CP20-RBPMSA (clone 7 IC50: 29.77 µg/ml and clone 8 IC50: 30.03 µg/ml) showed an increase in cisplatin sensitivity compared with the control, A2780CP20-EV (IC50: 57.73 µg/ml) (Figure 9A).

However, A2780CP20-RBPMSC (clone 3.3 IC50: 53.42 µg/ml and clone 3.10 IC50: 56.69 µg/ml) did not show a significant increase in cisplatin sensitivity compared to A2780CP20-EV (IC50: 58.99 µg/ml). (Figure 9B). A similar tendency was observed in OVCAR3CIS cells, as the obtained overexpression of RBPMSA in these cells exhibited an increase in cisplatin sensitivity (IC50: 18.89 µg/ml), compared with OVCAR3CIS-EV (IC50: 33.01 µg/ml) cells. OVCAR3CIS cells with RBPMSC overexpression did not show increases in cisplatin sensitivity (IC50: 31.69 µg/ml) compared to OVCAR3CIS-EV cells (Figure 9C). Together, these results suggest that RBPMSA levels, but not RBPMSC levels, increase the sensitivity of ovarian cancer cells to cisplatin treatment.

9A

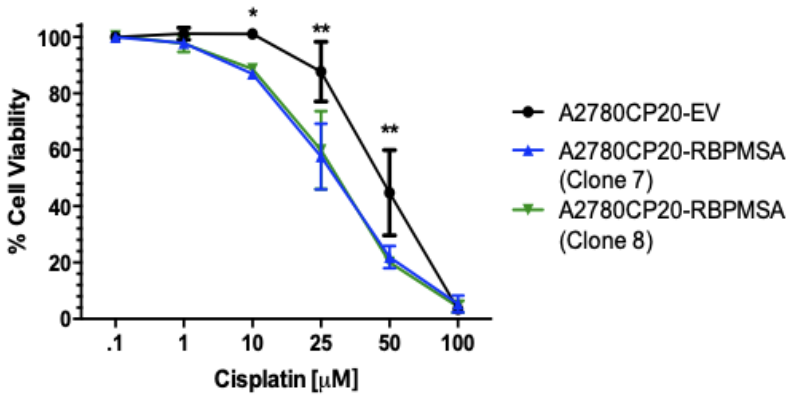

9B

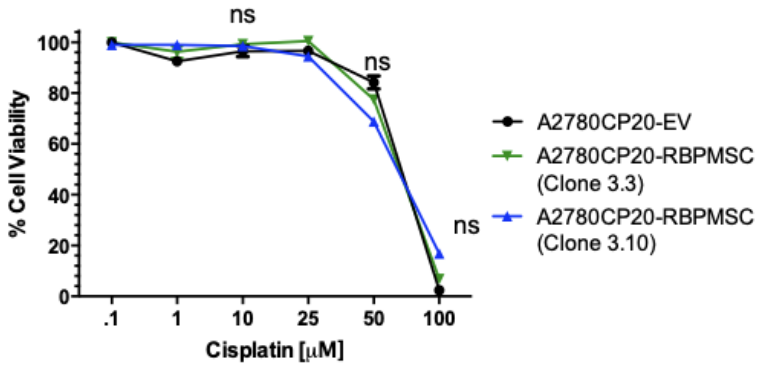

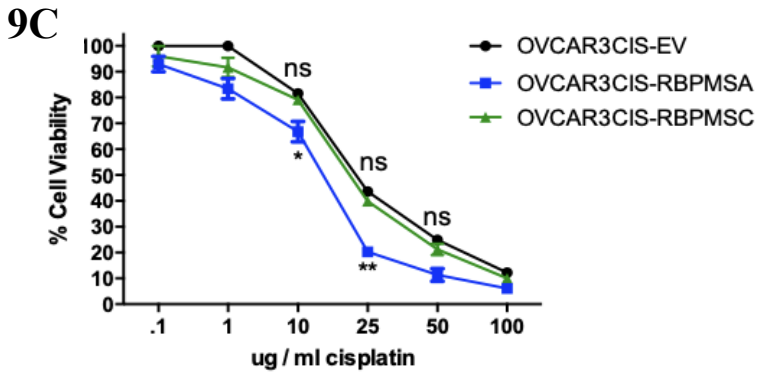

Figure 9. Viability Assays. (A and B) A2780CP20-EV, A2780CP20-RBPMSA (clones 7 and 8), and A2780CP20-RBPMSC (clones 3.10 and clones 3.3) and **(C)** OVCAR3CIS-EV, OVCAR3CIS-RBPMSA, and OVCAR3CIS-RBPMSC transiently transfected cells (all at 3 × 104 cell/mL) were exposed to different concentrations (0.1 µg/mL, 1.0 µg/mL, 10 µg/mL, 25 µg/mL, 50 µg/mL and 100 µg/mL) of cisplatin for 72 h. Percentages of cell viability were calculated relative to EV cells.

4.4 RBPMSA and RBPMSC overexpression decreased the migration and the invasion ability of ovarian cancer cells

RBPMS knockout has been associated with increased invasion ability in ovarian cancer [147]. The effect of RBPMSA and RBPMSC overexpression in the migration and invasiveness potential in ovarian cancer cells, was assessed. In transwell invasion assays, A2780CP20-RBPMSA decreased the invasion capacity of the cells in clones 7 (****$p<0.0001$) and 8 (****$p<0.0001$) when compared with the A2780CP20-EV clone. Similarly, results were observed in A2780CP20-RBPMSC clones 3.3 (****$p<0.0001$) and 3.10 (****$p<0.0001$). Remarkably, the number of invaded cells in A2780CP20-RBPMSA and A2780CP20-RBPMSC clones were 50% less than with the A2780CP20-EV clones (Figure 10A). In the wound healing assays, the A2780CP20-RBPMSA and A2780CP20-RBPMSC clones lost their ability to migrate, as shown in Figure 10B. Significant migration of cells was noted only with the A2780CP20-EV clones (Figure 10B). This data suggests that RBPMSA and RBPMSC significantly reduced the invasive and migration ability of cells when compared to A2780CP20-EV clones.

10A

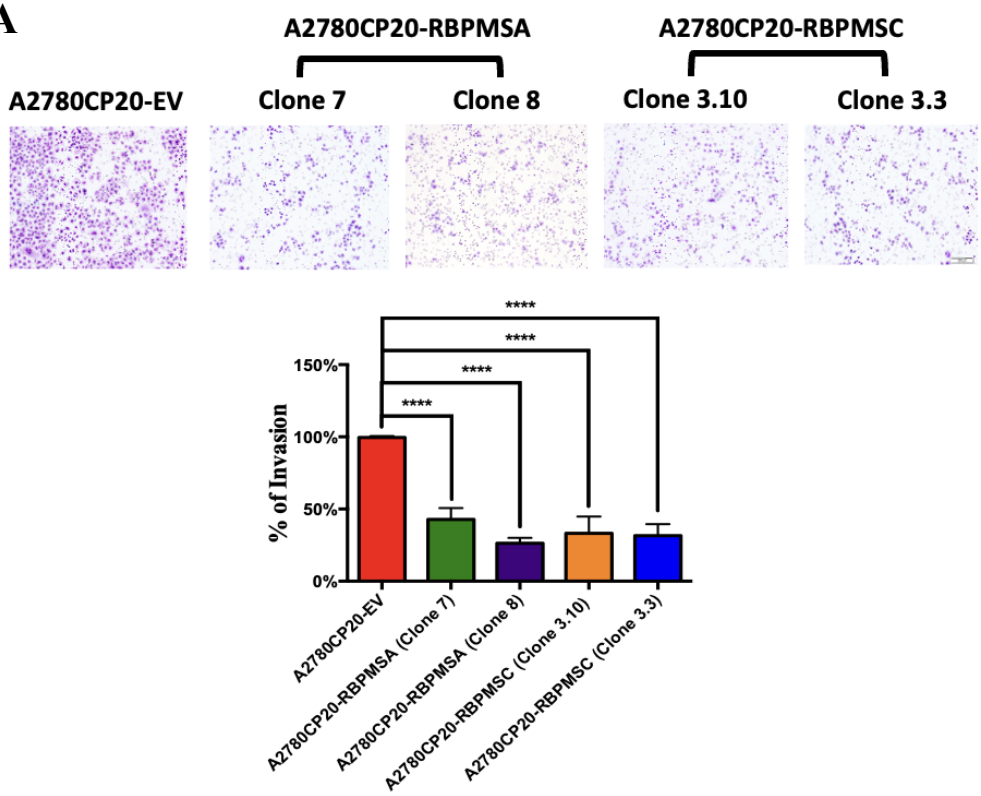
A2780CP20-RBPMSA
A2780CP20-RBPMSC
A2780CP20-EV
Clone 7
Clone 8
Clone 3.10
Clone 3.3
****
****
****
****
150%
100%
50%
0%
% of Invasion
A2780CP20-EV
A2780CP20-RBPMSA (Clone 7)
A2780CP20-RBPMSA (Clone 8)
A2780CP20-RBPMSC (Clone 3.10)
A2780CP20-RBPMSC (Clone 3.3)

10B

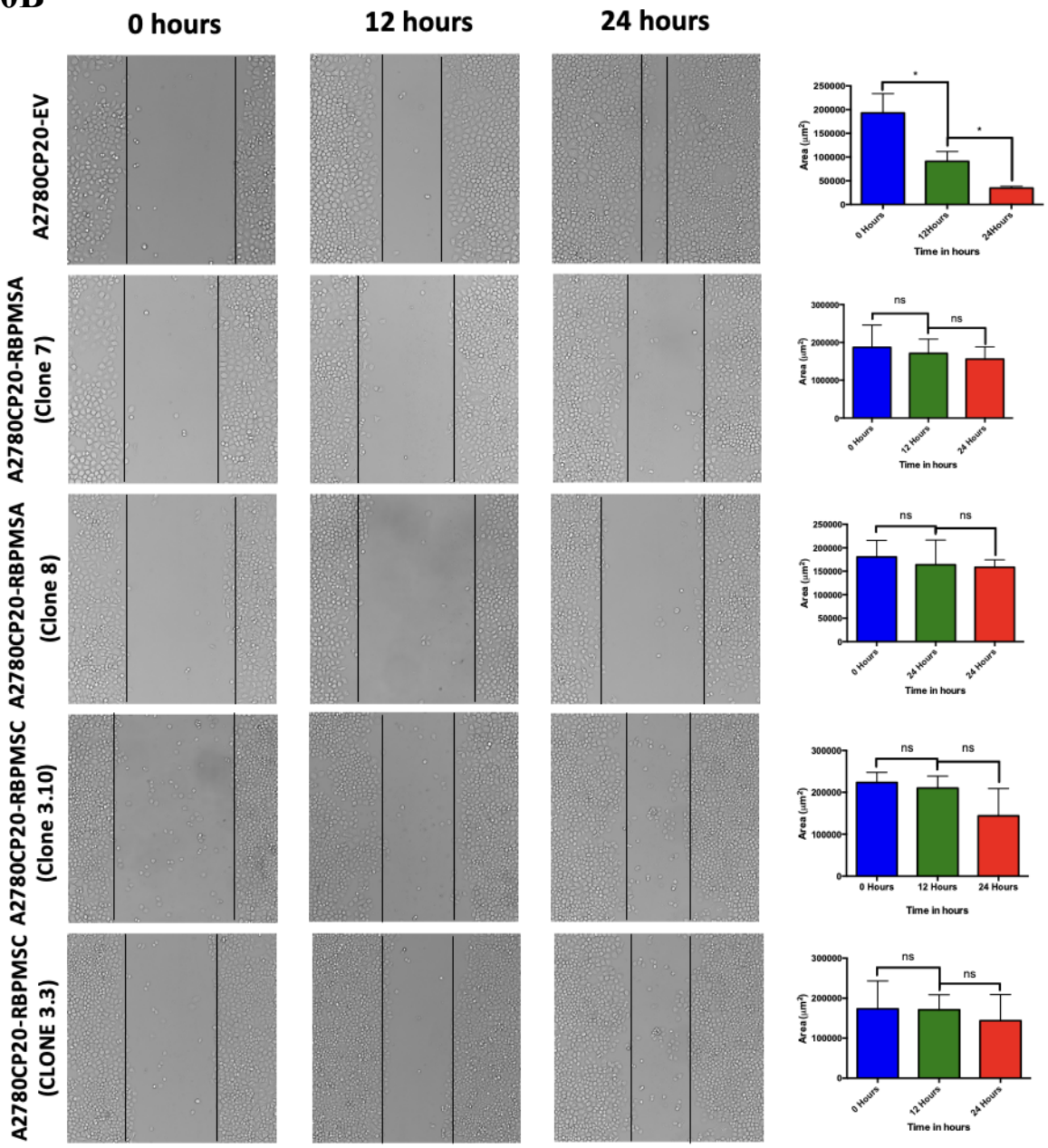

Figure: 10. Cell invasion and migration assays. (A) Percentages of invasion were calculated relative to A2780CP20-EV cells. Bars represent the means of triplicates ± S.E.M. (B) Representative images of scratch wound healing assays at 0, 12, and 24 h. Bars in the graph of (L) represent the area between the black lines in μm^2 in the cell migration images. Bars: mean of triplicates ± S.E.M. * $p < 0.05$, ** $p < 0.01$, *** $p < 0.001$, **** $p < 0.0001$ and ns = not significant.

4.5. RBPMSA and RBPMSC Overexpression Decreased the Senescence-Associated β-Galactosidase Levels

Evidence indicates that the acquisition of drug resistance by cancer cells is accompanied by senescence phenotypes [174]. Thus, further research was done to know if RBPMSA or RBPMSC overexpression promotes senescence phenotypes in ovarian cancer cells. Lower SA-β-Gal positive staining cells were observed in A2780CP20-RBPMSA or A2780CP20-RBPMSC clones, compared with A2780CP20-EV clones (Figure 11A). Figure 11B shows the number of SA-β-Gal-positive cells registered in Figure 3A, which confirmed our observations. The senescence-associated beta-galactosidase (β-Gal) levels were also quantified in A2780CP20-EV, A2780CP20-RBPMSA, and A2780CP20-RBPMSC clones. Smaller β-Gal levels were detected in A2780CP20-RBPMSA (* $p < 0.1$) or A2780CP20-RBPMSC (** $p < 0.01$) clones compared with A2780CP20-EV clones (Figure 11C). Increased levels of p21, p38, and p53 are associated with senescence phenotypes of cancer cells [174]. Figure 11D shows that the p53 and p38 protein levels were reduced in A2780CP20-RBPMSA and A2780CP20-RBPMSC clones, as compared with A2780CP20-EV clones or with A2780CP20 cells. Densitometry analysis of band intensities are shown in Figures 11E and 11F. P21 protein expression was not observed in A2780CP20 cells nor the clones.

11A

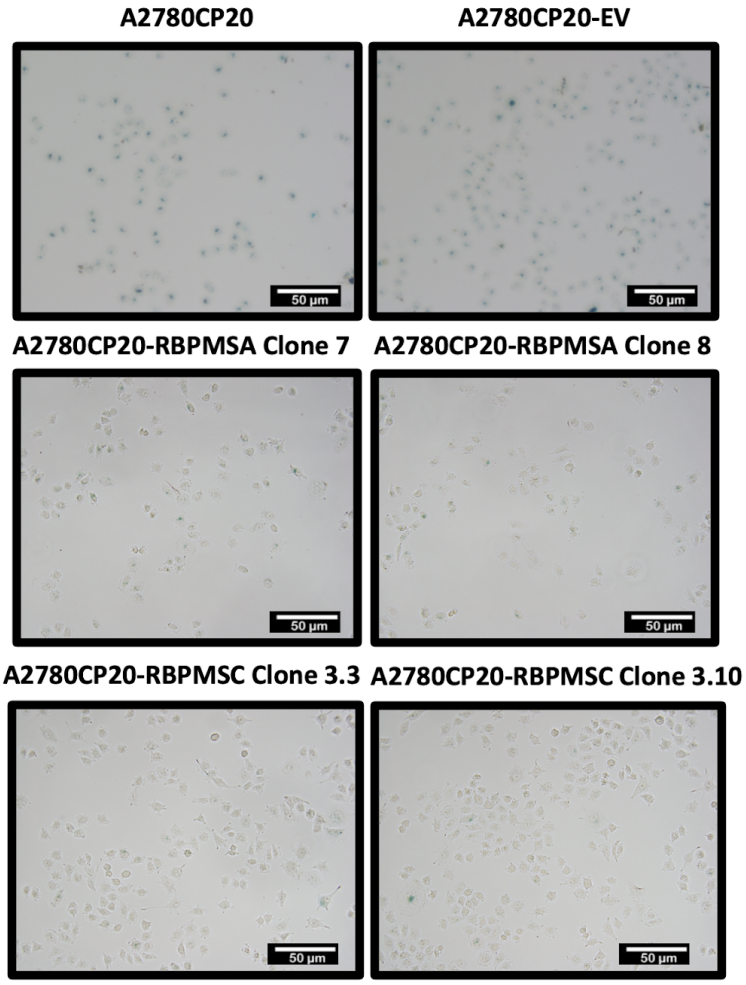
A2780CP20
A2780CP20-EV
A2780CP20-RBPMSA Clone 7
A2780CP20-RBPMSA Clone 8
A2780CP20-RBPMSC Clone 3.3
A2780CP20-RBPMSC Clone 3.10
50 µm

11B

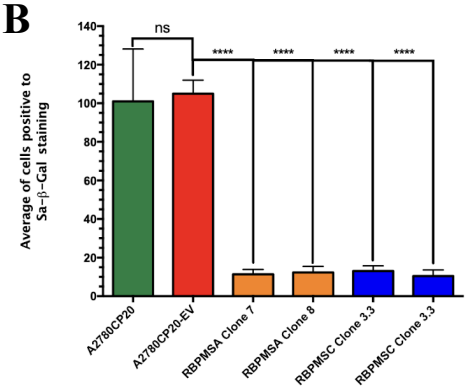
Average of cells positive to Sa-β-Gal staining
ns
****
A2780CP20
A2780CP20-EV
RBPMSA Clone 7
RBPMSA Clone 8
RBPMSC Clone 3.3
RBPMSC Clone 3.3

11C

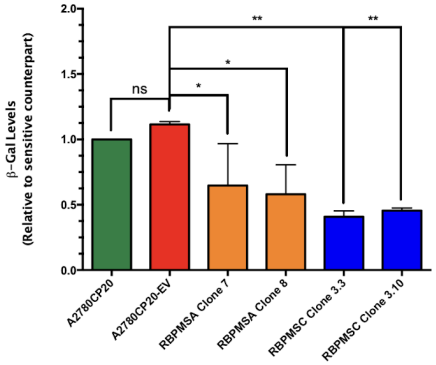
β-Gal Levels (Relative to sensitive counterpart)
ns
*
**
A2780CP20
A2780CP20-EV
RBPMSA Clone 7
RBPMSA Clone 8
RBPMSC Clone 3.3
RBPMSC Clone 3.10

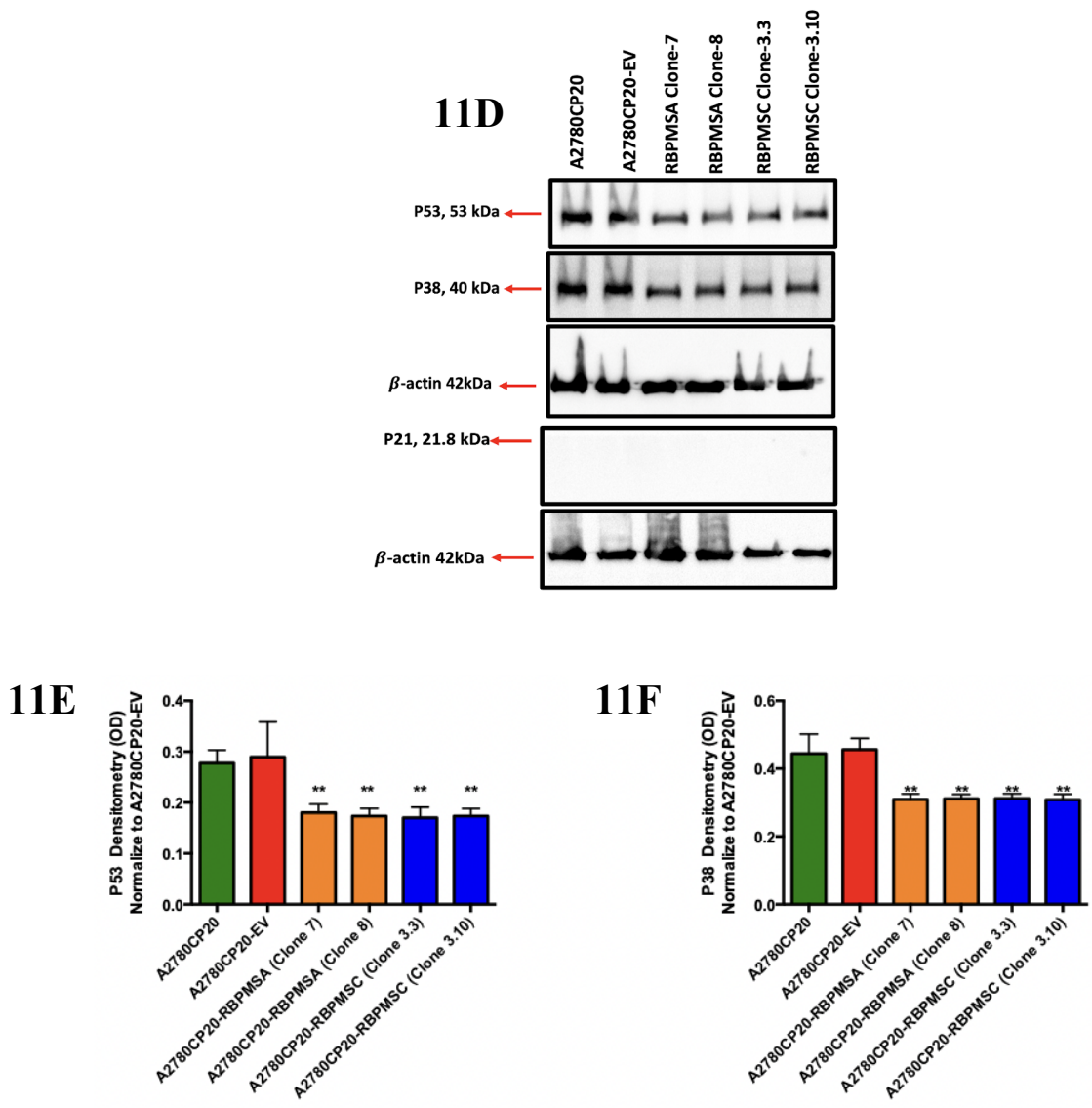

Figure 11. Effect of RBPMSA and RBPMSC overexpression on senescence. (**A**) Representative images of SA-β-Gal-stained cells. (**B**) Quantification of the positive SA-β-Gal-stained cells. Images scale bar: 50 µm (bars: five microscopic fields per condition). Staining was done according to manufacturer's specifications. * $p < 0.05$, ** $p < 0.01$, **** $p < 0.0001$ and ns = no significant. (**C**) Cells (1×10^4 cells/mL) were plated in Petri dishes. Next day, cells were rinsed with PBS, and protein extracts were prepared at 1 µg/mL protein concentration. Senescence-associated β-galactosidase activity (SA-β-gal) was assessed via fluorescence. β-galactosidase levels were calculated relative to A2780CP20-EV cells. Averages ± SEM are shown for three independent experiments. (**D**) Western blots were performed with 50 µg of protein extracts, and β-actin was used as a loading control. (**E and F**) Densitometry analysis of band intensities shown in (**D**). Fold changes in protein levels were calculated relative to the A2780CP20-EV clones (** $p < 0.01$).

4.6 Effects of Subcutaneous Implantation of RBPMSA and RBPMSC Overexpressing Cells in tumor growth in an Ovarian Cancer Mouse Model

The effect of RBPMSA or RBPMSC on tumor progression in a subcutaneous ovarian cancer mouse model, was assessed. A2780CP20-RBPMSA (clone 8), A2780CP20-RBPMSC (clone 3.10), and A2780CP20-EV cells (see Figure 7H and 7I) were subcutaneously injected into the right dorsal flank of female athymic mice (Figure 12A). Seven days after cell implantation, tumor size was measured with a Vernier caliper, three times per week for three weeks. Figure 12B shows that the tumors of A2780CP20-RBPMSA and A2780CP20-RBPMSC clones grew slower compared with tumors of A2780CP20-EV clones. At the end of the experiment, the difference in the tumor sizes between A2780CP20-RBPMSA or A2780CP20-RBPMSC and the control group (A2780CP20-EV) was statistically significant (** $p < 0.01$, and * $p < 0.05$, respectively). Figure 12C shows the appearance of the tumors at the end of the experiment. Additionally, tumor weight and the number of nodules showed a statistically significant difference between the A2780CP20-RBPMSA or A2780CP20-RBPMSC groups, and the A2780CP20-EV group (Figure 12D and 12E).

12A

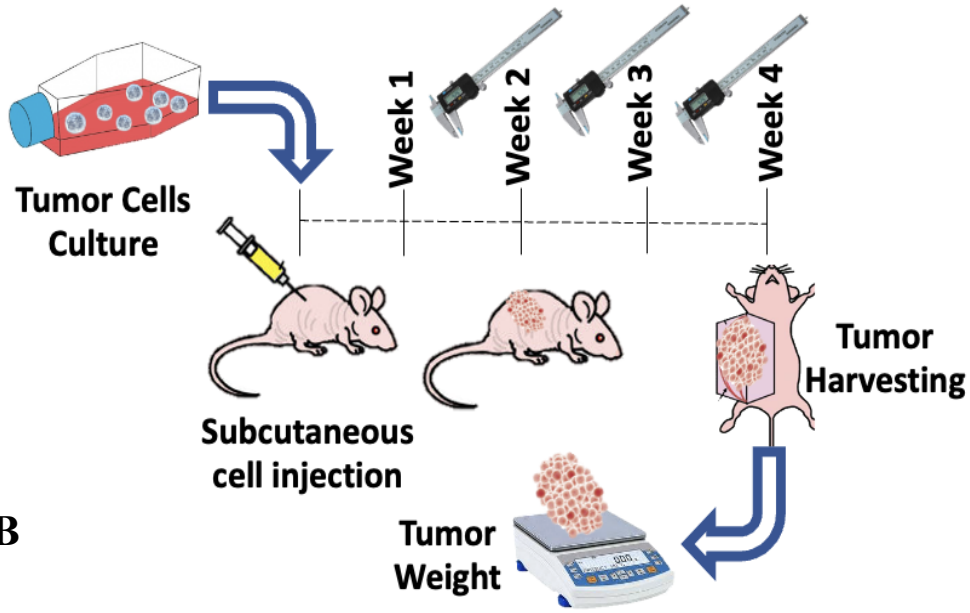
Tumor Cells Culture
Week 1
Week 2
Week 3
Week 4
Subcutaneous cell injection
Tumor Harvesting
Tumor Weight

12B

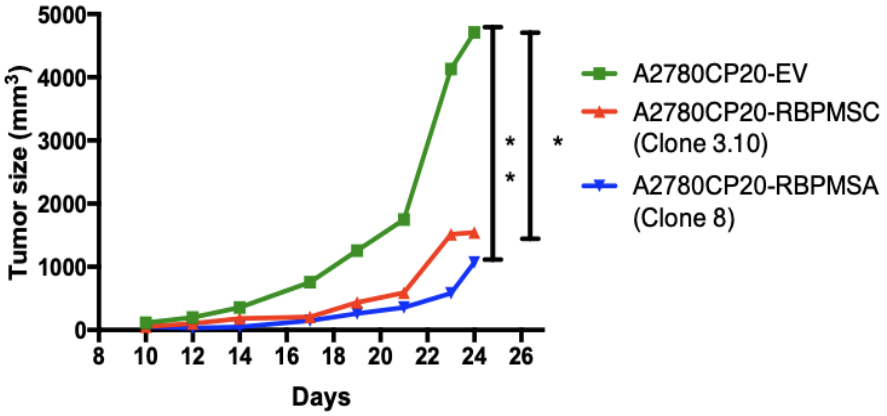
Tumor size (mm3)
5000
4000
3000
2000
1000
0
8
10
12
14
16
18
20
22
24
26
Days
A2780CP20-EV
A2780CP20-RBPMSC (Clone 3.10)
A2780CP20-RBPMSA (Clone 8)
*
*
*

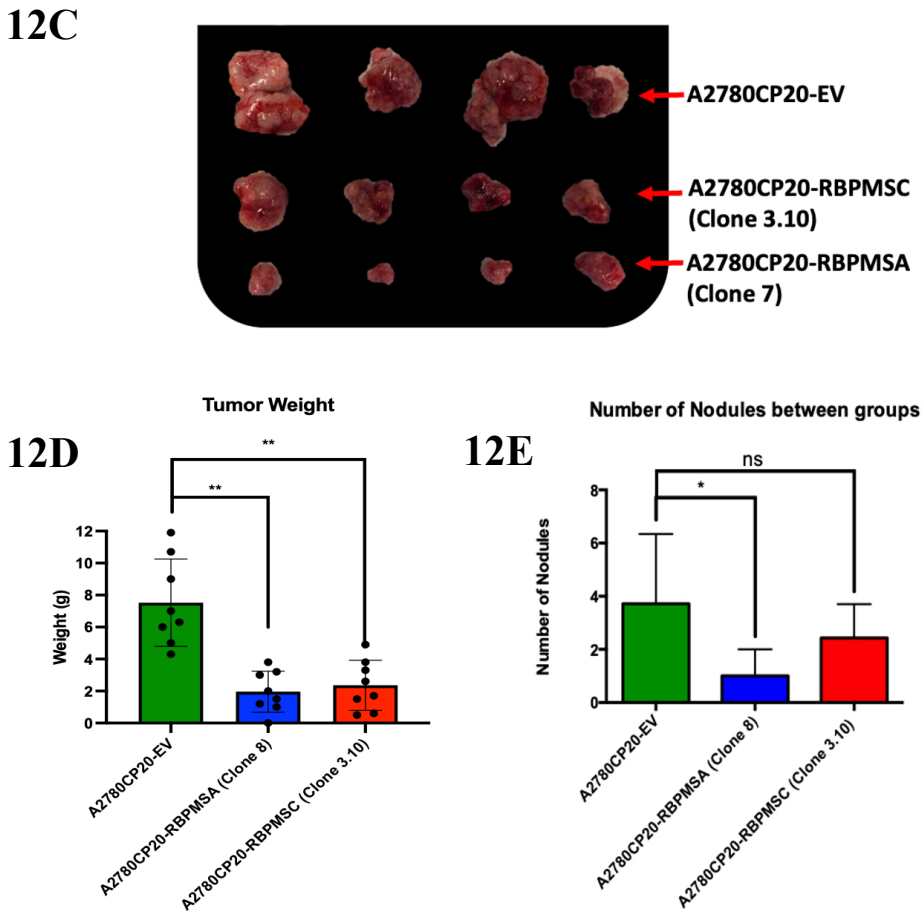

Figure 12. Effect of RBPMSA and RBPMSC overexpression on in vivo tumor growth. (A) Graphical image of the in vivo experiment. Mice were subcutaneously injected with A2780CP20-RBPMSA, A2780CP20-RBPMSC, and A2780CP20-EV (Number of mice, N = 7 per group). The tumor growth was monitored with a Vernier caliper, three times per week. **(B)** Tumor size measurements. **(C)** A visual image of tumor size at the end of the experiment. **(D)** Tumor weight **(E)** Number of nudes.

Then, IHC studies were performed to measure the RBPMS protein levels, tumor cell proliferation rates (Ki67), and blood vessel formation (CD31) in tissue sections of the mice tumors (Figure 13A-C). As expected, the RBPMS immunoreactivity was significantly higher for A2780CP20-RBPMSA (*** $p < 0.0001$) or A2780CP20-RBPMSC (** $p < 0.01$) tumor tissues compared with A2780CP20-EV tumor tissues (Figure 13A). The tumor tissues of A2780CP20-RBPMSA or A2780CP20-RBPMSC overexpressing cells had a significantly lower percentage of Ki67 positive stained cells (proliferative index), compared with tumor tissues of A2780CP20-EV cells (Figure 13B). Tumor tissue sections were also stained with the endothelial CD31 marker to

assess angiogenesis. As shown in Figure 13C, tissues of A2780CP20-RBPMSA (**** $p < 0.0001$) or A2780CP20-RBPMSC (**** $p < 0.0001$) had a significantly lower percentage of positive blood vessels, as compared with A2780CP20-EV tumor tissues.

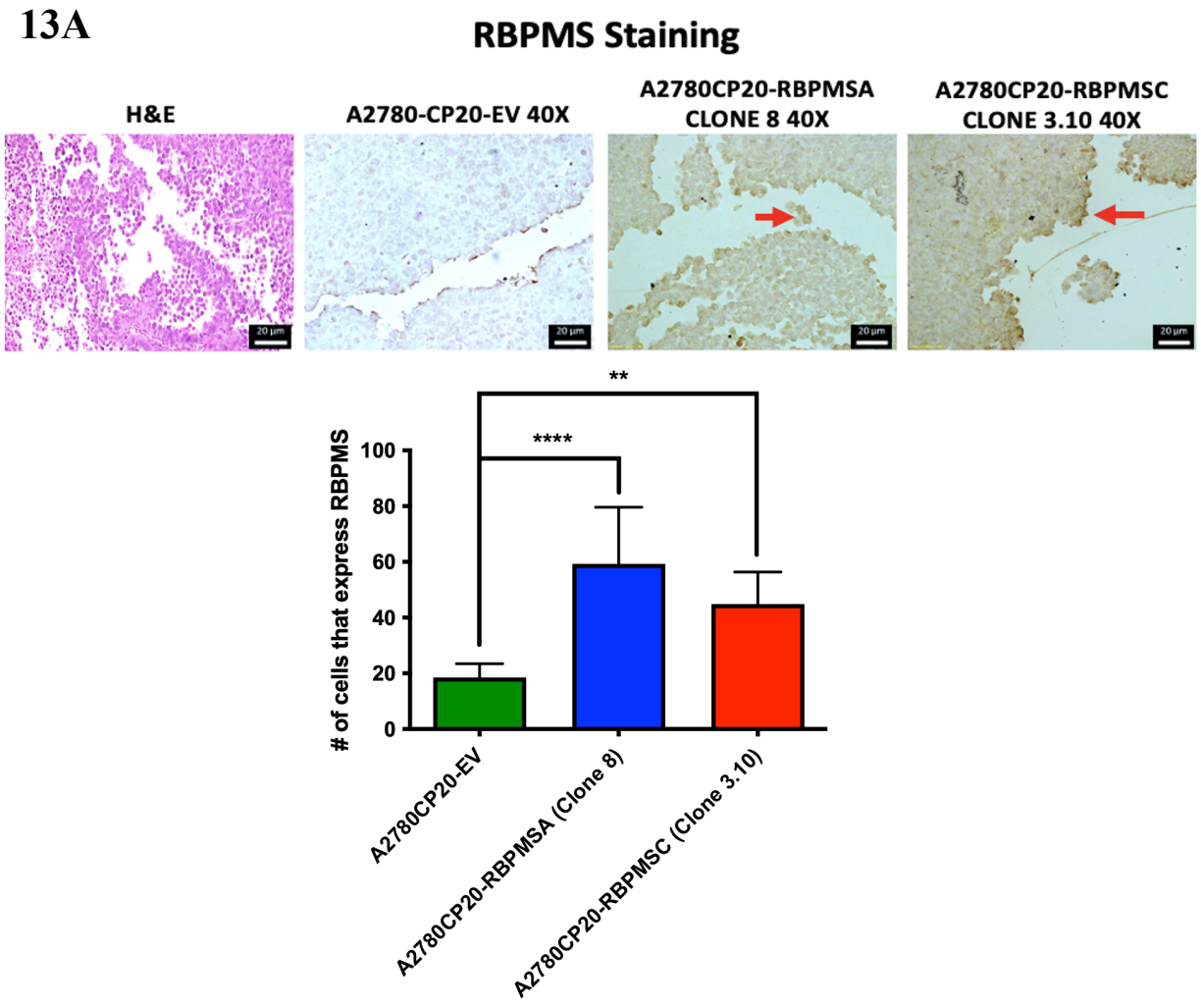

13B

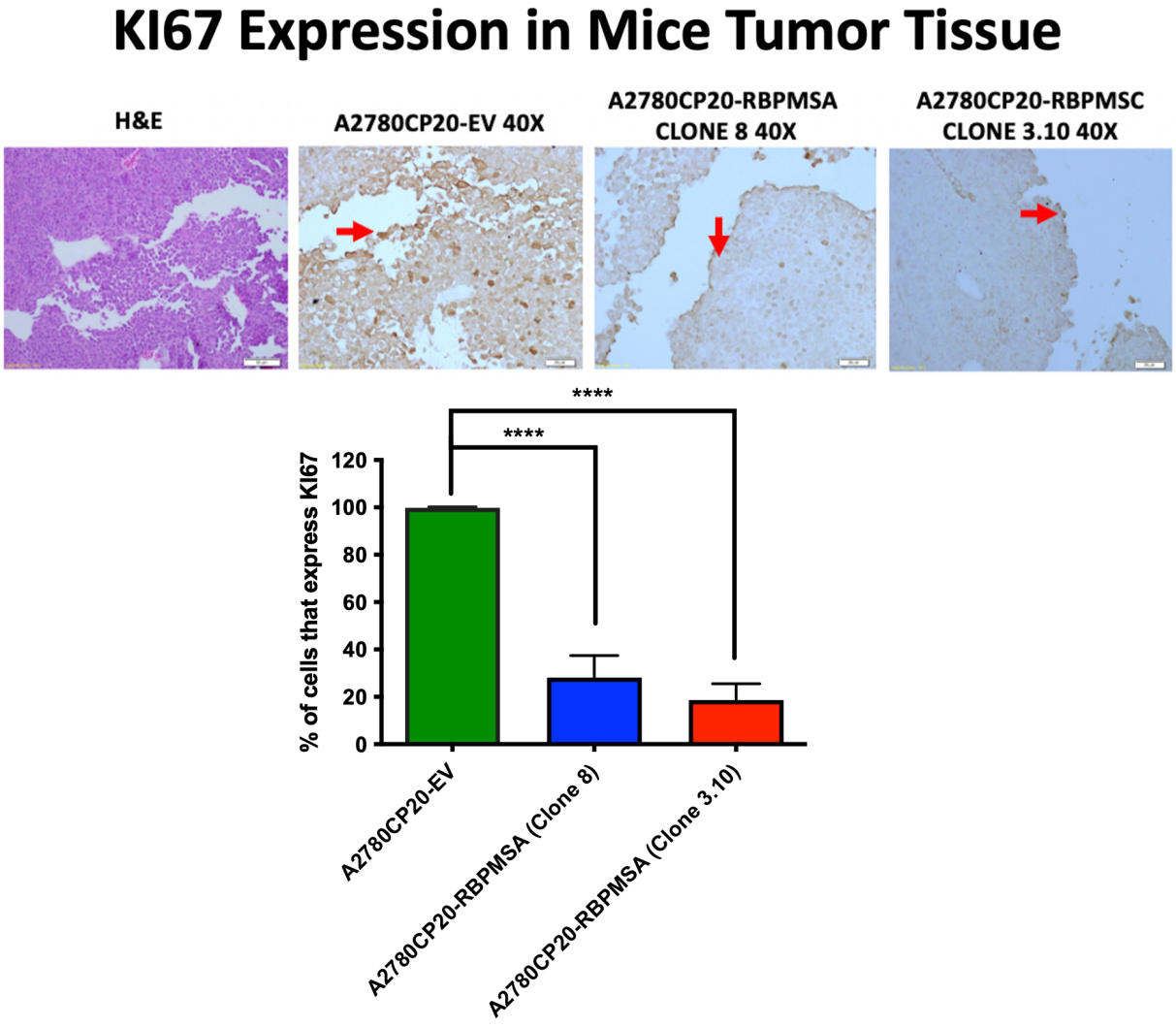
KI67 Expression in Mice Tumor Tissue
H&E
A2780CP20-EV 40X
A2780CP20-RBPMSA CLONE 8 40X
A2780CP20-RBPMSC CLONE 3.10 40X
****
****
% of cells that express KI67
120
100
80
60
40
20
0
A2780CP20-EV
A2780CP20-RBPMSA (Clone 8)
A2780CP20-RBPMSA (Clone 3.10)

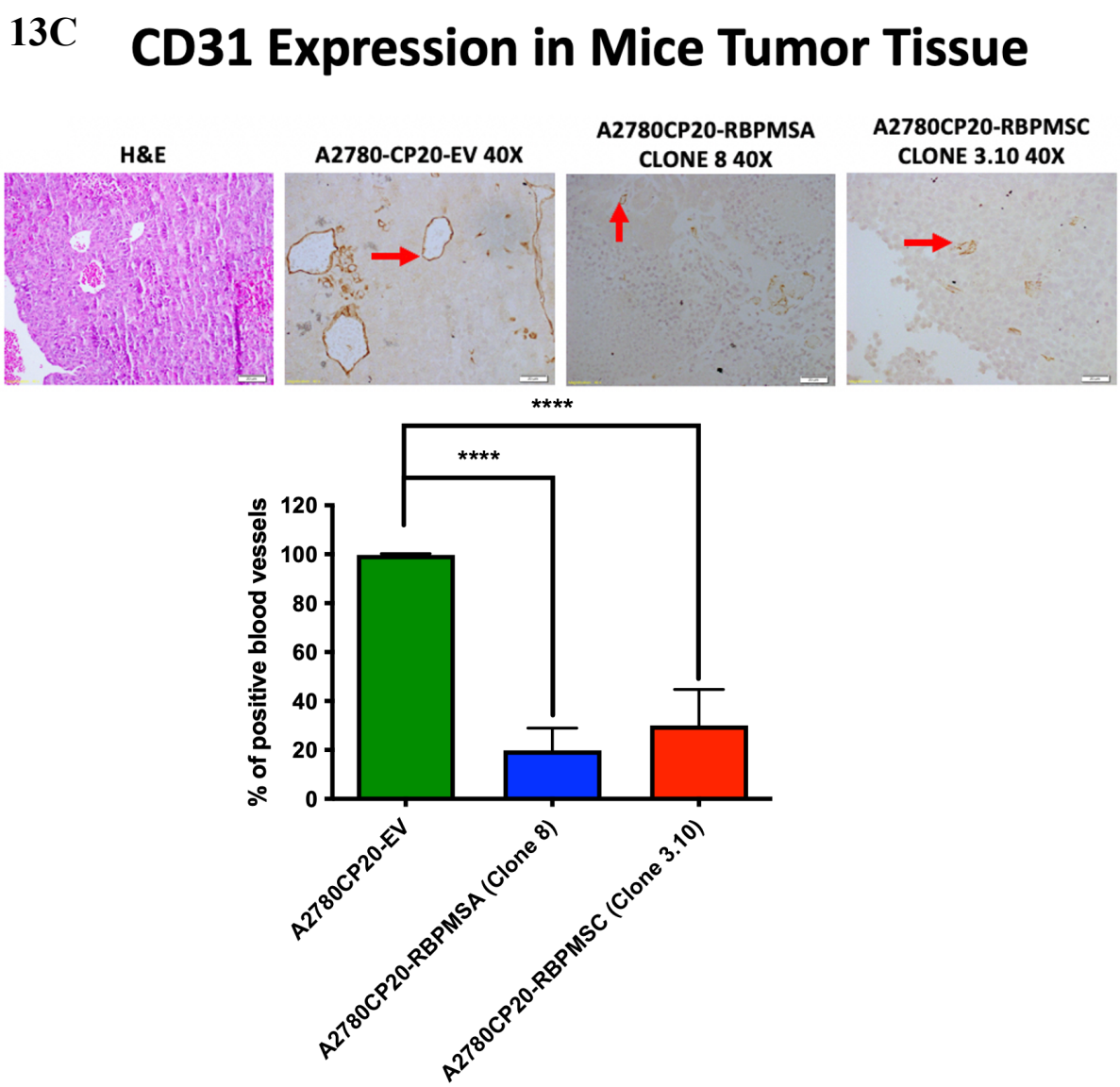

Figure 13. Representative images of IHC experiments for RBPMS protein levels, proliferation (KI-67), and blood vessel formation (CD31). Microscopy images were taken at 40× magnification. Red arrow shows a positive cell staining signal with respective antibody. Quantification of RBPMS **(13A)**, CD31 **(13B)**, and KI67 **(13C)** staining was determined by Image J software. Data is presented as the mean ± SEM of staining relative to A2780CP20-EV. Significant variations between groups and A2780CP20-EV control were determined by Student's t-test. * $p < 0.05$, ** $p < 0.01$, **** $p < 0.0001$ and ns = no significant.

4.7 Effects of cisplatin in RBPMS overexpressing in cell proliferation

Seeing that the RBPMSA and RBPMSC overexpressing clones dramatically reduced the number of colonies formed by cells, the cells were treated with cisplatin (2μM) to determine whether RBPMS splice variants A and C potentiated cell growth inhibition. In clonogenic assays

presented in Figures 14A and 14B, a significant increase was observed in the number of colonies in cisplatin-untreated than in cisplatin-treated RBPMS splice variants A and C overexpressing clones (****p<0.0001 and *p <0.1, respectively). In addition, the colony area did not show any statistical significance between A2780CP20-EV treated and untreated with cisplatin. The data suggests that RBPMS A and C overexpressing clones enhance the reduction of colony formation when cells are treated with cisplatin, in comparison with the untreated counterparts, making RBPMS A and C viable options as adjunct treatment for ovarian cancer.

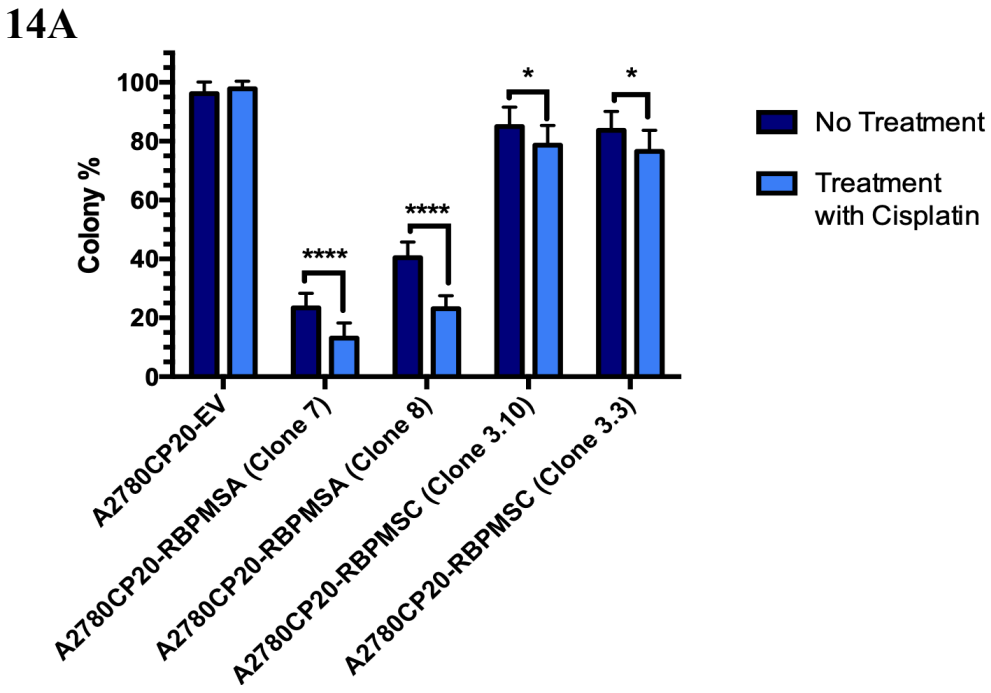

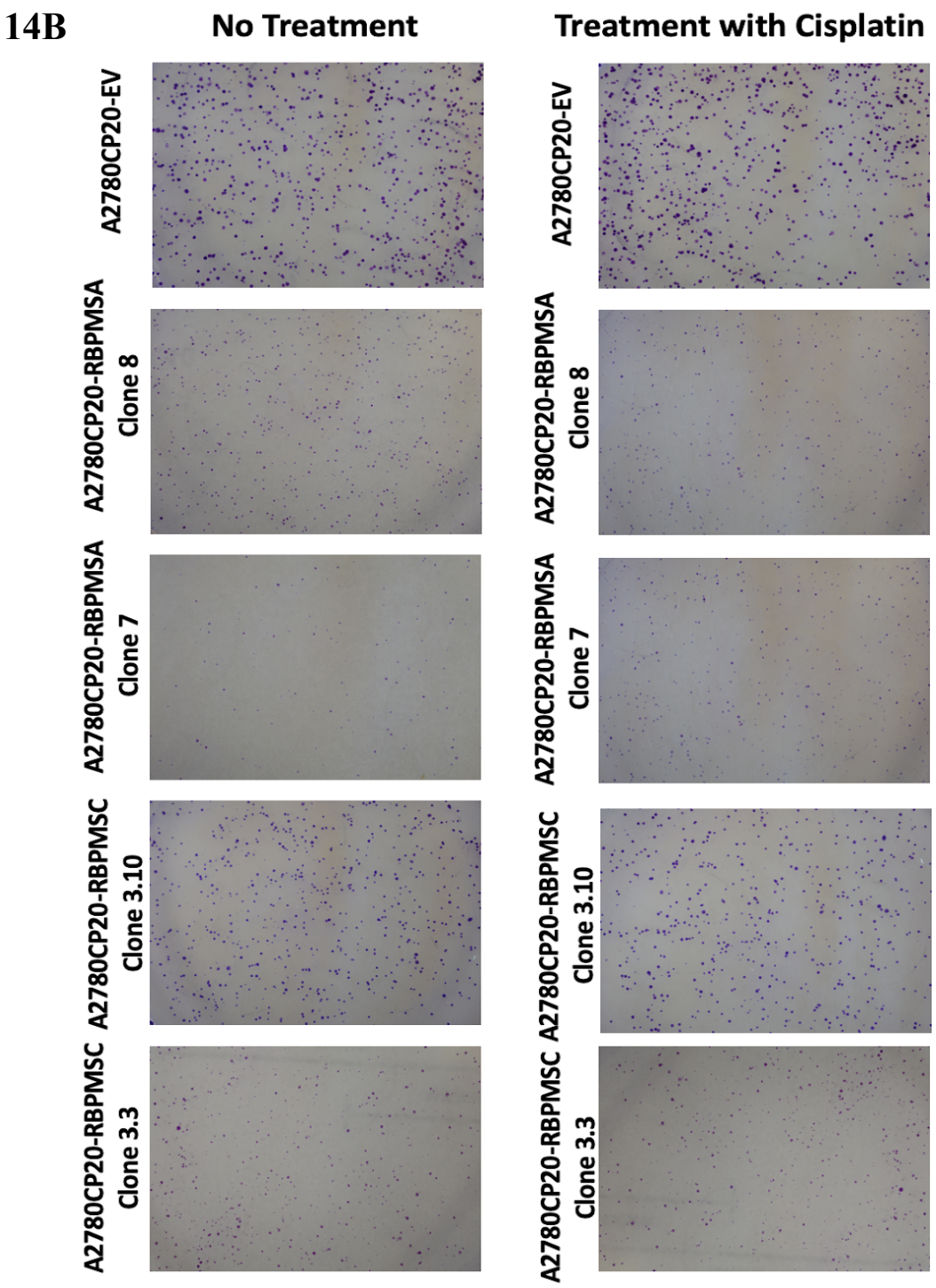

Figure 14: Effect on proliferation of RBPMS splice variants A and C overexpressing clones treated with or without cisplatin. Number of colonies was counted on RBPMSA (clones 7 and 8) and RBPMSC (clones 3.10 and 3.3) treated and not treated with cisplatin. RBPMS spice variant A and C showed significant reduction tendencies (****P<0.0001 and *P<0.1, respectively) when exposed to cisplatin compared with the untreated condition (Figures 14A and 14B).

Aim 2: Results

4.8 Ectopic expression of RBPMSA+Tag and RBPMSC+Tag in cisplatin resistant ovarian cancer cells

A2780CP20 cells were stable transfected with pCMV6-RBPMSA or pCMV6-RBPMSC plasmids. Figure 15A and 15C show a western blot of the protein levels of A2780CP20-RBPMSA (31.8 kDa) and A2780CP20-RBPMSC (34.2 kDa) clones. Figure 15B and 15D are densitometric analyses of the Western blot images' band intensities. The increase in molecular weight of the RBPMSA and RBPMSC bands correspond to the additional 12 mino acids of the DDK-Flag-Tag sequence, included in the pCMV6 vector. Moreover, DDK-Flag-Tag sequence was detected in the western blot to corroborate the successful transfection, as seen below in Figures 15A and 15C.

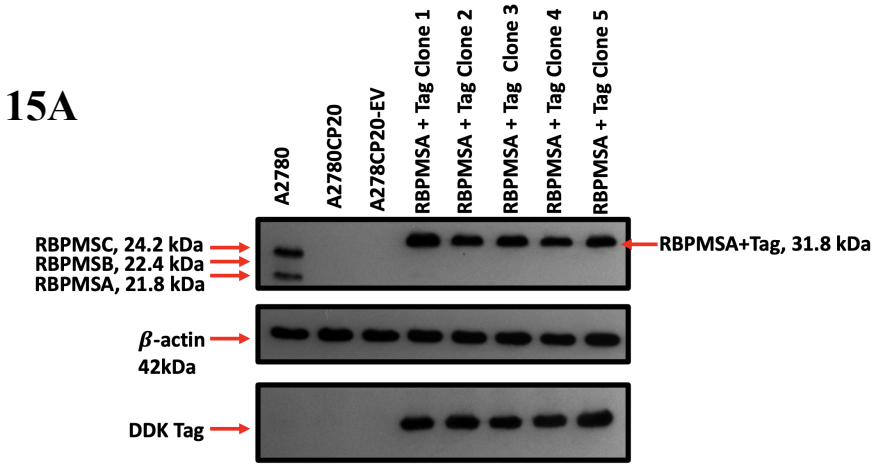

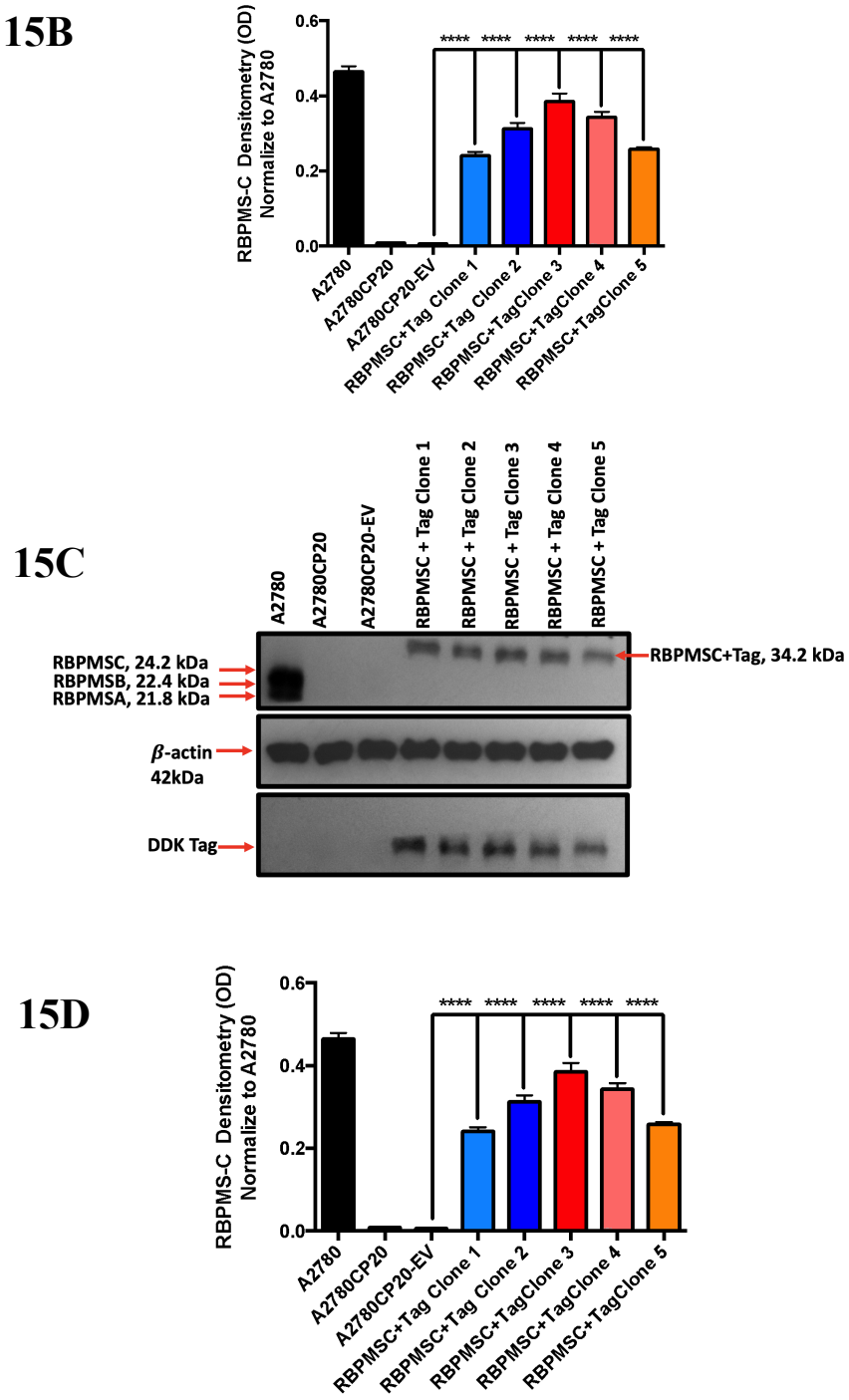

Figure 15: Overexpression of RBPMS+Flag-Tag (DDK) isoform A and C in ovarian cancer A2780CP20 cell line. (A) Western Blot showed overexpression of RBPMSA in A2780-CP20 cells using stable transfection. High density band of 31.8kDa is visible on clones 1 to 5 in RBPMS A stable transfected clones. **(B)** Densitometry analysis showed overexpression of RBPMSA band (31.4 kDa) when compared with A2780CP20-EV. **(C)** Western Blot showed overexpression of RBPMSC in A2780CP20 cells using stable transfection. High density band of 34.8kDa is visible on clones 1 to 5 in RBPMSC stable transfected clones. **(D)** Densitometry analysis showed overexpression of

RBPMSC band (34.8 kDa) when compared with A2780CP20-EV. Flag-Tag (DDK) Sequence has been detected to confirm the successful transfection of RBPMSA and RBPMSC clones, figure 15A and 15C lower image.

4.9 RBPMSA and RBPMSC interacts with AP-1 members (c-Fos and c-Jun) and Smad's proteins

Evidence indicates that RBPMS binds to AP-1 members [130]. Thus, to assess if this interaction occurs also in ovarian cancer cells, the interaction between RBPMSA and RBPMSC with AP-1 protein members (c-Jun and c-Fos), was investigated. Fu et al. (2015) showed that in breast cancer, each RBPMS isoform interacts differentially with AP-1 members (c-Fos and c-Jun). Particularly, the RNA-recognition motif (RRM) and C-terminus of the RBPMS isoforms (RBPMSA and RBPMSC, but not RBPMSB,) interacted with c-Fos. To elucidate if RBPMSA and RBPMSC interacts with AP-1 protein members in ovarian cancer, an immunoprecipitation (IP) with anti-DDK-antibody was performed, followed by blotting with RBPMS, c-Fos, c-Jun, Smad 2/3, and Smad4 antibodies. RBPMSA and RBPMSC were detected on the immunoprecipitated samples from RBPMSA+Tag clones and RBPMSC+Tag clones (Figure 16A), which indicate successful IP. The DDK Tag signal was also detected which confirmed the positive IP (Figure 16A, lower image). RBPMS or DDK-protein bands in the IP sample from A2780CP20-EV, used as control, was unable to be detected. Similar results were observed in the western blot image from the RBPMSA+Tag clones, RBPMSC+Tag clones, and A2780CP20-EV input samples (Figure 16A, upper image). Moreover, IP assays followed by western blot showed that RBPMSA+Tag and RBPMSC+Tag interacted with c-Fos, c-Jun, Smad 2/3, and Smad 4 (Figures 16B, 16C, 16D and 16E, lower image). As expected, A2780CP20-EV failed to coimmunoprecipitate to members of the AP-1 protein members (c-Fos and c-Jun) or Smad's proteins. c-Fos, c-Jun, Smad 2/3, and Smad 4 antibody signal were detected in the western blots input sample fraction from RBPMSA+Tag clones, RBPMSC+Tag clones and A2780CP20-EV.

16A

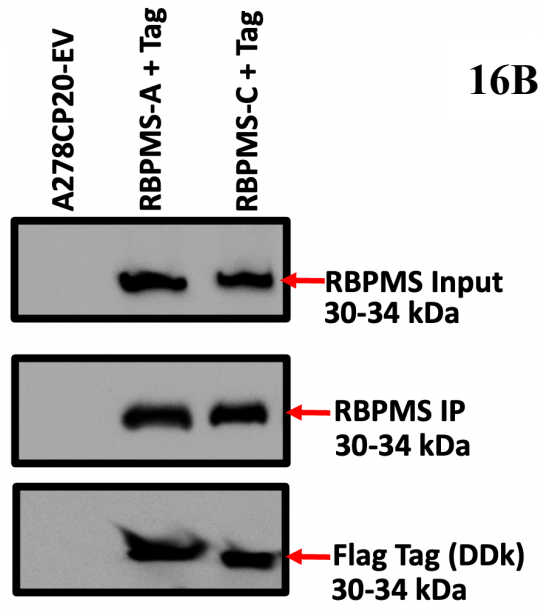

16B

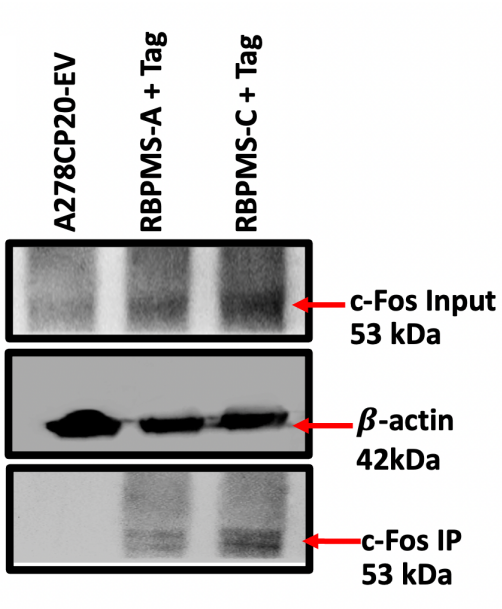

16C

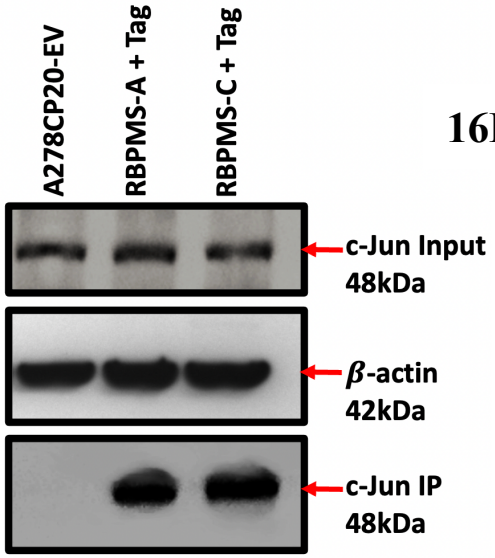

16D

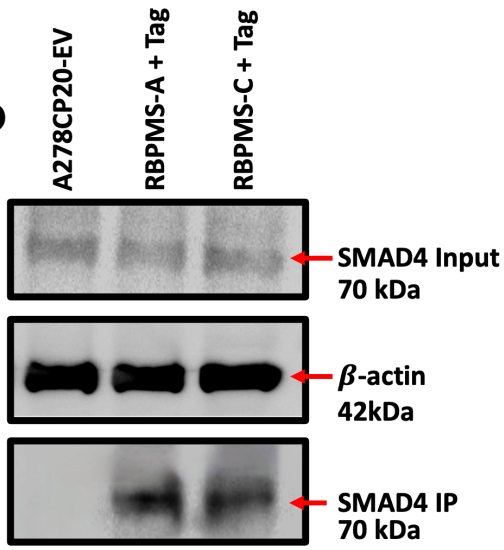

16E

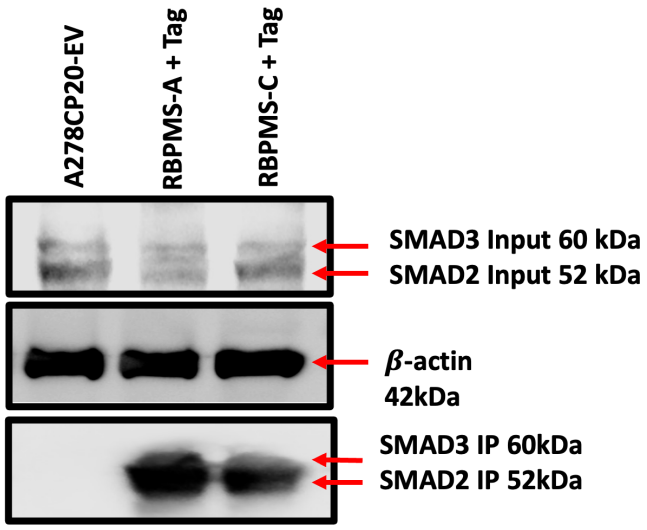

Figure 16: Interaction of RBPMSA and RBPMSC with c-Fos, c- Jun, Smad 2/3 and Smad 4. (A) A2780CP20 cells were stable transfected with RBPMSA+Tag and RBPMSC+Tag vector, IP immunoblotting with RBPMS antibody confirmed the successful transfection. **(B)** RBPMSA+Tag and RBPMSC+Tag cell lysates were immunoprecipitated (IP) with anti-FLAG beads, followed by western blot with the c-Fos antibody. **(C)** RBPMSA+Tag and RBPMSC+Tag cell lysates were immunoprecipitated (IP) with anti-DDK FLAG beads, followed by western blot with the c-Jun antibody. **(D)** RBPMSA+Tag and RBPMSC+Tag cell lysates were immunoprecipitated (IP) with anti-DDK FLAG beads, followed by western blot with the Smad4 antibody. **(E)** RBPMSA+Tag and RBPMSC+Tag cell lysates were immunoprecipitated (IP) with anti-DDK FLAG beads, followed by western blot with the Smad2/3 antibody.

4.10 Effect of overexpression of RBPMSA and RBPMS C in pre-mir-21 transcription

MicroRNA-21 (miR-21) is overexpressed in most cancers and has been implicated in tumor initiation, progression, and chemoresistance [162]. Evidence indicates that AP-1 members regulate the expression of miR-21 in ovarian cancer cells [168]. Since RBPMS isoforms binds to AP-1 members, the study sought to determine if RBPMS splice variants regulate this molecular pathway. Thus, the effect of RBPMSA or RBPMSC ectopic expression in pre-mir-21 transcription, was explored. As showed in the agarose gel (Figure 17A), expression of RBPMSA or RBPMSC decreased pre-mir-21 expresion when compared to A2780CP20-EV, which was used as the control. Densitometric analysis of the bands in agarose gel confirmed these observations (Figure 17B). To validate these results, RBPMS was knocked down with small-interference RNAs

(siRNAs). In Figures 17B and 17C, RBPMS-targeted siRNA-1 and siRNA-2 (see sequences in the “Material and Methods" section) was successfully reduced more than 50% of the RBPMS expression in the RBPMS overexpressed clones, compared with the untreated sample and the samples treated with a negative control siRNA. After the transfection with the siRNAs, cells and isolated the total RNA were collected from each experimental condition. RT-PCR was performed to detect changes in the pre-mir-21 levels after RBPMS siRNA transfection. As shown in Figure 17E and their corresponding densitometric analysis (Figure 17F), increased levels of pre-mir-21 were obtained in RBPMSA clones, after siRNA treatment when compared with RBPMSA-NC samples. Moreover, band intensity appears to be similar for A2780CP20-NC, A2780CP20-siRNA, and A2780CP20-EV. The NC-siRNA did not increase pre-mir-21 expression levels in RBPMSA overexpressing clones. The same experiments were performed with RBPMSC clones. As shown in Figure 17G and its corresponding densitometric analysis, Figure 17H, increased levels of pre-mir-21 were obtained in RBPMSC clones after siRNA treatment, when compared with RBPMSC-NC and A2780CP20-EV siRNA. Also, band intensity looks similar for A2780CP20-NC, A2780CP20-siRNA, and A2780CP20-EV. The NC-siRNA did not increase pre-mir-21 expression levels in RBPMSC overexpressing clones. The attained data suggests that RBPMSA and RBPMSC control the AP-1-mediated pre-mir-21 expression in ovarian cancer cells.

17A

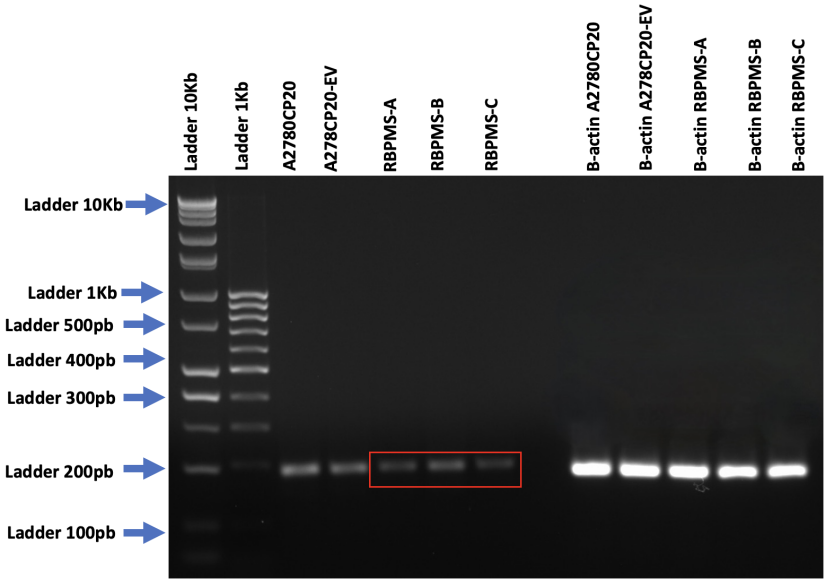
Ladder 10Kb
Ladder 1Kb
A2780CP20
A278CP20-EV
RBPMS-A
RBPMS-B
RBPMS-C
B-actin A2780CP20
B-actin A278CP20-EV
B-actin RBPMS-A
B-actin RBPMS-B
B-actin RBPMS-C
Ladder 10Kb
Ladder 1Kb
Ladder 500pb
Ladder 400pb
Ladder 300pb
Ladder 200pb
Ladder 100pb

17B

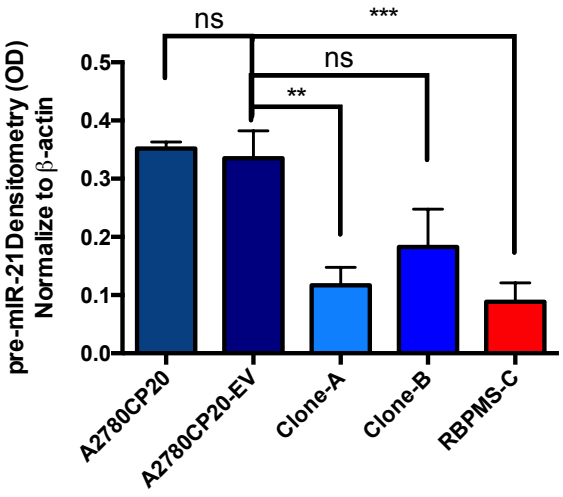
ns
***
ns
**
pre-mIR-21Densitometry (OD)
Normalize to β-actin
0.5
0.4
0.3
0.2
0.1
0.0
A2780CP20
A2780CP20-EV
Clone-A
Clone-B
RBPMS-C

17C

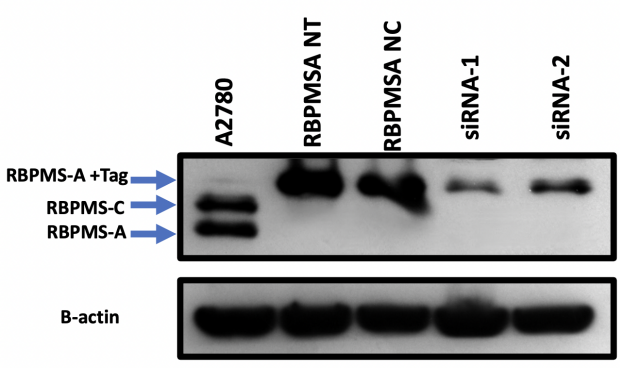
A2780
RBPMSA NT
RBPMSA NC
siRNA-1
siRNA-2
RBPMS-A +Tag
RBPMS-C
RBPMS-A
B-actin

17D

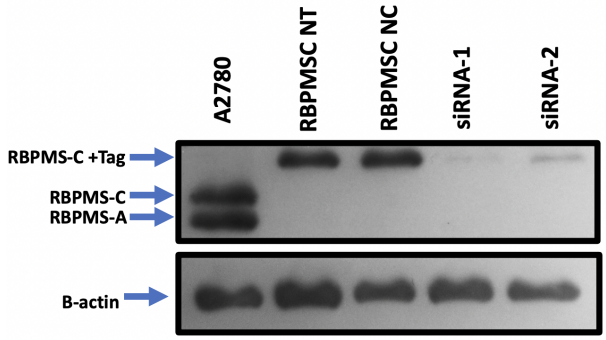
A2780
RBPMSC NT
RBPMSC NC
siRNA-1
siRNA-2
RBPMS-C +Tag
RBPMS-C
RBPMS-A
B-actin

17E

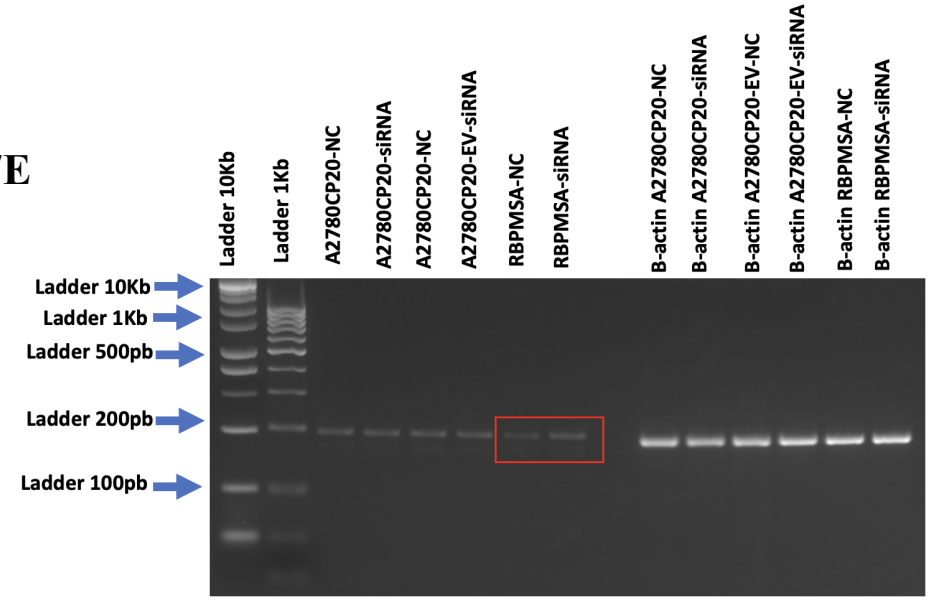
Ladder 10Kb
Ladder 1Kb
A2780CP20-NC
A2780CP20-siRNA
A2780CP20-NC
A2780CP20-EV-siRNA
RBPMSA-NC
RBPMSA-siRNA
B-actin A2780CP20-NC
B-actin A2780CP20-siRNA
B-actin A2780CP20-EV-NC
B-actin A2780CP20-EV-siRNA
B-actin RBPMSA-NC
B-actin RBPMSA-siRNA
Ladder 10Kb
Ladder 1Kb
Ladder 500pb
Ladder 200pb
Ladder 100pb

17F

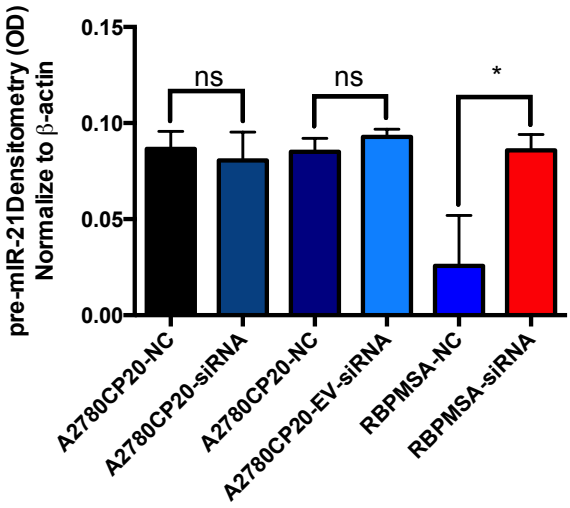
pre-miR-21Densitometry (OD)
Normalize to β-actin
0.15
0.10
0.05
0.00
ns
ns
*
A2780CP20-NC
A2780CP20-siRNA
A2780CP20-NC
A2780CP20-EV-siRNA
RBPMSA-NC
RBPMSA-siRNA

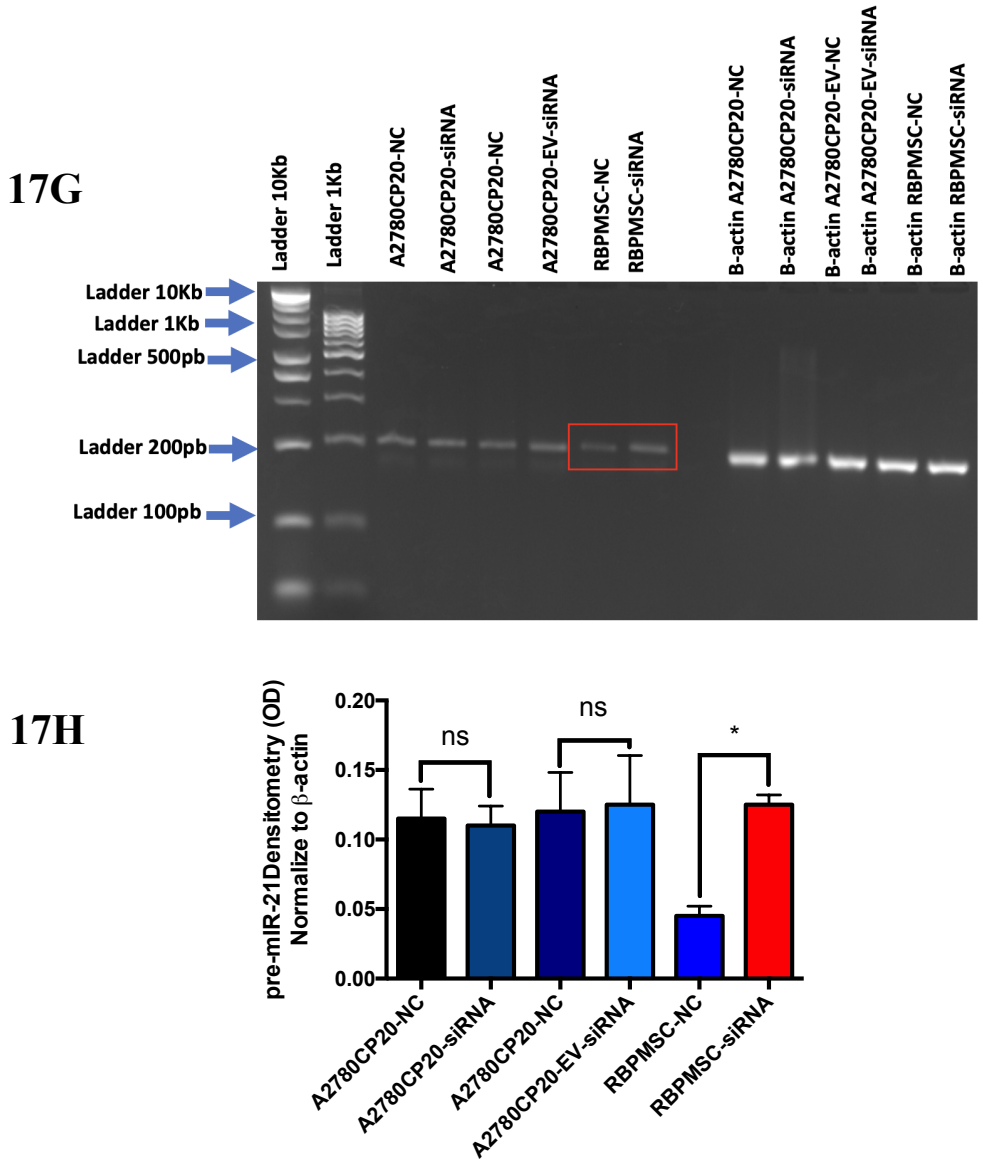

Figure 17: Effect of RBPMSA or RBPMSC on pri-mir-21 mRNA levels. (A and B) RT-PCR and densitometric analyses of the band intensities. The pre-mir-21 mRNA levels decreased when RBPMSA or RBPMSC were overexpressed in A2780CP20 clones. **(C and D)** SiRNA-mediated RBPMS knockdown. The western blots showed that the two RBPMS-targeted siRNAs successfully reduced by more than 50% the RBPMS expression. **(E and F)** RT-PCR gel (2% agarose) for pre-mir-21, after siRNA transfection of RBPMSA overexpressing cells. An increase in the pre-mir-21 levels is observed in RBPMSA clones. However, pre-mir-21 expression levels were still similar in A2780CP20-NC, A2780CP20-siRNA, A2780CP20-EV-NC and A2780CP20-EV-siRNA samples. **(G and H)** RT-PCR gel (2% agarose) for pre-mir-21 after siRNA transfection in RBPMSC overexpressing cells. An increase in the pre-mir-21 levels in RBPMSC is observed in de agarose gel. However, the pre-mir-21 expression levels were still similar in the A2780CP20-NC, A2780CP20-siRNA, A2780CP20-EV-NC and A2780CP20-EV-siRNA samples.

4.11 Identification of RBPMSA and RBPMSC downstream signaling pathways by RNAseq

To further identify additional downstream effectors of each RBPMS splice variant, RNAseq was performed with total RNA that was extracted from A2780CP20-EV, A2780CP20-RBPMSA, and A2780CP20-RBPMSC overexpressed clones. 16,968 RNA transcripts were initially identified in the A2780CP20-RBPMSA sample, and 16,717 in the A2780CP20-RBPMSC sample. Further filtering was done by using a cut-off p-value < 0.05 and fold change $\geq |2.0|$, which reduced the list of significantly expressed RNA transcripts to 4161 in A2780CP20-RBPMSA and 1869 for A2780CP20-RBPMSC samples (See Appendix C). A Venn diagram showed that 2995 RNA transcripts were exclusive to A2780CP20-RBPMSA and 703 for A2780CP20-RBPMSC. Moreover, 1161 transcripts were shared by the two RBPMS splice variants (Figure 18A). Table 2 includes the top 20 (10 upregulated and 10 downregulated, selected by fold change) differentially regulated transcripts in the A2780CP20-RBPMSA overexpression clones, and Table 3 shows the top 13 differentially regulated transcripts in the A2780CP20-RBPMSC overexpression clones (only three genes were significantly downregulated in the A2780CP20-RBPMSC clones). The RNAseq results were validated using quantitative real time PCR. The validation included the top 10 differentially expressed transcripts (7 upregulated and 3 downregulated) in RBPMSA vs. A2780CP20-EV. As shown in Table 5 and Figure 18B, nine (of the 10 genes validated by PCR) correlated well with the RNAseq results. The same validation was performed for the top eight differentially expressed transcripts in RBPMSC vs. A2780CP20-EV (five upregulated and three downregulated). The PCR data showed that five out of eight genes were validated and confirmed the RNAseq data (Table 6 and Figure 18C). Deregulation of most of these genes has already been associated with cancer progression, metastasis, and immune system response [184] [147, 185-187].

For example, interferon induced protein 44 (IFI44), one of the most increased transcripts upon A2780CP20-RBPMSA overexpression, has been linked to the suppression of the proliferation of human melanoma cell lines [188], as well as immune response to autoimmune disease [189]. Interestingly, two long non-coding RNAs (lncRNAs), LINC01504 (increased) and SNORD99 (decreased), were regulated in A2780CP20-RBPMSA clones. For A2780CP20-RBPMSC, Calbindin 2 (CALB2), the second most increased transcript, has been linked as an important mediator of 5-FU-induced cell death [190]. Moreover, in the list of common transcripts shared by A2780CP20-RBPMSA and A2780CP20-RBPMSC clones, ANKRD33B was identified, whose increase in CpG methylation was associated with oral and pharyngeal squamous cell carcinoma cell lines and primary non-neoplastic oral epithelial cells [191]. Also, RAD51 was identified, it has received considerable attention due to its function in tumor progression and decisive role in tumor resistance to chemotherapy. Moreover, RAD51 plays a role in maintaining genomic instability by mediating the DNA damage repair [192] (Table 4).

18A

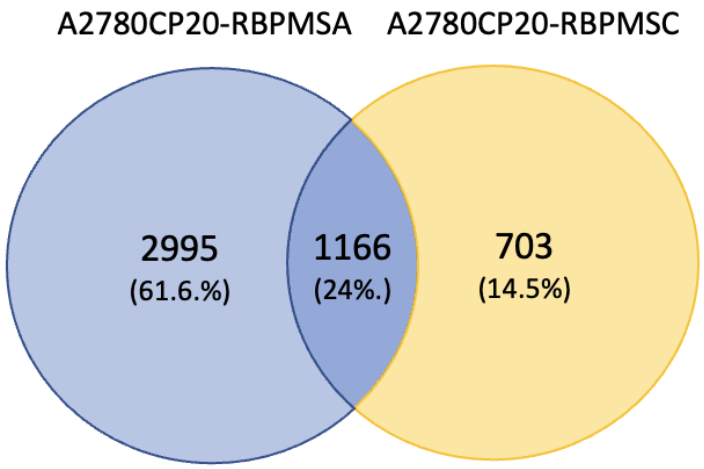

Table 2. Top 20 differentially expressed RNA transcripts in A2780CP20-RBPMSA vs. A2780CP20-EV clones.

Symbol	Gene Name	Fold Change	Biological Role	Reference
IFI44	Interferon induced protein 44	9.66541828	Plays a role in the immune response during autoimmune diseases.	[193]
XAF1	XIAP Associated Factor 1	8.297767889	A putative tumor suppressor candidate that junction to several pathways leading to apoptosis.	[185]
GBP4	Guanylate Binding Protein 4	6.931543382	Involved in the host-defense mechanisms response against cellular pathogens and tumorigenesis.	[194]
SLC15A3	Solute Carrier Family 15 Member 3	6.865730827	Transporting histidine, peptides and peptidomimetics from inside the lysosome to cytosol.	[195]
RBPMS	RNA Binding Protein	6.758908087	Regulate the RNA transport, stability and localization.	[147]
LINC01504	Long Intergenic Non-Protein Coding RNA 1504	6.554246988	A lncRNA which has a role on the suppression of malignant phenotypes of lung cancer.	[196]
NUPR1	Nuclear Protein 1, Transcriptional Regulator	6.087442834	Upregulation of this protein is associated with malignant characteristics of cancer as well as with chemoresistance.	[186]
BST2	Bone Marrow Stromal Cell Antigen 2	5.971957997	Lipid raft-associated type II transmembrane glycoprotein which mediates various facets of cancer progression and metastasis	[197]
FGF21	Fibroblast Growth Factor 21	5.930365363	Member of the FGF family which possess broad mitogenic and cell survival activities.	[198]
HSH2D	Hematopoietic SH2 Domain Containing	5.864666169	Play a role in various cellular functions such as apoptosis, membrane-associated intracellular trafficking, and the biogenesis of lipid and collagen remodeling.	[199]
S100A2	S100 Calcium Binding Protein A2	-2.477696881	Plays a role in metastasis process by transforming growth factor-β (TGF-β) mediated cancer cell invasion and migration.	[200]
KCNH4	Potassium Voltage-Gated Channel Subfamily H Member 4	-2.510279699	Transport positively charged potassium atoms between neighboring cells. KCNH4 plays a key role in the ability of cells to generate and transmit electrical signals.	[201]
SNORD99	Small Nucleolar RNA, C/D Box 99	-2.521724113	Related with diverse cellular functions such as regulation of T cell proliferation and death balance to promoting cancer cell plasticity.	[202]
LRRC8D-DT	LRRC8D Divergent Transcript	-3.051305443	Plays important pharmacological and physiological roles in supporting the transport of anti-cancer drugs and of the organic osmolyte taurine.	[203]
TXK	TXK Tyrosine Kinase	-3.120303742	Play important roles in the immune response and pathway signaling mediator	[204]
SGCZ	Sarcoglycan Zeta	-4.110780038	Part of the sarcoglycan complex which have a structural role in connecting cytoskeletal proteins with the extracellular matrix.	[205]
HIST1H2BH	H2B Clustered Histone 9	-4.323395136	Responsible for the nucleosome structure of the chromosomal fiber in eukaryotes. Low levels of HIST1H2BEH caused decreased proliferation in breast cancer cell lines.	[206]
COL12A1	Collagen Type XII Alpha 1 Chain	-4.332051747	Found in several cancer types and could be involved in tumor progression.	[207]

PREX2	Phosphatidylinositol-3,4,5-Trisphosphate Dependent Rac Exchange Factor 2	-4.381347741	Implicated in the inhibition of phosphatase and tensin homolog (PTEN). Overexpression significantly increases the proliferation, invasion, and migration of pancreatic cancer.	[208]
CCL2	C-C Motif Chemokine Ligand 2	-4.644149886	Strongest chemoattractant synthesized and secreted mainly by monocytic cells.	[209]

Table 3. Top 13 differentially expressed RNA transcripts in A2780CP20-RBPMSC vs. A2780CP20-EV clones.

Symbol	Gene Name	Fold Change	Biological Role	Reference
DAB2	DAB Adaptor Protein 2	7.15380118	Multi-function signaling molecule which catalytic enzyme activity suggest that it is an adaptor molecule involved in multiple receptor-mediated signalling pathways that plays a pivotal role in the cellular homeostasis.	[210]
CALB2	Calbindin 2	6.574845254	Important mediator of 5-FU-induced cell death and specific marker for the diagnosis of malignant mesothelioma.	[211]
CTNND2	Catenin Delta 2	6.484328261	Recognized to be a biomarker for cancers, overexpressed in various types of cancers, including prostate, breast, lung, and ovarian cancer.	[212]
CYP24A1	Cytochrome P450 Family 24 Subfamily A Member 1	6.041287981	Member of the cytochrome P450 superfamily of enzymes which catalyze many reactions involved in drug metabolism and synthesis of cholesterol, steroids, and other lipids.	[213]
FAR2P2	Fatty Acyl-CoA Reductase 2 Pseudogene 2	5.29742507	Catalyzes the reduction in saturated but not unsaturated C16 or C18 fatty acyl-CoA to fatty alcohols.	[214]
RBPMS	RNA Binding Protein	4.920050075	Regulate the RNA transport, stability and localization.	[147]
PPP1R1C	Protein Phosphatase 1 Regulatory Inhibitor Subunit 1C	4.253043369	Major serine/threonine phosphatase that regulates a variety of cellular functions and themselves regulated by phosphorylation.	[215]
SLFN11	Schlafen Family Member 11	3.827804248	DNA/RNA helicase that is recruited during stressed replication fork and irreversibly triggers replication block and cell death.	[216]
PTGER4	Prostaglandin E Receptor 4	3.770525307	Member of the G-protein coupled receptor family which bind and mediate cellular responses to PGE2 and other prostanoids.	[217]
FOXD3-AS1	FOXD3 Antisense RNA 1	3.654548595	Is abnormally expressed in many disease types. Reports suggest that FOXD3-AS1 is highly expressed in different cancer types promoting migration and invasion capacity.	[218]
TP63	Tumor Protein P63	-2.226163472	Functions as a transcription factor interacting with other proteins to turn different genes on and off at different times.	[187]
DTNA	Dystrobrevin Alpha	-2.582128781	Belongs to the dystrobrevin subfamily of the dystrophin family. Reports suggest that DTNA binds and activates STAT3 to induce TGFβ1 expression and repress P53 expression.	[219]
SCN3A	Sodium Voltage-Gated Channel Alpha Subunit 3	-4.437260362	Is a transmembrane glycoprotein responsible for the generation and propagation of action potentials in neurons and muscle.	[220]

Table 4. Top 20 RNA transcripts shared by A2780CP20-RBPMSA and A2780CP20-RBPMSC clones.

Symbol	Gene Name	Fold Change	Biological Role	Reference
FAR2P2	Fatty Acyl-CoA Reductase 2 Pseudogene 2	5.29742507	Acts as guanine nucleotide exchange factor that activates RAC1. Also, plays a role in the response to class 3 semaphorins and remodeling of the actin cytoskeleton.	[214]
RBPMS	RNA Binding Protein	4.920050075	Regulate the RNA transport, stability, and localization.	[147]
ANKRD33B	Ankyrin Repeat Domain 33B	4.556503793	Involved in negative regulation of transcription by RNA polymerase II and negative regulation of transcription regulatory region DNA binding activity.	[221]
PPP1R1C	Protein Phosphatase 1 Regulatory Inhibitor Subunit 1C	4.253043369	Major serine/threonine phosphatase that regulates a variety of cellular functions and themselves regulated by phosphorylation.	[215]
FGF12	Fibroblast Growth Factor 12	3.920423579	Involved in a broad mitogenic and cell survival activities, including embryonic development, cell growth, morphogenesis, tissue repair, tumor growth, and invasion.	[222]
GABRA2	Gamma-Aminobutyric Acid Type A Receptor Subunit Alpha2	3.844344607	Component of the heteropentameric receptor for GABA, the major inhibitory neurotransmitter in the brain.	[223]
FOXD3-AS1	FOXD3 Antisense RNA 1	3.654548595	Is abnormally expressed in many disease types. Reports suggest that FOXD3-AS1 is highly expressed in different cancer types promoting migration and invasion capacity.	[224]
NFATC1	Nuclear Factor of Activated T Cells 1	3.620469318	Family of proteins that play a central role in inducible gene transcription during immune response.	[225]
ROBO2	Roundabout Guidance Receptor 2	3.448549593	Transmembrane receptor for the slit homolog 2 protein that play a function in axon guidance and cell migration.	[226]
CDH6	Cadherin 6	3.421265843	Membrane glycoprotein that mediates homophilic cell-cell adhesion and play critical roles in cell differentiation and morphogenesis.	[227]
HOXD8	Homeobox D8	-2.593778164	Gene belongs to the homeobox family of genes which play an important role in morphogenesis in all multicellular organisms.	[228]
MYL7	Myosin Light Chain 7	-2.677248207	Part of the family motor proteins that have ATPase enzyme activity, actin binding, and potential for kinetic energy transduction.	[229]
SSUH2	Ssu-2 Homolog	-2.71336991	Gene that encodes a protein tyrosine phosphatase that plays a key role in the regulation of actin filaments.	[230]
HOXD9	Homeobox D9	-2.800133712	Transcription factor which is part of a developmental regulatory system providing cells the specific positional identities on the anterior-posterior axis.	[231]
DAPK1	Death-Associated Protein Kinase 1	-3.221475672	Mediator of gamma-interferon involved in multiple cellular signaling pathways that trigger cell survival, apoptosis, and autophagy.	[232]

SNTG1	Syntrophin Gamma 1	-3.228723507	Cytoplasmic peripheral membrane proteins that contain 2 pleckstrin domains.	[233]
NRP1	Neuropilin 1	-3.454159744	Cell membrane receptor involved in the development of cardiovascular system, angiogenesis, certain neuronal circuits, and organogenesis in nervous system.	[234]
ERICH3	Glutamate Rich 3	-3.951576843	Interacts with proteins function in vesicle biogenesis and may play a significant role in vesicular function in serotonergic, and other neuronal cell types.	[235]
JAG1	Jagged Canonical Notch Ligand 1	-6.91254142	Ligand for multiple Notch receptors involved in the mediation of Notch signaling, cell-fate decisions during, and cardiovascular development.	[236]
TRBV12-4	T Cell Receptor Beta Variable 12-4	-6.91254142	Antigen specific receptor which are essential to the immune response, and are present on the cell surface of T lymphocytes	[237]

To better examine the interaction networks of RBPMS downstream genes, the lists with 2995 transcripts of A2780CP20-RBPMSA, 703 of A2780CP20-RBPMSC, and the common 1161 transcripts were subjected to functional enrichment using Metascape via Gene Ontology (GO) and the Kyoto Encyclopedia of Genes and Genomes (KEGG), and uploaded into the Ingenuity Pathway Analysis (IPA) software [182]. Among the top 20 most significantly (p-value ≤ 0.05) enriched ontology clusters of A2780CP20-RBPMSA, the most relevant clusters included the metabolism of RNA, ribonucleoprotein complex biogenesis, and cell cycle (Figure 18D). Figure 18E shows the interactions between the top canonical pathways, identified in the A2780CP20-RBPMSA clones. The top canonical pathways were the hepatic fibrosis/hepatic stellate cell activation, inhibition of matrix metalloproteases, wound healing signaling, CDC42 signaling, and PD-1-PD-L1 cancer immunotherapy. The top five networks, in terms of the number of genes per pathway, are depicted in Appendix D. These pathways include Cancer, Cardiovascular System Development, and Function Organismal Development (31 genes); Cell Cycle, Cellular Development, Cellular Growth, and Proliferation (25 genes); and, Antimicrobial Response, Inflammatory Response, and Organismal Injury and Abnormality (55 genes).

Similarly, for the A2780CP20-RBPMSC, the top 20 most significantly (p-value ≤ 0.05) enriched ontology clusters included the cell junction organization, blood vessel development, and non-integrin membrane-ECM interactions (Figure 18F). Figure 18G includes the interaction network of the top canonical pathways that were identified for A2780CP20-RBPMSC clones. The top canonical pathways were the P53 signaling, hepatic fibrosis/hepatic stellate cell activation, pulmonary fibrosis idiopathic signaling, CDK5 signaling, and IGF1 signaling. The networks in terms of the number of genes per pathway for A2780CP20-RBPMSC are depicted in Appendix D. These pathways included cardiovascular system development and function, cell to cell signaling and interaction, cellular movement (2 genes), organ morphology, reproductive system development and function, tissue development (3 genes), antimicrobial response, cell cycle, and survival (2 genes).

A similar analysis was also completed with the common transcripts, regulated in both A2780CP20-RBPMSA and A2780CP20-RBPMSC clones. Among the top 20 most significantly (p-value ≤ 0.01) enriched ontology clusters, the most relevant included ribosome biogenesis, DNA metabolic process, and mitochondrial gene expression (Figure 18H). Figure 18I includes the interaction between the top canonical pathways, identified with the common transcripts between A2780CP20-RBPMSA and A2780CP20-RBPMSC clones. The top canonical pathways involved TGF-β signaling, role of tissue factor in cancer, and cytokine production in macrophages and T helped cells by IL-17A and IL-17F. The networks shared by A2780CP20-RBPMSA and A2780CP20-RBPMSC, in terms of the number of genes per pathway, included: Cancer, Cardiovascular Disease Hematological System Development and Function (2 genes); Cell to Cell

Signaling and Interaction, Cellular Development, Cellular growth, and Proliferation (2 genes); and Cancer, Cellular Movement, Organismal Injury, and Abnormality (2 genes) (Appendix D).

Table 5: Relative expression values of the differentially expressed RNA transcripts in A2780CP20-RBPMSA vs. A2780CP20-EV clones.

RBPMS-A Transcripts Validation Expression		
Gene ID	RT-qPCR FC	RNA-Seq FC
IF144	**9.666**	**9.665**
XAF1	**8.298**	**8.297**
GBP4	**6.932**	**6.931**
NUPR1	**6.087**	**6.087**
BST2	**5.972**	**5.971**
HSH2D	**5.865**	**5.864**
COL12A1	**-4.332**	**-4.332**
LLRC8D-DT	**-3.050**	**-3.058**
SLC15A3	-2.273	6.865
RBPMS	**6.499**	**6.758**

18B

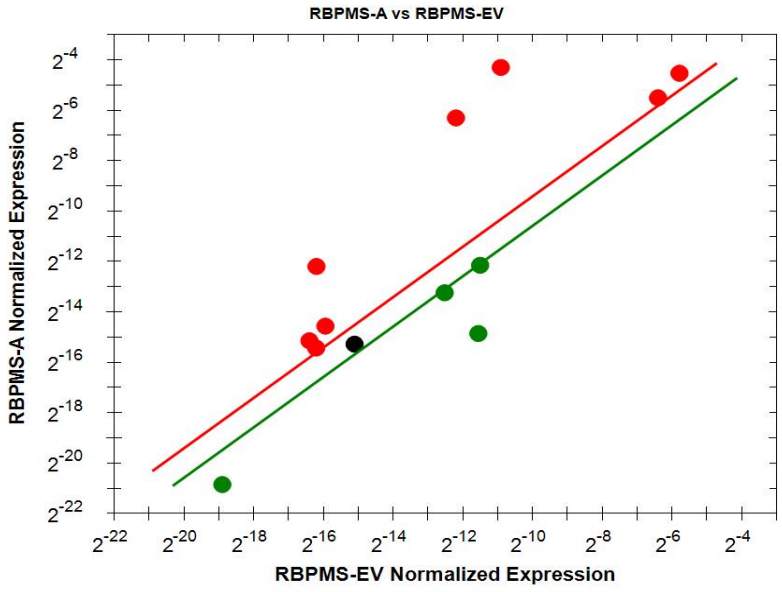

Table 6: Relative expression values of the differentially expressed RNA transcripts in A2780CP20-RBPMSC vs. A2780CP20-EV clones.

RBPMS-C Transcripts Validation Expression		
Gene ID	RT-qPCR FC	RNA-Seq FC
DAB2	**7.154**	**7.15**
CALB2	**6.575**	**6.57**
CYP24A1	**6.041**	**6.041**
SLFN11	**3.828**	**3.827**
PTGERR4	**3.771**	**3.770**
TP63	2.861	-2.226
DTNA	2.783	-2.582
SCN3A	2.775	-4.437

18C

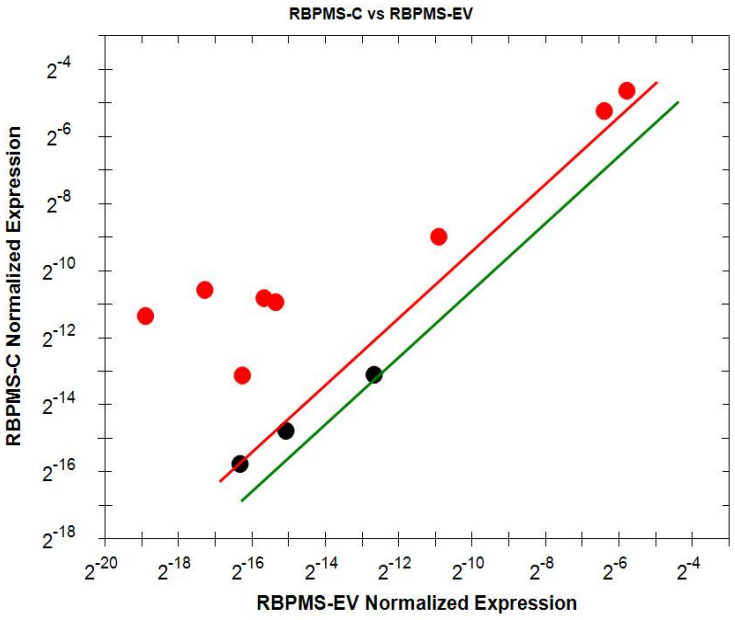

18D

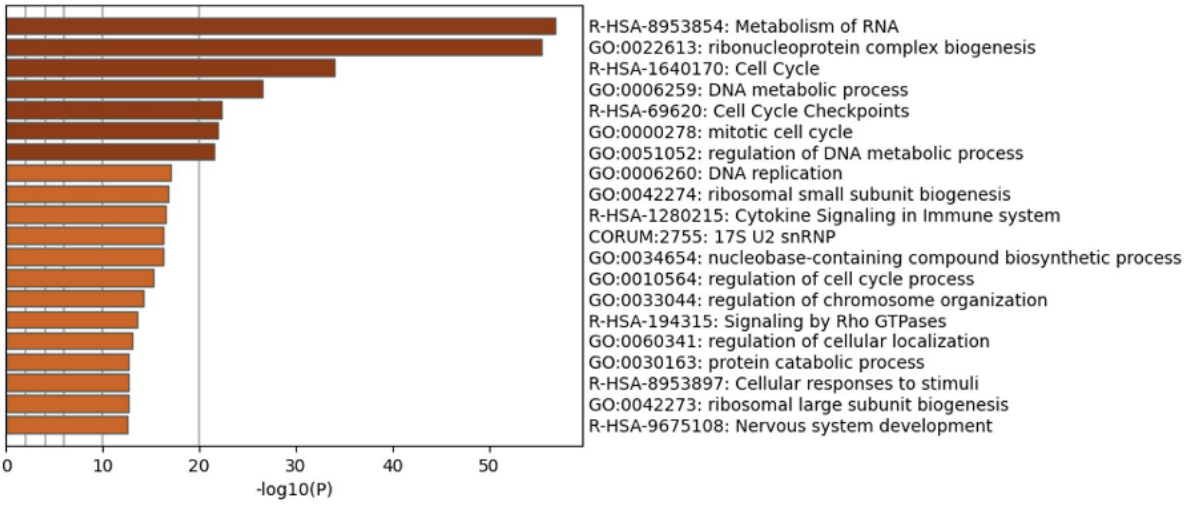
R-HSA-8953854: Metabolism of RNA
GO:0022613: ribonucleoprotein complex biogenesis
R-HSA-1640170: Cell Cycle
GO:0006259: DNA metabolic process
R-HSA-69620: Cell Cycle Checkpoints
GO:0000278: mitotic cell cycle
GO:0051052: regulation of DNA metabolic process
GO:0006260: DNA replication
GO:0042274: ribosomal small subunit biogenesis
R-HSA-1280215: Cytokine Signaling in Immune system
CORUM:2755: 17S U2 snRNP
GO:0034654: nucleobase-containing compound biosynthetic process
GO:0010564: regulation of cell cycle process
GO:0033044: regulation of chromosome organization
R-HSA-194315: Signaling by Rho GTPases
GO:0060341: regulation of cellular localization
GO:0030163: protein catabolic process
R-HSA-8953897: Cellular responses to stimuli
GO:0042273: ribosomal large subunit biogenesis
R-HSA-9675108: Nervous system development
0
10
20
30
40
50
-log10(P)

18E

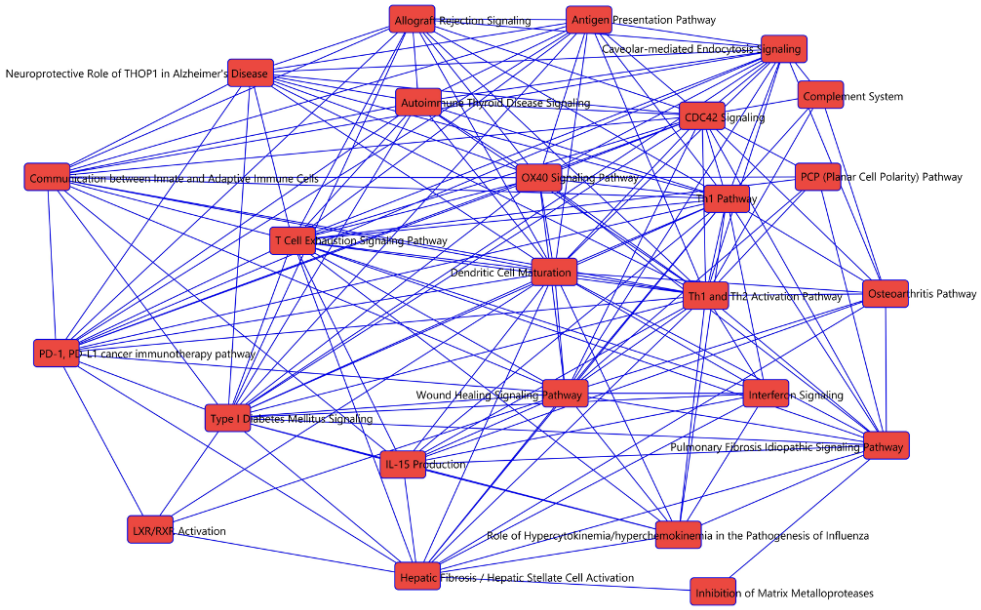
Allograft Rejection Signaling
Antigen Presentation Pathway
Caveolar-mediated Endocytosis Signaling
Neuroprotective Role of THOP1 in Alzheimer's Disease
Complement System
Autoimmune Thyroid Disease Signaling
CDC42 Signaling
Communication between Innate and Adaptive Immune Cells
OX40 Signaling Pathway
PCP (Planar Cell Polarity) Pathway
Th1 Pathway
T Cell Exhaustion Signaling Pathway
Dendritic Cell Maturation
Th1 and Th2 Activation Pathway
Osteoarthritis Pathway
PD-1, PD-L1 cancer immunotherapy pathway
Wound Healing Signaling Pathway
Interferon Signaling
Type I Diabetes Mellitus Signaling
Pulmonary Fibrosis Idiopathic Signaling Pathway
IL-15 Production
LXR/RXR Activation
Role of Hypercytokinemia/hyperchemokinemia in the Pathogenesis of Influenza
Hepatic Fibrosis / Hepatic Stellate Cell Activation
Inhibition of Matrix Metalloproteases

18F

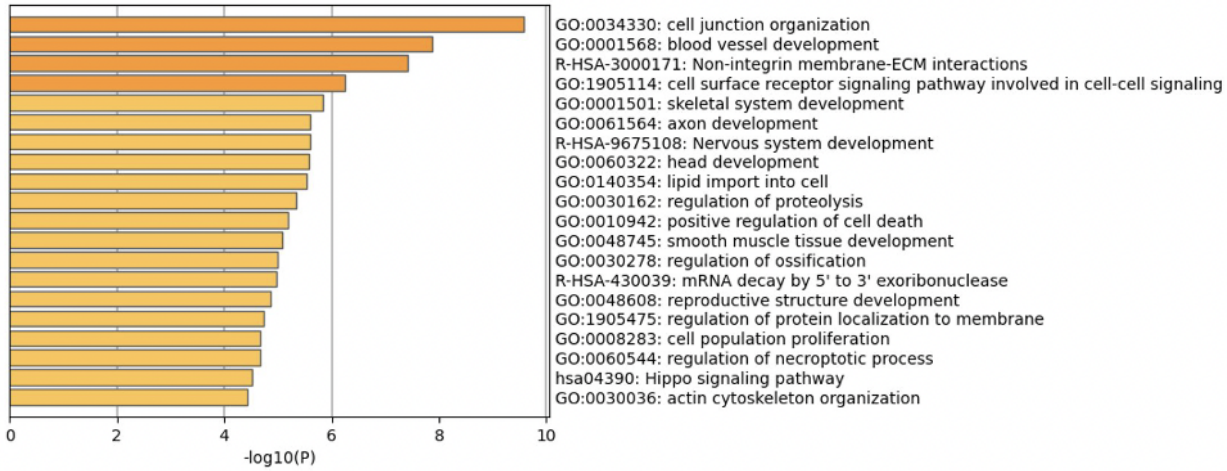
GO:0034330: cell junction organization
GO:0001568: blood vessel development
R-HSA-3000171: Non-integrin membrane-ECM interactions
GO:1905114: cell surface receptor signaling pathway involved in cell-cell signaling
GO:0001501: skeletal system development
GO:0061564: axon development
R-HSA-9675108: Nervous system development
GO:0060322: head development
GO:0140354: lipid import into cell
GO:0030162: regulation of proteolysis
GO:0010942: positive regulation of cell death
GO:0048745: smooth muscle tissue development
GO:0030278: regulation of ossification
R-HSA-430039: mRNA decay by 5' to 3' exoribonuclease
GO:0048608: reproductive structure development
GO:1905475: regulation of protein localization to membrane
GO:0008283: cell population proliferation
GO:0060544: regulation of necroptotic process
hsa04390: Hippo signaling pathway
GO:0030036: actin cytoskeleton organization
0
2
4
6
8
10
-log10(P)

18G

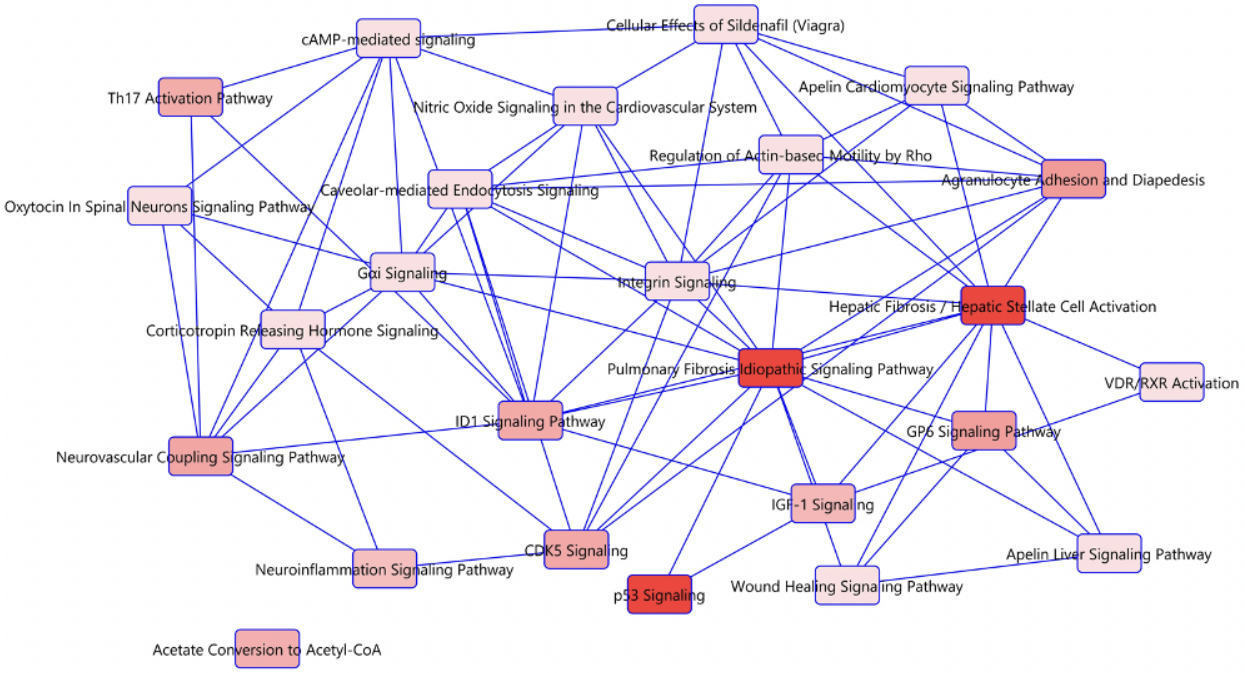
cAMP-mediated signaling
Cellular Effects of Sildenafil (Viagra)
Th17 Activation Pathway
Nitric Oxide Signaling in the Cardiovascular System
Apelin Cardiomyocyte Signaling Pathway
Regulation of Actin-based Motility by Rho
Caveolar-mediated Endocytosis Signaling
Agranulocyte Adhesion and Diapedesis
Oxytocin In Spinal Neurons Signaling Pathway
Gαi Signaling
Integrin Signaling
Hepatic Fibrosis / Hepatic Stellate Cell Activation
Corticotropin Releasing Hormone Signaling
Pulmonary Fibrosis Idiopathic Signaling Pathway
VDR/RXR Activation
ID1 Signaling Pathway
GP6 Signaling Pathway
Neurovascular Coupling Signaling Pathway
IGF-1 Signaling
CDK5 Signaling
Apelin Liver Signaling Pathway
Neuroinflammation Signaling Pathway
Wound Healing Signaling Pathway
p53 Signaling
Acetate Conversion to Acetyl-CoA

18H

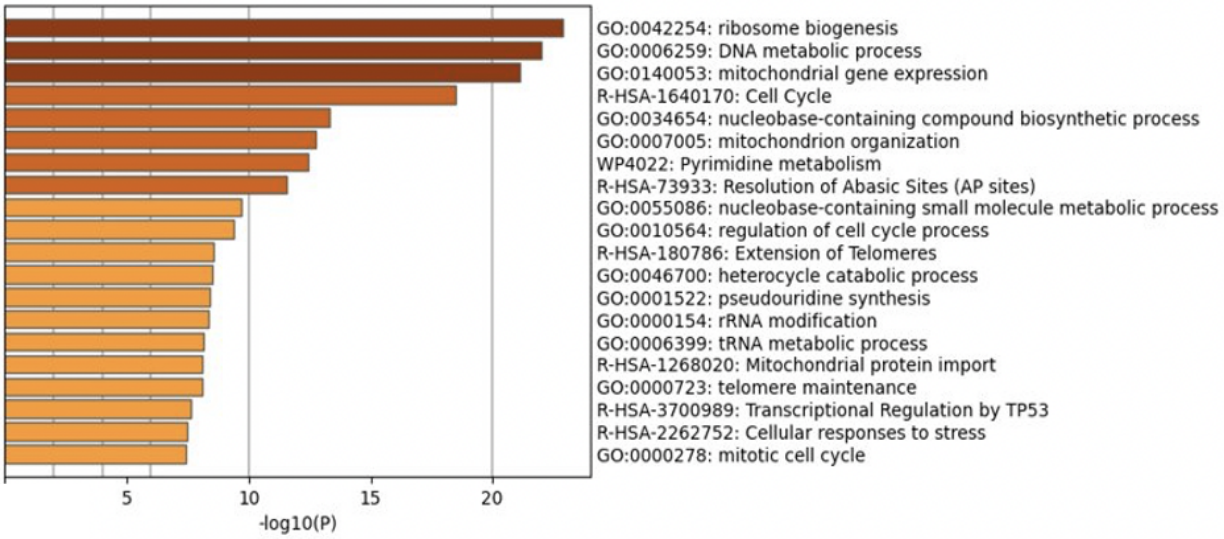

18I

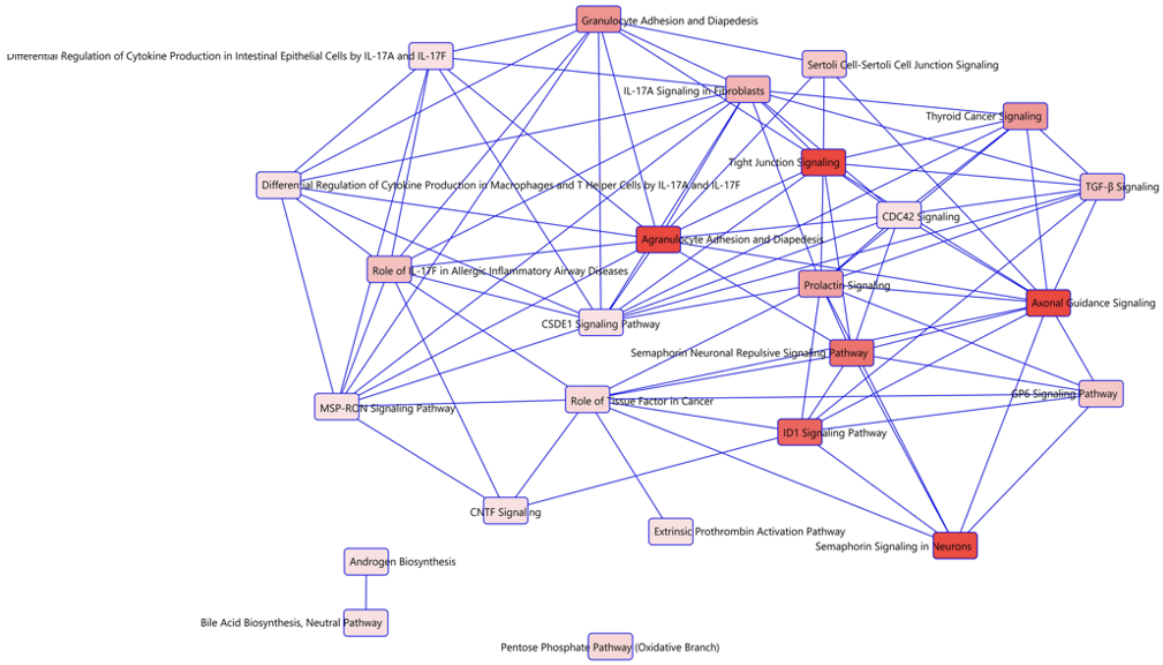

Figure 18. Ingenuity pathway analysis (IPA) and functional enrichment analysis of top deregulated transcripts in RBPMSA and RBPMSC clones. (A) Venn diagram showing that 2995 RNA transcripts were deferentially abundant in RBPMSA clones, 703 in RBPMSC clones, and 1166 were common to both, A2780CP20-RBPMSA and A2780CP20-RBPMSC clones. (B) Validation of 10 differentially abundant transcripts by RT−qPCR in A2780CP20-EV cells and A2780CP20-RBPMSA. The normalized expression values were calculated relative to A2780CP20-EV. Green and red symbols represent downregulated and upregulated genes, respectively. Diagonal green and red lines represent the selected threshold for significant fold changes. (C) Validation of 8 differentially abundant transcripts by RT−qPCR in A2780CP20-EV cells and A2780CP20-RBPMSC. The normalized expression values were calculated relative to A2780CP20-EV. Green and red symbols represent downregulated and upregulated genes, respectively. Diagonal green and red lines represent the selected threshold for significant fold changes. (D) The 20 top most significant (p-value ≤ 0.05) enriched ontology clusters by Gene ontology analysis of functional enrichment in A2780CP20-RBPMSA clones. (E) Interaction network of the top canonical pathways identified in the A2780CP20-RBPMSA clones. (F) The 13 top most significant (p-value ≤ 0.05) enriched ontology clusters by Gene ontology

analysis of functional enrichment in A2780CP20-RBPMSC clones. (G) Interaction network of the top canonical pathways identified in the A2780CP20-RBPMSC clones. (H) The 20 top most significant (p-value ≤ 0.05) enriched ontology clusters by Gene ontology analysis of functional enrichment in common transcripts between A2780CP20-RBPMSA and A2780CP20-RBPMSC clones. (I) Interaction network of the top canonical pathways identified in the common transcripts between A2780CP20-RBPMSA and A2780CP20-RBPMSC clones.

4.12 Prognostic Value of RBPMSA and RBPMSC Downstream Effectors

To assess the clinical relevance of the top differentiated abundant transcripts (see Table 2, Table 3 and Table 4) identified by RNAseq in A2780CP20-RBPMSA and A2780CP20-RBPMSC clones, the Kaplan-Meier plotter data base (KM plotter) was interrogated. The Ovarian Cancer KM plotter includes data from "The Cancer Genome Atlas" (TCGA), Gene Expression Omnibus (GEO), and European Genome Archive (EGA) for a total of 1436 ovarian cancer samples [238]. Overexpression of RBPMSA in A2780CP20 cell line increased the RNA levels of BST2 (also known as CD317), GBP4, and SLC15A. In agreement with these results, higher RNA expression levels of these genes were associated with better prognosis of the disease (OS; HR < 1) (Figure 19A–C). On the other hand, overexpression of RBPMSA reduced the expression levels of COL12A1 and CCL2. Again, KM plotter data analysis showed that lower expression levels of COL12A1 were associated with longer PFS (HR > 1) and better prognosis (OS; HR > 1) (Figure 6 D,E). High expression levels of CYP24A1, PPPIRIC, and FOXD3-AS1, detected in A2780CP20-RBPMSC clones, were associated with longer PFS (HR < 1) and better prognosis (OS; HR < 1) of ovarian cancer patients (Figure 6F–H). Moreover, decreased levels of DTNA in A2780CP20-RBPMSC clones were associated with longer PFS (HR > 1) and better prognosis (OS; HR > 1) in patients (Figure 6I).

19A-G

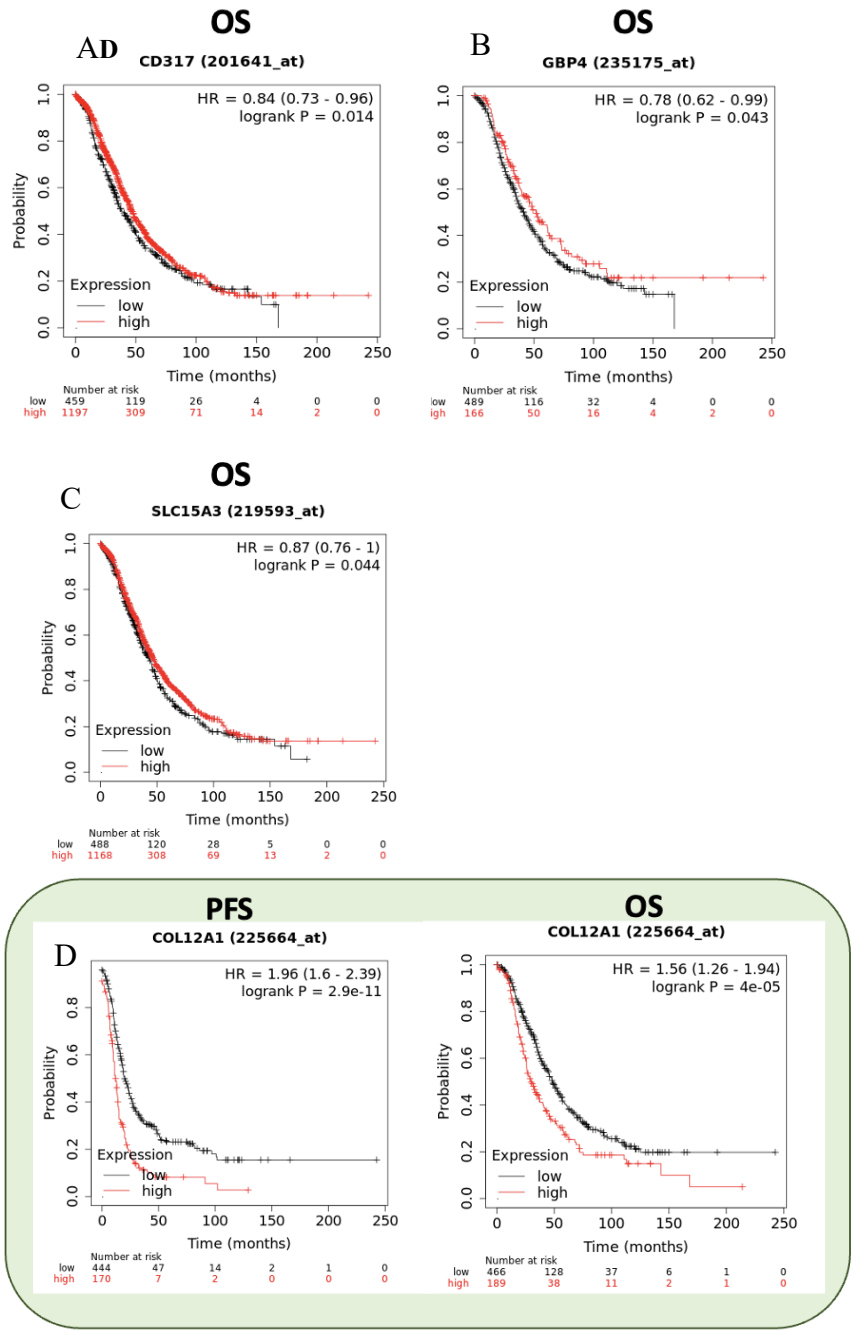
AD
OS
CD317 (201641_at)
HR = 0.84 (0.73 - 0.96)
logrank P = 0.014
B
OS
GBP4 (235175_at)
HR = 0.78 (0.62 - 0.99)
logrank P = 0.043
C
OS
SLC15A3 (219593_at)
HR = 0.87 (0.76 - 1)
logrank P = 0.044
D
PFS
COL12A1 (225664_at)
HR = 1.96 (1.6 - 2.39)
logrank P = 2.9e-11
OS
COL12A1 (225664_at)
HR = 1.56 (1.26 - 1.94)
logrank P = 4e-05
Probability
Expression
low
high
Time (months)
Number at risk

E

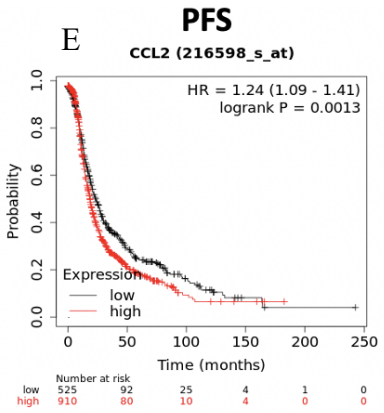
PFS
CCL2 (216598_s_at)
HR = 1.24 (1.09 - 1.41)
logrank P = 0.0013
Probability
Expression
low
high
Time (months)
Number at risk
low 525 92 25 4 1 0
high 910 80 10 4 0 0

F

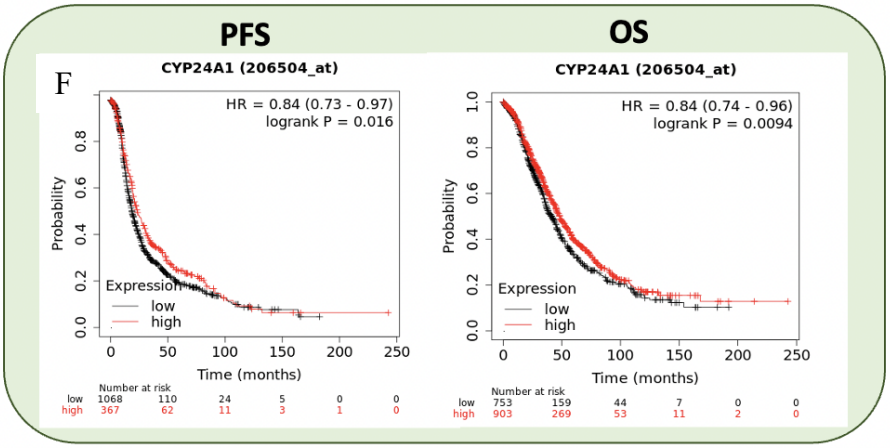
PFS
CYP24A1 (206504_at)
HR = 0.84 (0.73 - 0.97)
logrank P = 0.016
Probability
Expression
low
high
Time (months)
Number at risk
low 1068 110 24 5 0 0
high 367 62 11 3 1 0
OS
CYP24A1 (206504_at)
HR = 0.84 (0.74 - 0.96)
logrank P = 0.0094
Probability
Expression
low
high
Time (months)
Number at risk
low 753 159 44 7 0 0
high 903 269 53 11 2 0

G

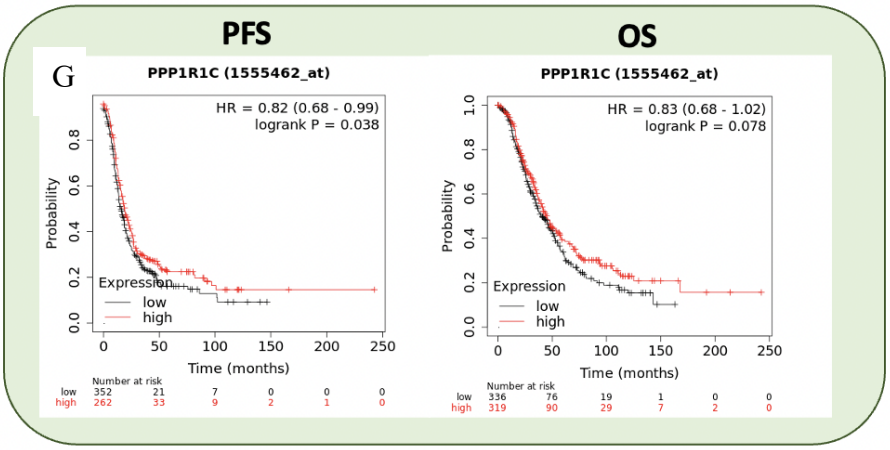
PFS
PPP1R1C (1555462_at)
HR = 0.82 (0.68 - 0.99)
logrank P = 0.038
Probability
Expression
low
high
Time (months)
Number at risk
low 352 21 7 0 0 0
high 262 33 9 2 1 0
OS
PPP1R1C (1555462_at)
HR = 0.83 (0.68 - 1.02)
logrank P = 0.078
Probability
Expression
low
high
Time (months)
Number at risk
low 336 76 19 1 0 0
high 319 90 29 7 2 0

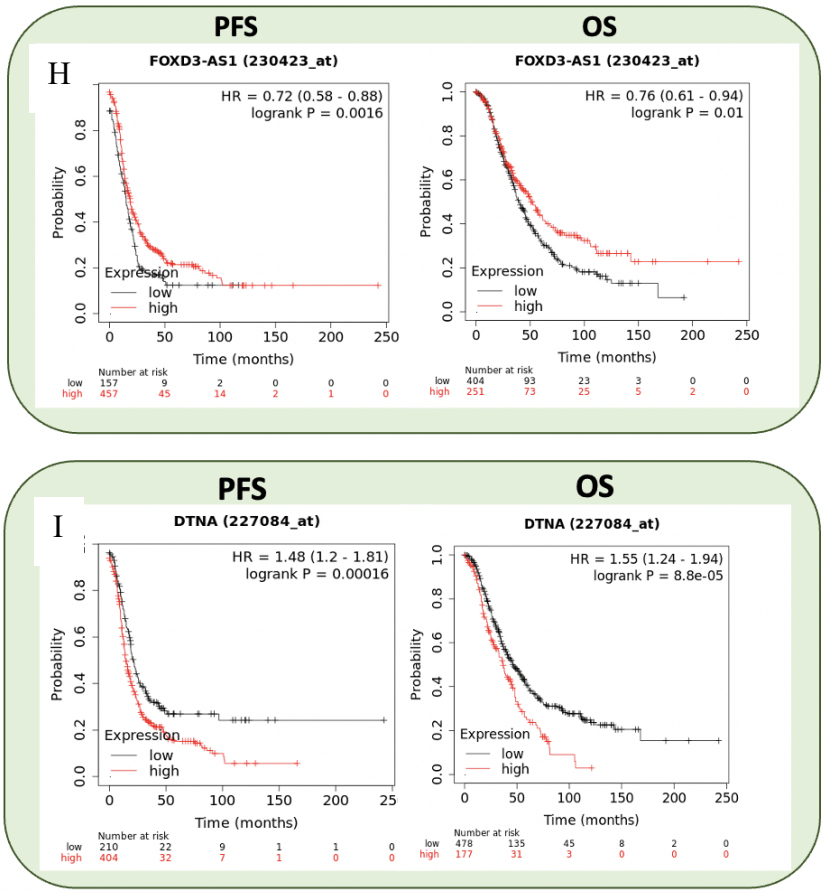

Figure 19: KM survival curves. KM plots for ovarian cancer patients were generated using the KM plotter database. The OS and PFS of the ovarian cancer patients were stratified based on the median RNA expression levels for each gene (**A**) CD3117 (**B**) GBP4 (**C**) SLC15A3 (**D**) COL12A1 (**E**) CCL2 (**F**) CYP24A1 (**G**) PPP1R1C (**H**) FOXD3-AS1 (**I**) DTNA.

Aim 3: Results

4.13 Identification of additional RBPMSA and RBPMSC-interacting proteins.

Following peptide separation and protein identification by mass spectroscopy (MS), the MS raw data was analyzed and filtered using Proteome Discoverer (PD) software version 2.5. Cutoff for considering significance in the proteins list was based on a fold change ≥ |2.0| and p-value ≤ 0.05. The human was the model organism for annotations. Through IP/MS assay, 49

proteins that may directly bind to A2780CP20-RBPMSA clones were found, and 29 for A2780CP20-RBPMSC (Appendix E). After subtracting the identified proteins in A2780CP20-EV cells, which were used as control, four proteins that differentially attached to A2780CP20-RBPMSA were able to be identified (Table 7), as well as three proteins to A2780CP20-RBPMSC (Table 8). Based on their biological roles, the unique group of proteins were selected for further validation by Western blots.

Table 7: Proteins identified in A2780CP20-RBPMSA overexpressing clones

Gene ID	Biological Role
NME1	Metastasis suppressor gene which inhibits the metastatic activity of tumor cells
MYH9	Involved in cytoskeletal reorganization, cellular pseudopodia formation, and migration. Proposed as suppressor gene playing an important role on re-Rho pathway.
MYH10	Plays and important role in cytokinesis, cell shape, cancer migration, invasion, extracellular matrix (ECM), production and, epithelial-mesenchymal transition (EMT).
IGK	Related with pathways involving the immune response CD16 signaling in NK cells and, immune response lectin induced complement pathway.

Table 8: Proteins identified in A2780CP20-RBPMSC overexpressing clones

Gene ID	Biological Role
NME1	Metastasis suppressor gene which inhibits the metastatic activity of tumor cells
MYH9	Involved in cytoskeletal reorganization, cellular pseudopodia formation, and migration. Proposed as suppressor gene playing an important role on re-Rho pathway.
MYH10	Plays and important role in cytokinesis, cell shape, cancer migration, invasion, extracellular matrix (ECM), production and, epithelial-mesenchymal transition (EMT).

The following proteins of the MS studies were validated by western blots: Diphosphate Kinase 1 (NME1), Immunoglobulin Kappa Locus (IGK), Myosin Heavy Chain 9 (MYH9) and Myosin Heavy Chain 10 (MYH10). Western blots band intensities showed significant differences in protein abundance between A2780CP20-EV vs. A2780CP20-RBPMSA, and A2780CP20-EV vs. A2780CP20-RBPMSC for NME1, IGK, MYH9 and MYH10. In Figure 20A, a band was observed near 17kDa, corresponding to NME1 in A2780CP20-RBPMSA and A2780CP20-RBPMSC IP samples. NME1 protein levels were absent in A2780CP20-EV as compared with A2780CP20-RBPMSA and A2780CP20-RBPMSC, where the NME1 levels were prominent. NME1 protein levels were detected with less intensity in the western blot of A2780CP20-EV, A2780CP20-RBPMSA, and A2780CP20-RBPMSC input samples. As expected, protein levels of IGK (56 kDa) were absent in A2780CP20-EV. Also, western blot of IGK in A2780CP20-EV, A2780CP20-RBPMSA, and A2780CP20-RBPMSC input samples showed a less signal intensity compared with the IP samples. On the other hand, bands corresponding to 210 kDa and 220 kDa (corresponding to MYH9 and MYH10, respectively) were detected in the western blots image of the A2780CP20-RBPMSA and A2780CP20-RBPMSC IP samples (Figures 20C and 20D). MYH9 and MYH10 proteins could not be detected in A2780CP20-EV IP samples. Input A2780CP20-EV, A2780CP20-RBPMSA, and A2780CP20-RBPMSC immunoblotting samples showed a lower intensity signal of MYH9 and MYH10 when compared with the IP samples. To corroborate the coimmunoprecipitation between RBPMS and the proteins identified by MS studies (NME1, IGK, MYH9 and MYH10), RBPMS was detected in the same immunoblotting IP samples membrane, as control of successful immunoprecipitation (Figure 20A, 20B, 20C and 20D, lower image). However, the biological role of these proteins in ovarian cancer cells and its association with cisplatin resistance is not well understood and needs further investigation.

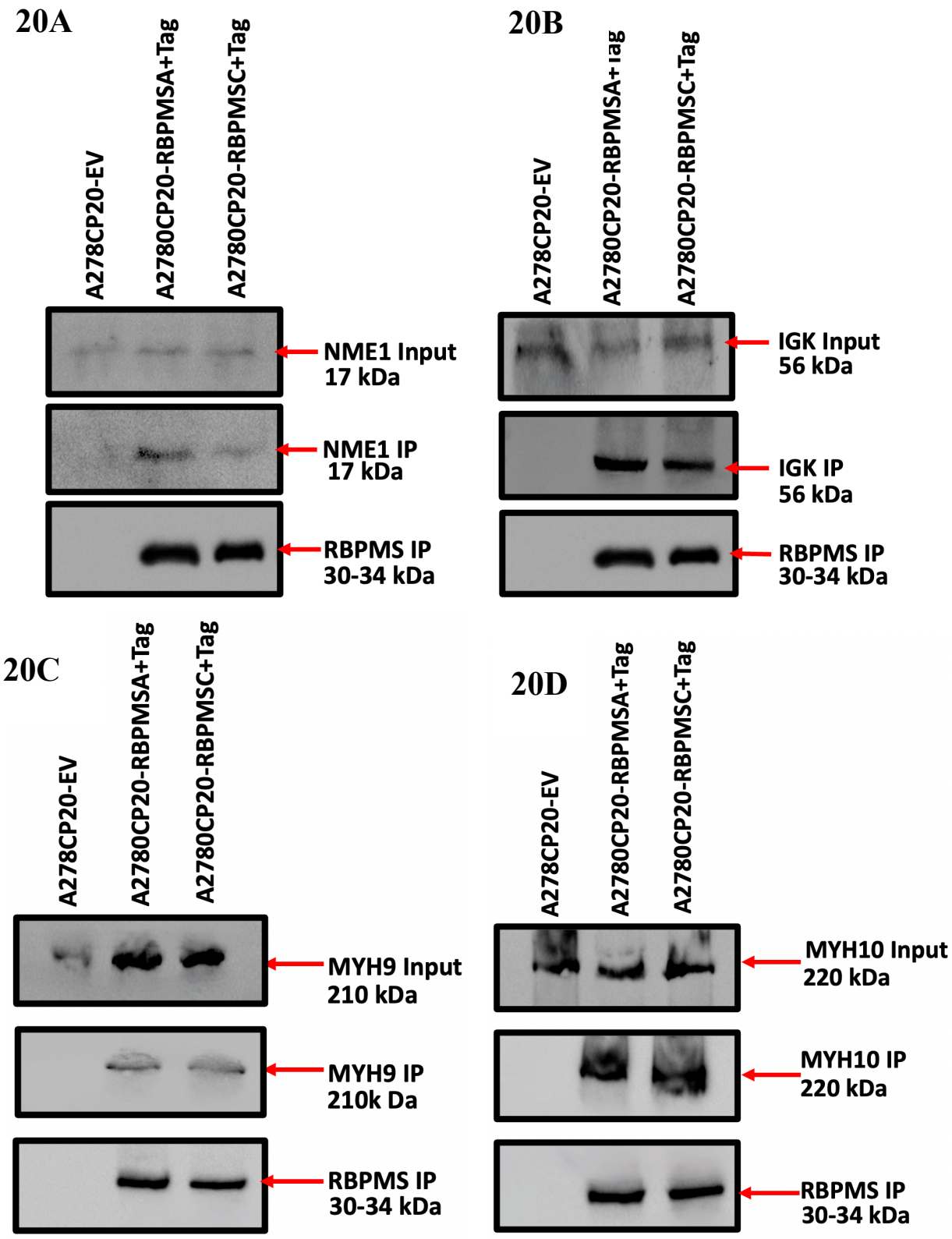
20A
A278CP20-EV
A2780CP20-RBPMSA+Tag
A2780CP20-RBPMSC+Tag
NME1 Input
17 kDa
NME1 IP
17 kDa
RBPMS IP
30-34 kDa
20B
A278CP20-EV
A2780CP20-RBPMSA+Tag
A2780CP20-RBPMSC+Tag
IGK Input
56 kDa
IGK IP
56 kDa
RBPMS IP
30-34 kDa
20C
A278CP20-EV
A2780CP20-RBPMSA+Tag
A2780CP20-RBPMSC+Tag
MYH9 Input
210 kDa
MYH9 IP
210k Da
RBPMS IP
30-34 kDa
20D
A278CP20-EV
A2780CP20-RBPMSA+Tag
A2780CP20-RBPMSC+Tag
MYH10 Input
220 kDa
MYH10 IP
220 kDa
RBPMS IP
30-34 kDa

Figure 20: Validation of proteins identified by IP/MS assay in RBPMSA and RBPMSC overexpressing clones. **(A)** NME1 input immunoblotting (upper image), follow by NME1 IP immunoblotting (middle image). RBPMS immunoblotting confirmed the successful coimmunopresipitation. **(B)** IGK input immunoblotting (upper image), follow by IGK IP immunoblotting (middle image). RBPMS immunoblotting confirmed the successful coimmunopresipitation. **(C)** MYH9 input immunoblotting (upper image), follow by MYH9 IP immunoblotting (middle image). RBPMS immunoblotting confirmed the successful coimmunopresipitation. **(D)** MYH10 input immunoblotting (upper image), follow by MYH10 IP immunoblotting (middle image). RBPMS immunoblotting confirmed the successful coimmunopresipitation.

4.14 Prognostic Value of RBPMSA and RBPMSC binds proteins NME1, IGK, MYH9 and MYH10

To assess the clinical relevance of the proteins identified by MS in A2780CP20-RBPMSA and A2780CP20-RBPMSC clones, the Kaplan-Meier plotter data base (KM plotter) was interrogated. NME1 and IGKC bind to RBPMSA and RBPMSC splice variants when overexpressed in the A2780CP20 cell line. In agreement with these results, higher expression levels of this protein were associated with better prognosis of the disease (OS; HR < 1) (Figures 21A and 21B). On the other hand, overexpression of RBPMSA and RBPMSC splice variants bind to MYH9 and MYH10 in A2780CP20. Again, KM plotter data analysis showed that lower expression levels of MYH9 and MYH10 were associated with unfavorable prognosis of the disease (OS; HR < 1) (Figures 21C and 21D). In summary, proteomic analysis showed that few proteins bound to each RBPMS splice variant. Moreover, RBPMS splice variants are associated with proteins which acts as tumor metastasis suppressors and cancer biomarkers.

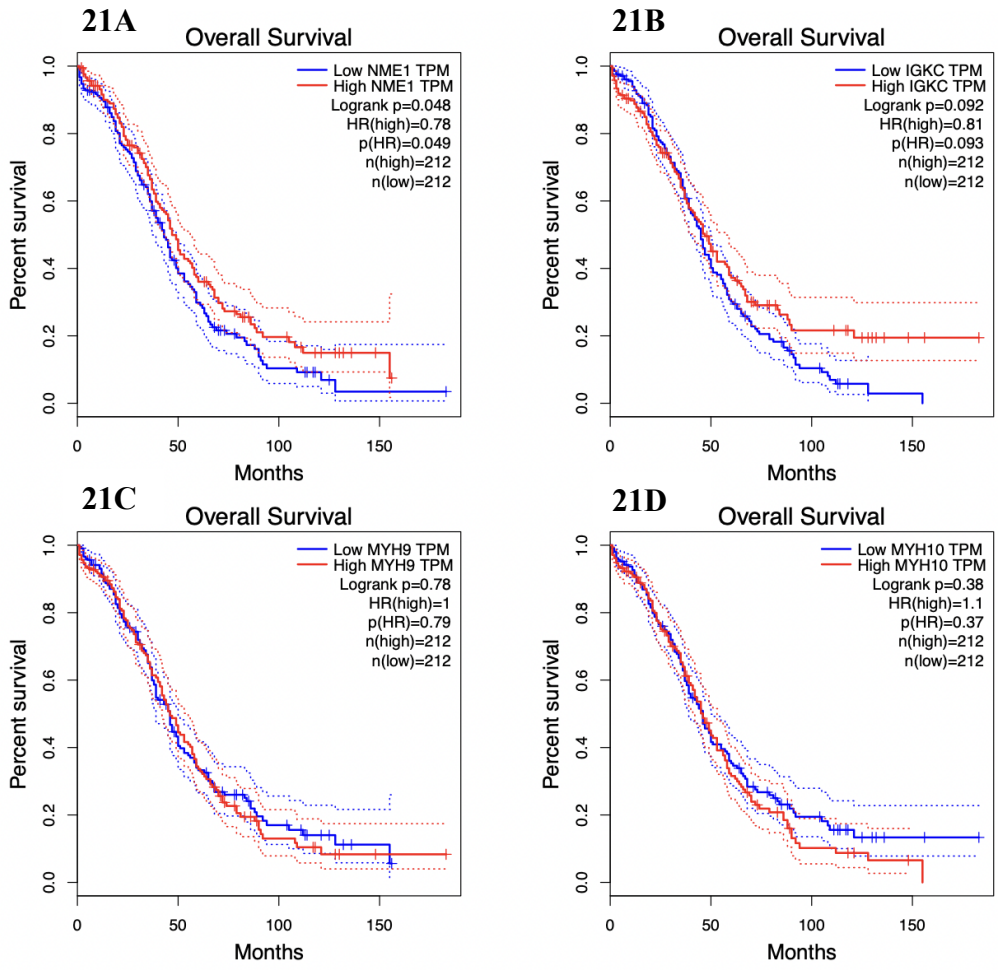

Figure 21: KM survival curves. KM plots for ovarian cancer patients were generated using the KM plotter database. The OS of the ovarian cancer patients was stratified based on the median RNA expression levels for each gene (**A**) NME1 (**B**) IGK (**C**) MYH9 (**D**) MYH10

Chapter 5. Discussion

Accumulating evidence indicates that RBPMS is a key RNA binding protein that is involved in the metabolism of RNA molecules. Several RBPMS splice variants originate from a single primary transcript; three of them have been reported at the protein level: RBPMSA, RBPMSB, and RBPMC. It is speculated that each RBPMS splice variant binds and processes its own group of RNAs [148]. In preliminary studies, CRISPR-mediated RBPMS knockdown reduced the sensitivity of ovarian cancer cells to cisplatin treatment [147]. However, the role of each RBPMS splice variant in ovarian cancer cells had not been studied previously. The reduction of mRNA and protein levels of RBPMSA and RBPMSC in cisplatin-resistant ovarian cancer cell lines, compared to their cisplatin-sensitive counterparts, was reported for the first time in this study. Non-significant mRNA and protein levels of RBPMSB were observed in cisplatin sensitive and cisplatin resistant ovarian cancer cells. Overexpression of RBPMSA and RBPMSC into cisplatin-resistant ovarian cancer cell line A2780CP20 decreased cell growth, migration, invasion, and reduced senescence that were associated with β-Galactosidase levels. Moreover, RBPMSA, but not RBPMSC, increased the sensitivity of ovarian cancer cells to cisplatin treatment. Similar results were obtained by using the HGSOC cell line OVCAR3CIS.

Nakagaki et al. (2019) showed that RBPMS is a master splicing regulator in vascular smooth muscle cells (SMCs) [148]. Knockdown of RBPMS in differentiated smooth muscle cell line PAC1 led to changes in mRNA abundance levels, promoting a differentiated alternative splicing program [148]. Also, Rastgoo et al. (2018) reported that RBPMS restauration by overexpressing miR-138 re-sensitized multiple myeloma cells to the proteasome inhibitor

bortezomib (BTZ) [159]. These two reports only interrogated the canonical RBPMS (RBPMSA, also known as RBPMS1). Fu et al. (2015) showed that decreased expression of RBMSA and RBPMSC promoted cell growth, survival and drug resistance of breast cancer cells [130]. The exact molecular mechanism by which each RBPMS splice variant exerts its biological effects are currently unknown; but Fu et al. (2015) reported that RBPMSA and RBPMSC bind and repress AP-1 transcription factor [130]. Also, Sun et al. (2006) reported that overexpression of RBPMS enhanced Smad's transcriptional activity in human embryonic kidney 293T cells. They showed that interaction of RBPMS with TGF-β receptor type I increased phosphorylation of Smad2 and Smad3, and promoted the nuclear accumulation of the Smad's proteins [239]. Therefore, each RBPMS splice variant could bind to key transcription factors and/or modify its own groups of RNA transcripts. These hypotheses can be further tested in future research endeavors.

The observed overexpression of RBPMSA and RBPMSC in A2780CP20 cells decreased the senescence-associated β-Gal levels of these cells. This effect was accompanied by the increased protein levels of p53 and p38. Curiously, A2780CP20 cells do not express p21 [174]. Decreased expression of p21 and p53, two key cell cycle progression regulators, had also been associated with a senescence phenotype of cancer cells [240]. Santana et al. (2020) studied the effect of Enolase-1 (ENO1) in ovarian cancer cells and observed that decreased expression of ENO1 promoted glucose accumulation, induced senescence, increased the p53 protein levels, and promoted cisplatin resistance of ovarian cancer cells [174]. In addition, the mitogen activated protein kinase p38 activates a wide range of substrates that include transcription factors, protein kinases, and nuclear proteins, thus leading to diverse responses, including senescence and chemoresistance processes [241]. Guo et al. (2008) studied the effect of phosphorylated p38 in the

human gastric cancer cells SGC7901/VCR cell line and observed that inhibition of p38 with the small molecule inhibitor SB203580 reversed the multidrug resistance of these cells [241]. Although evidence indicates that chemotherapy induces a beneficial short term senescence stage during treatment, it could promote changes in gene expression that lead to reprogramming in cancer cells. Reprogramming of these cancer cell populations in a tumor could be an adaptive pathway that later generates more aggressive and highly drug-resistant phenotype clones, characteristic of tumor heterogeneity [242]. Senescent cells are characterized by altered cell metabolism, increased lysosomal capacity, and their potential to secrete different molecules (i.e., pro-inflammatory cytokines and growth factors) to the microenvironment (TME) [240, 243]. The production of all these molecules is known as the senescence associated secretory phenotype (SASP). SASP promotes cell proliferation, induces epithelial to mesenchymal transition EMT [244], enhances invasion [245], and promotes chemo-resistant and radioresistant phenotypes [246]. In consequence, increasing the RBPMS levels could potentially take out cells of senescence stages, and reduce the cell growth and proliferation of cisplatin resistant ovarian cancer cells, which would require further research.

Reduced protein levels of RBPMS have been documented in bladder cancer [161], multiple myeloma [159], ovarian cancer [147], and osteoarthritic cartilage cell lines [149]. However, in these studies, only RBPMSA (RBPMS1) was studied. By using a subcutaneous ovarian cancer mouse model, the increased expression of RBPMSA and RBPMSC that was observed, resulted in smaller tumors compared with the controls. This effect was more noticeable with tumors that overexpressed the RBPMSA isoform. Tumors that overexpressed the RBPMSA isoform also had reduced blood vessel formation and proliferation by measuring CD31 and Ki-67. The results are

in agreement with the studies of Fu et al. (2015), which reported that RBPMSA and RBPMSC reduced proliferation and migration of breast cancer cells, in vitro and in vivo [130].

IP studies allowed us to identify proteins bound to RBPMSA and RBPMSC, including c-Jun, c-Fos, Smad2, Smad3 and Smad4. Sundqvist et al. (2020), suggested that Smad2/3-Fra1 complexes mediate the activation of the Smad/AP-1-dependent TGFβ-induced epithelial mesenchymal transition and invasion program [247]. In addition, Wong et al. (1999) demonstrated that Smad3-Smad4 is important for TGF-β induction of c-Jun, and that AP-1/CRE is also required for TGF-β regulation of the c-Jun promoter [248]. The RNA-binding protein with multiple splicing mediates the transcriptional activity of Smad's proteins, mainly by enhancing the phosphorylation of Smad2 and Smad3 [239]. Upon phosphorylation, Smad's accumulate in the cell nucleus and act as mediators of transcriptional activation [239]. Also, Fu, et al. (2015) reported that RBPMS inhibited breast cancer cell proliferation and migration by blocking the formation of c-Jun-c-Fos or c-Jun-Smad3 complexes. However, their function in ovarian cancer drug resistance needs to be further investigated.

High expression of miR-21 has been related with cancer proliferation in several types of cancer, such as colorectal cancer [249] [250], glioma [251], breast cancer [252], lung cancer [253], and prostate cancer [254]. Echevarria Vargas et al. (2014) showed that miR-21 is a downstream target gene of AP-1 [168]. AP-1 signaling pathway and its protein members c-Jun and c-Fos works as transcription factors involved in a wide variety of physiological responses including cancer. The study suggested that the JNK-1/c-Jun signaling pathway regulates miR-21 expression in ovarian cancer cells. [168]. Moreover, the association between c-Jun and pri-mir-21 DNA promoter

regions was demonstrated. Using a small interference RNA (siRNA) against JNK-1, the major activator of c-Jun phosphorylation, they decreased the expression of pre-mir-21 and increasing the expression of PDCD4 [168].

However, these studies did not address which RBPMS splice variant control the transcriptional activation of pre-miR-21 gene. Del Mar Díaz-González et al. (2019) demonstrated that c-Fos and c-Jun proteins are expressed and regulate the expression of miR-21 in cervical cancer cells [255]. Through DNA sequence analysis and EMSA analyses, they confirmed the presence of AP-1 DNA-binding sites in the human miR-21 promoter region [255]. In this project, siRNA mediated RBPMS knockdown increased the pre-miR-21 transcription activation. This suggests that RBPMSA and RBPMSC control the transcriptional activation of pre-miR-21 in cisplatin resistant ovarian cancer cells. Therefore, the data from this study strengthens the role of an interesting regulatory genetic network involving AP-1/RBPMS and miR-21, which modulates critical genes in ovarian cancer tumorigenesis. Eventually, this knowledge may encourage the use of AP-1, RBPMS and miR-21 as therapeutic targets in ovarian cancer treatment, and to overcome cisplatin resistance.

To further explore the downstream effectors of RBPMSA and RBPMSC in ovarian cancer cells, RNAseq was performed. Firstly, each RBPMS splice variant regulate its own group of transcripts. Within the RBPMSA downstream transcripts, multiple transcripts of genes associated with chemoresistance were identified, including NUPR1 and XAF1 (both increased in this study's RNAseq). Wen Jiang et al. (2006) reported that knockout of NUPR1 (also known as Com-1/p8) correlated with the increased invasiveness and growth of prostate cancer cells [256].

Overexpression of NUPR1 reduced the growth of prostate tumors in athymic mice model [256]. NUPR1 has been shown to interact with transcriptional regulators such as p300, PTIP, estrogen receptor-beta, and Smads [257]. Clack et al. (2008) reported that NUPR1 formed a complex with p53 and p300 in epithelial breast cancer cells [258]. These complexes bound the p21 DNA promoter and transcriptionally upregulated p21 expression [258]. Wen Jiang et al. (2006) suggested that in prostate cancer, NUPR1 acts as a tumor suppressor and facilitator of apoptosis because it was able to trans activates p53 following DNA damage [256]. Interestingly, Jiang et al. (2005) reported an association between low levels of NUPR1 expression with shorter survival in both ERα-positive and ERα-negative breast cancer patients [259]. Together, these observations show that RBPMSA could transcriptionally regulate the expression levels of NUPR1 by interacting with transcriptional regulators. Another possible scenario that would warrant further research is RBPMSA's interaction with the mRNA of NUPR1, which could increase translation into the NURP1 protein.

Increased levels of LINC01504 and decreased levels of SNORD99 were also observed in the RBPMSA overexpressed cells. Increased levels of LINC01504 in the non-small cell lung cancers cell lines A549, NCI-H1650, SK-MES-1, and NCI-H226 exposed to cinnamaldehyde promoted the production of cytokine signaling 1 (SOCS1), BTG anti-proliferation factor 2 (BTG2), and Bruton tyrosine kinase (BTK) [196]. Cinnamaldehyde is the main component extracted from cinnamon, which has antiviral and anti-tumor effects in HepG2 hepatocellular carcinoma cell line [260]. SNORD99, one of the downregulated transcripts in RBPMSA overexpressed clones, was expressed at a higher level in hepatocellular carcinoma patient tissue samples, and in the hepatocellular carcinoma cell lines SK-Hep1 and HCCLM9 [261]. Increased

levels of SNORD99 have been implicated in the regulation of cell proliferation and death balance by promoting cancer cell plasticity [261]. This evidence suggests that RBPMSA could inhibit transcription factors that regulate SNORD99 expression (i.e., AP-1). Moreover, RBPMSA expression levels could enhance the LINC01504 levels by promoting its RNA processing, through the JAK/STAT3 signaling pathway.

Overexpression of RBPMSC increased the RNA levels of DAB2, SLFN11, FOXD3-AS1, PTGER4, among others. These transcripts have been endowed with tumor suppressor capabilities and better prognostic patient outcomes [217, 262] [263]. For example, high levels of DAB and PTGER4, two of the top upregulated genes in RBPMS clones, act as tumor suppressor genes. Jia et al. (2014) reported that in human colorectal cancer, loss of DAB increased cellular migration, reduced sensitivity to chemotherapeutic agents, and markedly reduced survival rate [262]. Tseng et al. (1999) reported that the phosphorylation of the DOC-2/DAB2 protein complex inhibited the AP-1 activity [264]. In addition, Murn et al. (2008) reported that PTGER4 knockdown accelerated tumor growth, whereas PTGER4 overexpression yielded significant protection to B cell lymphoma development through the intrinsic activity between PTGER4 and PGE2–EP4 signaling target genes [217]. PTGER4 expression had an inhibitory effect on the transcriptional activity of the AP-1 components c-Fos and c-Jun [217]. Also, expression of PTGER4 decreased the expression of IL-2 promoter, which is critically important AP-1 signaling activation [217]. These reports are in agreement with Fu et al. (2015)'s study, in where RBPMS splice variants bind to c-Fos and c-Jun and inhibit the binding of the AP-1 complex to its DNA recognition sites [130].

Decreased mRNA levels of TP63 in RBPMSC overexpressing clones were also observed. TP63 is a critical suppressor of tumorigenesis and metastasis [265]. Sundqvist et al. (2020) reported that in breast cancer cell lines HCC1954, HCC202, MCF10A MI, and MII; TP63 is a AP-1 downstream effector [247]. In the same report, TP63 strongly potentiates TGFβ induction of AP-1 protein members, in particular c-Fos [247]. Moreover, TP63 stabilized the interactions between Smad's and AP-1, and enhanced the binding of Smad's/AP-1 complexed in the chromatin [247]. These reports are in agreement with evidence that RBPMS splice variants interact with Smad's and/or c-Jun and c-Fos to regulate AP-1/Smad's-dependent genes. Interestingly, Lau et al. (2013) reported that TP63 knockdown decreased the proliferation of neoplastic stromal cells, through CDC2 and CDC25C suppression [266]. Also, Senoo et al. (2013) reported that TP63 null tymus epithelial cells decreased their proliferative rate as compared with normal cells [267]. These pathways could contribute to the reduced cell proliferation of RBPMS overexpressed clones. However, the mechanism by which RBPMS regulates TP63 function needs further investigation.

Within the RNA regulated transcripts shared by both, A2780CP20-RBPMSA and A2780CP20-RBPMSC overexpressing clones, genes associated with biological processes including ion transportation, lipid biogenesis, collagen remodeling, tumor microenvironment, and immune response activity were identified. For example, decreased mRNA levels of NRP1 were observed in the top 20 RNA transcripts shared between A2780CP20-RBPMSA and A2780CP20-RBPMSC overexpressing clones. Neuropilin-1 (NRP1) is a cell surface glycoprotein that has been previously associated with nervous system axonal guidance and as a receptor for the collapsin/semaphorin family of proteins [268]. Soker et al. (1998) showed that coexpression of NRP1 with the kinase insert domain receptor (KDR) increased VEGF, angiogenesis as well as

chemotaxis in porcine aortic endothelial cells line PAE [269]. Also, Gagnon et al. (2000) reported that inhibition of AP-1 significantly attenuated VEGF-dependent NRP1 in human umbilical vascular endothelial cells (HUVECs) [234]. These results suggest that RBPMSA and RBPMSC could bind and metabolize RNA transcripts associated with a variety of cellular processes.

Using Kaplan–Meier analysis of publicly available mRNA expression (RNA-Seq data), it was further observed that several RNA transcripts differentially abundant in RBPMSA and RBPMSC overexpression clones are significantly associated with survival outcomes in ovarian cancer patients. In particular, BST2 (also known as CD317), GBP4, and SLC15A3 were associated with OS but not with PFS. Wang et al. (2018) observed that high expression of GBP4 was correlated with good overall survival in cutaneous skin melanoma [194]. SLC15A3 has been postulated by Song et al. (2018) as a prognostic biomarker and target in lung adenocarcinoma [195]. Yi et al. (2020) reported that overexpression of CYP24A1 plays an essential role in enhancing immune activity and inhibiting tumorigenesis [270]. Opposite, PPP1R1C has been linked by Liu et al. (2017) with the progression and resistance to temozolomide therapy in glioblastoma [215]. Wan et al. (2020) identified FOXD3-AS1 as a cancer-promoting gene in glioma [218]. In addition, Li et al. (2021) suggested that downregulation of COL12A1 has a key role in regulating tumor immune interactions [207]. Therefore, further studies are needed to confirm the biological role of these RBPMS downstream genes and their diagnostic, prognostic, and/or therapeutic potential in ovarian cancer.

Furthermore, IP/MS studies allowed us to identify proteins bound to RBPMA and RBPMSC variants including Diphosphate Kinase 1 (NME1), Immunoglobulin Kappa Locus

(IGK), Myosin Heavy Chain 9 (MYH9), and Myosin Heavy Chain 10 (MYH10). The nucleoside diphosphate kinase A is an enzyme that, in humans, is encoded by the NME1 gene, which catalyzes the exchange of terminal phosphate between different nucleoside diphosphates to produce nucleotide triphosphates [271]. The immunoglobulin kappa locus (IGK) is a region in chromosome 2, which contains genes for the kappa light chains of immunoglobulins. IGK locus includes the variable (V), joining (J), and constant (C) segments of the immunoglobulins. For that reason, their biological role crucial in the initiate immune responses, such as phagocytosis and the complement system. Myosin Heavy Chain 9 and Myosin Heavy Chain 10 are highly conserved ubiquitous actin-based motor proteins that drive a wide range of motile processes in eukaryotic cells. These proteins convert the chemical energy derived from hydrolysis of ATP into mechanical force. MYH9 and MYH10 drives a diverse motile process including cytokinesis, vesicular transport, and cellular locomotion.

The role of NME1, IGK, MYH9 and MYH10 in cancer has been studied in difference instances at transcriptional level [272-275]. Reduced levels of NME1 are associated with highly metastatic cells [271]. NME1 is also involved in cell proliferation, differentiation and development, signal transduction, G protein-coupled receptor endocytosis, and gene expression [276]. Also, studies demonstrated an affinity of NME1 for single-stranded motifs in the promoter regions of c-MYC, TP53 and PDGFA, as well as the ability to regulate transcription from those promoters [277-279]. Therefore, the interaction of NME1 and RBPMS splice variants A and C, could be control the expression of proto-oncogene and tumor suppressor genes such as c-MYC and TP53, respectively. Moreover, IGK plays a role in pathways related with CD16 in NK cells during immune system response [273, 280]. IGK is altered in 0.18% of all cancers such as breast

invasive ductal carcinoma, endometrial endometrioid adenocarcinoma, diffuse large B-cell lymphoma, bladder urothelial carcinoma, and Burkitt lymphoma having the greatest prevalence of alterations [281]. The interaction between IGK and RBPMSA could be controlling the transcription of genes related to the tumor microenvironment and immune system response. Previous studies suggested that the interaction between RBPMS and MET proteins promotes an aberrant cell signaling pathway expression related with tumor microenvironment [273]. Perhaps, the interaction between IGK and RBPMSA could have the same function.

MYH10 has diverse functions that include regulation of cytokinesis, cell motility, and cell polarity. This protein is involved in the stabilization of type I collagen mRNAs for CO1A1 and CO1A2 [282]. MYH9 plays a role in cytokinesis, cell shape, and specialized functions such as secretion and capping. Also, during cell spreading, MYH9 is involved in cell motility maintenance of cell and cell focal contact formation [274]. Nakagaki-Silva et al. (2019) showed that RBPMS directly regulates components of the actin cytoskeleton and focal adhesion machineries, whose activity is critical for vascular smooth muscle cell's function [153]. The interaction between RBPMS splice variants A and C, MYH9, and MYH10, presented in this study, could explain the role of RBPMS in the RNA splicing involved in cytoskeletal signaling pathways.

Using Kaplan Meier analysis, high levels of NME1 were observed and seen to be related with a good overall survival outcome in ovarian cancer patients. In agreement with these results, Shi et al. (2018) reported that NME1 was linked to improve overall survival in gastric cancer [272]. Also, increased level of IGK in RBPMSA and RBPMSC overexpressing clones is associated with good overall survival in cancer patients. Kacsoh et al. (2022) reported that high levels of IGK in

pediatric neuroblastoma, one of the most common pediatric cancers, is associated with better overall survival [283]. In contrast, increased levels of MYH9 and MYH10 remarkably correlate with poor prognosis and represents a novel biomarker and drug target for the diagnosis and treatment of esophageal cancer [284]. Wang et al. (2018) showed that overexpression of MYH10 protein is associated with malignant tumors [275]. However, the biological consequences of these proteins NME1, IGK, MYH9, and MYH10 in ovarian cancer cells, and their association with cisplatin resistance are not well understood which demands further investigation.

Overall, this study provides evidence that increased expression of RBPMSA and RBPMSC contribute to the reduction of ovarian cancer cell proliferation, invasion, and migration. However, only RBPMSA was associated with the cisplatin sensitivity of ovarian cancer cells. RBPMSA and RBPMSC negatively regulated the pre-miR-21 transcriptional activation. Furthermore, RBPMSA and RBPMSC bind to c-Fos and c-Jun, protein members of the AP-1 transcription factor. RBPMSA and RBPMSC emerge as possible candidates that could control the transcriptional activation of the AP-1 downstream target genes. Also, RBPMSA and RBPMSC control the expression of RNAs that is associated with the remodeling of the tumor microenvironment, cell proliferation, cell survival, and cell integrity, among others. These findings highlight the important role of RBPMS splice variants in the regulation of gene expression in health and disease.

Although this study focused on the biological role of RBPMSA and RBPMSC in ovarian cancer, we identified several other downstream target genes whose clinical and therapeutic relevance remains unknown. Future studies need to be conducted to confirm their potential as therapy and their relevance in cancer drug resistance. Also, studies should be performed to

investigate the relation of RBPMSA and RBPMSC with other microRNAs in addition to pre-miR-21. Moreover, further studies should assess if RBPMS interacts or is associated with other transcription factors by regulating gene expression at the transcriptional and posttranscriptional level. Lastly, the role in cancer of RBPMS predicted splice variants (RBPMSB, RBPMSE) needs to be investigated.

Chapter 6. Conclusions and Future Directions

Cancer is one of the leading cause of death worldwide. In 2020, the International Agency for Research on Cancer, in collaboration with the World Health Organization, reported 19,094,716 million new cases and 10 million deaths. Today, 1.3% of people in the worldwide population live with cancer. Ovarian cancer is one of the six most common cancers among women and the most common cause of gynecological cancer-related deaths in western countries, with a survival proportion of 40% to 50% in the first five years of diagnosis [6]. Depending on the type of ovarian cancer and how advanced it is, the standard medical care plans for patients can include cytoreductive surgery combined with platinum and taxane based chemotherapy. Unfortunately, this disease remains the most aggressive and malignant gynecological cancer. Though 60%-80% of patients initially respond to the traditional treatment, only 10% to 30% of them eventually recur and develop resistance to platinum-based chemotherapy [170]. Furthermore, a combination of cytotoxic agents (gemcitabine, pegylated liposomal doxorubicin, and topotecan) and a second cycle of chemotherapy are recommended for these patients, but the efficacy has not yet been determined. Platinum-based chemotherapy such as cisplatin, is one of the most active anticancer agents now used, and resistance represents a major obstacle to overcome. As a result, the survival

rate for patients with ovarian cancer has not improved over the past 20 years [159]. It is imperative to understand and identify molecules that are involved in the platinum resistance/sensitivity-related mechanisms.

RNA binding protein with multiple splicing (RBPMS) is a member of a family of proteins that bind to the nascent RNA and control their pre-mRNA processing, splicing, alternative splicing, RNA editing, mRNA export, mRNA stability, pre-rRNA complex formation, translational regulation, and protein degradation [147]. However, the functions of many more biological processes and their relevance to disease states remain to be elucidated. Recently, studies explored the functions of RBPMS in vascular smooth muscle cell differentiation, aging, oogenesis, and retina ganglion cell. Nakagaki-Silva et al. (2019) reported that RBPMS highly down-regulated phenotypic switching of smooth muscle cells from a contractile to a motile [153]. Moreover, RBPMS is responsible for 20% of the alternative splicing changes during this transition. In breast cancer, RBPMS interacts with AP-1 protein members in vitro. Fu et al. (2015) demonstrated that RBPMS inhibited the growth and migration of breast cancer cells through its interaction with c-Fos or Smad3. RBPMS inhibited c-Fos or Smad3-mediated AP-1 transactivation and the expression of AP-1 target genes known to be the key regulators of cancer growth and progression. Some of the AP-1 target genes include the vascular endothelial growth factor (VEGF) and cyclin D1. Mechanistically, it is speculated that RBPMS blocks the formation of the c-Fos/c-Jun or Smad3/c-Jun complex as well as the recruitment of c-Fos or Smad3 to the promoters of AP-1 target genes [133].

This study is novel because it reports, for the first time, CRISPR-mediated RBPMS knockdown promoted cell proliferation and invasion, as well as increased the cisplatin resistance of ovarian cancer cells. The study also concluded that RBPMS expression levels can be reduced in ovarian cancer patients, since they were reduced in cisplatin resistant ovarian cancer cells, compared to cisplatin sensitive cells. Until today, no previous scientific evidence reported the biological function of RBPMS in ovarian cancer; much less, which splice variants are related to cisplatin resistance.

In this dissertation, a systematic experimental validation and bioinformatic analysis was developed to unravel the role of RBPMSA and RBPMSC splice variants in ovarian cancer and cisplatin drug resistance. Western blot analyses were performed to determine the protein expression of RBPMS splice variants A and C in ovarian cancer cell panels. RBPMSA and RBPMSC was highly expressed in cisplatin-sensitive, compared with cisplatin-resistant ovarian cancer cells. The results also demonstrate that increased expression of RBPMSA and RBPMSC splice variants reduced cell proliferation, invasion, and migration in ovarian cancer cells. However, only RBPMSA was associated with the cisplatin sensitivity of ovarian cancer cells. Using a mouse model, increased expression of RBPMSA and RBPMSC was seen to result in smaller tumors compared with controls. This effect was more noticeable with tumors overexpressing the RBPMSA isoform. Tumors overexpressing the RBPMSA and RBPMSC splice variants also had reduced cell proliferation rate and blood vessel formation.

In addition, evidence was provided on how RBPMSA and RBPMSC interact with the transcription factors c-Fos, c-Jun, Smad2, Smad3, and Smad4. Previous research suggested that

RBPMS is a critical repressor of AP-1 signaling [130]. The data of this dissertation demonstrated that RBPMSA and RBPMSC interacted with c-Fos and c-Jun in ovarian cancer cells. Therefore, in agreement with previous reports, RBPMSA and RBPMSC could be critical repressors of AP-1 signaling and its activation should be a valuable strategy for ovarian cancer treatment.

Using RNA sequencing of RBPMSA and RBPMSC overexpressing clones unveiled the transcriptional changes that these cells go through when they express one of these protein splice variants. Evidence indicates that RBPMSA and RBPMSC control the expression of RNA transcripts associated with remodeling the tumor microenvironment, cell proliferation, cell survival, cell integrity, among others. These findings highlight the vital role of RBPMS splice variants in the regulation of gene expression in health and disease. Moreover, through CO-IP/MS assay, RBPMS was found to directly bind to proteins such as NME1 and IGK, among others. High levels of NME1 and IGK in cancer patients are significantly related with overall survival in ovarian cancer patients. However, their function in ovarian cancer and relation with RBPMSA and RBPMSC merits further investigation.

This project contributes significant findings for understanding the role of RBPMS and their splice variants in cancer. It identifies RBPMS splice variants A and C as potential tumor suppressors in ovarian cancer. Despite the significant impacts of this project, many questions remain unanswered. Notwithstanding, this project could pave the way for the future development of further research projects, with the following suggested aims:

1. To perform a comprehensive identification of the RNA interacting with each of the RBPMS splice variants in nuclear and cytoplasm fraction by immunoprecipitation, followed by sequencing (Clip-seq). Clip-seq is a novel technique that has become one of the standard techniques to identify in vivo transcriptome-wide binding sites of RNA binding proteins. In general, the cells are treated by UV, which introduces covalent bonds between the RNA and protein that are in direct contact. Then, the cells are lysed and treated with an RNase to degrade naked RNAs, but not RNA regions bound by proteins. The target RNA Binding Protein (in our case RBPMS) and the RNA fragments it binds are isolated via immunoprecipitation. The RNA and protein complex are then resolved on an SDS-PAGE gel, followed by transferal to a membrane. The RNA-protein complexes are cut in the membrane, and proteinase K digestion is used to separate the RNA Binding Protein from the RNA-protein complexes. The resulting RNA fragments are subject to library construction, followed by high throughput sequencing.

2. To generate CRISPR/Cas9 RBPMS knockout mouse models by injecting Cas9 mRNA and multiple single guide RNAs directly into the embryos to induce precise genomic edits. Following these embryos will be transfer into oviduct of surrogate mother. Genotype the mice that develop from these embryos to determine if they carry the RBPMS knockout, and those that do, breed to confirm germline transmission. These genetically engineered animal models should be used to study the biological process and pathological diseases in which RBPMS was involved.

3. To confirm the role of RBPMS as a tumor suppressor gene in mice. In these experiments, double allele mutations RBPMS-/- need to be generated, combined with mutations in other critical oncogenes/tumor suppressor genes, including c-MYC, PTEN, AKT, APC, ATM, CHK2, VHL, or TP53. For this experiment, advantage can be taken of the CRISPR-mediated lentivirus transfections to generate a new clone. The generated doble mutated clones would be implanted

into the mice's ovaries or fallopian tubes, by micro injection. These studies could evaluate the molecular and physiological effects of RBPMS in vivo, and elucidate the effect on angiogenesis, apoptosis, and cellular proliferation.

4. To identify whether other RBPMS splice variants (RBPMSB, RBPMSD, and RBPMSE) are expressed in normal and cancer cells. Specific antibodies could be generated against the C-terminal of the RBPMSB, RBPMSD, and RBPMSE. This would require the determination of protein and mRNA levels of RBPMSB, RBPMSD, and RBPMSE in a panel of cisplatin-sensitive and cisplatin-resistant ovarian cancer cells using a western blot and RT-PCR, respectively.

5. To perform comprehensive identification of the sites, at which RBPMS binds to the RNA within RNA-protein complexes. In this technique, the RNA-protein complexes are immunoprecipitated with the antibodies targeted to the protein of interest (In our case, we can use the DDK-Tag-RBPMS clones). Then, RNase digestion is performed where RNA, protected by protein binding, is extracted and reverse transcribed to cDNA. The exact locations of the proteins and RNA's interactions can then be mapped back to the genome.

6. To perform IP-Ms experiments after crosslink proteins interact with different RBPMS splice variants. Crosslinking is the process of chemically joining two molecules by a covalent bond. This process could help identify more RBPMS interacting proteins; in this study, there was loss during the multiple washing steps while completing the IP protocol.

7. To assess RBPMS as a diagnostic biomarker for ovarian cancer and other types of cancer. To consider RBPMS as good biomarker, it must meet the following criteria:

a. Be specific for ovarian cancer

b. Easy to measure and safe for the patients

c. Rapid detection which allows for faster diagnosis

e. Able to give accurate results within a short period of time

f. Be consistent between ethnic groups or genders.

The expression levels of RBPMS in tumor biopsies could be evaluated in a large group of samples by qRT-PCR and immunohistochemistry to predict cancer drug response.

8. To assess whether the RBPMS splice variants levels are related to the sensitivity of ovarian cancer cells in other chemotherapeutic agents, such as carboplatin, vinorelbine, gemcitabine, paclitaxel, docetaxel, etoposide, and pemetrexed.

9. To identify other miRNAs that potentially able to potentially regulate the RBPMS splice variants at the posttranscriptional level.

Appendix A

Isoforms messenger RNA aliments of NM_001008710.3 Homo sapiens RNA binding protein, mRNA processing factor (RBPMS), transcript variant 1, mRNA (Isoform A), NM_001008711.3 Homo sapiens RNA binding protein, mRNA processing factor (RBPMS), transcript variant 2, mRNA (Isoform B) and NM_001008712.2 Homo sapiens RNA binding protein, mRNA processing factor (RBPMS), transcript variant 3, mRNA (Isoform C). In Blue the sequence that not has been share between mRNA sequence isoforms.

Isoform A: agagcctgcc tggagcgcgt actcagcggc tctcgggtcc cagcgtccca gccgcggccc gcgctcctcc gccccgctcc

Isoform B: agagcctgcc tggagcgcgt actcagcggc tctcgggtcc cagcgtccca gccgcggccc gcgctcctcc gccccgctcc

Isoform C: aaggcgagag aaagggagct gcttccatcc cggacttccc agagcctgcc tggagcgcgt actcagcggc tctcgggtcc

Isoform A: tcctcctcct cttcctcctc ctcctcctct ctaggcaccc ccgtcccctc cttccagcgg ctgcagcccc cagccccaac

Isoform B: tcctcctcct cttcctcctc ctcctcctct ctaggcaccc ccgtcccctc cttccagcgg ctgcagcccc cagccccaac

Isoform C: cagcgtccca gccgcggccc gcgctcctcc gccccgctcc tcctcctcct cttcctcctc ctcctcctct ctaggcaccc ccgtcccctc

Isoform A: tctccgcgct tactcctggg acgcgcgtcc tcgccccatc ctttgcttcc ttccttcctt ccttcttcct tcctcccctg gctcccgccc tccctctcca

Isoform B: tctccgcgct tactcctggg acgcgcgtcc tcgccccatc ctttgcttcc ttccttcctt ccttcttcct tcctcccctg gctcccgccc tccctctcca

Isoform C: cttccagcgg ctgcagcccc cagccccaac tctccgcgct tactcctggg acgcgcgtcc tcgccccatc ctttgcttcc ttccttcctt

Isoform A: ggtcgccctc ccggggcccg attgtctcgg tgccccgctc ccggcccgcg ccctgccccg tctctccctt gcacttcctg agtcgcccgc

Isoform B: ggtcgccctc ccggggcccg attgtctcgg tgccccgctc ccggcccgcg ccctgccccg tctctccctt gcacttcctg agtcgcccgc

Isoform C: ccttcttcct tcctcccctg gctcccgccc tccctctcca ggtcgccctc ccggggcccg attgtctcgg tgccccgctc ccggcccgcg

Isoform A: gcagactcgc cgcgggagcc ccagcccaac ccgagcccga cagccactgc cccggctcca gctccagccc cacagcccgc

Isoform B: gcagactcgc cgcgggagcc ccagcccaac ccgagcccga cagccactgc cccggctcca gctccagccc cacagcccgc

Isoform C: ccctgccccg tctctccctt gcacttcctg agtcgcccgc cgccgccgtc gcagactcgc cgcgggagcc ccagcccaac

Isoform A: ggcgcccgcc cgagggagcc ccggcgcccg gggaaggctc cagtgggcta gcgcgccctc gcccagcccc gcgccccagc

Isoform B: ggcgcccgcc cgagggagcc ccggcgcccg gggaaggctc cagtgggcta gcgcgccctc gcccagcccc gcgccccagc

Isoform C: ccgagcccga cagccactgc cccggctcca gctccagccc cacagcccgc ccgagcccga cagccactgc cccggctcca

Isoform A: cctgcccggc ccggcgagga aggaccggga agatgaacaa cggcggcaaa gccgagaagg agaacacccc gagcgaggcc

Isoform B: cctgcccggc ccggcgagga aggaccggga agatgaacaa cggcggcaaa gccgagaagg agaacacccc gagcgaggcc

Isoform C: gctccagccc cacagcccgc ggcgcccgcc cgagggagcc ccggcgcccg gggaaggctc cagtgggcta gcgcgccctc

Isoform A: aaccttcagg aggaggaggt ccggacccta tttgtcagtg gccttcctct ggatatcaaa cctcgggagc tctatctgct

Isoform B: aaccttcagg aggaggaggt ccggacccta tttgtcagtg gccttcctct ggatatcaaa cctcgggagc tctatctgct

Isoform C: gcccagcccc gcgccccagc cctgcccggc ccggcgagga aggaccggga agatgaacaa cggcggcaaa gccgagaagg

Isoform A: tttcagacca tttaagggct atgagggttc tcttataaag ctcacatcta aacagcctgt aggttttgtc agttttgaca gtcgctcaga

Isoform B: tttcagacca tttaagggct atgagggttc tcttataaag ctcacatcta aacagcctgt aggttttgtc agttttgaca gtcgctcaga

Isoform C: agaacacccc gagcgaggcc aaccttcagg aggaggaggt ccggacccta tttgtcagtg gccttcctct ggatatcaaa cctcgggagc

Isoform A: agcagaggct gcaaagaatg ctttgaatgg catccgcttc gatcctgaaa ttccgcaaac actacgacta gagtttgcta aggcaaacac

Isoform B: agcagaggct gcaaagaatg ctttgaatgg catccgcttc gatcctgaaa ttccgcaaac actacgacta gagtttgcta aggcaaacac

Isoform C: tctatctgct tttcagacca tttaagggct atgagggttc tcttataaag ctcacatcta aacagcctgt aggttttgtc agttttgaca gtcgctcaga

Isoform A: gaagatggcc aagaacaaac tcgtagggac tccaaacccc agtactcctc tgcccaacac tgtacctcag ttcattgcca gagagccata

Isoform B: gaagatggcc aagaacaaac tcgtagggac tccaaacccc agtactcctc tgcccaacac tgtacctcag ttcattgcca gagagccata

Isoform C: agcagaggct gcaaagaatg ctttgaatgg catccgcttc gatcctgaaa ttccgcaaac actacgacta gagtttgcta aggcaaacac

Isoform A: tgagctcaca gtgcctgcac tttaccccag tagccctgaa gtgtgggccc cgtaccctct gtacccagcg gagttagcgc ctgctctacc

Isoform B: tgagctcaca gtgcctgcac tttaccccag tagccctgaa gtgtgggccc cgtaccctct gtacccagcg gagttagcgc ctgctctacc

Isoform C: gaagatggcc aagaacaaac tcgtagggac tccaaacccc agtactcctc tgcccaacac tgtacctcag ttcattgcca gagagccata

Isoform A: tcctcctgct ttcacctatc ccgcttcact gcatgcccag atgcgctggc tccctccctc cgaggctact tctcagggct ggaagtcccg

Isoform B: gagttagcgc ctgctctacc tcctcctgct ttcacctatc ccgcttcact gcatgcccag ctctgtgaag gtcagactgt gaggagaagc

Isoform C: tgagctcaca gtgcctgcac tttaccccag tagccctgaa gtgtgggccc cgtaccctct gtacccagcg gagttagcgc ctgctctacc

Isoform A: tcagttctgc tgaatactat gtcccaggtg tgtgatggcg gctgcaatct gtcttgtggg tattaatgca atcttcagtg gtggctactg

Isoform B: caccccttga gcgctccgtc tcctgatagt gccagcctgg cctggtttcc tgtttgatgc gctggctccc tccctccgag gctacttctc

Isoform C: tcctcctgct ttcacctatc ccgcttcact gcatgcccag tgtttctctc ctgaggcaaa gcccaacaca cctgtctttt gtccacttct

Isoform A: ttctctagct gttctacaaa actggagcat gctggcttga aaaaccctg cccagttttg atcccttcaa gactttgtca cagcctctat

Isoform B: gccagcctgg cctggtttcc tgtttgatgc gctggctccc tccctccgag gctacttctc agggctggaa gtcccgtcag ttctgctgaa

Isoform C: ccagcaaatt gcccaacaca cctgtctttt gtccacttct ccagcaaatt agatttgtct ctgggaatgt gtttgtaaca taccaaccta

Isoform A: cacacatctg tttttctcga agaaaaaaat ataattaata aaaatgtttt actcttttac actgtataat tttttctcga agaaaaaaat

Isoform B: tactatgtcc caggtgtgtg atggcggctg caatctgtct tgtgggtatt aatgcaatct tcagtggtgg ctactgttct ctagctgttc

Isoform C: ctgcagacca gcagagggag ctcccatgtt gaatttgttt gttagctatt ttccccccctt tcacaaaaac tatttcttga cgacctttga

Isoform A: ataattaata aaaatgtttt actcttttac actgtataat tgtaagaaat agcgtattat ttgtgaatgc atggtctgaa atttctgtac

Isoform B: tacaaaactg gagcatgctg gcttgaaaaa cccttgccca gttttgatcc cttcaagact ttgtcacagc ctctatcaca catctgtttt

Isoform C: gagatttcaa taaaaatttt aatcagagca aaaatgaact caaaaaaaaa aaaaaa

Isoform A: agtttggaga tgtaagaaat agcgtattat ttgtgaatgc atggtctgaa atttctgtac agtttggaga tattttcaaa cgaaacgtaa

Isoform B: ttgtcacagc ctctatcaca catctgtttt tctcgaagaa aaaaatataa ttaataaaaa tgttttactc ttttacactg tataattgta

Isoform A: tattttcaaa cgaaacgtaa gagaagtcaa caataaaacc aagaaaagtg agtattttta taccaaacat tttaagtatg ctgggatgga

Isoform B: agaaatagcg tattatttgt gaatgcatgg tctgaaattt ctgtacagtt tggagatatt ttcaaacgaa acgtaagaga agtcaacaat

Isoform A: cgatcttaca ctggtttgga tcacagtttt tgttcttgac ttttgaatgc ttgtaattaa aaatatctat ttttttcctc tgaagtaagt

Isoform B: aaaaccaaga aaagtgagta tttttatacc aaacatttta agtatgctgg gatggacgat cttacactgg tttggatcac agtttttgtt

Isoform A: tgcatgtttg aggcatgttt ccaaatatta tcaaaatatc ctgaattgta ttgtgaatat atagaaatct gtgcctggcc ggagtccagg

Isoform B: cttgactttt gaatgcttgt aattaaaaat atctattttt ttcctctgaa gtaagttgca tgtttgaggc atgtttccaa atattatcaa

Isoform A: gtaaattagt agcatggtgt tagatgttag aaacagaact gttatttgca gtgttaggtc taggatccca gttctagtag gacagccctg

Isoform B: atctatttttt ttcctctgaa gtaagttgca tgtttgaggc atgtttccaa atattatcaa aatatcctga attgtattgt gaatatatag

Isoform A: caagacaatc aaccagaagc ctccaggagc ttctacctat ggcttattca caactgggca agaaaacatc attggtaaga actgctgagt

Isoform B: aaatctgtgc ctggccggag tccagggtaa attagtagca tggtgttaga tgttagaaac agaactgtta tttgcagtgt taggtctagg

Isoform A: gtgcccttag aaagccctag tagctccagc tgtgactata tcaactgtgt gccaagtgtg actttgtaca gttttatgtt tccactctcc

Isoform B: atcccagttc tagtaggaca gccctgcaag acaatcaacc agaagcctcc aggagcttct acctatggct tattcacaac tgggcaagaa

Isoform A: tgtgactata tcaactgtgt gccaagtgtg actttgtaca gttttatgtt tccactctcc tgtgactata tcaactgtgt gccaagtgtg

Isoform B: aacatcattg gtaagaactg ctgagtgtgc ccttagaaag ccctagtagc tccagctgtg actatatcaa ctgtgtgcca agtgtgactt

Isoform A: actttgtaca gttttatgtt tccactctcc tgtatgtgta gccactcgat gcctaaccta ccttccacaa gccagccccg catccctgct

Isoform B: tgtacagttt tatgtttcca ctctcctgta tgtgtagcca ctcgatgcct aacctacctt ccacaagcca gccccgcatc cctgctcccg

Isoform A: cccgcagtgt aagtgcagag cctgcctcac tggtaaggga aaaccttggc ttgggaggcc agccctggcc cttgaagggg

Isoform B: ccacaagcca gccccgcatc cctgctcccg cagtgtaagt gcagagcctg cctcactggt aagggaaaac cttggcttgg

Isoform A: ttggctgtgc ccagcccacc tggctgcagt gggcagctca tgtctgtatc tccaaagtga tgtttgtttg caaaacaccg

Isoform B: gaggccagcc ctggcccttg aaggggttgg ctgtgcccag cccacctggc tgcagtgggc agctcatgtc tgtatctcca

Isoform A: gctgaactga gctggtgttg ccaactcttg gcagcactgg gccaaaccga ccacatacca tgagctccca aatggcgtg

Isoform B: aagtgatgtt tgtttgcaaa acaccggctg aactgagctg gtgttgccaa ctcttggcag cactgggcca aaccgaccac

Isoform A: gctcactgtg agacgtcctg ccacacccca caggagacgg aggcagtggg catttggaac caattctatt cagacttcgt

Isoform B: ataccatgag ctcccaaatg gcgtgtgctc actgtgagac gtcctgccac accccacagg agacggaggc agtgggcatt

Isoform A: caaagccaaa gtcagtctgg tgttgtcagt tgacacatct ccagagttca tgacagctca acctctcccc ttgtacagaa

Isoform B: tggaaccaat tctattcaga cttcgtcaaa gccaaagtca gtctggtgtt gtcagttgac acatctccag agttcatgac

Isoform A: gccatttttg taaaaccaca ctgacctaaa ttcagctgcc aaacacagtc tttcctattg atccgctcgg cttatgttga aaatttcaat

Isoform B: agctcaacct ctccccttgt acagaagcca tttttgtaaa accacactga cctaaattca gctgccaaac acagtctttc ctattgatcc

Isoform A: gtcatgatta cctggttggt ttgggttttt gttttgttat tttccattag aaatataaag atgtcaagaa gcttttaaag gtcaacacaa

Isoform B: gctcggctta tgttgaaaat ttcaatgtca tgattacctg gttggtttgg gtttttgttt tgttattttc cattagaaat ataaagatgt

Isoform A: aaaaccaagg ccaggagtga ggggctcttt cttaccgtaa ataaggggaa aaggcagtta gctcaaggac ttgtgacgga

Isoform B: caagaagctt ttaaaggtca acacaaaaaa ccaaggccag gagtgagggg ctctttctta ccgtaaataa ggggaaaagg

Isoform A: tccactttgg tgttcaagga cctgcttatg ccctcagtgc caatcggctc ttggtgagat gactgtactc ctaaggaaaa

Isoform B: cagttagctc aaggacttgt gacggatcca ctttggtgtt caaggacctg cttatgccct cagtgccaat cggctcttgg

Isoform A: tagccacttc tgcagtctat tatgctttta taactgttta aaggtacttt tctattgtca tttttaaaaa ataaagtgct tattccagct gtca

Isoform B: tgagatgact gtactcctaa ggaaaatagc cacttctgca gtctattatg cttttataac tgtttaaagg tacttttcta ttgtcatttt

Isoform B: taaaaaataa agtgcttatt ccagctgtca ccagctgtca

Appendix B

Amino acid alignment of the three well studied RBPMS protein isoforms. Isoform Protein sequences according to Unitpro.org, Accession number: Q93062. We performed alignments with the Multiple Sequence Alignment by CLUSTALW program (https://www.genome.jp/tools-bin/clustalw). In red, the amino acid sequence that changes between isoforms. In blue, the RRM domain characteristic of RNA binding proteins. In green, the antibody sequence that recognized the sigma RBPMS antibody.

Isoform A: MNNGGKAEKENTPSEANLQEEEVRTLFVSGLPLDIKPRELYLLFRPFKGYEG
Isoform B: MNNGGKAEKENTPSEANLQEEEVRTLFVSGLPLDIKPRELYLLFRPFKGYEG
Isoform C: MNNGGKAEKENTPSEANLQEEEVRTLFVSGLPLDIKPRELYLLFRPFKGYEG

Isoform A: SLIKLTSKQPVGFVSFDSRSEAEAAKNALNGIRFDPEIPQTLRLEFAKANTKM
Isoform B: SLIKLTSKQPVGFVSFDSRSEAEAAKNALNGIRFDPEIPQTLRLEFAKANTKM
Isoform C: SLIKLTSKQPVGFVSFDSRSEAEAAKNALNGIRFDPEIPQTLRLEFAKANTKM

Isoform A: AKNKLVGTPNPSTPLPNTVPQFIAREPYELTVPALYPSSPEVWAPYPLYPAELA
Isoform B: AKNKLVGTPNPSTPLPNTVPQFIAREPYELTVPALYPSSPEVWAPYPLYPAELA
Isoform C: AKNKLVGTPNPSTPLPNTVPQFIAREPYELTVPALYPSSPEVWAPYPLYPAELA

Isoform A: PALPPPAFTYPASLHAQMRWLPPSEATSQGWKSRQFC
Isoform B: PALPPPAFTYPASLHAQLCEGQTVRRSHPLSAPSPDSASLAWFPV
Isoform C:PALPPPAFTYPASLHAQCFSPEAKPNTPVFCPLLQQIRFVSGNVFVTYQPTADQQRELPC

Appendix C

List of Transcripts in A2780CP20-RBPMSA

ID	log2FoldChange	pvalue	Gene.name
ENSG00000117281	7.061648	#########	CD160
ENSG00000081138	6.696741	#########	CDH7
ENSG00000248905	4.229346	#########	FMN1
ENSG00000174827	3.581563	#########	PDZK1
ENSG00000156453	3.547803	#########	PCDH1
ENSG00000184731	3.815345	#########	FAM110C
ENSG00000141750	1.94467	#########	STAC2
ENSG00000137965	9.665418	#########	IFI44
ENSG00000168952	2.699767	#########	STXBP6
ENSG00000183248	2.73186	#########	PRR36
ENSG00000165821	1.660758	#########	SALL2
ENSG00000160963	2.703602	#########	COL26A1
ENSG00000224536	4.079151	#########	AC096677.1
ENSG00000151012	2.875087	#########	SLC7A11
ENSG00000130224	3.450166	#########	LRCH2
ENSG00000137962	4.55751	#########	ARHGAP29
ENSG00000066468	3.37452	#########	FGFR2
ENSG00000170271	2.57907	#########	FAXDC2
ENSG00000241644	4.53226	#########	INMT
ENSG00000149021	7.72195	#########	SCGB1A1
ENSG00000115461	4.808982	#########	IGFBP5
ENSG00000133321	4.104905	#########	RARRES3
ENSG00000100593	1.627568	#########	ISM2
ENSG00000138764	1.794789	#########	CCNG2
ENSG00000152952	2.618066	#########	PLOD2
ENSG00000260807	2.48413	#########	AC009041.2
ENSG00000137573	1.683238	#########	SULF1
ENSG00000148942	2.789883	#########	SLC5A12
ENSG00000223396	3.818768	#########	RPS10P7
ENSG00000138606	2.385711	#########	SHF
ENSG00000129244	2.693013	#########	ATP1B2
ENSG00000128284	4.522353	#########	APOL3
ENSG00000040731	2.481557	#########	CDH10
ENSG00000166448	2.922946	#########	TMEM130
ENSG00000272931	-3.05131	#########	AC099568.2
ENSG00000106868	2.446266	#########	SUSD1
ENSG00000046889	-4.38135	#########	PREX2
ENSG00000186470	1.404181	#########	BTN3A2

ENSG00000160323	1.323483	#########	ADAMTS13
ENSG00000137203	2.177523	#########	TFAP2A
ENSG00000050767	2.152862	#########	COL23A1
ENSG00000187268	-2.02028	#########	FAM9C
ENSG00000072195	1.512706	#########	SPEG
ENSG00000261051	4.93514	#########	AC107021.2
ENSG00000166816	1.669122	#########	LDHD
ENSG00000259884	5.486558	#########	AC025259.3
ENSG00000250033	5.666149	#########	SLC7A11-AS1
ENSG00000052344	3.02167	#########	PRSS8
ENSG00000157514	2.529853	#########	TSC22D3
ENSG00000214274	1.474773	#########	ANG
ENSG00000069812	3.354458	#########	HES2
ENSG00000134013	1.697994	#########	LOXL2
ENSG00000265972	3.958924	#########	TXNIP
ENSG00000173157	2.683433	#########	ADAMTS20
ENSG00000215915	-1.912	#########	ATAD3C
ENSG00000183049	1.538965	#########	CAMK1D
ENSG00000108947	1.623675	#########	EFNB3
ENSG00000148143	1.813476	#########	ZNF462
ENSG00000157303	3.73631	#########	SUSD3
ENSG00000136378	1.645541	#########	ADAMTS7
ENSG00000262001	1.456036	#########	DLGAP1-AS2
ENSG00000100167	1.033558	#########	SEPT3
ENSG00000108984	1.732926	#########	MAP2K6
ENSG00000061656	1.342071	#########	SPAG4
ENSG00000108771	2.637488	#########	DHX58
ENSG00000168350	2.497218	#########	DEGS2
ENSG00000160818	-1.29756	#########	GPATCH4
ENSG00000128394	1.449079	#########	APOBEC3F
ENSG00000107968	1.568218	#########	MAP3K8
ENSG00000165675	-1.12983	#########	ENOX2
ENSG00000181513	1.136722	#########	ACBD4
ENSG00000242574	2.202546	#########	HLA-DMB
ENSG00000068831	1.711108	#########	RASGRP2
ENSG00000130304	1.428097	#########	SLC27A1
ENSG00000225434	6.554247	#########	LINC01504
ENSG00000168062	2.241166	#########	BATF2
ENSG00000240694	2.343762	#########	PNMA2
ENSG00000119922	4.629633	#########	IFIT2
ENSG00000102683	2.931468	#########	SGCG

ENSG00000162654	6.931543	#########	GBP4
ENSG00000204767	4.905735	#########	FAM196B
ENSG00000213420	1.776686	#########	GPC2
ENSG00000120738	2.273067	#########	EGR1
ENSG00000176406	1.292923	#########	RIMS2
ENSG00000092068	3.223802	#########	SLC7A8
ENSG00000188897	2.956762	#########	AC099489.1
ENSG00000143226	4.501612	#########	FCGR2A
ENSG00000124143	1.695956	#########	ARHGAP40
ENSG00000120217	2.573364	#########	CD274
ENSG00000128165	4.651843	#########	ADM2
ENSG00000158710	-1.5107	#########	TAGLN2
ENSG00000205795	3.048989	#########	CYS1
ENSG00000185561	2.174608	#########	TLCD2
ENSG00000105639	1.25664	#########	JAK3
ENSG00000184678	2.287248	#########	HIST2H2BE
ENSG00000164086	-1.08132	#########	DUSP7
ENSG00000179041	-1.05868	#########	RRS1
ENSG00000126583	1.244188	#########	PRKCG
ENSG00000196684	5.864666	#########	HSH2D
ENSG00000111801	1.391975	#########	BTN3A3
ENSG00000186868	1.271379	#########	MAPT
ENSG00000282851	3.518552	#########	BISPR
ENSG00000139572	3.170133	#########	GPR84
ENSG00000208028	4.426901	#########	MIR616
ENSG00000108829	-1.22479	#########	LRRC59
ENSG00000154874	1.956932	#########	CCDC144B
ENSG00000130528	3.743749	#########	HRC
ENSG00000196415	3.62375	#########	PRTN3
ENSG00000106305	-1.06491	#########	AIMP2
ENSG00000132603	-0.95678	#########	NIP7
ENSG00000014914	1.229848	#########	MTMR11
ENSG00000232721	1.745501	#########	AC239800.2
ENSG00000105327	2.193872	#########	BBC3
ENSG00000168209	2.165621	#########	DDIT4
ENSG00000214357	1.10629	#########	NEURL1B
ENSG00000124383	-0.94133	#########	MPHOSPH10
ENSG00000128917	2.024312	#########	DLL4
ENSG00000185053	-4.11078	#########	SGCZ
ENSG00000033050	-0.81629	#########	ABCF2
ENSG00000155961	2.263183	#########	RAB39B

ENSG00000116254	1.605628	#########	CHD5
ENSG00000052850	2.731533	#########	ALX4
ENSG00000054392	1.317658	#########	HHAT
ENSG00000169418	1.117657	#########	NPR1.00
ENSG00000136045	-0.87764	#########	PWP1
ENSG00000011600	3.647828	#########	TYROBP
ENSG00000119917	4.321095	#########	IFIT3
ENSG00000234160	-1.38825	#########	AL513165.1
ENSG00000142046	1.678942	#########	TMEM91
ENSG00000005513	1.674885	#########	SOX8
ENSG00000105173	-1.18391	#########	CCNE1
ENSG00000233967	1.871983	#########	AL359715.1
ENSG00000140450	2.00479	#########	ARRDC4
ENSG00000072133	1.439895	0.0001	RPS6KA6
ENSG00000196337	2.127355	0.000101	CGB7
ENSG00000108018	5.895097	0.000101	SORCS1
ENSG00000072274	-1.41207	0.000103	TFRC
ENSG00000151224	2.433938	0.000103	MAT1A
ENSG00000188452	3.677324	0.000104	CERKL
ENSG00000172828	1.594397	0.000104	CES3
ENSG00000186994	3.080561	0.000106	KANK3
ENSG00000260001	1.999004	0.000108	TGFBR3L
ENSG00000125508	2.965505	0.000111	SRMS
ENSG00000147183	6.930851	0.000112	CPXCR1
ENSG00000115946	-0.79827	0.00012	PNO1
ENSG00000235863	1.371934	0.000121	B3GALT4
ENSG00000165271	-1.02282	0.000122	NOL6
ENSG00000143319	-0.8002	0.000131	ISG20L2
ENSG00000139174	2.762563	0.000135	PRICKLE1
ENSG00000108840	1.442705	0.000135	HDAC5
ENSG00000184500	1.150706	0.000136	PROS1
ENSG00000213928	2.513039	0.000137	IRF9
ENSG00000248514	1.470285	0.000138	AC008443.4
ENSG00000130303	5.971958	0.000138	BST2
ENSG00000130513	5.715488	0.000139	GDF15
ENSG00000100889	1.786649	0.000139	PCK2
ENSG00000117266	1.155845	0.00014	CDK18
ENSG00000261236	-1.45662	0.000144	BOP1.00
ENSG00000116761	1.482136	0.000144	CTH
ENSG00000109654	1.604518	0.000144	TRIM2
ENSG00000163811	-0.76875	0.000147	WDR43

ENSG00000127415	1.674184	0.000147	IDUA
ENSG00000101255	2.084738	0.000148	TRIB3
ENSG00000101076	6.743273	0.000149	HNF4A
ENSG00000125347	1.750063	0.000152	IRF1
ENSG00000070182	3.002206	0.000155	SPTB
ENSG00000172426	1.581787	0.000155	RSPH9
ENSG00000160190	1.155402	0.000156	SLC37A1
ENSG00000104888	1.188479	0.000162	SLC17A7
ENSG00000197989	-1.44691	0.000163	SNHG12
ENSG00000127585	1.491184	0.000164	FBXL16
ENSG00000115226	1.623698	0.00017	FNDC4
ENSG00000278962	3.808058	0.000173	AC092645.1
ENSG00000129451	5.034537	0.000177	KLK10
ENSG00000177337	1.054721	0.000178	DLGAP1-AS1
ENSG00000144136	-0.94663	0.000183	SLC20A1
ENSG00000104369	-1.58449	0.000185	JPH1
ENSG00000168899	1.552272	0.00019	VAMP5
ENSG00000176533	1.428823	0.00019	GNG7
ENSG00000135763	-0.98839	0.000192	URB2
ENSG00000229950	3.506545	0.000194	TFAP2A-AS1
ENSG00000105668	1.792068	0.000198	UPK1A
ENSG00000168333	6.108959	0.0002	PPDPFL
ENSG00000155846	-0.95619	0.000201	PPARGC1B
ENSG00000103522	4.790108	0.000203	IL21R
ENSG00000274021	2.152944	0.000205	AC024909.2
ENSG00000038945	-1.37995	0.000209	MSR1
ENSG00000259953	4.355291	0.00021	AL138756.1
ENSG00000160208	-0.83872	0.000212	RRP1B
ENSG00000131067	1.400825	0.000213	GGT7
ENSG00000106665	1.918251	0.000213	CLIP2
ENSG00000217442	2.442425	0.000215	SYCE3
ENSG00000206503	2.298012	0.000225	HLA-A
ENSG00000166197	-0.73624	0.000232	NOLC1
ENSG00000266302	4.851928	0.000234	AC098850.3
ENSG00000115761	-0.92179	0.000236	NOL10
ENSG00000117360	-0.77911	0.000238	PRPF3
ENSG00000095596	3.087763	0.000245	CYP26A1
ENSG00000144152	1.802502	0.000248	FBLN7
ENSG00000154358	1.587232	0.000256	OBSCN
ENSG00000167632	1.053381	0.000257	TRAPPC9
ENSG00000128285	2.718826	0.000261	MCHR1

ENSG00000187486	1.105937	0.000269	KCNJ11
ENSG00000121552	3.88724	0.000271	CSTA
ENSG00000105447	-1.28767	0.000272	GRWD1
ENSG00000187140	5.270456	0.000276	FOXD3
ENSG00000035862	1.415516	0.000277	TIMP2
ENSG00000105550	5.930365	0.000282	FGF21
ENSG00000162367	3.35196	0.000283	TAL1
ENSG00000173638	-1.21905	0.000284	SLC19A1
ENSG00000074966	-3.1203	0.000286	TXK
ENSG00000100439	1.080637	0.000287	ABHD4
ENSG00000103196	2.835103	0.000291	CRISPLD2
ENSG00000187994	3.602864	0.000301	RINL
ENSG00000165684	-0.88105	0.00031	SNAPC4
ENSG00000183666	-1.4586	0.000314	GUSBP1
ENSG00000112238	-1.87762	0.000317	PRDM13
ENSG00000167601	1.304903	0.000317	AXL
ENSG00000186517	1.650674	0.000318	ARHGAP30
ENSG00000146054	0.890051	0.000322	TRIM7
ENSG00000188747	1.506754	0.000326	NOXA1
ENSG00000118292	1.207673	0.000327	C1orf54
ENSG00000087269	-1.0707	0.00033	NOP14
ENSG00000173208	1.923978	0.00033	ABCD2
ENSG00000104870	1.590767	0.000331	FCGRT
ENSG00000130517	1.047937	0.000334	PGPEP1
ENSG00000135424	1.085419	0.000338	ITGA7
ENSG00000115053	-1.24438	0.000341	NCL
ENSG00000141682	1.769668	0.000346	PMAIP1
ENSG00000244041	0.951575	0.000348	LINC01011
ENSG00000131467	-0.91799	0.000348	PSME3
ENSG00000088881	2.314594	0.000352	EBF4
ENSG00000145014	0.886872	0.000353	TMEM44
ENSG00000187091	1.141992	0.00037	PLCD1
ENSG00000145194	-1.26919	0.000372	ECE2
ENSG00000174564	2.908358	0.000373	IL20RB
ENSG00000162591	2.381914	0.000374	MEGF6
ENSG00000167721	-0.85816	0.000381	TSR1
ENSG00000198944	1.511651	0.000383	SOWAHA
ENSG00000099953	1.364167	0.000388	MMP11
ENSG00000136875	-1.03039	0.00039	PRPF4
ENSG00000206559	1.391151	0.000391	ZCWPW2
ENSG00000104765	0.874577	0.000394	BNIP3L

ENSG00000089195	-0.73627	0.000396	TRMT6
ENSG00000003400	1.151111	0.000398	CASP10
ENSG00000176046	6.087443	0.000401	NUPR1
ENSG00000041802	-0.73961	0.000403	LSG1
ENSG00000170581	1.355389	0.000405	STAT2
ENSG00000162426	1.57107	0.000405	SLC45A1
ENSG00000115271	2.74221	0.000406	GCA
ENSG00000007314	3.036166	0.000424	SCN4A
ENSG00000165475	1.032925	0.000428	CRYL1
ENSG00000170684	-1.26783	0.000429	ZNF296
ENSG00000188933	2.206837	0.000433	USP32P1
ENSG00000130363	1.524602	0.000434	RSPH3
ENSG00000183072	-0.78738	0.000434	NKX2-5
ENSG00000066185	1.528207	0.000441	ZMYND12
ENSG00000101361	-1.12897	0.000442	NOP56
ENSG00000125999	3.962015	0.000447	BPIFB1
ENSG00000170412	2.155127	0.000452	GPRC5C
ENSG00000099194	1.498504	0.000452	SCD
ENSG00000053918	4.926976	0.000458	KCNQ1
ENSG00000082516	-0.95806	0.000461	GEMIN5
ENSG00000168961	6.507802	0.00047	LGALS9
ENSG00000170017	1.284602	0.000473	ALCAM
ENSG00000152583	3.388799	0.000474	SPARCL1
ENSG00000131069	1.227859	0.000479	ACSS2
ENSG00000167157	1.955894	0.000482	PRRX2
ENSG00000151789	2.655202	0.000483	ZNF385D
ENSG00000232352	2.212548	0.000485	SEMA3B-AS1
ENSG00000170390	1.159124	0.000486	DCLK2
ENSG00000149131	1.613542	0.000488	SERPING1
ENSG00000197324	1.323296	0.000506	LRP10
ENSG00000184060	2.014594	0.000507	ADAP2
ENSG00000009950	1.401053	0.00051	MLXIPL
ENSG00000253500	0.963641	0.000513	AF121898.1
ENSG00000197948	0.898571	0.000519	FCHSD1
ENSG00000110446	6.865731	0.000523	SLC15A3
ENSG00000182871	1.242694	0.000525	COL18A1
ENSG00000198223	1.786365	0.000526	CSF2RA
ENSG00000130826	-0.81684	0.000527	DKC1
ENSG00000185155	3.548535	0.000528	MIXL1
ENSG00000260645	1.548169	0.000529	AL359715.2
ENSG00000235300	2.125238	0.000529	AC090627.1

ENSG00000128298	1.740278	0.000529	BAIAP2L2
ENSG00000221539	-2.52172	0.000538	SNORD99
ENSG00000235831	2.12688	0.000539	BHLHE40-AS1
ENSG00000247077	-0.84183	0.000541	PGAM5
ENSG00000160781	1.70834	0.000542	PAQR6
ENSG00000172409	-0.9373	0.000546	CLP1
ENSG00000155158	1.545619	0.000549	TTC39B
ENSG00000111641	-0.72175	0.000564	NOP2
ENSG00000184481	1.126321	0.000579	FOXO4
ENSG00000108592	-0.8383	0.000581	FTSJ3
ENSG00000088205	-0.71422	0.000582	DDX18
ENSG00000159173	3.106137	0.000584	TNNI1
ENSG00000136819	-0.71452	0.000586	C9orf78
ENSG00000244219	2.804392	0.000586	TMEM225B
ENSG00000198176	-0.9902	0.000588	TFDP1
ENSG00000110104	-1.04317	0.000592	CCDC86
ENSG00000162699	3.076529	0.000609	DNAJA1P5
ENSG00000130294	1.875152	0.00061	KIF1A
ENSG00000145703	3.045269	0.000615	IQGAP2
ENSG00000104356	-1.07932	0.000616	POP1
ENSG00000102984	1.183785	0.00062	ZNF821
ENSG00000170542	1.565508	0.000626	SERPINB9
ENSG00000270666	2.925138	0.000627	AL021918.1
ENSG00000100100	1.105258	0.000639	PIK3IP1
ENSG00000181350	1.30698	0.000642	LRRC75A
ENSG00000119801	1.266204	0.000645	YPEL5
ENSG00000277459	-1.87699	0.000651	AP001527.2
ENSG00000185163	-0.87273	0.000655	DDX51
ENSG00000160111	1.921754	0.000658	CPAMD8
ENSG00000100285	-1.42852	0.000664	NEFH
ENSG00000175938	1.173002	0.000665	ORAI3
ENSG00000070814	-1.0779	0.000665	TCOF1
ENSG00000105849	-0.94017	0.000671	TWISTNB
ENSG00000223669	5.638946	0.000679	AL357033.2
ENSG00000111271	0.980663	0.000689	ACAD10
ENSG00000100029	-0.98635	0.000689	PES1.00
ENSG00000172037	1.072857	0.000689	LAMB2
ENSG00000114315	1.789226	0.00069	HES1
ENSG00000070669	1.884527	0.000695	ASNS
ENSG00000159199	-1.2184	0.000703	ATP5MC1
ENSG00000107798	1.545303	0.000706	LIPA

ENSG00000114648	-0.75376	0.000715	KLHL18
ENSG00000171798	2.332277	0.000718	KNDC1
ENSG00000239282	1.792082	0.000719	CASTOR1
ENSG00000133067	4.870829	0.000726	LGR6
ENSG00000070540	1.429653	0.000738	WIPI1
ENSG00000134697	-0.79121	0.000745	GNL2
ENSG00000175356	1.913444	0.000754	SCUBE2
ENSG00000131781	1.393061	0.000757	FMO5
ENSG00000070444	1.392247	0.000757	MNT
ENSG00000073150	1.394323	0.000759	PANX2
ENSG00000117305	0.799632	0.000769	HMGCL
ENSG00000197496	1.360388	0.000771	SLC2A10
ENSG00000132530	8.297768	0.000782	XAF1
ENSG00000171223	1.508508	0.000792	JUNB
ENSG00000258580	5.077016	0.000795	AL136298.1
ENSG00000101445	1.40552	0.000801	PPP1R16B
ENSG00000130529	1.217643	0.000803	TRPM4
ENSG00000111540	0.895376	0.000807	RAB5B
ENSG00000196517	1.799331	0.000813	SLC6A9
ENSG00000220008	2.161571	0.000814	LINGO3
ENSG00000155438	-0.8871	0.00082	NIFK
ENSG00000121297	3.446574	0.000835	TSHZ3
ENSG00000265817	3.321043	0.000841	FSBP
ENSG00000239779	0.830244	0.000842	WBP1
ENSG00000139625	0.683821	0.00086	MAP3K12
ENSG00000204305	1.139591	0.000868	AGER
ENSG00000168939	1.81469	0.000876	SPRY3
ENSG00000075043	-1.31207	0.000877	KCNQ2
ENSG00000204282	2.826788	0.000883	TNRC6C-AS1
ENSG00000188573	2.464702	0.000884	FBLL1
ENSG00000065183	-0.73201	0.000892	WDR3
ENSG00000196363	-0.80091	0.000893	WDR5
ENSG00000111319	2.021261	0.000899	SCNN1A
ENSG00000258837	1.794881	0.000899	AL133370.1
ENSG00000115263	1.494541	0.000907	GCG
ENSG00000162733	1.464615	0.000921	DDR2
ENSG00000129932	-0.89564	0.000924	DOHH
ENSG00000142235	0.88357	0.000933	LMTK3
ENSG00000138759	4.07941	0.000942	FRAS1
ENSG00000148229	-1.02633	0.000943	POLE3
ENSG00000139597	1.603627	0.000948	N4BP2L1

ENSG00000115468	1.127388	0.00095	EFHD1
ENSG00000131981	1.97137	0.000966	LGALS3
ENSG00000163017	-2.19861	0.000978	ACTG2
ENSG00000105821	-0.9853	0.001012	DNAJC2
ENSG00000162849	-1.57858	0.001012	KIF26B
ENSG00000105967	3.039575	0.001013	TFEC
ENSG00000184669	1.63048	0.001019	OR7E14P
ENSG00000126217	1.518953	0.001019	MCF2L
ENSG00000100077	1.328656	0.001024	GRK3
ENSG00000206341	2.19888	0.001037	HLA-H
ENSG00000163840	1.752244	0.001054	DTX3L
ENSG00000232530	1.50365	0.001055	LIF-AS1
ENSG00000162413	-0.88015	0.001055	KLHL21
ENSG00000186496	1.167034	0.001059	ZNF396
ENSG00000261270	2.795555	0.001064	AC012181.2
ENSG00000100462	-0.95241	0.001066	PRMT5
ENSG00000133874	0.815955	0.001067	RNF122
ENSG00000099617	3.144231	0.001068	EFNA2
ENSG00000044090	0.985887	0.001069	CUL7
ENSG00000154134	1.223226	0.001074	ROBO3
ENSG00000230615	1.609283	0.001076	AL139220.2
ENSG00000205250	-0.84169	0.00108	E2F4
ENSG00000011021	1.110713	0.001088	CLCN6
ENSG00000078081	4.07203	0.001089	LAMP3
ENSG00000119812	-0.83138	0.001101	FAM98A
ENSG00000130726	-1.07741	0.001108	TRIM28
ENSG00000251381	5.683703	0.001109	LINC00958
ENSG00000178685	3.893206	0.001114	PARP10
ENSG00000065717	0.840534	0.001116	TLE2
ENSG00000261884	-1.23635	0.001118	AC040162.1
ENSG00000113356	-0.93226	0.001133	POLR3G
ENSG00000121579	-0.73091	0.001141	NAA50
ENSG00000129103	0.845156	0.001142	SUMF2
ENSG00000168924	-0.97	0.001163	LETM1
ENSG00000154553	1.347746	0.001176	PDLIM3
ENSG00000196421	2.411486	0.001194	C20orf204
ENSG00000131171	0.849941	0.0012	SH3BGRL
ENSG00000272512	2.521189	0.001205	AL645608.8
ENSG00000259319	2.397304	0.001207	AF111167.2
ENSG00000151576	-0.81386	0.001212	QTRT2
ENSG00000182919	1.074684	0.001243	C11orf54

ENSG00000158156	3.208944	0.001245	XKR8
ENSG00000204128	1.484981	0.001253	C2orf72
ENSG00000183431	-1.0957	0.001257	SF3A3
ENSG00000228203	-3.66095	0.001258	RNF144A-AS1
ENSG00000135636	1.592639	0.001263	DYSF
ENSG00000184564	2.550643	0.001265	SLITRK6
ENSG00000172183	3.311568	0.00127	ISG20
ENSG00000167123	1.279362	0.001283	CERCAM
ENSG00000224843	1.635311	0.00129	LINC00240
ENSG00000275713	-4.3234	0.001298	HIST1H2BH
ENSG00000186998	1.446607	0.001309	EMID1
ENSG00000125744	1.030243	0.00131	RTN2
ENSG00000135521	-0.75194	0.001312	LTV1
ENSG00000111912	1.596153	0.001316	NCOA7
ENSG00000170791	-0.98918	0.001318	CHCHD7
ENSG00000071967	1.167342	0.001319	CYBRD1
ENSG00000148300	-0.72738	0.001326	REXO4
ENSG00000214212	1.87927	0.001369	C19orf38
ENSG00000164889	-0.98199	0.001372	SLC4A2
ENSG00000123999	1.269927	0.00138	INHA
ENSG00000187266	0.756913	0.001403	EPOR
ENSG00000227946	0.986452	0.00141	AC007383.2
ENSG00000142303	1.153839	0.001411	ADAMTS10
ENSG00000104081	1.316	0.00142	BMF
ENSG00000198865	2.240307	0.001426	CCDC152
ENSG00000184787	-0.68048	0.001436	UBE2G2
ENSG00000134668	1.012588	0.001436	SPOCD1
ENSG00000138772	1.687598	0.001453	ANXA3
ENSG00000168065	3.818054	0.001459	SLC22A11
ENSG00000175309	1.011259	0.001461	PHYKPL
ENSG00000086827	-0.91364	0.001475	ZW10
ENSG00000149150	1.501306	0.001478	SLC43A1
ENSG00000167995	4.703248	0.001483	BEST1
ENSG00000162772	3.853352	0.001519	ATF3
ENSG00000105472	-1.37629	0.00152	CLEC11A
ENSG00000111364	-0.7048	0.001558	DDX55
ENSG00000099875	1.586125	0.00156	MKNK2
ENSG00000150471	4.14806	0.001561	ADGRL3
ENSG00000007944	1.026902	0.001561	MYLIP
ENSG00000182040	1.046929	0.001595	USH1G
ENSG00000162572	0.832052	0.001615	SCNN1D

ENSG00000187244	1.457612	0.001616	BCAM
ENSG00000231925	0.903551	0.001619	TAPBP
ENSG00000090006	0.901549	0.001622	LTBP4
ENSG00000130254	-0.77888	0.001629	SAFB2
ENSG00000171490	-0.65487	0.001631	RSL1D1
ENSG00000107165	-2.31519	0.001634	TYRP1
ENSG00000179409	-0.92364	0.001647	GEMIN4
ENSG00000105204	0.834029	0.001651	DYRK1B
ENSG00000167600	0.989229	0.00168	CYP2S1
ENSG00000258952	1.378909	0.001684	SALRNA1
ENSG00000130935	-0.82417	0.001685	NOL11
ENSG00000196843	-1.26967	0.001708	ARID5A
ENSG00000179598	-0.91381	0.001724	PLD6
ENSG00000136699	-0.88749	0.001732	SMPD4
ENSG00000169439	1.873355	0.001744	SDC2
ENSG00000128590	1.167184	0.001745	DNAJB9
ENSG00000225138	1.264902	0.001753	SLC9A3-AS1
ENSG00000115257	0.896892	0.001776	PCSK4
ENSG00000127561	1.162663	0.001783	SYNGR3
ENSG00000181938	-1.18565	0.001801	GINS3
ENSG00000144331	2.940823	0.001802	ZNF385B
ENSG00000164093	-1.51512	0.001804	PITX2
ENSG00000112578	-0.715	0.001816	BYSL
ENSG00000196605	1.066519	0.001825	ZNF846
ENSG00000108679	3.687035	0.001831	LGALS3BP
ENSG00000135372	-0.71824	0.001847	NAT10
ENSG00000120158	-0.86171	0.001849	RCL1
ENSG00000124593	1.047899	0.001859	AL365205.1
ENSG00000138675	-2.16884	0.001886	FGF5
ENSG00000136718	-0.852	0.001888	IMP4
ENSG00000168216	1.010756	0.001899	LMBRD1
ENSG00000070047	-0.73089	0.001922	PHRF1
ENSG00000125485	-0.84531	0.00193	DDX31
ENSG00000167552	0.695483	0.001956	TUBA1A
ENSG00000179532	1.178888	0.001958	DNHD1
ENSG00000152518	-0.68631	0.001977	ZFP36L2
ENSG00000175634	-0.80962	0.001989	RPS6KB2
ENSG00000069122	2.898767	0.00199	ADGRF5
ENSG00000110002	1.145685	0.001995	VWA5A
ENSG00000125630	-0.75847	0.002009	POLR1B
ENSG00000086717	1.703989	0.002024	PPEF1

ENSG00000228705	2.502071	0.002031	LINC00659
ENSG00000159784	1.997729	0.002033	FAM131B
ENSG00000106263	-0.88979	0.002035	EIF3B
ENSG00000144659	-0.75792	0.00204	SLC25A38
ENSG00000181544	-1.37618	0.002043	FANCB
ENSG00000158423	0.921364	0.002055	RIBC1
ENSG00000138613	0.863329	0.002066	APH1B
ENSG00000241288	1.275762	0.002078	AC092902.2
ENSG00000107902	1.204279	0.002086	LHPP
ENSG00000104901	1.212409	0.002089	DKKL1
ENSG00000237441	0.812275	0.002096	RGL2
ENSG00000160471	1.863782	0.002103	COX6B2
ENSG00000262468	0.94625	0.002103	LINC01569
ENSG00000184220	-0.71386	0.002107	CMSS1
ENSG00000116922	-0.67765	0.002116	C1orf109
ENSG00000101004	0.800173	0.002133	NINL
ENSG00000102057	1.672556	0.002135	KCND1
ENSG00000254858	-0.98466	0.002142	MPV17L2
ENSG00000187955	4.329544	0.002142	COL14A1
ENSG00000080608	-0.65679	0.002148	PUM3
ENSG00000141756	0.921956	0.002151	FKBP10
ENSG00000085741	1.973227	0.002154	WNT11
ENSG00000106948	3.393675	0.002172	AKNA
ENSG00000099864	1.11459	0.002176	PALM
ENSG00000148296	-0.72887	0.002178	SURF6
ENSG00000007516	2.005964	0.002182	BAIAP3
ENSG00000166145	1.631715	0.002189	SPINT1
ENSG00000188511	3.32028	0.002193	C22orf34
ENSG00000278771	-1.63419	0.002198	RN7SL3
ENSG00000226510	1.497186	0.002217	UPK1A-AS1
ENSG00000162496	1.280727	0.002232	DHRS3
ENSG00000165959	1.524454	0.002238	CLMN
ENSG00000189283	1.173916	0.002262	FHIT
ENSG00000178075	0.841085	0.002278	GRAMD1C
ENSG00000174951	4.949331	0.002284	FUT1
ENSG00000147251	1.299587	0.002293	DOCK11
ENSG00000198723	1.010794	0.002311	TEX45
ENSG00000166224	1.08451	0.002323	SGPL1
ENSG00000068976	2.080847	0.002332	PYGM
ENSG00000100196	0.828866	0.002337	KDELR3
ENSG00000154127	-1.55144	0.002338	UBASH3B

ENSG00000244675	3.021661	0.002369	AC108676.1
ENSG00000116455	-1.22857	0.00237	WDR77
ENSG00000064703	-0.73916	0.002374	DDX20
ENSG00000167874	-1.66872	0.002383	TMEM88
ENSG00000183496	0.73595	0.002385	MEX3B
ENSG00000119599	-0.81824	0.002385	DCAF4
ENSG00000100299	1.048743	0.002399	ARSA
ENSG00000182447	2.815431	0.00241	OTOL1
ENSG00000117533	0.952639	0.00244	VAMP4
ENSG00000205129	1.067256	0.00244	C4orf47
ENSG00000144021	-0.60369	0.002459	CIAO1
ENSG00000170919	1.249101	0.002459	TPT1-AS1
ENSG00000142207	-0.77556	0.002467	URB1
ENSG00000175606	-0.81253	0.002483	TMEM70
ENSG00000162194	0.946058	0.002491	LBHD1
ENSG00000165733	-0.76013	0.002493	BMS1
ENSG00000099337	1.208696	0.002497	KCNK6
ENSG00000188729	3.122175	0.002499	OSTN
ENSG00000107815	-0.6797	0.002512	TWNK
ENSG00000055044	-0.93487	0.002516	NOP58
ENSG00000165259	1.000282	0.002538	HDX
ENSG00000070081	0.867175	0.002552	NUCB2
ENSG00000110628	1.13728	0.002569	SLC22A18
ENSG00000168734	1.211622	0.002576	PKIG
ENSG00000157212	-0.89557	0.002579	PAXIP1
ENSG00000107949	-0.79959	0.002579	BCCIP
ENSG00000114491	-1.02175	0.002581	UMPS
ENSG00000198467	-1.25086	0.002599	TPM2
ENSG00000128973	-1.06811	0.002604	CLN6
ENSG00000162377	-0.60187	0.002614	COA7
ENSG00000261716	0.782954	0.002617	AC239868.1
ENSG00000141030	-0.83499	0.002646	COPS3
ENSG00000116584	1.411329	0.002663	ARHGEF2
ENSG00000185133	0.921647	0.002666	INPP5J
ENSG00000135124	1.117942	0.002716	P2RX4
ENSG00000240303	1.301837	0.002718	ACAD11
ENSG00000118816	0.88625	0.002741	CCNI
ENSG00000008086	1.661895	0.002752	CDKL5
ENSG00000162913	1.790539	0.002758	OBSCN-AS1
ENSG00000159210	-0.80434	0.002771	SNF8
ENSG00000198604	-0.66315	0.002787	BAZ1A

ENSG00000079385	2.687623	0.002795	CEACAM1
ENSG00000234494	-1.25009	0.00281	SP2-AS1
ENSG00000181744	1.083811	0.002826	C3orf58
ENSG00000111799	-4.33205	0.002829	COL12A1
ENSG00000165997	1.417375	0.002863	ARL5B
ENSG00000103005	-0.71804	0.002872	USB1
ENSG00000147224	-0.66495	0.002877	PRPS1
ENSG00000188312	-1.19348	0.002878	CENPP
ENSG00000167085	-0.9573	0.002896	PHB
ENSG00000163354	1.347519	0.002909	DCST2
ENSG00000175198	0.78743	0.002915	PCCA
ENSG00000184619	1.559467	0.002915	KRBA2
ENSG00000161921	0.831697	0.002939	CXCL16
ENSG00000068971	1.270825	0.00294	PPP2R5B
ENSG00000168872	-0.68048	0.002953	DDX19A
ENSG00000137767	0.748623	0.002976	SQOR
ENSG00000231721	1.266401	0.002981	LINC-PINT
ENSG00000168672	3.598847	0.002997	FAM84B
ENSG00000052802	1.247247	0.003006	MSMO1
ENSG00000134453	-0.72482	0.003009	RBM17
ENSG00000160097	1.146588	0.003011	FNDC5
ENSG00000105538	1.415622	0.003012	RASIP1
ENSG00000148411	-0.75564	0.003022	NACC2
ENSG00000165269	3.601286	0.003023	AQP7
ENSG00000105642	1.024791	0.003023	KCNN1
ENSG00000141622	2.865455	0.003023	RNF165
ENSG00000115902	1.588239	0.003027	SLC1A4
ENSG00000217801	1.383159	0.003029	AL390719.1
ENSG00000123505	-0.84011	0.003036	AMD1.00
ENSG00000146416	0.760942	0.003061	AIG1
ENSG00000136271	-0.8592	0.003074	DDX56
ENSG00000176624	0.962218	0.003094	MEX3C
ENSG00000132254	-0.67819	0.003097	ARFIP2
ENSG00000166986	1.041665	0.003097	MARS
ENSG00000204131	1.490151	0.00312	NHSL2
ENSG00000188486	-0.89076	0.003128	H2AFX
ENSG00000128965	3.265234	0.003133	CHAC1
ENSG00000116990	1.480099	0.003134	MYCL
ENSG00000112761	2.215649	0.003147	WISP3
ENSG00000135074	1.732943	0.003148	ADAM19
ENSG00000092096	1.07761	0.00315	SLC22A17

ENSG00000004399	0.953944	0.003201	PLXND1
ENSG00000278259	-0.92587	0.003203	MYO19
ENSG00000100968	0.787404	0.00322	NFATC4
ENSG00000123453	2.352911	0.003231	SARDH
ENSG00000169083	3.150837	0.003233	AR
ENSG00000162552	2.801586	0.00324	WNT4
ENSG00000120334	-0.7534	0.003247	CENPL
ENSG00000163491	-1.52769	0.00328	NEK10
ENSG00000159166	2.49192	0.003291	LAD1
ENSG00000198911	0.966325	0.003306	SREBF2
ENSG00000225345	-1.66716	0.003307	SNX18P3
ENSG00000175305	-1.48428	0.003321	CCNE2
ENSG00000133216	2.120514	0.003322	EPHB2
ENSG00000133119	-0.80865	0.003325	RFC3
ENSG00000138119	1.195491	0.003362	MYOF
ENSG00000007402	1.098709	0.003364	CACNA2D2
ENSG00000119899	0.99877	0.003381	SLC17A5
ENSG00000135829	-0.94523	0.003393	DHX9
ENSG00000188807	-0.66333	0.003397	TMEM201
ENSG00000105737	1.590278	0.0034	GRIK5
ENSG00000156697	-0.88671	0.003411	UTP14A
ENSG00000270441	1.755716	0.003423	AC135506.1
ENSG00000067334	-0.65473	0.003425	DNTTIP2
ENSG00000177606	1.463565	0.003433	JUN
ENSG00000236698	-1.04599	0.003445	EIF1AXP1
ENSG00000197444	0.918165	0.003452	OGDHL
ENSG00000143443	0.690894	0.003472	C1orf56
ENSG00000213024	-0.74471	0.003478	NUP62
ENSG00000214944	2.058477	0.003487	ARHGEF28
ENSG00000118733	0.84407	0.003509	OLFM3
ENSG00000084090	-0.80542	0.003519	STARD7
ENSG00000115828	1.741262	0.003522	QPCT
ENSG00000146909	-0.81224	0.003523	NOM1
ENSG00000198496	0.944866	0.003526	NBR2
ENSG00000167371	0.720219	0.003529	PRRT2
ENSG00000136856	-1.02192	0.00355	SLC2A8
ENSG00000102967	-1.00831	0.003566	DHODH
ENSG00000171298	0.896372	0.003594	GAA
ENSG00000225648	-0.7062	0.003608	SBDSP1
ENSG00000181381	2.794727	0.003618	DDX60L
ENSG00000104381	-0.89134	0.003627	GDAP1

ENSG00000164211	1.352051	0.00363	STARD4
ENSG00000179528	2.568181	0.003637	LBX2
ENSG00000138074	-0.81003	0.003641	SLC5A6
ENSG00000256268	1.135328	0.003686	LINC02454
ENSG00000021300	0.946305	0.003708	PLEKHB1
ENSG00000108785	1.69217	0.003711	HSD17B1P1
ENSG00000167617	1.322195	0.003722	CDC42EP5
ENSG00000116711	-1.15491	0.003736	PLA2G4A
ENSG00000140105	1.324156	0.003747	WARS
ENSG00000162664	-0.7224	0.003749	ZNF326
ENSG00000160193	-1.20309	0.003774	WDR4
ENSG00000107371	-1.03997	0.003778	EXOSC3
ENSG00000132470	1.031135	0.00379	ITGB4
ENSG00000261114	1.942156	0.003816	AC012181.1
ENSG00000164742	1.199394	0.00382	ADCY1
ENSG00000263812	2.790646	0.00382	LINC00908
ENSG00000148840	-0.6252	0.003827	PPRC1
ENSG00000181085	1.276191	0.003834	MAPK15
ENSG00000127995	0.943069	0.003841	CASD1
ENSG00000120942	-0.67474	0.003846	UBIAD1
ENSG00000104921	2.814961	0.003856	FCER2
ENSG00000226349	1.545496	0.003856	AC099066.1
ENSG00000105376	1.243778	0.003861	ICAM5
ENSG00000248383	-1.03465	0.003868	PCDHAC1
ENSG00000204815	1.450282	0.003878	TTC25
ENSG00000196449	-0.62915	0.003885	YRDC
ENSG00000170954	2.679253	0.003902	ZNF415
ENSG00000277161	-1.15568	0.003907	PIGW
ENSG00000172346	1.403289	0.003909	CSDC2
ENSG00000144401	0.626177	0.003941	METTL21A
ENSG00000146731	-0.81835	0.003941	CCT6A
ENSG00000165905	1.274048	0.003962	LARGE2
ENSG00000130706	-0.78874	0.003969	ADRM1
ENSG00000110723	1.253173	0.004006	EXPH5
ENSG00000258634	0.910167	0.004007	AL160006.1
ENSG00000135698	-0.77957	0.004011	MPHOSPH6
ENSG00000170965	1.693196	0.004012	PLAC1
ENSG00000197536	1.674059	0.004041	C5orf56
ENSG00000196998	1.008333	0.004056	WDR45
ENSG00000170558	1.306178	0.004064	CDH2
ENSG00000206053	-0.77046	0.00408	JPT2

ENSG00000160401	-1.17522	0.004089	CFAP157
ENSG00000138685	1.102373	0.004104	FGF2
ENSG00000120053	1.196739	0.00411	GOT1
ENSG00000261438	1.95512	0.00413	AL157394.1
ENSG00000132170	-0.80617	0.004134	PPARG
ENSG00000102878	0.81602	0.004146	HSF4
ENSG00000198042	-0.55228	0.004216	MAK16
ENSG00000140057	0.742774	0.004217	AK7
ENSG00000176619	-0.77992	0.00423	LMNB2
ENSG00000146242	0.785493	0.004233	TPBG
ENSG00000165480	-1.19655	0.004255	SKA3
ENSG00000188157	1.18558	0.004262	AGRN
ENSG00000138750	-0.58584	0.00427	NUP54
ENSG00000145526	4.578614	0.004302	CDH18
ENSG00000123737	-0.9848	0.004305	EXOSC9
ENSG00000170396	-0.89038	0.004318	ZNF804A
ENSG00000260412	1.427883	0.004321	AL353746.1
ENSG00000099251	1.190758	0.004353	HSD17B7P2
ENSG00000135899	1.857665	0.00436	SP110
ENSG00000115241	-0.86348	0.004362	PPM1G
ENSG00000162063	-1.11073	0.004366	CCNF
ENSG00000101003	-1.11296	0.004377	GINS1
ENSG00000181163	-1.01301	0.004379	NPM1
ENSG00000169188	-0.76664	0.004383	APEX2
ENSG00000011007	-0.68071	0.004416	ELOA
ENSG00000055163	1.202493	0.004426	CYFIP2
ENSG00000158290	0.640063	0.004439	CUL4B
ENSG00000135678	1.382991	0.004445	CPM
ENSG00000116237	-0.61654	0.004483	ICMT
ENSG00000181577	2.82111	0.004488	C6orf223
ENSG00000139233	-0.73614	0.004496	LLPH
ENSG00000070423	-0.69889	0.004502	RNF126
ENSG00000155816	2.264344	0.004516	FMN2
ENSG00000116117	1.664614	0.00454	PARD3B
ENSG00000204592	1.262801	0.004552	HLA-E
ENSG00000092929	1.863712	0.004561	UNC13D
ENSG00000077092	2.887572	0.004587	RARB
ENSG00000167578	0.837738	0.004598	RAB4B
ENSG00000185090	-0.68894	0.004602	MANEAL
ENSG00000174804	0.726124	0.004611	FZD4
ENSG00000065357	0.681843	0.004638	DGKA

ENSG00000143878	0.956542	0.004645	RHOB
ENSG00000102547	1.131594	0.004654	CAB39L
ENSG00000142864	-0.69336	0.00466	SERBP1
ENSG00000185437	0.933571	0.004678	SH3BGR
ENSG00000156265	0.990422	0.004685	MAP3K7CL
ENSG00000163485	-1.29056	0.004696	ADORA1
ENSG00000184634	0.819141	0.004704	MED12
ENSG00000138642	1.489441	0.004718	HERC6
ENSG00000183145	0.720404	0.004731	RIPPLY3
ENSG00000054793	0.993103	0.004735	ATP9A
ENSG00000180801	-2.8782	0.004743	ARSJ
ENSG00000261652	0.831758	0.004747	C15orf65
ENSG00000152778	1.406144	0.004772	IFIT5
ENSG00000134516	5.548323	0.004782	DOCK2
ENSG00000135316	-0.78634	0.00479	SYNCRIP
ENSG00000133315	1.166111	0.00481	MACROD1
ENSG00000140688	0.783342	0.004833	C16orf58
ENSG00000188051	1.282842	0.004834	TMEM221
ENSG00000135269	3.664881	0.004839	TES
ENSG00000122884	0.984086	0.004855	P4HA1
ENSG00000175868	1.896796	0.004862	CALCB
ENSG00000135540	1.319979	0.004869	NHSL1
ENSG00000132522	-1.06111	0.00488	GPS2
ENSG00000178177	0.895782	0.00488	LCORL
ENSG00000226137	0.696824	0.004882	BAIAP2-AS1
ENSG00000112146	-0.63522	0.004883	FBXO9
ENSG00000212232	-1.61319	0.004888	SNORD17
ENSG00000130164	1.303815	0.00489	LDLR
ENSG00000171421	-1.11431	0.004891	MRPL36
ENSG00000120075	0.86738	0.004893	HOXB5
ENSG00000155970	0.805152	0.004895	MICU3
ENSG00000147124	0.996425	0.004926	ZNF41
ENSG00000182459	1.852202	0.004939	TEX19
ENSG00000185838	-0.93007	0.004977	GNB1L
ENSG00000113161	1.066427	0.004996	HMGCR
ENSG00000145604	-0.87121	0.005008	SKP2
ENSG00000244242	2.552465	0.005008	IFITM10
ENSG00000145736	-0.64902	0.005022	GTF2H2
ENSG00000249242	0.838051	0.005057	TMEM150C
ENSG00000109971	-0.92727	0.005067	HSPA8
ENSG00000114867	-0.76212	0.005074	EIF4G1

ENSG00000145907	-0.70586	0.005077	G3BP1
ENSG00000205978	1.114565	0.005077	NYNRIN
ENSG00000240849	1.137896	0.00509	TMEM189
ENSG00000137266	1.018394	0.005095	SLC22A23
ENSG00000090554	1.413735	0.005095	FLT3LG
ENSG00000165240	0.882406	0.005097	ATP7A
ENSG00000134815	-0.77025	0.005103	DHX34
ENSG00000176595	1.328586	0.005119	KBTBD11
ENSG00000196981	0.681788	0.005126	WDR5B
ENSG00000136450	-0.93945	0.005126	SRSF1
ENSG00000255284	1.097078	0.005129	AP006621.3
ENSG00000267649	1.397807	0.005141	AC010327.4
ENSG00000186635	0.755335	0.005162	ARAP1
ENSG00000100372	-0.65393	0.005192	SLC25A17
ENSG00000231503	-1.0666	0.005193	PTMAP4
ENSG00000087076	1.291444	0.0052	HSD17B14
ENSG00000077585	0.978401	0.005217	GPR137B
ENSG00000249464	0.989367	0.005222	LINC01091
ENSG00000232445	-0.69773	0.005234	AC006329.1
ENSG00000134001	-0.58522	0.005271	EIF2S1
ENSG00000100216	-1.00962	0.005276	TOMM22
ENSG00000125457	0.639037	0.005288	MIF4GD
ENSG00000162408	-0.8542	0.005294	NOL9
ENSG00000066923	1.262264	0.005333	STAG3
ENSG00000250899	-0.79712	0.005341	AC125807.2
ENSG00000135625	2.025347	0.005346	EGR4
ENSG00000172432	1.160136	0.005375	GTPBP2
ENSG00000013275	-0.76902	0.005382	PSMC4
ENSG00000166341	1.508488	0.00539	DCHS1
ENSG00000132561	1.440611	0.005449	MATN2
ENSG00000130158	0.913109	0.005467	DOCK6
ENSG00000165556	2.739589	0.005468	CDX2
ENSG00000187193	-0.91223	0.005484	MT1X
ENSG00000171793	-0.85299	0.005501	CTPS1
ENSG00000111142	-0.61835	0.005522	METAP2
ENSG00000158828	0.973797	0.005528	PINK1
ENSG00000162231	-0.58226	0.005555	NXF1
ENSG00000136891	-0.53473	0.005592	TEX10
ENSG00000149547	-0.62892	0.005602	EI24
ENSG00000170322	-0.63744	0.005616	NFRKB
ENSG00000163597	-0.85881	0.005622	SNHG16

ENSG00000231607	-1.05746	0.005689	DLEU2
ENSG00000104723	0.761522	0.005712	TUSC3
ENSG00000047644	1.248184	0.005712	WWC3
ENSG00000187372	2.204105	0.005731	PCDHB13
ENSG00000185345	1.713553	0.005823	PRKN
ENSG00000282826	0.795296	0.005826	FRG1CP
ENSG00000156374	-0.63566	0.005837	PCGF6
ENSG00000172216	1.335832	0.005852	CEBPB
ENSG00000114698	2.1244	0.005874	PLSCR4
ENSG00000255008	1.827645	0.00589	AP000442.1
ENSG00000160678	1.241846	0.005892	S100A1
ENSG00000168003	1.329833	0.005894	SLC3A2
ENSG00000145833	-1.06186	0.005898	DDX46
ENSG00000130725	-0.72026	0.005899	UBE2M
ENSG00000144231	-0.67912	0.005902	POLR2D
ENSG00000130766	2.700174	0.005922	SESN2
ENSG00000101493	0.977298	0.005925	ZNF516
ENSG00000261824	1.09104	0.005927	LINC00662
ENSG00000267309	0.94617	0.005929	AC092295.2
ENSG00000134107	1.248276	0.005932	BHLHE40
ENSG00000116120	-0.76692	0.00596	FARSB
ENSG00000231689	4.7308	0.005967	LINC01090
ENSG00000106462	-0.93034	0.00598	EZH2
ENSG00000108312	-0.63637	0.005993	UBTF
ENSG00000145414	-0.67705	0.006008	NAF1
ENSG00000091651	-0.83011	0.006022	ORC6
ENSG00000103227	0.729168	0.006031	LMF1
ENSG00000130700	1.266087	0.006039	GATA5
ENSG00000266947	1.190431	0.006039	AC022916.1
ENSG00000130830	-0.87729	0.006045	MPP1
ENSG00000105928	0.715115	0.006085	GSDME
ENSG00000103326	-0.656	0.006096	CAPN15
ENSG00000139112	1.379842	0.0061	GABARAPL1
ENSG00000012061	1.024426	0.006102	ERCC1
ENSG00000078804	0.88339	0.006105	TP53INP2
ENSG00000282988	1.639146	0.006117	AL031777.3
ENSG00000262528	1.40637	0.006131	AL022341.2
ENSG00000130733	1.147514	0.006137	YIPF2
ENSG00000058729	-0.58592	0.006138	RIOK2
ENSG00000237877	2.126064	0.006139	LINC01473
ENSG00000167670	-0.8464	0.006145	CHAF1A

ENSG00000125434	0.799146	0.006146	SLC25A35
ENSG00000006638	-1.09081	0.006219	TBXA2R
ENSG00000171435	1.437392	0.006222	KSR2
ENSG00000090861	1.108857	0.006251	AARS
ENSG00000205571	-0.88983	0.006271	SMN2
ENSG00000140941	1.180686	0.006279	MAP1LC3B
ENSG00000172062	-0.72244	0.0063	SMN1
ENSG00000163762	1.885176	0.006305	TM4SF18
ENSG00000164024	-0.62396	0.006305	METAP1
ENSG00000177370	-0.79372	0.006314	TIMM22
ENSG00000141101	-0.55958	0.006317	NOB1
ENSG00000104936	0.72393	0.00632	DMPK
ENSG00000186298	-0.71015	0.006339	PPP1CC
ENSG00000197771	-0.76892	0.006376	MCMBP
ENSG00000165410	-0.69683	0.0064	CFL2
ENSG00000131876	-0.80598	0.006423	SNRPA1
ENSG00000100276	1.884189	0.006423	RASL10A
ENSG00000133466	1.444649	0.006424	C1QTNF6
ENSG00000117399	-1.30321	0.006437	CDC20
ENSG00000112033	0.849995	0.006439	PPARD
ENSG00000170160	2.053248	0.006455	CCDC144A
ENSG00000090273	-0.89632	0.006503	NUDC
ENSG00000198133	1.016221	0.006509	TMEM229B
ENSG00000168883	-0.61716	0.006525	USP39
ENSG00000204709	1.680752	0.006526	LINC01556
ENSG00000106031	-2.70321	0.006527	HOXA13
ENSG00000146250	1.317754	0.006547	PRSS35
ENSG00000111012	1.265756	0.006558	CYP27B1
ENSG00000124784	-0.58015	0.006568	RIOK1
ENSG00000185669	1.703981	0.006571	SNAI3
ENSG00000150990	-0.67324	0.006577	DHX37
ENSG00000197905	-0.87457	0.006582	TEAD4
ENSG00000184702	0.694177	0.006611	SEPT5
ENSG00000102900	-0.67498	0.006623	NUP93
ENSG00000159588	1.365763	0.006624	CCDC17
ENSG00000021762	0.788672	0.006632	OSBPL5
ENSG00000168843	4.94718	0.00665	FSTL5
ENSG00000008735	-1.16274	0.006692	MAPK8IP2
ENSG00000196743	0.636441	0.00671	GM2A
ENSG00000167037	1.556845	0.006726	SGSM1
ENSG00000156587	2.372796	0.006744	UBE2L6

ENSG00000112651	-0.68778	0.006749	MRPL2
ENSG00000161036	-0.88875	0.006756	LRWD1
ENSG00000255310	1.214584	0.006757	AF131215.5
ENSG00000113739	2.332185	0.006764	STC2
ENSG00000164338	-0.57533	0.006805	UTP15
ENSG00000118655	-0.75057	0.006814	DCLRE1B
ENSG00000241399	1.298645	0.006814	CD302
ENSG00000166226	-0.82189	0.006823	CCT2
ENSG00000185615	1.063076	0.006834	PDIA2
ENSG00000133424	2.705624	0.00685	LARGE1
ENSG00000138073	-0.77277	0.006857	PREB
ENSG00000205959	2.381591	0.006877	AC105345.1
ENSG00000234928	1.332892	0.006883	LINC01659
ENSG00000130487	5.258587	0.006892	KLHDC7B
ENSG00000106560	1.333218	0.0069	GIMAP2
ENSG00000235513	2.121719	0.006902	AL035681.1
ENSG00000260920	0.928661	0.00694	AL031985.3
ENSG00000197461	3.403128	0.006949	PDGFA
ENSG00000173545	-0.56496	0.00695	ZNF622
ENSG00000001497	-0.93774	0.006982	LAS1L
ENSG00000109107	0.658175	0.006988	ALDOC
ENSG00000105127	-0.61475	0.007041	AKAP8
ENSG00000005194	-0.67258	0.007054	CIAPIN1
ENSG00000166710	1.187799	0.007061	B2M
ENSG00000176723	1.414916	0.007064	ZNF843
ENSG00000196220	1.226719	0.007078	SRGAP3
ENSG00000116750	-0.5969	0.007095	UCHL5
ENSG00000105401	-0.73199	0.007103	CDC37
ENSG00000120800	-0.82514	0.007109	UTP20
ENSG00000166246	-1.7883	0.007123	C16orf71
ENSG00000279520	1.565297	0.007136	AC093525.8
ENSG00000113657	-2.1884	0.007152	DPYSL3
ENSG00000167711	1.072229	0.007191	SERPINF2
ENSG00000107959	-0.68254	0.007207	PITRM1
ENSG00000133863	-0.90219	0.007208	TEX15
ENSG00000162461	1.898423	0.007251	SLC25A34
ENSG00000275700	-0.67572	0.007271	AATF
ENSG00000177679	1.606904	0.007272	SRRM3
ENSG00000099783	-0.90868	0.007274	HNRNPM
ENSG00000206190	1.165111	0.007277	ATP10A
ENSG00000185513	0.81976	0.007295	L3MBTL1

ENSG00000228397	1.405689	0.007296	LINC01635
ENSG00000232656	2.130902	0.007297	IDI2-AS1
ENSG00000271581	1.723136	0.007342	AL671883.2
ENSG00000158406	1.485064	0.007348	HIST1H4H
ENSG00000106976	0.731387	0.00736	DNM1
ENSG00000227799	1.531926	0.007399	AC012358.2
ENSG00000148843	-0.62693	0.007399	PDCD11
ENSG00000109323	0.746678	0.007401	MANBA
ENSG00000181444	0.886386	0.007404	ZNF467
ENSG00000084731	0.923911	0.00741	KIF3C
ENSG00000164161	2.015097	0.007422	HHIP
ENSG00000129472	0.787955	0.007428	RAB2B
ENSG00000104324	1.181046	0.007429	CPQ
ENSG00000163879	2.108345	0.007441	DNALI1
ENSG00000104805	0.755593	0.007463	NUCB1
ENSG00000135365	0.807944	0.007498	PHF21A
ENSG00000197768	1.090463	0.007522	STPG3
ENSG00000185046	1.501764	0.007531	ANKS1B
ENSG00000260428	1.94505	0.007532	SCX
ENSG00000268108	3.241492	0.007544	AC008687.2
ENSG00000236824	-1.35418	0.007545	BCYRN1
ENSG00000225855	0.655936	0.007554	RUSC1-AS1
ENSG00000142871	0.98857	0.007561	CYR61
ENSG00000140464	1.175763	0.007573	PML
ENSG00000117407	1.108559	0.007593	ARTN
ENSG00000254819	1.145439	0.007611	AC021698.1
ENSG00000162069	1.301047	0.007618	BICDL2
ENSG00000148835	-0.74023	0.00763	TAF5
ENSG00000186567	1.173666	0.007638	CEACAM19
ENSG00000197555	0.81804	0.007651	SIPA1L1
ENSG00000229431	1.696551	0.007687	AL139289.1
ENSG00000198125	1.912676	0.007689	MB
ENSG00000125459	-0.92132	0.007705	MSTO1
ENSG00000213551	-0.98965	0.007727	DNAJC9
ENSG00000169499	1.091793	0.00773	PLEKHA2
ENSG00000165105	2.985848	0.007784	RASEF
ENSG00000168827	-0.51992	0.007789	GFM1
ENSG00000250241	1.504081	0.007814	AC105383.1
ENSG00000224152	0.821469	0.007818	AC009506.1
ENSG00000104969	-0.5838	0.007833	SGTA
ENSG00000126953	-0.76597	0.00785	TIMM8A

ENSG00000133302	0.794871	0.007905	SLF1
ENSG00000111845	-0.64423	0.007906	PAK1IP1
ENSG00000138381	-0.68932	0.007907	ASNSD1
ENSG00000264364	-0.51213	0.007943	DYNLL2
ENSG00000156639	1.042015	0.007948	ZFAND3
ENSG00000196787	0.980645	0.007953	HIST1H2AG
ENSG00000037897	-0.73016	0.007961	METTL1
ENSG00000100410	-0.7361	0.007963	PHF5A
ENSG00000139438	-1.54524	0.007972	FAM222A
ENSG00000185250	0.72973	0.007993	PPIL6
ENSG00000150593	1.267347	0.008016	PDCD4
ENSG00000118473	-3.36286	0.008061	SGIP1
ENSG00000066427	0.741958	0.008078	ATXN3
ENSG00000113460	-0.66321	0.008083	BRIX1
ENSG00000174938	0.850089	0.008097	SEZ6L2
ENSG00000065150	-0.6336	0.008171	IPO5
ENSG00000141576	0.993122	0.008175	RNF157
ENSG00000280734	0.724077	0.008178	LINC01232
ENSG00000145244	-2.26965	0.008182	CORIN
ENSG00000198053	0.906435	0.008223	SIRPA
ENSG00000166401	1.633047	0.008228	SERPINB8
ENSG00000227620	-1.23109	0.008242	ALG1L8P
ENSG00000104413	6.499193	0.008245	ESRP1
ENSG00000130522	1.089629	0.008284	JUND
ENSG00000095752	1.052653	0.008308	IL11
ENSG00000164308	0.787818	0.008308	ERAP2
ENSG00000100031	1.050294	0.008321	GGT1
ENSG00000181610	-0.69078	0.008342	MRPS23
ENSG00000107937	-0.53926	0.008363	GTPBP4
ENSG00000141314	2.225795	0.008399	RHBDL3
ENSG00000160087	-0.64667	0.008399	UBE2J2
ENSG00000088247	-0.59002	0.008404	KHSRP
ENSG00000131979	0.960035	0.008411	GCH1
ENSG00000169245	3.305495	0.00842	CXCL10
ENSG00000224419	1.399324	0.008453	KRT18P27
ENSG00000152795	-0.87651	0.008459	HNRNPDL
ENSG00000248333	-0.63147	0.008465	CDK11B
ENSG00000087087	-0.83847	0.008483	SRRT
ENSG00000033011	-0.95245	0.008493	ALG1
ENSG00000138316	1.784879	0.008525	ADAMTS14
ENSG00000239900	-0.79583	0.008558	ADSL

ENSG00000241489	1.648713	0.008563	AC244197.3
ENSG00000174243	-0.926	0.008583	DDX23
ENSG00000185359	-0.62109	0.008625	HGS
ENSG00000167772	1.123448	0.008665	ANGPTL4
ENSG00000143390	0.594044	0.008671	RFX5
ENSG00000096384	-0.72044	0.008694	HSP90AB1
ENSG00000155508	0.557777	0.008712	CNOT8
ENSG00000179292	1.461138	0.008713	TMEM151A
ENSG00000163412	2.211316	0.008715	EIF4E3
ENSG00000163866	-0.73357	0.008716	SMIM12
ENSG00000132780	-0.91729	0.008737	NASP
ENSG00000163938	-0.59188	0.008759	GNL3
ENSG00000135776	-0.71125	0.008761	ABCB10
ENSG00000174446	-0.63867	0.00878	SNAPC5
ENSG00000164136	2.281411	0.008782	IL15
ENSG00000147813	-1.2163	0.008784	NAPRT
ENSG00000153187	-0.66392	0.008799	HNRNPU
ENSG00000156502	-0.49531	0.008803	SUPV3L1
ENSG00000187642	-0.90989	0.008836	PERM1
ENSG00000117477	-1.51666	0.00884	CCDC181
ENSG00000144381	-0.79705	0.008844	HSPD1
ENSG00000100219	0.911438	0.008861	XBP1
ENSG00000146197	1.540049	0.008868	SCUBE3
ENSG00000278828	1.021229	0.008884	HIST1H3H
ENSG00000103064	-0.71167	0.00889	SLC7A6
ENSG00000066135	0.885289	0.008891	KDM4A
ENSG00000132256	1.072452	0.008906	TRIM5
ENSG00000240065	1.069189	0.008918	PSMB9
ENSG00000228084	1.220535	0.008949	AC118553.1
ENSG00000060688	-0.70716	0.008964	SNRNP40
ENSG00000168779	0.861114	0.00897	SHOX2
ENSG00000268964	3.201666	0.008994	ERVV-2
ENSG00000112343	1.657062	0.009015	TRIM38
ENSG00000226699	2.194883	0.009016	AL360181.1
ENSG00000103550	-0.56225	0.009019	KNOP1
ENSG00000114349	2.813419	0.009019	GNAT1
ENSG00000108424	-0.66033	0.00905	KPNB1
ENSG00000120162	-1.0076	0.009054	MOB3B
ENSG00000232859	0.928395	0.00906	LYRM9
ENSG00000128923	0.797144	0.009095	MINDY2
ENSG00000064300	1.780035	0.009098	NGFR

ENSG00000133816	-1.20321	0.009102	MICAL2
ENSG00000158526	-0.69991	0.009108	TSR2
ENSG00000268655	1.092847	0.00912	AC008687.4
ENSG00000174013	-0.57808	0.009139	FBXO45
ENSG00000189114	-0.69447	0.009152	BLOC1S3
ENSG00000185386	0.724452	0.009164	MAPK11
ENSG00000251129	3.429092	0.00918	LINC02506
ENSG00000074211	1.020064	0.00919	PPP2R2C
ENSG00000143368	-0.75979	0.009227	SF3B4
ENSG00000092201	-0.58087	0.009254	SUPT16H
ENSG00000245248	-1.1404	0.009256	USP2-AS1
ENSG00000108306	0.962369	0.009277	FBXL20
ENSG00000127990	0.665333	0.009305	SGCE
ENSG00000112365	-0.60225	0.00932	ZBTB24
ENSG00000179846	2.779643	0.009335	NKPD1
ENSG00000144043	-0.8217	0.00937	TEX261
ENSG00000120725	0.856758	0.009443	SIL1
ENSG00000136828	0.696319	0.009449	RALGPS1
ENSG00000197283	0.86138	0.009452	SYNGAP1
ENSG00000125740	2.481283	0.009469	FOSB
ENSG00000142449	2.982606	0.009476	FBN3
ENSG00000107317	1.513799	0.009496	PTGDS
ENSG00000276900	1.068783	0.009499	AC023157.3
ENSG00000163507	-0.98183	0.0095	CIP2A
ENSG00000169180	-0.64348	0.009508	XPO6
ENSG00000138380	1.025093	0.009548	CARF
ENSG00000149084	0.81437	0.009577	HSD17B12
ENSG00000185880	1.18495	0.009607	TRIM69
ENSG00000198369	0.964371	0.009622	SPRED2
ENSG00000225921	-0.77372	0.009625	NOL7
ENSG00000186088	0.705307	0.009652	GSAP
ENSG00000139620	-0.54189	0.009662	KANSL2
ENSG00000197299	-1.04135	0.009664	BLM
ENSG00000169756	0.864414	0.009678	LIMS1
ENSG00000168259	-0.6979	0.009681	DNAJC7
ENSG00000121851	0.864651	0.009697	POLR3GL
ENSG00000122952	-1.21505	0.009707	ZWINT
ENSG00000128191	-0.59418	0.00971	DGCR8
ENSG00000183760	2.587608	0.009716	ACP7
ENSG00000137171	0.784143	0.009727	KLC4
ENSG00000151135	0.626781	0.009764	TMEM263

ENSG00000171843	-1.8719	0.009768	MLLT3
ENSG00000163320	0.61685	0.009815	CGGBP1
ENSG00000080839	-0.74815	0.009842	RBL1
ENSG00000106078	0.821284	0.009854	COBL
ENSG00000184916	-0.72283	0.009858	JAG2
ENSG00000181409	0.905744	0.009869	AATK
ENSG00000124279	-0.63606	0.009904	FASTKD3
ENSG00000137547	-0.74663	0.009909	MRPL15
ENSG00000148408	1.68156	0.00991	CACNA1B
ENSG00000188493	0.613945	0.009971	C19orf54
ENSG00000162385	-0.69436	0.009997	MAGOH
ENSG00000117122	1.048136	0.010011	MFAP2
ENSG00000158717	-0.5869	0.010034	RNF166
ENSG00000107938	-0.61467	0.010035	EDRF1
ENSG00000105171	-0.74398	0.010046	POP4
ENSG00000130270	1.030632	0.010052	ATP8B3
ENSG00000183474	-0.55091	0.010064	GTF2H2C
ENSG00000147676	1.860456	0.010065	MAL2
ENSG00000091127	-0.65735	0.010072	PUS7
ENSG00000123607	0.669867	0.010103	TTC21B
ENSG00000154845	-0.67038	0.010167	PPP4R1
ENSG00000112658	-0.54134	0.010176	SRF
ENSG00000111261	0.640316	0.010237	MANSC1
ENSG00000100027	1.996108	0.010254	YPEL1
ENSG00000165861	0.804034	0.010275	ZFYVE1
ENSG00000160469	0.911871	0.010281	BRSK1
ENSG00000144867	-0.56607	0.01029	SRPRB
ENSG00000093217	-0.98812	0.010297	XYLB
ENSG00000124532	-0.58275	0.010303	MRS2
ENSG00000198892	1.062316	0.010337	SHISA4
ENSG00000159200	-0.58911	0.010377	RCAN1
ENSG00000042493	1.218815	0.010377	CAPG
ENSG00000182481	-0.86612	0.010382	KPNA2
ENSG00000198482	1.057014	0.010415	ZNF808
ENSG00000143845	1.102208	0.010452	ETNK2
ENSG00000051596	-0.86207	0.010493	THOC3
ENSG00000173805	1.175175	0.010512	HAP1
ENSG00000132688	-0.84419	0.010519	NES
ENSG00000235385	4.836401	0.010529	LINC02154
ENSG00000251201	1.223396	0.010534	TMED7-TICAM2
ENSG00000130600	-2.06108	0.010551	H19

ENSG00000076344	2.623139	0.010564	RGS11
ENSG00000168913	-1.18499	0.010613	ENHO
ENSG00000112294	0.737078	0.010682	ALDH5A1
ENSG00000101084	-0.8024	0.010686	C20orf24
ENSG00000173145	-0.50499	0.010687	NOC3L
ENSG00000070950	-0.77897	0.010696	RAD18
ENSG00000168101	-0.97975	0.010752	NUDT16L1
ENSG00000172071	1.03839	0.010787	EIF2AK3
ENSG00000087191	-0.89642	0.010806	PSMC5
ENSG00000110944	1.20949	0.010813	IL23A
ENSG00000177302	-0.61429	0.010815	TOP3A
ENSG00000145777	2.763066	0.010829	TSLP
ENSG00000255717	-0.72689	0.010848	SNHG1
ENSG00000155393	-0.6636	0.010858	HEATR3
ENSG00000130881	-0.71066	0.010898	LRP3
ENSG00000165304	-0.78762	0.010925	MELK
ENSG00000140443	1.215952	0.010941	IGF1R
ENSG00000183520	-0.63653	0.010945	UTP11
ENSG00000177706	1.230647	0.010972	FAM20C
ENSG00000187522	-0.68394	0.010975	HSPA14
ENSG00000139323	0.623159	0.011051	POC1B
ENSG00000013503	-0.67576	0.011074	POLR3B
ENSG00000174943	0.752571	0.011155	KCTD13
ENSG00000204525	1.182465	0.011173	HLA-C
ENSG00000213996	1.416497	0.011187	TM6SF2
ENSG00000125482	-0.70962	0.011212	TTF1
ENSG00000138760	0.785542	0.011226	SCARB2
ENSG00000075131	-0.63728	0.011238	TIPIN
ENSG00000185798	-0.656	0.01127	WDR53
ENSG00000265354	-0.61505	0.011305	TIMM23
ENSG00000127528	1.007571	0.011307	KLF2
ENSG00000198551	0.718072	0.011322	ZNF627
ENSG00000113360	-0.62311	0.011393	DROSHA
ENSG00000148331	-0.59526	0.011401	ASB6
ENSG00000129484	-0.53322	0.011404	PARP2
ENSG00000196943	-0.58664	0.011414	NOP9
ENSG00000163468	-0.88285	0.011417	CCT3
ENSG00000099999	0.999341	0.011419	RNF215
ENSG00000185633	1.640183	0.01145	NDUFA4L2
ENSG00000132872	2.66812	0.011471	SYT4
ENSG00000100170	2.074889	0.011473	SLC5A1

ENSG00000260776	3.325417	0.011509	AC104758.3
ENSG00000166508	-1.05465	0.011509	MCM7
ENSG00000090661	0.87895	0.011528	CERS4
ENSG00000184371	1.431866	0.011554	CSF1
ENSG00000224481	3.173755	0.011574	AC245100.1
ENSG00000105926	-0.76509	0.011576	MPP6
ENSG00000065320	2.45223	0.011584	NTN1
ENSG00000169136	1.34858	0.011624	ATF5
ENSG00000132386	1.062858	0.011641	SERPINF1
ENSG00000279713	2.809525	0.011646	AC080038.3
ENSG00000105559	1.021521	0.011651	PLEKHA4
ENSG00000185418	-0.92327	0.011663	TARSL2
ENSG00000169727	-0.71616	0.011677	GPS1
ENSG00000175792	-0.85739	0.011682	RUVBL1
ENSG00000120694	-0.70281	0.011706	HSPH1
ENSG00000165689	-0.5892	0.011731	SDCCAG3
ENSG00000071994	-0.65821	0.011747	PDCD2
ENSG00000258818	1.220907	0.011772	RNASE4
ENSG00000237440	0.846359	0.011782	ZNF737
ENSG00000125450	-0.67851	0.011788	NUP85
ENSG00000164687	-1.2212	0.01179	FABP5
ENSG00000236104	0.744767	0.011832	ZBTB22
ENSG00000104497	0.744419	0.011864	SNX16
ENSG00000171488	-0.9029	0.01187	LRRC8C
ENSG00000186480	0.856488	0.011879	INSIG1
ENSG00000142178	-0.68587	0.011911	SIK1
ENSG00000137692	-0.60229	0.011915	DCUN1D5
ENSG00000088002	0.990275	0.011924	SULT2B1
ENSG00000090889	-0.83369	0.011938	KIF4A
ENSG00000160563	-0.66796	0.011948	MED27
ENSG00000108883	-0.61816	0.011951	EFTUD2
ENSG00000101040	0.700106	0.011955	ZMYND8
ENSG00000099995	-0.59385	0.011964	SF3A1
ENSG00000132507	-0.90823	0.011965	EIF5A
ENSG00000072858	2.052408	0.01197	SIDT1
ENSG00000184898	0.723759	0.011972	RBM43
ENSG00000230306	2.033695	0.011989	BANF1P2
ENSG00000080224	1.925639	0.012013	EPHA6
ENSG00000215808	0.556611	0.012048	LINC01139
ENSG00000144647	-0.74522	0.012073	POMGNT2
ENSG00000197498	-0.62806	0.012085	RPF2

ENSG00000237276	1.536644	0.012103	ANO7L1
ENSG00000163376	-1.31114	0.012122	KBTBD8
ENSG00000074695	0.719717	0.012127	LMAN1
ENSG00000110108	-0.61324	0.012136	TMEM109
ENSG00000148308	-0.58635	0.01218	GTF3C5
ENSG00000109674	-0.96647	0.01221	NEIL3
ENSG00000104897	-0.68151	0.012214	SF3A2
ENSG00000198522	-0.58887	0.01222	GPN1
ENSG00000106244	-0.5468	0.012231	PDAP1
ENSG00000128604	1.160224	0.012234	IRF5
ENSG00000086619	1.208421	0.012251	ERO1B
ENSG00000258216	2.947775	0.012358	AC084200.1
ENSG00000124562	-0.73327	0.012376	SNRPC
ENSG00000129968	-0.73994	0.012389	ABHD17A
ENSG00000185963	-0.6239	0.012392	BICD2
ENSG00000156983	-0.5997	0.012397	BRPF1
ENSG00000187942	1.969259	0.012401	LDLRAD2
ENSG00000000460	-0.99346	0.012417	C1orf112
ENSG00000268713	1.02489	0.012422	AC005261.3
ENSG00000100320	0.723066	0.012445	RBFOX2
ENSG00000271601	0.653965	0.012471	LIX1L
ENSG00000164053	-0.92851	0.012476	ATRIP
ENSG00000182325	-0.65787	0.012535	FBXL6
ENSG00000103342	-0.50982	0.012556	GSPT1
ENSG00000164362	-1.24864	0.012601	TERT
ENSG00000101189	-0.5139	0.012602	MRGBP
ENSG00000023318	0.688413	0.012626	ERP44
ENSG00000180817	-0.87486	0.012639	PPA1
ENSG00000030419	3.402612	0.012653	IKZF2
ENSG00000167216	2.020267	0.012669	KATNAL2
ENSG00000274020	0.691495	0.012675	LINC01138
ENSG00000160888	0.889659	0.01268	IER2
ENSG00000099817	-0.66835	0.012682	POLR2E
ENSG00000149136	-0.76902	0.012686	SSRP1
ENSG00000197472	-0.88587	0.012749	ZNF695
ENSG00000005884	0.740283	0.012764	ITGA3
ENSG00000167671	0.655141	0.012776	UBXN6
ENSG00000140678	3.077356	0.012777	ITGAX
ENSG00000272419	0.850914	0.012789	AC241585.2
ENSG00000183837	0.896457	0.012797	PNMA3
ENSG00000239306	-0.77205	0.012824	RBM14

ENSG00000102226	0.58019	0.012894	USP11
ENSG00000198435	-0.70272	0.012903	NRARP
ENSG00000163684	-0.49784	0.012904	RPP14
ENSG00000171453	-0.67915	0.012924	POLR1C
ENSG00000235119	3.746313	0.012954	AL138895.1
ENSG00000129636	0.64034	0.012984	ITFG1
ENSG00000129566	0.915726	0.013016	TEP1
ENSG00000132109	1.266632	0.013041	TRIM21
ENSG00000089351	0.724337	0.01306	GRAMD1A
ENSG00000171388	-1.84474	0.013067	APLN
ENSG00000242861	1.069698	0.013087	AL591895.1
ENSG00000156469	-0.71599	0.01309	MTERF3
ENSG00000105612	0.925224	0.013111	DNASE2
ENSG00000245526	-3.29377	0.013169	LINC00461
ENSG00000080644	1.352919	0.013184	CHRNA3
ENSG00000156471	-0.77004	0.013192	PTDSS1
ENSG00000120820	0.669445	0.013211	GLT8D2
ENSG00000166548	0.660585	0.013232	TK2
ENSG00000204634	0.743904	0.013236	TBC1D8
ENSG00000020129	-0.6061	0.013251	NCDN
ENSG00000156966	2.691517	0.013257	B3GNT7
ENSG00000152292	1.153327	0.013275	SH2D6
ENSG00000139926	0.612842	0.013283	FRMD6
ENSG00000267365	0.884269	0.013327	KCNJ2-AS1
ENSG00000067840	1.132129	0.013363	PDZD4
ENSG00000181031	0.831253	0.013383	RPH3AL
ENSG00000095739	2.401039	0.013417	BAMBI
ENSG00000102032	1.479426	0.013438	RENBP
ENSG00000132334	0.852587	0.013454	PTPRE
ENSG00000163754	-0.75339	0.01346	GYG1
ENSG00000106571	1.59275	0.013499	GLI3
ENSG00000132819	-0.57953	0.013508	RBM38
ENSG00000115816	-0.53136	0.013526	CEBPZ
ENSG00000087995	-0.55113	0.013571	METTL2A
ENSG00000132664	-0.64853	0.013582	POLR3F
ENSG00000202337	-1.4865	0.013596	RNU6-8
ENSG00000085832	0.688097	0.013596	EPS15
ENSG00000241015	-0.66341	0.0136	TPM3P9
ENSG00000162607	-0.54065	0.013635	USP1
ENSG00000259494	-0.65105	0.01364	MRPL46
ENSG00000250722	3.084155	0.013718	SELENOP

ENSG00000182700	1.082261	0.013734	IGIP
ENSG00000105825	1.724721	0.013782	TFPI2
ENSG00000165879	1.185605	0.013787	FRAT1
ENSG00000105810	-1.81628	0.013827	CDK6
ENSG00000050820	-0.67955	0.013833	BCAR1
ENSG00000101868	-0.75824	0.01388	POLA1
ENSG00000171766	0.791297	0.013886	GATM
ENSG00000182718	-0.74756	0.013933	ANXA2
ENSG00000186765	1.583494	0.013947	FSCN2
ENSG00000124212	2.557832	0.013952	PTGIS
ENSG00000132326	-0.68379	0.013964	PER2
ENSG00000175063	-0.98711	0.013968	UBE2C
ENSG00000198908	0.743159	0.013982	BHLHB9
ENSG00000130066	1.151974	0.013989	SAT1
ENSG00000204104	-0.5697	0.014004	TRAF3IP1
ENSG00000160392	-0.61716	0.014019	C19orf47
ENSG00000153574	-0.59022	0.014026	RPIA
ENSG00000204055	2.236248	0.014034	AL158151.1
ENSG00000130720	2.095724	0.01407	FIBCD1
ENSG00000246339	1.424355	0.014071	EXTL3-AS1
ENSG00000108561	-0.78963	0.014081	C1QBP
ENSG00000275325	0.753875	0.014105	PDCD6IPP1
ENSG00000111644	2.503834	0.01412	ACRBP
ENSG00000153879	1.053092	0.014132	CEBPG
ENSG00000181924	-0.65886	0.014155	COA4
ENSG00000161547	-0.83374	0.014162	SRSF2
ENSG00000181004	0.690629	0.014169	BBS12
ENSG00000149483	-0.6392	0.014199	TMEM138
ENSG00000138111	-0.95852	0.014212	MFSD13A
ENSG00000005073	-2.5424	0.01422	HOXA11
ENSG00000134375	-0.7609	0.014267	TIMM17A
ENSG00000133687	2.656361	0.014277	TMTC1
ENSG00000145687	0.618225	0.014307	SSBP2
ENSG00000157224	0.781419	0.014324	CLDN12
ENSG00000119705	-0.91961	0.014333	SLIRP
ENSG00000142156	1.216118	0.014361	COL6A1
ENSG00000163002	-0.79438	0.014363	NUP35
ENSG00000087086	-0.58752	0.01437	FTL
ENSG00000165175	0.75311	0.014382	MID1IP1
ENSG00000146918	-0.81158	0.014385	NCAPG2
ENSG00000068654	-0.59642	0.014386	POLR1A

ENSG00000175467	-0.68531	0.014399	SART1
ENSG00000142784	0.729968	0.014419	WDTC1
ENSG00000136937	-0.64665	0.014449	NCBP1
ENSG00000006634	-0.58875	0.014497	DBF4
ENSG00000184900	-0.5712	0.014528	SUMO3
ENSG00000129250	-0.57081	0.014567	KIF1C
ENSG00000141384	-0.9109	0.014624	TAF4B
ENSG00000249992	-0.82077	0.014649	TMEM158
ENSG00000143549	-0.5555	0.01468	TPM3
ENSG00000149260	0.666443	0.014687	CAPN5
ENSG00000184979	1.066297	0.014708	USP18
ENSG00000170049	0.744857	0.014713	KCNAB3
ENSG00000143412	0.753737	0.014734	ANXA9
ENSG00000182612	0.930639	0.014815	TSPAN10
ENSG00000165121	0.780795	0.014819	AL353743.1
ENSG00000184661	-0.85193	0.014822	CDCA2
ENSG00000185033	0.986993	0.014833	SEMA4B
ENSG00000160633	-0.57414	0.014853	SAFB
ENSG00000204574	-0.56483	0.014883	ABCF1
ENSG00000188282	5.034788	0.014913	RUFY4
ENSG00000144655	1.188625	0.014918	CSRNP1
ENSG00000005961	2.457238	0.014941	ITGA2B
ENSG00000174799	-0.77013	0.014969	CEP135
ENSG00000235245	1.818486	0.015046	AL360181.2
ENSG00000185269	0.977585	0.015082	NOTUM
ENSG00000167553	-0.67838	0.015092	TUBA1C
ENSG00000049769	1.01882	0.015097	PPP1R3F
ENSG00000142687	0.640238	0.015127	KIAA0319L
ENSG00000075618	0.60487	0.015146	FSCN1
ENSG00000142444	-0.65707	0.015163	TIMM29
ENSG00000107719	-0.53314	0.015179	PALD1
ENSG00000146540	-0.68105	0.015217	C7orf50
ENSG00000110060	-0.63148	0.015237	PUS3
ENSG00000136122	-0.74467	0.015255	BORA
ENSG00000156650	0.660699	0.01527	KAT6B
ENSG00000249082	-1.34133	0.015299	C5orf66-AS1
ENSG00000161270	2.24425	0.015306	NPHS1
ENSG00000197415	2.906312	0.015306	VEPH1
ENSG00000116985	0.608318	0.015307	BMP8B
ENSG00000196118	-0.90027	0.015348	CCDC189
ENSG00000262712	-1.78791	0.015377	AC012676.1

ENSG00000106554	-0.70029	0.015385	CHCHD3
ENSG00000126254	-0.64576	0.015386	RBM42
ENSG00000199753	-0.9445	0.01542	SNORD104
ENSG00000139131	-0.62162	0.015465	YARS2
ENSG00000109576	-0.79076	0.015502	AADAT
ENSG00000114923	0.864469	0.015508	SLC4A3
ENSG00000138160	-0.81586	0.015551	KIF11
ENSG00000262768	1.384171	0.015643	AC100791.2
ENSG00000182389	1.123109	0.015685	CACNB4
ENSG00000205702	1.504532	0.015701	CYP2D7
ENSG00000175470	-0.63192	0.015733	PPP2R2D
ENSG00000110237	0.721273	0.015742	ARHGEF17
ENSG00000234664	-0.95985	0.015853	HMGN2P5
ENSG00000133226	-0.66681	0.015867	SRRM1
ENSG00000157856	1.930431	0.015874	DRC1
ENSG00000155100	-0.57559	0.015881	OTUD6B
ENSG00000059728	1.33938	0.015893	MXD1
ENSG00000121390	-0.5257	0.015902	PSPC1
ENSG00000165521	-2.47373	0.015911	EML5
ENSG00000123374	-0.75013	0.015917	CDK2
ENSG00000172201	0.740394	0.015942	ID4
ENSG00000158941	-0.60646	0.015942	CCAR2
ENSG00000177889	-0.64397	0.016028	UBE2N
ENSG00000101346	-0.49079	0.016029	POFUT1
ENSG00000135378	0.952429	0.016079	PRRG4
ENSG00000084092	-0.57254	0.016085	NOA1
ENSG00000136158	0.639968	0.016125	SPRY2
ENSG00000213700	1.51358	0.016145	RPL17P50
ENSG00000185100	0.834846	0.016163	ADSSL1
ENSG00000174442	-0.68317	0.016177	ZWILCH
ENSG00000248663	2.861861	0.016195	LINC00992
ENSG00000100065	0.785446	0.016202	CARD10
ENSG00000149050	0.813613	0.01623	ZNF214
ENSG00000172469	0.544248	0.016233	MANEA
ENSG00000150938	-1.26804	0.016236	CRIM1
ENSG00000164543	-0.61693	0.016249	STK17A
ENSG00000136944	0.787803	0.01625	LMX1B
ENSG00000254470	-0.58491	0.016275	AP5B1
ENSG00000196263	0.889652	0.016275	ZNF471
ENSG00000159267	0.809873	0.016287	HLCS
ENSG00000261512	0.980575	0.016295	AC092368.3

ENSG00000108671	-0.54125	0.016308	PSMD11
ENSG00000067798	-3.04959	0.016353	NAV3
ENSG00000124587	0.627311	0.016365	PEX6
ENSG00000066044	-0.60288	0.016399	ELAVL1
ENSG00000141522	-0.76296	0.01641	ARHGDIA
ENSG00000114423	0.825546	0.016422	CBLB
ENSG00000107611	0.631652	0.016425	CUBN
ENSG00000090863	0.639013	0.016438	GLG1
ENSG00000224596	2.033609	0.016452	ZMIZ1-AS1
ENSG00000102241	-0.65052	0.016453	HTATSF1
ENSG00000275064	3.767117	0.016458	AC239860.1
ENSG00000089737	-0.52478	0.016494	DDX24
ENSG00000163629	1.00237	0.016498	PTPN13
ENSG00000110321	-0.53588	0.016526	EIF4G2
ENSG00000274307	1.607653	0.016538	AC023449.2
ENSG00000118004	0.912724	0.016543	COLEC11
ENSG00000124160	-0.908	0.016543	NCOA5
ENSG00000138668	-0.85181	0.016612	HNRNPD
ENSG00000141456	-0.52368	0.016627	PELP1
ENSG00000165943	0.690432	0.016666	MOAP1
ENSG00000171241	-0.93597	0.016668	SHCBP1
ENSG00000089159	-0.88279	0.016671	PXN
ENSG00000138092	-0.73547	0.016678	CENPO
ENSG00000180957	-0.50361	0.016685	PITPNB
ENSG00000134690	-0.83806	0.016696	CDCA8
ENSG00000126500	1.785051	0.016699	FLRT1
ENSG00000115841	0.482022	0.016728	RMDN2
ENSG00000054654	0.736222	0.016735	SYNE2
ENSG00000166888	0.559024	0.016761	STAT6
ENSG00000164134	-0.5001	0.016777	NAA15
ENSG00000137074	-0.58797	0.016785	APTX
ENSG00000257261	0.792639	0.016831	AC008014.1
ENSG00000184205	0.979622	0.016852	TSPYL2
ENSG00000257337	0.659756	0.01686	AC068888.1
ENSG00000186591	0.726465	0.016872	UBE2H
ENSG00000125124	0.521502	0.016881	BBS2
ENSG00000150275	0.758507	0.016888	PCDH15
ENSG00000124228	-0.49512	0.016894	DDX27
ENSG00000151694	1.06786	0.016908	ADAM17
ENSG00000159079	-0.58871	0.016917	C21orf59
ENSG00000184178	-0.79142	0.016951	SCFD2

ENSG00000068079	2.301491	0.016968	IFI35
ENSG00000160803	-0.52612	0.017023	UBQLN4
ENSG00000184557	0.754748	0.017043	SOCS3
ENSG00000061794	-0.47298	0.017056	MRPS35
ENSG00000179348	-0.79732	0.017056	GATA2
ENSG00000228649	-1.07488	0.017071	SNHG26
ENSG00000154743	-0.70223	0.01708	TSEN2
ENSG00000130649	1.775671	0.017088	CYP20.00
ENSG00000126778	0.564983	0.017091	SIX1
ENSG00000011260	-0.48563	0.017119	UTP18
ENSG00000159322	-0.58247	0.017137	ADPGK
ENSG00000170734	-0.68498	0.017166	POLH
ENSG00000186020	0.718229	0.017173	ZNF529
ENSG00000136518	-0.53283	0.017194	ACTL6A
ENSG00000106003	-1.38337	0.01723	LFNG
ENSG00000124207	-0.76209	0.017234	CSE1L
ENSG00000143815	-0.6333	0.017237	LBR
ENSG00000171307	-0.69732	0.017342	ZDHHC16
ENSG00000122507	0.613653	0.017345	BBS9
ENSG00000136059	1.344912	0.017366	VILL
ENSG00000101938	1.783118	0.017367	CHRDL1
ENSG00000168993	-0.83904	0.017392	CPLX1
ENSG00000100814	0.953239	0.017517	CCNB1IP1
ENSG00000170445	-0.53352	0.017521	HARS
ENSG00000107796	-0.97437	0.017545	ACTA2
ENSG00000241852	-0.80674	0.017549	C8orf58
ENSG00000225206	0.745308	0.017579	MIR137HG
ENSG00000107537	0.644451	0.017606	PHYH
ENSG00000104218	-0.59354	0.01761	CSPP1
ENSG00000141431	2.636202	0.017695	ASXL3
ENSG00000177200	0.634952	0.017708	CHD9
ENSG00000164649	-0.60652	0.017711	CDCA7L
ENSG00000198841	-0.65319	0.017722	KTI12
ENSG00000139714	1.421569	0.01774	MORN3
ENSG00000146950	1.91415	0.017755	SHROOM2
ENSG00000116729	0.765631	0.017762	WLS
ENSG00000196230	-0.83797	0.017772	TUBB
ENSG00000183605	-0.59922	0.017779	SFXN4
ENSG00000126947	1.83981	0.01778	ARMCX1
ENSG00000214160	-0.61751	0.017817	ALG3
ENSG00000266208	0.744575	0.017858	AC080112.1

ENSG00000132467	-0.48137	0.017888	UTP3
ENSG00000225913	-1.66434	0.017894	AL138767.3
ENSG00000225530	1.039019	0.017913	SP3P
ENSG00000115368	-0.65361	0.017924	WDR75
ENSG00000145743	0.594415	0.017955	FBXL17
ENSG00000229132	-1.10047	0.017959	EIF4A1P10
ENSG00000119669	0.889568	0.017971	IRF2BPL
ENSG00000225678	1.500831	0.017986	AP000619.1
ENSG00000198000	-0.62201	0.017989	NOL8
ENSG00000150527	1.004101	0.017995	CTAGE5
ENSG00000165568	0.864038	0.017997	AKR1E2
ENSG00000221923	1.621258	0.018026	ZNF880
ENSG00000175985	2.237603	0.018028	PLEKHD1
ENSG00000171865	-0.55632	0.01805	RNASEH1
ENSG00000010165	-0.60356	0.018056	METTL13
ENSG00000262521	1.608513	0.018087	AJ003147.1
ENSG00000243989	0.645879	0.018097	ACY1
ENSG00000261428	-1.63657	0.018101	AC097461.1
ENSG00000169612	-0.57381	0.018105	FAM103A1
ENSG00000196497	-1.03447	0.018108	IPO4
ENSG00000161847	-0.69081	0.018113	RAVER1
ENSG00000234653	-1.28696	0.018121	AC079117.1
ENSG00000213430	-1.02164	0.018152	HSPD1P1
ENSG00000108773	-0.66213	0.018176	KAT2A
ENSG00000164761	1.93678	0.01821	TNFRSF11B
ENSG00000165490	-0.84674	0.018213	DDIAS
ENSG00000093000	-0.60125	0.018244	NUP50
ENSG00000156170	-0.72768	0.018272	NDUFAF6
ENSG00000083290	0.845094	0.018276	ULK2
ENSG00000196358	1.084823	0.018303	NTNG2
ENSG00000135446	-0.58284	0.018333	CDK4
ENSG00000065978	-0.64054	0.018335	YBX1
ENSG00000004478	-0.79143	0.018385	FKBP4
ENSG00000215251	-0.53381	0.018418	FASTKD5
ENSG00000139405	-0.59748	0.018425	RITA1
ENSG00000185818	-0.51729	0.018427	NAT8L
ENSG00000144802	1.05121	0.018435	NFKBIZ
ENSG00000169758	1.239367	0.018439	TMEM266
ENSG00000136932	-0.66196	0.018471	TRMO
ENSG00000163026	-0.71812	0.018486	WDCP
ENSG00000112592	-0.51746	0.018493	TBP

ENSG00000100395	-0.63423	0.018498	L3MBTL2
ENSG00000039560	-0.6491	0.018499	RAI14
ENSG00000103707	-0.58698	0.018551	MTFMT
ENSG00000167491	-0.4723	0.01856	GATAD2A
ENSG00000150991	0.690586	0.018569	UBC
ENSG00000158428	2.26167	0.018594	CATIP
ENSG00000129455	2.424792	0.018612	KLK8
ENSG00000119335	-0.4941	0.018618	SET
ENSG00000272841	-0.78885	0.018628	AL139393.2
ENSG00000164176	2.251833	0.018644	EDIL3
ENSG00000165424	0.799986	0.018668	ZCCHC24
ENSG00000198089	0.48581	0.018689	SFI1
ENSG00000166987	0.642388	0.018755	MBD6
ENSG00000170860	-0.83845	0.018793	LSM3.00
ENSG00000108064	-0.64495	0.018801	TFAM
ENSG00000197599	1.851574	0.018913	CCDC154
ENSG00000121057	-0.67443	0.018943	AKAP1
ENSG00000063127	0.934631	0.018956	SLC6A16
ENSG00000130813	0.98364	0.01897	C19orf66
ENSG00000104679	-0.70209	0.018978	R3HCC1
ENSG00000138131	2.667509	0.01898	LOXL4
ENSG00000188229	-0.73328	0.01898	TUBB4B
ENSG00000111224	0.684528	0.018984	PARP11
ENSG00000260231	0.706542	0.018988	JHDM1D-AS1
ENSG00000248238	0.922776	0.019	LINC02438
ENSG00000133028	-0.56298	0.019033	SCO1
ENSG00000080031	1.035862	0.019078	PTPRH
ENSG00000104859	-0.57253	0.019078	CLASRP
ENSG00000267317	0.740799	0.019122	AC027307.2
ENSG00000204392	-0.69654	0.019123	LSM2.00
ENSG00000136367	0.638168	0.019131	ZFHX2
ENSG00000131015	1.11661	0.019139	ULBP2
ENSG00000175662	0.548893	0.019144	TOM1L2
ENSG00000162694	0.686963	0.019152	EXTL2
ENSG00000013573	-0.77335	0.019155	DDX11
ENSG00000153292	2.913408	0.019156	ADGRF1
ENSG00000107731	2.472672	0.019159	UNC5B
ENSG00000104825	-0.62141	0.019159	NFKBIB
ENSG00000176087	-0.78268	0.019173	SLC35A4
ENSG00000148154	0.64918	0.01921	UGCG
ENSG00000172336	-0.76271	0.019236	POP7

ENSG00000227057	-0.58936	0.019247	WDR46
ENSG00000271992	2.139841	0.01929	AL354872.2
ENSG00000259605	0.870679	0.019306	AC074212.1
ENSG00000147874	-0.65522	0.019354	HAUS6
ENSG00000063244	-0.50274	0.019366	U2AF2
ENSG00000239857	-0.66543	0.01937	GET4
ENSG00000151491	1.22082	0.0194	EPS8
ENSG00000163138	-0.71995	0.019409	PACRGL
ENSG00000137198	1.471684	0.019415	GMPR
ENSG00000136866	0.624837	0.019415	ZFP37
ENSG00000071626	-0.61462	0.019423	DAZAP1
ENSG00000141968	1.112092	0.019442	VAV1
ENSG00000122644	0.607376	0.019447	ARL4A
ENSG00000138385	-0.66795	0.019519	SSB
ENSG00000167770	-0.65314	0.019528	OTUB1
ENSG00000268041	2.518552	0.019531	AC010616.1
ENSG00000160255	1.659267	0.019554	ITGB2
ENSG00000100625	0.757763	0.019578	SIX4
ENSG00000224805	1.020996	0.019597	LINC00853
ENSG00000149503	-0.84705	0.019621	INCENP
ENSG00000100591	-0.69996	0.019641	AHSA1
ENSG00000182853	0.88122	0.019641	VMO1
ENSG00000139890	2.08123	0.019658	REM2
ENSG00000123473	-0.6023	0.019686	STIL
ENSG00000181991	-0.73572	0.019695	MRPS11
ENSG00000125835	-0.72011	0.0197	SNRPB
ENSG00000165238	-0.60418	0.019739	WNK2
ENSG00000075336	-0.90158	0.019752	TIMM21
ENSG00000101849	0.792631	0.01976	TBL1X
ENSG00000214646	2.429339	0.019807	AC104758.1
ENSG00000183153	1.369592	0.019825	GJD3
ENSG00000090674	-0.78939	0.01983	MCOLN1
ENSG00000280423	2.077301	0.019887	AL359852.1
ENSG00000257194	1.45775	0.019892	AC126178.1
ENSG00000007923	-0.65974	0.019971	DNAJC11
ENSG00000138496	2.122313	0.019993	PARP9
ENSG00000062038	1.54849	0.020005	CDH3
ENSG00000120008	0.725631	0.020022	WDR11
ENSG00000125912	-0.63022	0.020033	NCLN
ENSG00000078699	0.592053	0.02004	CBFA2T2
ENSG00000070882	-0.52182	0.020103	OSBPL3

ENSG00000111186	1.233583	0.020104	WNT5B
ENSG00000100226	0.922433	0.020118	GTPBP1
ENSG00000152223	0.716031	0.020134	EPG5
ENSG00000165626	0.722672	0.020161	BEND7
ENSG00000269343	-0.7853	0.020183	ZNF587B
ENSG00000086200	-0.56648	0.020233	IPO11
ENSG00000102595	0.789491	0.020263	UGGT2
ENSG00000142961	0.685608	0.020273	MOB3C
ENSG00000167680	0.838268	0.020318	SEMA6B
ENSG00000169718	-0.64044	0.020338	DUS1L
ENSG00000100867	1.406243	0.020341	DHRS2
ENSG00000255471	1.962484	0.020361	AP001528.2
ENSG00000120438	-0.75949	0.020397	TCP1
ENSG00000151883	0.643848	0.020413	PARP8
ENSG00000246523	1.255416	0.020414	AP001528.1
ENSG00000144736	-0.63162	0.020424	SHQ1
ENSG00000171943	0.676828	0.020461	SRGAP2C
ENSG00000157895	-0.53737	0.020474	C12orf43
ENSG00000058804	-0.55236	0.020514	NDC1
ENSG00000241622	2.015374	0.020532	RARRES2P1
ENSG00000173821	0.922955	0.020558	RNF213
ENSG00000138623	0.819947	0.020578	SEMA7A
ENSG00000100626	0.861811	0.02058	GALNT16
ENSG00000159917	-0.75556	0.020637	ZNF235
ENSG00000111252	0.840913	0.020667	SH2B3
ENSG00000172301	-0.7473	0.020711	COPRS
ENSG00000080561	0.766207	0.020716	MID2
ENSG00000232040	0.811128	0.020751	ZBED9
ENSG00000085433	0.941383	0.020777	WDR47
ENSG00000129951	0.791859	0.020794	PLPPR3
ENSG00000071127	-0.74676	0.020832	WDR1
ENSG00000134597	-0.53304	0.020851	RBMX2
ENSG00000102316	0.628597	0.020863	MAGED2
ENSG00000104361	0.735984	0.020902	NIPAL2
ENSG00000138346	-0.94368	0.020914	DNA2
ENSG00000112787	-0.57395	0.020926	FBRSL1
ENSG00000180353	2.406001	0.020965	HCLS1
ENSG00000105711	1.610075	0.021031	SCN1B
ENSG00000132763	-0.75841	0.021045	MMACHC
ENSG00000197093	2.109429	0.021111	GAL3ST4
ENSG00000101182	-0.74008	0.021174	PSMA7

ENSG00000140263	-0.50626	0.021182	SORD
ENSG00000250326	1.74164	0.021212	AC104596.1
ENSG00000186871	-0.99304	0.021225	ERCC6L
ENSG00000171219	1.021764	0.021266	CDC42BPG
ENSG00000135452	0.635804	0.021269	TSPAN31
ENSG00000156802	-0.62919	0.021273	ATAD2
ENSG00000185730	-0.52585	0.021298	ZNF696
ENSG00000225159	-1.47468	0.021316	NPM1P39
ENSG00000127837	-0.49805	0.021323	AAMP
ENSG00000170291	-0.58989	0.021329	ELP5
ENSG00000110851	-0.50099	0.021357	PRDM4
ENSG00000167088	-0.7424	0.021386	SNRPD1
ENSG00000179403	-0.6954	0.021398	VWA1
ENSG00000186792	-1.10419	0.021405	HYAL3
ENSG00000152818	2.325129	0.021428	UTRN
ENSG00000251661	1.008361	0.021428	AC136475.1
ENSG00000120949	2.464825	0.021456	TNFRSF8
ENSG00000260276	0.965889	0.021463	AC022167.2
ENSG00000170144	-0.5656	0.021474	HNRNPA3
ENSG00000134057	-0.92493	0.021505	CCNB1
ENSG00000111696	-0.58577	0.021515	NT5DC3
ENSG00000150753	-0.6455	0.021551	CCT5
ENSG00000163636	-0.58532	0.021558	PSMD6
ENSG00000123545	-0.67059	0.021558	NDUFAF4
ENSG00000160993	-0.62198	0.021598	ALKBH4
ENSG00000041880	0.763687	0.021607	PARP3
ENSG00000106344	-0.48046	0.021624	RBM28
ENSG00000101391	-0.46962	0.021711	CDK5RAP1
ENSG00000070495	-0.71355	0.021808	JMJD6
ENSG00000169045	-0.48655	0.02186	HNRNPH1
ENSG00000128512	-1.08719	0.021875	DOCK4
ENSG00000225972	-0.79259	0.021882	MTND1P23
ENSG00000164654	-0.64324	0.021901	MIOS
ENSG00000133641	-0.63934	0.02194	C12orf29
ENSG00000159055	-0.74134	0.021967	MIS18A
ENSG00000005100	-0.5908	0.022011	DHX33
ENSG00000204406	0.673934	0.022028	MBD5
ENSG00000177000	0.783337	0.022064	MTHFR
ENSG00000101489	1.97975	0.022081	CELF4
ENSG00000112511	0.818512	0.022084	PHF1
ENSG00000125818	-0.54666	0.022108	PSMF1

ENSG00000136153	0.925043	0.02211	LMO7
ENSG00000172766	-0.65157	0.022113	NAA16
ENSG00000176845	1.690372	0.022126	METRNL
ENSG00000146530	0.787762	0.022135	VWDE
ENSG00000188566	-0.72803	0.022163	NDOR1
ENSG00000110442	-0.8669	0.022182	COMMD9
ENSG00000161328	0.758319	0.022208	LRRC56
ENSG00000135900	-0.55655	0.02222	MRPL44
ENSG00000111199	1.27584	0.022276	TRPV4
ENSG00000177570	0.75638	0.022307	SAMD12
ENSG00000101911	-0.62891	0.022337	PRPS2
ENSG00000136868	0.888781	0.022365	SLC31A1
ENSG00000101236	0.718087	0.022405	RNF24
ENSG00000213889	0.771418	0.022442	PPM1N
ENSG00000183019	1.743293	0.022452	MCEMP1
ENSG00000173418	-0.64282	0.022456	NAA20
ENSG00000104998	0.745621	0.022478	IL27RA
ENSG00000174950	1.392201	0.022498	CD164L2
ENSG00000124766	2.544515	0.022503	SOX4
ENSG00000164074	0.519245	0.022512	ABHD18
ENSG00000078674	0.738581	0.02252	PCM1
ENSG00000139636	0.582626	0.022523	LMBR1L
ENSG00000104140	-0.64831	0.022536	RHOV
ENSG00000030304	1.00959	0.022562	MUSK
ENSG00000145293	-0.52469	0.022594	ENOPH1
ENSG00000146409	0.606302	0.022601	SLC18B1
ENSG00000126749	-0.61281	0.022618	EMG1
ENSG00000261026	2.69551	0.022619	AC105046.1
ENSG00000149599	1.365248	0.022628	DUSP15
ENSG00000114686	-0.66794	0.022631	MRPL3
ENSG00000170653	0.563789	0.022702	ATF7
ENSG00000115541	-0.90682	0.02278	HSPE1
ENSG00000136279	-0.72639	0.022794	DBNL
ENSG00000114841	1.087943	0.022798	DNAH1
ENSG00000282965	1.031164	0.022808	AP001005.3
ENSG00000146834	-0.49586	0.022812	MEPCE
ENSG00000130382	-0.56902	0.022847	MLLT1
ENSG00000132341	-0.80878	0.02285	RAN
ENSG00000183479	-1.47856	0.02286	TREX2
ENSG00000096063	-0.46117	0.02289	SRPK1
ENSG00000113649	-0.63059	0.0229	TCERG1

ENSG00000080824	-0.74704	0.022926	HSP90AA1
ENSG00000164163	-0.49427	0.022944	ABCE1
ENSG00000091527	-0.43828	0.022997	CDV3
ENSG00000068400	0.543902	0.023006	GRIPAP1
ENSG00000138032	0.672287	0.023009	PPM1B
ENSG00000183763	-0.8601	0.023036	TRAIP
ENSG00000118242	-0.70005	0.023041	MREG
ENSG00000283667	2.260119	0.023045	AC009802.1
ENSG00000166451	-0.53564	0.023054	CENPN
ENSG00000112096	-0.48245	0.02311	SOD2
ENSG00000128346	1.210387	0.023165	C22orf23
ENSG00000146090	0.948468	0.02318	RASGEF1C
ENSG00000173213	0.803698	0.023194	TUBB8P12
ENSG00000214655	0.59613	0.023198	ZSWIM8
ENSG00000166689	0.773217	0.02322	PLEKHA7
ENSG00000095539	0.571074	0.023228	SEMA4G
ENSG00000172915	0.663486	0.023232	NBEA
ENSG00000165312	1.376569	0.023302	OTUD1
ENSG00000167676	1.097066	0.023309	PLIN4
ENSG00000168140	-0.99457	0.023362	VASN
ENSG00000197275	-0.75212	0.023362	RAD54B
ENSG00000175416	-0.62399	0.023441	CLTB
ENSG00000161204	-0.52737	0.023515	ABCF3
ENSG00000279414	2.0868	0.023542	CR392039.2
ENSG00000255652	2.184135	0.02356	AC140847.2
ENSG00000171262	-0.56346	0.023573	FAM98B
ENSG00000106479	0.77775	0.023573	ZNF862
ENSG00000231431	1.045401	0.02358	FAR2P4
ENSG00000144935	0.840489	0.02361	TRPC1
ENSG00000013306	-0.59061	0.023663	SLC25A39
ENSG00000146147	0.594308	0.0237	MLIP
ENSG00000162729	0.738833	0.023705	IGSF8
ENSG00000067533	-0.56615	0.023731	RRP15
ENSG00000118939	-0.82622	0.02375	UCHL3
ENSG00000001461	0.661209	0.023769	NIPAL3
ENSG00000100600	0.786153	0.023792	LGMN
ENSG00000115268	-0.64595	0.023794	RPS15
ENSG00000166920	2.135623	0.023826	C15orf48
ENSG00000274911	-0.69796	0.023826	AL627230.2
ENSG00000196295	0.596244	0.023873	AC005154.1
ENSG00000136048	0.819915	0.023925	DRAM1

ENSG00000135624	-0.5633	0.023955	CCT7
ENSG00000146143	-0.65387	0.023957	PRIM2
ENSG00000149532	-0.44894	0.023974	CPSF7
ENSG00000187961	-0.66843	0.02398	KLHL17
ENSG00000105618	-0.62512	0.023982	PRPF31
ENSG00000169248	0.92082	0.02401	CXCL11
ENSG00000167766	0.669651	0.024023	ZNF83
ENSG00000187531	-0.6684	0.024024	SIRT7
ENSG00000272031	0.573473	0.024059	ANKRD34A
ENSG00000226037	1.596064	0.024064	LINC01040
ENSG00000160161	1.213448	0.024083	CILP2
ENSG00000167925	0.621301	0.024084	GHDC
ENSG00000259781	-0.91026	0.024087	HMGB1P6
ENSG00000119285	-0.53622	0.024088	HEATR1
ENSG00000148019	-0.80689	0.0241	CEP78
ENSG00000105298	-0.55814	0.024124	CACTIN
ENSG00000141385	-0.47675	0.024124	AFG3L2
ENSG00000197937	0.82115	0.024148	ZNF347
ENSG00000259448	2.043348	0.024188	LINC02352
ENSG00000117411	-0.56637	0.024203	B4GALT2
ENSG00000170876	-0.572	0.024232	TMEM43
ENSG00000063180	0.540618	0.02427	CA11
ENSG00000118257	2.158898	0.024277	NRP2
ENSG00000162512	0.721237	0.02432	SDC3
ENSG00000132436	-0.85795	0.024342	FIGNL1
ENSG00000211460	-0.44131	0.024397	TSN
ENSG00000163794	1.766374	0.024441	UCN
ENSG00000183770	1.948954	0.024485	FOXL2
ENSG00000196584	-0.97159	0.024509	XRCC2
ENSG00000085117	1.201393	0.024541	CD82
ENSG00000188825	1.071802	0.024548	LINC00910
ENSG00000100416	-0.71809	0.024562	TRMU
ENSG00000174004	1.250972	0.024604	NRROS
ENSG00000092853	-1.07208	0.024608	CLSPN
ENSG00000079337	1.273741	0.024633	RAPGEF3
ENSG00000183647	-0.80064	0.024702	ZNF530
ENSG00000260942	-0.97495	0.024816	CAPN10-AS1
ENSG00000053900	-0.65295	0.024829	ANAPC4
ENSG00000109794	1.257404	0.024853	FAM149A
ENSG00000071462	-0.55622	0.024879	BUD23
ENSG00000204060	1.131514	0.024887	FOXO6

ENSG00000079785	-0.46541	0.024893	DDX1
ENSG00000253626	-1.00106	0.024899	EIF5AL1
ENSG00000021355	0.855908	0.024905	SERPINB1
ENSG00000105136	0.70128	0.024948	ZNF419
ENSG00000139044	1.157778	0.024969	B4GALNT3
ENSG00000265458	-1.17239	0.024981	AC132938.3
ENSG00000153234	2.166373	0.025058	NR4A2
ENSG00000143621	-0.61871	0.02507	ILF2
ENSG00000095370	1.527857	0.025089	SH2D3C
ENSG00000163075	-0.87608	0.025096	CFAP221
ENSG00000023734	-0.46211	0.025125	STRAP
ENSG00000258102	1.327757	0.025181	MAP1LC3B2
ENSG00000198901	-0.70915	0.025189	PRC1
ENSG00000123983	0.651991	0.025196	ACSL3
ENSG00000128050	-0.70794	0.025208	PAICS
ENSG00000108799	0.645601	0.025221	EZH1
ENSG00000186056	0.937537	0.025253	MATN1-AS1
ENSG00000181104	0.787921	0.025256	F2R
ENSG00000101695	1.133495	0.025256	RNF125
ENSG00000088280	0.667027	0.025263	ASAP3
ENSG00000100897	0.507606	0.025268	DCAF11
ENSG00000181035	0.633676	0.025307	SLC25A42
ENSG00000196422	0.59241	0.025454	PPP1R26
ENSG00000158604	0.642868	0.025473	TMED4
ENSG00000203485	-0.65198	0.025494	INF2
ENSG00000142528	-0.50851	0.025544	ZNF473
ENSG00000105251	2.000697	0.025545	SHD
ENSG00000145817	0.604858	0.025579	YIPF5
ENSG00000260912	0.727113	0.02558	AL158206.1
ENSG00000172780	1.115316	0.025587	RAB43
ENSG00000138821	-2.27262	0.025598	SLC39A8
ENSG00000150510	-1.1377	0.025606	FAM124A
ENSG00000119865	-1.84542	0.025646	CNRIP1
ENSG00000116560	-0.74269	0.025722	SFPQ
ENSG00000273802	1.242303	0.025759	HIST1H2BG
ENSG00000173064	0.826781	0.02578	HECTD4
ENSG00000187583	-0.76984	0.02578	PLEKHN1
ENSG00000143799	-0.60358	0.025801	PARP1
ENSG00000236107	2.139859	0.025815	AC010127.1
ENSG00000101365	-0.57853	0.025885	IDH3B
ENSG00000204632	1.536632	0.025901	HLA-G

ENSG00000173273	0.68474	0.025913	TNKS
ENSG00000155099	0.669779	0.025917	PIP4P2
ENSG00000259585	1.010988	0.026013	RBM17P4
ENSG00000170191	-0.5406	0.026026	NANP
ENSG00000127863	0.720001	0.02604	TNFRSF19
ENSG00000174796	0.506999	0.026087	THAP6
ENSG00000254860	1.131256	0.026109	TMEM9B-AS1
ENSG00000255112	0.672846	0.026116	CHMP1B
ENSG00000108176	0.941011	0.026123	DNAJC12
ENSG00000177426	0.611536	0.026124	TGIF1
ENSG00000257923	0.535136	0.026125	CUX1
ENSG00000011304	-0.53796	0.026149	PTBP1
ENSG00000233098	0.624584	0.026176	CCDC144NL-AS1
ENSG00000138621	-0.71321	0.026181	PPCDC
ENSG00000108344	-0.62224	0.026277	PSMD3
ENSG00000165732	-0.59394	0.026294	DDX21
ENSG00000215190	-0.9606	0.026322	LINC00680
ENSG00000122861	0.942639	0.026337	PLAU
ENSG00000106686	1.330515	0.0264	SPATA6L
ENSG00000118420	-0.73062	0.026401	UBE3D
ENSG00000160194	-0.62884	0.026438	NDUFV3
ENSG00000062485	-0.55575	0.026454	CS
ENSG00000094804	-0.91351	0.026516	CDC6
ENSG00000181873	-0.69515	0.026532	IBA57
ENSG00000237154	2.574669	0.026542	MCFD2P1
ENSG00000145632	2.311472	0.026577	PLK2
ENSG00000197037	-0.56341	0.026597	ZSCAN25
ENSG00000186017	0.687505	0.026601	ZNF566
ENSG00000004487	-0.45752	0.026632	KDM1A
ENSG00000007080	-0.65051	0.026654	CCDC124
ENSG00000197841	0.584538	0.026656	ZNF181
ENSG00000086967	1.99592	0.026707	MYBPC2
ENSG00000214114	-0.67346	0.026721	MYCBP
ENSG00000121871	1.932821	0.026737	SLITRK3
ENSG00000253846	1.540391	0.026748	PCDHGA10
ENSG00000113643	-0.41454	0.026801	RARS
ENSG00000124575	1.682951	0.026861	HIST1H1D
ENSG00000115596	2.795112	0.026923	WNT6
ENSG00000197170	-0.60087	0.02695	PSMD12
ENSG00000119844	0.577174	0.027012	AFTPH
ENSG00000280968	-1.48922	0.02707	MIR3653

ENSG00000083093	-0.49235	0.027097	PALB2
ENSG00000005075	-0.66159	0.027119	POLR2J
ENSG00000100084	-0.62198	0.027146	HIRA
ENSG00000112237	-0.54979	0.027174	CCNC
ENSG00000276390	-1.20514	0.027193	AC004241.3
ENSG00000272108	1.894253	0.027295	AC244517.1
ENSG00000173193	1.865971	0.02731	PARP14
ENSG00000106028	-0.90209	0.027337	SSBP1
ENSG00000143476	-0.62672	0.02734	DTL
ENSG00000167986	-0.50779	0.027348	DDB1
ENSG00000225178	-0.72561	0.027353	RPSAP58
ENSG00000182175	1.13817	0.027396	RGMA
ENSG00000064393	0.935545	0.027406	HIPK2
ENSG00000137831	0.54887	0.027416	UACA
ENSG00000276644	2.716767	0.027423	DACH1
ENSG00000079435	1.286373	0.027502	LIPE
ENSG00000070371	0.570178	0.027524	CLTCL1
ENSG00000128581	-0.75191	0.027526	IFT22
ENSG00000178104	0.480422	0.027557	PDE4DIP
ENSG00000088325	-0.61747	0.027566	TPX2
ENSG00000143748	-0.51415	0.02759	NVL
ENSG00000171497	-0.65623	0.0276	PPID
ENSG00000175582	0.738108	0.027624	RAB6A
ENSG00000170619	-0.59527	0.027714	COMMD5
ENSG00000261762	-1.17982	0.027717	AC027228.2
ENSG00000204519	-0.62813	0.027742	ZNF551
ENSG00000165527	-0.49014	0.02775	ARF6
ENSG00000254480	-1.30579	0.027756	AC015689.1
ENSG00000280987	-0.70653	0.027771	MATR3
ENSG00000183625	1.435828	0.027791	CCR3
ENSG00000205269	1.169229	0.027837	TMEM170B
ENSG00000160233	0.936461	0.027841	LRRC3
ENSG00000239322	-1.16632	0.027874	ATP6V1B1-AS1
ENSG00000163521	0.635322	0.027875	GLB1L
ENSG00000079246	-0.54487	0.027883	XRCC5
ENSG00000129991	0.707951	0.027894	TNNI3
ENSG00000147459	0.716716	0.027895	DOCK5
ENSG00000273674	1.028263	0.027902	AC021752.1
ENSG00000161800	-0.5571	0.027907	RACGAP1
ENSG00000128245	-0.59089	0.027913	YWHAH
ENSG00000162458	0.667502	0.027979	FBLIM1

ENSG00000106266	-0.54095	0.027988	SNX8
ENSG00000127054	-0.46241	0.027994	INTS11
ENSG00000083223	0.691442	0.027999	ZCCHC6
ENSG00000075223	2.117765	0.028148	SEMA3C
ENSG00000085563	1.001651	0.028168	ABCB1
ENSG00000164951	0.617155	0.028168	PDP1
ENSG00000163702	0.483124	0.028206	IL17RC
ENSG00000129460	-0.54749	0.02822	NGDN
ENSG00000099810	-0.45104	0.028234	MTAP
ENSG00000271395	2.581269	0.028249	LINC02336
ENSG00000065361	0.814037	0.028277	ERBB3
ENSG00000100764	-0.51057	0.028294	PSMC1
ENSG00000254221	1.316169	0.028328	PCDHGB1
ENSG00000177455	2.017585	0.028378	CD19
ENSG00000161970	-0.57173	0.028381	RPL26
ENSG00000270084	1.319778	0.028463	GAS5-AS1
ENSG00000125651	-0.42489	0.028465	GTF2F1
ENSG00000158270	6.824146	0.028469	COLEC12
ENSG00000141934	1.152945	0.028527	PLPP2
ENSG00000139192	0.692799	0.02854	TAPBPL
ENSG00000177082	-0.78215	0.028599	WDR73
ENSG00000108639	-0.71454	0.028634	SYNGR2
ENSG00000205560	0.88751	0.028664	CPT1B
ENSG00000008283	-0.55263	0.028696	CYB561
ENSG00000146733	0.874974	0.028706	PSPH
ENSG00000087365	-0.43987	0.028718	SF3B2
ENSG00000100485	0.719595	0.02874	SOS2
ENSG00000156869	0.678188	0.028757	FRRS1
ENSG00000106628	-0.63525	0.028788	POLD2
ENSG00000161526	-0.4729	0.028846	SAP30BP
ENSG00000215784	-0.73286	0.028856	FAM72D
ENSG00000065154	-0.61925	0.028857	OAT
ENSG00000135622	0.653591	0.02888	SEMA4F
ENSG00000147118	0.688103	0.02894	ZNF182
ENSG00000071073	0.653418	0.02898	MGAT4A
ENSG00000175764	-1.15281	0.029115	TTLL11
ENSG00000047346	0.70657	0.029116	FAM214A
ENSG00000166147	0.671261	0.029125	FBN1
ENSG00000108559	-0.48926	0.029132	NUP88
ENSG00000131462	-0.68033	0.029187	TUBG1
ENSG00000135185	-0.58992	0.029199	TMEM243

ENSG00000147180	0.643066	0.029226	ZNF711
ENSG00000162736	0.521853	0.029276	NCSTN
ENSG00000106459	-0.51164	0.029329	NRF1
ENSG00000115840	-0.64803	0.029347	SLC25A12
ENSG00000164124	0.620929	0.029388	TMEM144
ENSG00000164002	-0.81835	0.029389	EXO5
ENSG00000067248	-0.55385	0.029391	DHX29
ENSG00000115641	-0.65254	0.029414	FHL2
ENSG00000170464	0.656205	0.029446	DNAJC18
ENSG00000198515	-2.18202	0.02947	CNGA1
ENSG00000198055	-0.44329	0.029491	GRK6
ENSG00000072182	2.177772	0.029514	ASIC4
ENSG00000151304	-0.62118	0.02952	SRFBP1
ENSG00000104213	1.03488	0.029609	PDGFRL
ENSG00000257108	1.510962	0.029609	NHLRC4
ENSG00000120948	-0.66854	0.029611	TARDBP
ENSG00000184117	0.590762	0.02962	NIPSNAP1
ENSG00000136527	-0.64838	0.029664	TRA2B
ENSG00000223764	0.66138	0.029671	AL645608.1
ENSG00000162433	-0.45244	0.029695	AK4
ENSG00000185436	0.636984	0.029717	IFNLR1
ENSG00000111602	-0.7424	0.029786	TIMELESS
ENSG00000134308	-0.57799	0.029815	YWHAQ
ENSG00000135406	1.163962	0.02989	PRPH
ENSG00000135476	-0.82114	0.02992	ESPL1
ENSG00000029363	-0.71652	0.029961	BCLAF1
ENSG00000162927	0.55704	0.029981	PUS10
ENSG00000084463	-0.53241	0.030001	WBP11
ENSG00000119772	0.502036	0.030015	DNMT3A
ENSG00000064195	-2.05293	0.03004	DLX3
ENSG00000157873	1.02872	0.030052	TNFRSF14
ENSG00000159885	0.839873	0.030052	ZNF222
ENSG00000259425	0.763476	0.03009	AC011767.1
ENSG00000092621	1.126545	0.03016	PHGDH
ENSG00000122591	-0.47706	0.030187	FAM126A
ENSG00000104823	0.498517	0.030189	ECH1
ENSG00000248278	-0.8182	0.030205	SUMO2P17
ENSG00000270647	-0.49054	0.030246	TAF15
ENSG00000205937	-0.42574	0.030246	RNPS1
ENSG00000139722	-0.4617	0.030249	VPS37B
ENSG00000083750	0.603951	0.030251	RRAGB

ENSG00000141569	-0.50399	0.0303	TRIM65
ENSG00000159640	0.989206	0.030358	ACE
ENSG00000272933	0.755056	0.030383	AL391121.1
ENSG00000075702	-0.80794	0.030395	WDR62
ENSG00000091664	1.796146	0.030397	SLC17A6
ENSG00000162614	-0.63001	0.030404	NEXN
ENSG00000136010	1.839527	0.030413	ALDH1L2
ENSG00000184428	-0.55377	0.030418	TOP1MT
ENSG00000167325	-0.80311	0.030434	RRM1
ENSG00000158417	-0.63043	0.030457	EIF5B
ENSG00000163131	1.914559	0.030493	CTSS
ENSG00000166833	2.025323	0.030525	NAV2
ENSG00000173848	-0.53376	0.030536	NET1
ENSG00000136950	-0.55513	0.030552	ARPC5L
ENSG00000197808	0.735263	0.030574	ZNF461
ENSG00000004838	-1.18657	0.030588	ZMYND10
ENSG00000115042	0.52829	0.030651	FAHD2A
ENSG00000106367	-0.71108	0.030678	AP1S1
ENSG00000283696	1.139888	0.030765	AL592295.4
ENSG00000237438	-0.60347	0.030765	CECR7
ENSG00000177464	1.558408	0.030833	GPR4
ENSG00000124222	0.732523	0.030833	STX16
ENSG00000179476	0.715358	0.030855	C14orf28
ENSG00000170190	0.673776	0.030904	SLC16A5
ENSG00000167701	1.385588	0.030943	GPT
ENSG00000215492	-0.80038	0.030965	HNRNPA1P7
ENSG00000011426	-0.77365	0.031037	ANLN
ENSG00000227755	1.177077	0.03105	AP000344.1
ENSG00000037965	0.645863	0.031125	HOXC8
ENSG00000144848	-0.5548	0.031139	ATG3
ENSG00000078579	2.313254	0.031154	FGF20
ENSG00000111911	0.66375	0.03118	HINT3
ENSG00000085721	-0.46943	0.031241	RRN3
ENSG00000151468	0.803075	0.031255	CCDC3
ENSG00000164109	-0.91842	0.031278	MAD2L1
ENSG00000119326	-0.46778	0.031328	CTNNAL1
ENSG00000231259	0.999491	0.031331	AC125232.1
ENSG00000146083	0.813189	0.031346	RNF44
ENSG00000060656	0.668848	0.031349	PTPRU
ENSG00000136379	-0.58563	0.031391	ABHD17C
ENSG00000139915	1.603321	0.031393	MDGA2

ENSG00000174607	-1.91168	0.031443	UGT8
ENSG00000256628	-0.63266	0.031487	ZBTB11-AS1
ENSG00000185989	-0.96914	0.031514	RASA3
ENSG00000132792	-0.45752	0.031521	CTNNBL1
ENSG00000073849	0.630997	0.03155	ST6GAL1
ENSG00000124641	-0.5469	0.03166	MED20
ENSG00000281398	-0.95242	0.031721	SNHG4
ENSG00000139132	0.958926	0.031738	FGD4
ENSG00000101811	-0.6232	0.031757	CSTF2
ENSG00000236404	3.223543	0.03176	VLDLR-AS1
ENSG00000143507	1.34884	0.03184	DUSP10
ENSG00000122691	-2.64697	0.031841	TWIST1
ENSG00000260086	0.767164	0.031848	AC007611.1
ENSG00000277147	0.626486	0.031849	LINC00869
ENSG00000235652	1.27314	0.031872	AL356599.1
ENSG00000168234	0.724364	0.031902	TTC39C
ENSG00000168394	0.970268	0.031913	TAP1
ENSG00000125510	0.877398	0.031919	OPRL1
ENSG00000088833	-0.5226	0.031926	NSFL1C
ENSG00000114904	-0.53987	0.031933	NEK4
ENSG00000078142	0.555813	0.031952	PIK3C3
ENSG00000165637	-0.53611	0.032006	VDAC2
ENSG00000005001	1.859095	0.032023	PRSS22
ENSG00000067064	0.609222	0.032055	IDI1
ENSG00000126458	0.758147	0.032063	RRAS
ENSG00000125885	-0.70519	0.032069	MCM8
ENSG00000265666	0.811382	0.032094	RARA-AS1
ENSG00000210196	-0.64059	0.032107	MT-TP
ENSG00000155893	0.622932	0.032111	PXYLP1
ENSG00000110958	-0.6046	0.032142	PTGES3
ENSG00000076706	-1.34002	0.032181	MCAM
ENSG00000175040	0.887549	0.032199	CHST2
ENSG00000140545	0.640897	0.032202	MFGE8
ENSG00000213553	-0.67662	0.03226	RPLP0P6
ENSG00000205593	0.628534	0.032326	DENND6B
ENSG00000075218	-0.84032	0.032364	GTSE1
ENSG00000108591	-0.54615	0.03244	DRG2
ENSG00000111581	-0.6606	0.032445	NUP107
ENSG00000087077	-0.51392	0.032517	TRIP6
ENSG00000096696	1.094292	0.032604	DSP
ENSG00000123600	-0.60881	0.032609	METTL8

ENSG00000109572	0.687785	0.032629	CLCN3
ENSG00000066697	-0.53602	0.032638	MSANTD3
ENSG00000168439	-0.57187	0.03275	STIP1
ENSG00000109272	0.872243	0.032766	PF4V1
ENSG00000100028	-0.73476	0.032784	SNRPD3
ENSG00000169071	1.150325	0.032788	ROR2
ENSG00000167311	1.38727	0.032792	ART5
ENSG00000115211	-0.54869	0.032807	EIF2B4
ENSG00000167930	0.51357	0.032824	FAM234A
ENSG00000130021	-0.62182	0.032828	PUDP
ENSG00000105829	0.538968	0.032838	BET1
ENSG00000102312	0.490787	0.032865	PORCN
ENSG00000140391	-0.51294	0.032882	TSPAN3
ENSG00000170909	1.058076	0.032884	OSCAR
ENSG00000198431	-0.46858	0.032893	TXNRD1
ENSG00000141401	-0.68839	0.032908	IMPA2
ENSG00000244300	-0.71105	0.032917	GATA2-AS1
ENSG00000117751	-0.44015	0.03292	PPP1R8
ENSG00000125734	0.57721	0.032935	GPR108
ENSG00000232838	-0.54991	0.032957	PET117
ENSG00000225173	0.71853	0.032991	AL662890.1
ENSG00000175189	1.944918	0.032996	INHBC
ENSG00000133103	0.69661	0.033035	COG6
ENSG00000226415	-1.02217	0.033046	TPI1P1
ENSG00000225975	-1.07416	0.033072	LINC01534
ENSG00000102053	0.687436	0.033089	ZC3H12B
ENSG00000137726	1.544876	0.033099	FXYD6
ENSG00000256862	-1.07372	0.033179	AC005842.1
ENSG00000171824	-0.56313	0.033259	EXOSC10
ENSG00000123146	0.63448	0.033357	ADGRE5
ENSG00000119632	0.708565	0.033373	IFI27L2
ENSG00000164902	-0.43459	0.033431	PHAX
ENSG00000101447	-0.82884	0.033515	FAM83D
ENSG00000150768	-0.64168	0.033535	DLAT
ENSG00000116209	0.62029	0.033557	TMEM59
ENSG00000216331	1.893573	0.033592	HIST1H1PS1
ENSG00000259577	1.03634	0.033635	CERNA1
ENSG00000085185	0.568055	0.033667	BCORL1
ENSG00000109339	1.312506	0.033674	MAPK10
ENSG00000106049	0.570895	0.033686	HIBADH
ENSG00000113758	-0.52764	0.033745	DBN1

ENSG00000138411	0.924179	0.033765	HECW2
ENSG00000169519	0.551364	0.033772	METTL15
ENSG00000078668	-0.80839	0.033825	VDAC3
ENSG00000162878	-1.24653	0.033872	PKDCC
ENSG00000164181	0.95952	0.0339	ELOVL7
ENSG00000270060	1.410543	0.0339	AC090589.3
ENSG00000205559	-1.1417	0.033935	CHKB-AS1
ENSG00000074582	-0.60452	0.033952	BCS1L
ENSG00000163633	0.582996	0.033953	C4orf36
ENSG00000132004	-0.62265	0.033964	FBXW9
ENSG00000261189	1.797823	0.034005	AL031058.1
ENSG00000083444	0.831626	0.034035	PLOD1
ENSG00000110200	-0.7993	0.03415	ANAPC15
ENSG00000130311	-0.55806	0.034167	DDA1
ENSG00000130332	-0.726	0.034174	LSM7.00
ENSG00000175193	-0.52957	0.034301	PARL
ENSG00000156011	0.684328	0.034328	PSD3
ENSG00000184154	0.706409	0.034328	LRTOMT
ENSG00000200879	-1.15893	0.034356	SNORD14E
ENSG00000183032	0.541955	0.034366	SLC25A21
ENSG00000173141	-0.58273	0.034374	MRPL57
ENSG00000147650	0.726489	0.034401	LRP12
ENSG00000118518	0.453079	0.034513	RNF146
ENSG00000163882	-0.64289	0.034514	POLR2H
ENSG00000180900	-0.6051	0.03456	SCRIB
ENSG00000172889	0.838939	0.034621	EGFL7
ENSG00000205309	0.966662	0.034673	NT5M
ENSG00000172250	1.16024	0.034712	SERHL
ENSG00000157227	0.959817	0.034714	MMP14
ENSG00000267395	0.950703	0.034722	DM1-AS
ENSG00000154065	1.742496	0.034749	ANKRD29
ENSG00000166278	1.355545	0.034752	C2
ENSG00000147649	-0.47525	0.034753	MTDH
ENSG00000260329	0.693791	0.03476	AC007541.1
ENSG00000103356	-0.45123	0.034865	EARS2
ENSG00000204314	0.533816	0.034868	PRRT1
ENSG00000012223	1.425483	0.03489	LTF
ENSG00000183978	-0.6835	0.034897	COA3
ENSG00000119125	3.235166	0.034952	GDA
ENSG00000081721	-0.50389	0.034953	DUSP12
ENSG00000100290	1.062906	0.034993	BIK

ENSG00000121766	-0.56769	0.035	ZCCHC17
ENSG00000142233	1.742244	0.035009	NTN5
ENSG00000164031	0.637035	0.035025	DNAJB14
ENSG00000126067	-0.58326	0.035034	PSMB2
ENSG00000156504	-0.55039	0.035062	FAM122B
ENSG00000152642	-0.46484	0.035107	GPD1L
ENSG00000272405	-0.82804	0.035167	AL365181.3
ENSG00000132906	0.475718	0.035181	CASP9
ENSG00000167699	-0.50083	0.035194	GLOD4
ENSG00000267698	-0.95682	0.035201	AC002116.2
ENSG00000182552	-0.48063	0.03521	RWDD4
ENSG00000184939	0.702497	0.035233	ZFP90
ENSG00000104833	0.586184	0.035262	TUBB4A
ENSG00000115486	0.611889	0.035362	GGCX
ENSG00000055950	-0.6232	0.035399	MRPL43
ENSG00000182134	0.439567	0.03546	TDRKH
ENSG00000133997	-0.51919	0.035489	MED6
ENSG00000134986	0.50032	0.035601	NREP
ENSG00000031698	0.804644	0.035647	SARS
ENSG00000085872	-0.51417	0.035675	CHERP
ENSG00000257950	-1.09305	0.035753	P2RX5-TAX1BP3
ENSG00000162526	1.210709	0.035761	TSSK3
ENSG00000156970	-0.87055	0.035766	BUB1B
ENSG00000260448	-0.84645	0.035805	LCMT1-AS1
ENSG00000132383	-0.53238	0.03582	RPA1
ENSG00000105088	0.633005	0.035846	OLFM2
ENSG00000177721	0.82993	0.035886	ANXA2R
ENSG00000177084	-0.63153	0.035915	POLE
ENSG00000126457	-0.66426	0.035923	PRMT1
ENSG00000228549	0.946765	0.035952	BX284668.2
ENSG00000255108	1.408891	0.035963	AP006621.1
ENSG00000182759	1.357977	0.035978	MAFA
ENSG00000205356	0.548809	0.036001	TECPR1
ENSG00000167110	0.656449	0.036038	GOLGA2
ENSG00000238105	0.674459	0.03606	GOLGA2P5
ENSG00000067606	0.476868	0.036102	PRKCZ
ENSG00000228013	1.876125	0.036126	IL6R-AS1
ENSG00000240489	-0.7567	0.036175	SETP14
ENSG00000154319	1.423385	0.036185	FAM167A
ENSG00000160124	-0.7127	0.036201	CCDC58
ENSG00000176749	-0.6985	0.03621	CDK5R1

ENSG00000166262	0.593495	0.03621	FAM227B
ENSG00000102384	-0.79408	0.036224	CENPI
ENSG00000196504	-0.41119	0.036279	PRPF40A
ENSG00000119820	0.547771	0.036338	YIPF4
ENSG00000112081	-0.70988	0.036339	SRSF3
ENSG00000132967	-0.94581	0.036373	HMGB1P5
ENSG00000197312	-0.51541	0.036396	DDI2
ENSG00000143294	-0.45232	0.036408	PRCC
ENSG00000042753	-0.66242	0.036455	AP2S1
ENSG00000147439	-0.54412	0.036482	BIN3
ENSG00000105339	0.775436	0.036504	DENND3
ENSG00000134905	-0.67993	0.036529	CARS2
ENSG00000175482	0.665531	0.036532	POLD4
ENSG00000167733	0.656975	0.036537	HSD11B1L
ENSG00000110013	0.587899	0.036583	SIAE
ENSG00000124201	1.046596	0.036662	ZNFX1
ENSG00000171574	-0.46866	0.036701	ZNF584
ENSG00000165792	-0.58032	0.036706	METTL17
ENSG00000271936	-0.84863	0.03671	AC012073.1
ENSG00000168811	-1.18628	0.03671	IL12A
ENSG00000138801	0.6029	0.036737	PAPSS1
ENSG00000119227	0.640724	0.03676	PIGZ
ENSG00000115415	2.068253	0.036864	STAT1
ENSG00000266904	0.733875	0.036867	LINC00663
ENSG00000116161	-0.7732	0.03691	CACYBP
ENSG00000244045	-0.55616	0.036918	TMEM199
ENSG00000116062	-0.45871	0.03692	MSH6
ENSG00000213064	-0.5502	0.036984	SFT2D2
ENSG00000164756	1.132209	0.03701	SLC30A8
ENSG00000111328	-0.61981	0.037014	CDK2AP1
ENSG00000145335	1.464457	0.037028	SNCA
ENSG00000224861	-0.68274	0.037119	YBX1P1
ENSG00000137804	-0.65845	0.03715	NUSAP1
ENSG00000157653	-1.20718	0.037157	C9orf43
ENSG00000101605	0.947901	0.037158	MYOM1
ENSG00000203772	-0.8764	0.037158	SPRN
ENSG00000144895	-0.52307	0.0372	EIF2A
ENSG00000085415	-0.49612	0.037221	SEH1L
ENSG00000176438	1.77757	0.037235	SYNE3
ENSG00000151503	-0.57416	0.037348	NCAPD3
ENSG00000065060	0.881515	0.037367	UHRF1BP1

ENSG00000176024	0.563363	0.037384	ZNF613
ENSG00000111348	-2.4183	0.037456	ARHGDIB
ENSG00000112624	0.671848	0.037507	BICRAL
ENSG00000170364	-0.70304	0.037542	SETMAR
ENSG00000269952	1.196946	0.037593	AL117336.2
ENSG00000163918	-0.74106	0.037614	RFC4
ENSG00000182263	0.894426	0.037616	FIGN
ENSG00000257524	1.105069	0.03762	AL157935.2
ENSG00000187122	1.54427	0.037648	SLIT1
ENSG00000204580	0.525204	0.037713	DDR1
ENSG00000225963	2.326577	0.037719	AC009950.1
ENSG00000158467	0.593607	0.037724	AHCYL2
ENSG00000112130	-0.46878	0.037777	RNF8
ENSG00000205002	0.982437	0.037802	AARD
ENSG00000164933	-0.39614	0.037806	SLC25A32
ENSG00000153207	-0.55413	0.037856	AHCTF1
ENSG00000153029	0.500393	0.037883	MR1
ENSG00000278948	0.995116	0.037897	AL031587.5
ENSG00000132153	-0.42091	0.037901	DHX30
ENSG00000115998	0.580669	0.037921	C2orf42
ENSG00000258727	0.752491	0.037928	AL135999.1
ENSG00000112029	-0.77218	0.037928	FBXO5
ENSG00000176386	-0.58332	0.037929	CDC26
ENSG00000170854	-0.51854	0.037935	RIOX2
ENSG00000145494	-0.70311	0.038032	NDUFS6
ENSG00000116977	0.586237	0.038059	LGALS8
ENSG00000108774	-0.57166	0.038064	RAB5C
ENSG00000170638	-0.53153	0.038082	TRABD
ENSG00000135506	0.563795	0.038118	OS9
ENSG00000151790	-1.42975	0.03812	TDO2
ENSG00000272760	0.995874	0.038149	AC093726.1
ENSG00000123609	0.708561	0.038174	NMI
ENSG00000132591	-0.50349	0.038174	ERAL1
ENSG00000126016	0.871347	0.038199	AMOT
ENSG00000135519	0.76023	0.038255	KCNH3
ENSG00000105357	0.578316	0.038285	MYH14
ENSG00000103174	-0.67278	0.038288	NAGPA
ENSG00000272221	-1.0361	0.038338	AL645933.2
ENSG00000125870	-0.5683	0.038422	SNRPB2
ENSG00000113575	-0.41642	0.038448	PPP2CA
ENSG00000163481	-0.52351	0.038469	RNF25

ENSG00000198569	1.970515	0.038484	SLC34A3
ENSG00000248918	0.991966	0.038492	AC008808.1
ENSG00000186185	-0.87912	0.038519	KIF18B
ENSG00000159217	-0.79448	0.038544	IGF2BP1
ENSG00000100092	-0.5182	0.038561	SH3BP1
ENSG00000185267	1.066547	0.038562	CDNF
ENSG00000189060	0.797046	0.038565	H1F0
ENSG00000108813	1.154338	0.03857	DLX4
ENSG00000213585	-0.50948	0.038582	VDAC1
ENSG00000160131	-0.43098	0.038633	VMA21
ENSG00000070785	-0.58512	0.038648	EIF2B3
ENSG00000174915	-0.5261	0.038752	PTDSS2
ENSG00000138193	-0.67979	0.03876	PLCE1
ENSG00000012963	-0.45413	0.038773	UBR7
ENSG00000136560	0.523442	0.038778	TANK
ENSG00000139832	1.238931	0.038851	RAB20
ENSG00000247746	0.748637	0.038851	USP51
ENSG00000116459	-0.637	0.038896	ATP5PB
ENSG00000156261	-0.50538	0.038901	CCT8
ENSG00000138081	0.753465	0.038947	FBXO11
ENSG00000137460	1.037285	0.038979	FHDC1
ENSG00000178038	1.007789	0.039003	ALS2CL
ENSG00000134531	0.712689	0.039054	EMP1
ENSG00000147852	2.249868	0.03906	VLDLR
ENSG00000179387	0.569506	0.039114	ELMOD2
ENSG00000129173	-0.9018	0.039153	E2F8
ENSG00000185664	0.858579	0.039166	PMEL
ENSG00000214756	-0.68439	0.039315	CSKMT
ENSG00000117245	0.693453	0.039375	KIF17
ENSG00000079308	1.110295	0.039382	TNS1
ENSG00000167380	0.58567	0.039391	ZNF226
ENSG00000137807	-0.6621	0.039455	KIF23
ENSG00000019485	0.77808	0.039485	PRDM11
ENSG00000183576	-0.39407	0.039508	SETD3
ENSG00000143321	-0.44575	0.039514	HDGF
ENSG00000164929	1.789806	0.039518	BAALC
ENSG00000234072	0.560885	0.039522	AC074117.1
ENSG00000221968	0.592506	0.039559	FADS3
ENSG00000275549	1.024919	0.039561	STPG3-AS1
ENSG00000119537	0.608828	0.03963	KDSR
ENSG00000188785	0.721106	0.039634	ZNF548

ENSG00000171763	-0.44779	0.039651	SPATA5L1
ENSG00000197969	0.461725	0.039659	VPS13A
ENSG00000243323	1.744083	0.03969	PTPRVP
ENSG00000213341	-0.42916	0.039696	CHUK
ENSG00000163607	-0.50999	0.039733	GTPBP8
ENSG00000082458	0.540878	0.039764	DLG3
ENSG00000174327	0.644849	0.039805	SLC16A13
ENSG00000229953	-1.07508	0.03982	AL590666.2
ENSG00000172922	-0.97451	0.039871	RNASEH2C
ENSG00000260917	0.925159	0.039899	AL158212.3
ENSG00000154920	-0.84974	0.039964	EME1
ENSG00000198355	-0.46973	0.039969	PIM3
ENSG00000149929	-0.80781	0.039992	HIRIP3
ENSG00000125629	0.536829	0.039995	INSIG2
ENSG00000111206	-0.68253	0.040031	FOXM1
ENSG00000241685	-0.52321	0.040037	ARPC1A
ENSG00000180769	0.69888	0.040073	WDFY3-AS2
ENSG00000134283	-0.50711	0.040082	PPHLN1
ENSG00000116016	1.826556	0.040085	EPAS1
ENSG00000263818	1.389436	0.040091	AC091178.1
ENSG00000250644	1.737505	0.040095	AC068580.4
ENSG00000144893	-0.71516	0.040102	MED12L
ENSG00000137575	0.441987	0.040153	SDCBP
ENSG00000089053	-0.53449	0.040215	ANAPC5
ENSG00000159147	-0.53096	0.040216	DONSON
ENSG00000163293	-1.34036	0.040243	NIPAL1
ENSG00000223482	-0.51738	0.040258	NUTM2A-AS1
ENSG00000160325	0.802589	0.040264	CACFD1
ENSG00000068383	-0.44513	0.040267	INPP5A
ENSG00000139514	0.928073	0.040336	SLC7A1
ENSG00000204564	-0.56926	0.040337	C6orf136
ENSG00000007255	0.659404	0.040354	TRAPPC6A
ENSG00000086506	-0.70281	0.040439	HBQ1
ENSG00000049449	0.609327	0.040444	RCN1
ENSG00000250510	0.657109	0.040456	GPR162
ENSG00000143303	0.522667	0.040459	RRNAD1
ENSG00000129347	-0.49195	0.040483	KRI1
ENSG00000164647	-0.78919	0.040537	STEAP1
ENSG00000269899	1.77208	0.040566	AC025857.2
ENSG00000150787	-0.59768	0.040663	PTS
ENSG00000104904	-0.56729	0.040719	OAZ1

ENSG00000183765	-0.57676	0.04077	CHEK2
ENSG00000168411	-0.59657	0.040781	RFWD3
ENSG00000069020	1.610969	0.040783	MAST4
ENSG00000187555	-0.43066	0.040791	USP7
ENSG00000112167	-0.69068	0.040845	SAYSD1
ENSG00000168056	0.532506	0.040984	LTBP3
ENSG00000249565	-0.90521	0.040992	SERBP1P5
ENSG00000131584	-0.71275	0.04101	ACAP3
ENSG00000157216	-0.5515	0.041056	SSBP3
ENSG00000171067	-0.51169	0.041067	C11orf24
ENSG00000110172	-0.69821	0.041087	CHORDC1
ENSG00000068878	-0.52335	0.04113	PSME4
ENSG00000269918	0.949751	0.041246	AF131215.6
ENSG00000188033	1.260681	0.041307	ZNF490
ENSG00000153006	-0.52396	0.041313	SREK1IP1
ENSG00000055130	-0.46796	0.041337	CUL1
ENSG00000204272	0.619968	0.041343	NBDY
ENSG00000106682	-0.48873	0.041353	EIF4H
ENSG00000105223	0.660915	0.041354	PLD3
ENSG00000139865	1.355026	0.041374	TTC6
ENSG00000104290	0.62384	0.041405	FZD3
ENSG00000280194	1.004994	0.041405	AD000864.1
ENSG00000125944	-0.43762	0.041432	HNRNPR
ENSG00000272968	1.680627	0.041497	RBAK-RBAKDN
ENSG00000262668	1.048335	0.041509	AJ003147.2
ENSG00000140830	-0.45684	0.041539	TXNL4B
ENSG00000102904	0.704473	0.041545	TSNAXIP1
ENSG00000128274	0.910477	0.041577	A4GALT
ENSG00000179899	0.811893	0.041584	PHC1P1
ENSG00000064995	-0.47522	0.041602	TAF11
ENSG00000077238	0.550194	0.041618	IL4R
ENSG00000167723	0.853142	0.041639	TRPV3
ENSG00000146966	2.224907	0.041729	DENND2A
ENSG00000224424	0.885669	0.041743	PRKAR2A-AS1
ENSG00000151967	-1.15777	0.04177	SCHIP1
ENSG00000277534	-0.92913	0.041853	AC007996.1
ENSG00000145794	2.365694	0.041988	MEGF10
ENSG00000148773	-0.83099	0.042004	MKI67
ENSG00000243244	1.014328	0.042012	STON1
ENSG00000182600	0.933213	0.04204	SNORC
ENSG00000133069	0.904735	0.042059	TMCC2

ENSG00000143028	0.938597	0.042155	SYPL2
ENSG00000182180	-0.49854	0.042179	MRPS16
ENSG00000079313	-0.41739	0.042184	REXO1
ENSG00000179833	0.531069	0.042186	SERTAD2
ENSG00000269473	-0.7798	0.0422	AC012313.8
ENSG00000088832	-0.55264	0.042209	FKBP1A
ENSG00000187601	0.751669	0.042218	MAGEH1
ENSG00000188610	-0.56923	0.042298	FAM72B
ENSG00000116032	1.87579	0.042355	GRIN3B
ENSG00000116874	-0.4816	0.042377	WARS2
ENSG00000144285	2.637162	0.042385	SCN1A
ENSG00000159176	0.812582	0.042424	CSRP1
ENSG00000170089	-0.77318	0.042455	AC106795.1
ENSG00000261474	1.853583	0.042488	AC026471.4
ENSG00000125484	-0.4303	0.04254	GTF3C4
ENSG00000132275	-0.47658	0.042545	RRP8
ENSG00000102265	0.96297	0.042551	TIMP1
ENSG00000173334	0.872495	0.042556	TRIB1
ENSG00000137404	-0.91404	0.042571	NRM
ENSG00000062822	-0.64358	0.042604	POLD1
ENSG00000224157	1.621164	0.042609	HCG14
ENSG00000101294	-0.53237	0.042626	HM13
ENSG00000263874	1.709318	0.042643	LINC00672
ENSG00000171202	-0.71679	0.042681	TMEM126A
ENSG00000249115	-0.69707	0.042683	HAUS5
ENSG00000142544	-0.58786	0.042699	CTU1
ENSG00000152208	0.905238	0.042735	GRID2
ENSG00000279453	0.767965	0.04286	Z99129.4
ENSG00000113231	0.780161	0.042873	PDE8B
ENSG00000196756	-0.46828	0.042887	SNHG17
ENSG00000222041	-0.57817	0.042909	CYTOR
ENSG00000082153	-0.52481	0.042914	BZW1
ENSG00000131368	-0.66325	0.042934	MRPS25
ENSG00000143384	0.55478	0.042957	MCL1
ENSG00000170385	-0.60395	0.043004	SLC30A1
ENSG00000031823	-0.52635	0.043063	RANBP3
ENSG00000132849	0.876406	0.043098	PATJ
ENSG00000131558	0.501209	0.043099	EXOC4
ENSG00000018408	0.555391	0.043299	WWTR1
ENSG00000130707	2.105313	0.043318	ASS1
ENSG00000142065	0.543242	0.043329	ZFP14

ENSG00000149328	-0.60897	0.04336	GLB1L2
ENSG00000123179	-0.55127	0.043376	EBPL
ENSG00000119950	0.630935	0.04346	MXI1
ENSG00000230453	-0.50051	0.04346	ANKRD18B
ENSG00000138180	-0.65754	0.043513	CEP55
ENSG00000147883	0.663584	0.043539	CDKN2B
ENSG00000174989	0.552704	0.043599	FBXW8
ENSG00000080986	-0.65457	0.043609	NDC80
ENSG00000137216	0.532862	0.043624	TMEM63B
ENSG00000254413	0.860713	0.043629	CHKB-CPT1B
ENSG00000110888	0.538081	0.04363	CAPRIN2
ENSG00000148688	-0.63649	0.043654	RPP30
ENSG00000104818	1.496865	0.04367	CGB2
ENSG00000143436	-0.56615	0.043749	MRPL9
ENSG00000115364	-0.4797	0.043753	MRPL19
ENSG00000052795	-0.49568	0.043754	FNIP2
ENSG00000177728	0.469889	0.043797	TMEM94
ENSG00000027869	-0.49998	0.043819	SH2D2A
ENSG00000198931	-0.60391	0.043846	APRT
ENSG00000169871	0.864968	0.043849	TRIM56
ENSG00000102003	-0.55198	0.043862	SYP
ENSG00000110075	-0.49722	0.04396	PPP6R3
ENSG00000267696	7.873377	0.043965	ERVK-28
ENSG00000138771	0.773699	0.044004	SHROOM3
ENSG00000158186	-0.40213	0.044039	MRAS
ENSG00000114107	0.447715	0.044058	CEP70
ENSG00000139343	-0.71773	0.044096	SNRPF
ENSG00000108468	-0.60952	0.044149	CBX1
ENSG00000124795	-0.42094	0.044165	DEK
ENSG00000213676	0.383935	0.044169	ATF6B
ENSG00000135423	0.841874	0.044203	GLS2
ENSG00000135597	-0.40988	0.04421	REPS1
ENSG00000138078	0.475067	0.044221	PREPL
ENSG00000130433	1.194916	0.044279	CACNG6
ENSG00000197405	0.950795	0.044287	C5AR1
ENSG00000160791	1.023512	0.044287	CCR5
ENSG00000206262	1.251009	0.044338	FOXL2NB
ENSG00000198205	0.661488	0.044376	ZXDA
ENSG00000278053	-0.41279	0.044482	DDX52
ENSG00000251322	0.645921	0.044508	SHANK3
ENSG00000212127	0.999828	0.044515	TAS2R14

ENSG00000163050	-0.53013	0.044525	COQ8A
ENSG00000196748	1.189911	0.044579	CLPSL2
ENSG00000086061	-0.48425	0.044601	DNAJA1
ENSG00000117479	-0.49985	0.044714	SLC19A2
ENSG00000186684	0.979134	0.044717	CYP27C1
ENSG00000155827	-0.40703	0.044769	RNF20
ENSG00000214367	-0.58953	0.044769	HAUS3
ENSG00000183077	-0.55329	0.044801	AFMID
ENSG00000167971	0.801135	0.044804	CASKIN1
ENSG00000051523	-1.28559	0.044808	CYBA
ENSG00000160867	0.613389	0.044848	FGFR4
ENSG00000040531	-0.67667	0.04489	CTNS
ENSG00000181097	1.03	0.04491	AC105219.1
ENSG00000162409	0.599792	0.044913	PRKAA2
ENSG00000171502	2.31048	0.044914	COL24A1
ENSG00000163249	0.514561	0.044967	CCNYL1
ENSG00000181781	0.756964	0.044968	ODF3L2
ENSG00000196547	0.568257	0.044974	MAN2A2
ENSG00000244151	-0.95363	0.044974	AC010973.2
ENSG00000115875	-0.55375	0.044976	SRSF7
ENSG00000273492	1.028111	0.045021	AP000229.1
ENSG00000065621	0.865047	0.045066	GSTO2
ENSG00000125122	0.909714	0.045093	LRRC29
ENSG00000008710	0.788944	0.045165	PKD1
ENSG00000234028	0.676461	0.04518	AC062029.1
ENSG00000011198	-0.62975	0.045193	ABHD5
ENSG00000169548	0.629871	0.04524	ZNF280A
ENSG00000143256	-0.5584	0.04524	PFDN2
ENSG00000167779	0.683042	0.045265	IGFBP6
ENSG00000168679	1.77782	0.045312	SLC16A4
ENSG00000233369	0.519376	0.045319	GTF2IP4
ENSG00000111615	-0.45139	0.045323	KRR1
ENSG00000255992	1.790147	0.045333	AC131009.1
ENSG00000088826	0.943126	0.045355	SMOX
ENSG00000153395	-0.55377	0.04536	LPCAT1
ENSG00000188322	0.72772	0.045384	SBK1
ENSG00000182327	0.930989	0.045445	GLTPD2
ENSG00000137872	0.667897	0.04546	SEMA6D
ENSG00000105520	-0.61712	0.04549	PLPPR2
ENSG00000248456	7.815316	0.04555	LINC02485
ENSG00000119953	-0.47043	0.045605	SMNDC1

ENSG00000091262	0.547332	0.045609	ABCC6
ENSG00000123485	-0.65205	0.045655	HJURP
ENSG00000157613	1.082982	0.045657	CREB3L1
ENSG00000115307	-0.55242	0.045669	AUP1
ENSG00000243927	-0.70048	0.045695	MRPS6
ENSG00000229474	1.166961	0.045699	PATL2
ENSG00000156256	-0.49855	0.045706	USP16
ENSG00000197417	-0.78443	0.045727	SHPK
ENSG00000057608	-0.47564	0.045802	GDI2
ENSG00000110925	0.566487	0.045863	CSRNP2
ENSG00000244026	-0.481	0.045891	FAM86DP
ENSG00000157916	-0.44482	0.045914	RER1
ENSG00000277475	1.25109	0.04597	AC213203.1
ENSG00000237187	0.628135	0.046126	NR2F1-AS1
ENSG00000213047	0.620838	0.046133	DENND1B
ENSG00000267278	0.648082	0.046151	MAP3K14-AS1
ENSG00000139372	-0.48042	0.046163	TDG
ENSG00000228109	0.574865	0.046175	MELTF-AS1
ENSG00000183579	-0.44032	0.04622	ZNRF3
ENSG00000152455	-0.57763	0.046298	SUV39H2
ENSG00000132837	1.766317	0.046466	DMGDH
ENSG00000132535	0.592654	0.0465	DLG4
ENSG00000214455	0.95013	0.046513	RCN1P2
ENSG00000258732	0.772441	0.046528	AC025884.1
ENSG00000143633	-0.52421	0.046646	C1orf131
ENSG00000122696	-0.54529	0.046657	SLC25A51
ENSG00000108370	-0.52726	0.046798	RGS9
ENSG00000132313	-0.63434	0.0468	MRPL35
ENSG00000197106	-1.81882	0.046802	SLC6A17
ENSG00000156876	-0.64199	0.046824	SASS6
ENSG00000174885	1.83643	0.046902	NLRP6
ENSG00000108439	-0.58601	0.046962	PNPO
ENSG00000261578	1.310923	0.046963	AP003119.3
ENSG00000130640	-0.47303	0.046972	TUBGCP2
ENSG00000187051	-0.59127	0.046993	RPS19BP1
ENSG00000156500	0.595389	0.047038	FAM122C
ENSG00000135916	0.606204	0.047043	ITM2C
ENSG00000244627	0.673712	0.047049	Z98749.2
ENSG00000141574	1.23338	0.047084	SECTM1
ENSG00000182379	1.271106	0.047175	NXPH4
ENSG00000164733	0.569888	0.047184	CTSB

ENSG00000105497	0.498786	0.047206	ZNF175
ENSG00000149575	1.402673	0.047235	SCN2B
ENSG00000248592	1.164356	0.047258	TMEM110-MUSTN1
ENSG00000149930	-0.60281	0.047318	TAOK2
ENSG00000168135	1.447439	0.047354	KCNJ4
ENSG00000154839	-0.58017	0.04737	SKA1
ENSG00000233822	1.066371	0.047405	HIST1H2BN
ENSG00000128272	0.714168	0.047414	ATF4
ENSG00000153291	2.282465	0.047422	SLC25A27
ENSG00000131591	-0.45533	0.047424	C1orf159
ENSG00000157823	0.542383	0.047438	AP3S2
ENSG00000227398	0.798554	0.047613	KIF9-AS1
ENSG00000245552	1.38206	0.047635	AP000787.1
ENSG00000115252	1.690583	0.04767	PDE1A
ENSG00000197670	1.784665	0.047678	AL157838.1
ENSG00000135144	1.478746	0.047681	DTX1
ENSG00000137822	-0.49637	0.047741	TUBGCP4
ENSG00000127586	-0.66157	0.047746	CHTF18
ENSG00000136811	-0.58041	0.047791	ODF2
ENSG00000273261	1.029635	0.047802	AC092953.2
ENSG00000168310	0.537799	0.04783	IRF2
ENSG00000119574	-0.51261	0.047837	ZBTB45
ENSG00000091622	1.493216	0.047852	PITPNM3
ENSG00000204618	1.202153	0.047853	RNF39
ENSG00000154229	0.543684	0.047907	PRKCA
ENSG00000146701	-0.50156	0.047946	MDH2
ENSG00000141524	0.716258	0.047982	TMC6
ENSG00000234545	-0.41869	0.048013	FAM133B
ENSG00000176928	1.306405	0.048024	GCNT4
ENSG00000112110	-0.66185	0.048026	MRPL18
ENSG00000153558	0.538979	0.048055	FBXL2
ENSG00000103365	-0.50517	0.04809	GGA2
ENSG00000122566	-0.64573	0.048112	HNRNPA2B1
ENSG00000280099	0.826706	0.048118	AL603750.1
ENSG00000154639	0.4379	0.048163	CXADR
ENSG00000213593	-0.47173	0.048201	TMX2
ENSG00000141582	0.680984	0.048233	CBX4
ENSG00000151465	-0.54557	0.048251	CDC123
ENSG00000271380	1.157913	0.048271	AL451085.2
ENSG00000111846	0.639853	0.048302	GCNT2
ENSG00000145362	1.106771	0.04832	ANK2

ENSG00000228343	-0.94108	0.04833	AC115618.2
ENSG00000204540	1.059208	0.048374	PSORS1C1
ENSG00000119421	-0.60199	0.048472	NDUFA8
ENSG00000086159	1.245768	0.04853	AQP6
ENSG00000076685	-0.76715	0.048564	NT5C2
ENSG00000104427	0.602312	0.048612	ZC2HC1A
ENSG00000138376	-0.59075	0.048629	BARD1
ENSG00000260176	1.742723	0.048645	AC141586.2
ENSG00000163714	-0.45549	0.048672	U2SURP
ENSG00000174514	0.644796	0.048674	MFSD4A
ENSG00000082996	0.545939	0.048676	RNF13
ENSG00000250067	0.596565	0.048752	YJEFN3
ENSG00000174840	-0.38056	0.048758	PDE12
ENSG00000161203	-0.58978	0.048809	AP2M1
ENSG00000151726	-0.39008	0.04885	ACSL1
ENSG00000055332	0.913394	0.048876	EIF2AK2
ENSG00000089597	0.484259	0.048931	GANAB
ENSG00000168124	1.106584	0.04895	OR1F1
ENSG00000175166	-0.58358	0.04896	PSMD2
ENSG00000188313	1.852786	0.049031	PLSCR1
ENSG00000139445	0.908228	0.049079	FOXN4
ENSG00000261663	-0.65362	0.049082	AC009065.8
ENSG00000256340	0.65064	0.049108	ABCC6P1
ENSG00000167566	0.543701	0.049166	NCKAP5L
ENSG00000130827	0.486992	0.049172	PLXNA3
ENSG00000100490	-0.68919	0.049203	CDKL1
ENSG00000110955	-0.47183	0.049251	ATP5F1B
ENSG00000167657	-0.57069	0.049334	DAPK3
ENSG00000134470	0.693131	0.049353	IL15RA
ENSG00000143924	-1.02373	0.049362	EML4
ENSG00000140259	-0.42666	0.04939	MFAP1
ENSG00000114346	-0.58409	0.049422	ECT2
ENSG00000214922	0.553898	0.049483	HLA-F-AS1
ENSG00000131697	-0.56571	0.04949	NPHP4
ENSG00000144504	-0.49546	0.049541	ANKMY1
ENSG00000064547	0.503817	0.049549	LPAR2
ENSG00000203995	-0.52479	0.049591	ZYG11A
ENSG00000130175	0.467412	0.049625	PRKCSH
ENSG00000133961	0.520108	0.049669	NUMB
ENSG00000113272	-0.4596	0.049681	THG1L
ENSG00000157259	0.502785	0.049692	GATAD1

ENSG00000260552	0.965846	0.049813	AC023043.1
ENSG00000113719	-0.44669	0.049898	ERGIC1
ENSG00000004779	-0.57705	0.049968	NDUFAB1
ENSG00000162623	-0.51029	0.049999	TYW3
ENSG00000112763	0.581937	0.050073	BTN2A1
ENSG00000234290	1.865678	0.050091	AC116366.1
ENSG00000164674	0.934928	0.050106	SYTL3
ENSG00000213949	-1.2745	0.05016	ITGA1
ENSG00000160446	-0.91784	0.050232	ZDHHC12
ENSG00000233966	-0.88613	0.050249	UBE2SP1
ENSG00000204920	0.709058	0.050303	ZNF155
ENSG00000259943	0.533769	0.050307	AL050341.2
ENSG00000163923	-0.60778	0.050327	RPL39L
ENSG00000136492	-0.70258	0.050331	BRIP1
ENSG00000132017	-0.51973	0.050383	DCAF15
ENSG00000171320	-0.80142	0.050469	ESCO2
ENSG00000092020	-0.48221	0.050543	PPP2R3C
ENSG00000103154	1.964635	0.050577	NECAB2
ENSG00000115266	0.765093	0.050582	APC2
ENSG00000236088	-0.62765	0.050628	COX10-AS1
ENSG00000128596	0.835483	0.05069	CCDC136
ENSG00000075275	0.510704	0.050722	CELSR1
ENSG00000143106	-0.59625	0.050784	PSMA5
ENSG00000099625	0.748784	0.050801	CBARP
ENSG00000239523	-0.85744	0.050869	MYLK-AS1
ENSG00000235706	0.796541	0.050917	DICER1-AS1
ENSG00000106105	0.795012	0.050931	GARS
ENSG00000160716	-1.63798	0.051056	CHRNB2
ENSG00000134317	0.978475	0.051067	GRHL1
ENSG00000186812	0.77039	0.051147	ZNF397
ENSG00000245017	0.85721	0.051186	LINC02453
ENSG00000154359	0.666623	0.051198	LONRF1
ENSG00000142945	-0.54011	0.051207	KIF2C
ENSG00000182107	0.577398	0.051217	TMEM30B
ENSG00000135070	-0.44831	0.051226	ISCA1
ENSG00000275601	1.357967	0.051234	AC011330.2
ENSG00000100344	0.720329	0.051236	PNPLA3
ENSG00000152270	-0.56828	0.051297	PDE3B
ENSG00000274523	-0.45536	0.051334	RCC1L
ENSG00000185504	-0.39826	0.051338	FAAP100
ENSG00000169372	-0.79889	0.051355	CRADD

ENSG00000258659	1.737518	0.051454	TRIM34
ENSG00000187801	0.724028	0.051454	ZFP69B
ENSG00000109321	1.987033	0.051523	AREG
ENSG00000135966	-0.47692	0.051528	TGFBRAP1
ENSG00000185022	2.126989	0.051544	MAFF
ENSG00000100109	-0.41831	0.051602	TFIP11
ENSG00000261645	1.254827	0.051622	DISC1FP1
ENSG00000253910	1.59681	0.051693	PCDHGB2
ENSG00000169288	-0.9241	0.051744	MRPL1
ENSG00000197114	-0.50578	0.051761	ZGPAT
ENSG00000140743	-0.43027	0.051774	CDR2
ENSG00000140326	-0.54397	0.051789	CDAN1
ENSG00000165752	-0.60744	0.051792	STK32C
ENSG00000214300	-0.76481	0.051801	SPDYE3
ENSG00000232450	1.332945	0.051825	AL133517.1
ENSG00000164638	0.627198	0.051853	SLC29A4
ENSG00000167136	-0.72127	0.05186	ENDOG
ENSG00000172757	-0.67999	0.051888	CFL1
ENSG00000261150	-1.79096	0.051892	EPPK1
ENSG00000091428	1.076891	0.051901	RAPGEF4
ENSG00000197121	0.522125	0.051907	PGAP1
ENSG00000214402	1.301836	0.05191	LCNL1
ENSG00000115290	1.050264	0.051928	GRB14
ENSG00000173110	0.785542	0.051935	HSPA6
ENSG00000174482	0.577691	0.051953	LINGO2
ENSG00000131848	-0.64881	0.051967	ZSCAN5A
ENSG00000100601	-0.39546	0.052012	ALKBH1
ENSG00000236609	0.666497	0.052031	ZNF853
ENSG00000109881	-0.80339	0.052101	CCDC34
ENSG00000053524	1.363086	0.05218	MCF2L2
ENSG00000204334	1.893241	0.05223	ERICH2
ENSG00000143702	0.558147	0.052243	CEP170
ENSG00000113812	-0.38696	0.052247	ACTR8
ENSG00000189403	-0.76111	0.052282	HMGB1
ENSG00000245614	-0.99437	0.0523	DDX11-AS1
ENSG00000119121	1.21333	0.052302	TRPM6
ENSG00000105137	-0.52647	0.052378	SYDE1
ENSG00000226690	1.72258	0.052408	AC013470.2
ENSG00000171813	-0.45211	0.052424	PWWP2B
ENSG00000109046	0.606305	0.05245	WSB1
ENSG00000137414	0.561976	0.052487	FAM8A1

ENSG00000228526	0.925537	0.052496	MIR34AHG
ENSG00000109917	-0.40582	0.052537	ZPR1
ENSG00000197217	0.467939	0.05257	ENTPD4
ENSG00000178952	-0.56312	0.052573	TUFM
ENSG00000135541	0.625308	0.052576	AHI1
ENSG00000127445	-0.66241	0.052599	PIN1
ENSG00000258302	1.58047	0.052606	AC025034.1
ENSG00000250802	0.887503	0.052644	ZBED3-AS1
ENSG00000102172	-0.51338	0.052662	SMS
ENSG00000100519	-0.56232	0.052672	PSMC6
ENSG00000162997	1.080999	0.05268	PRORSD1P
ENSG00000037241	-0.59979	0.052703	RPL26L1
ENSG00000113456	-0.42176	0.052747	RAD1
ENSG00000276291	0.623342	0.052755	FRG1HP
ENSG00000070961	0.497868	0.052757	ATP2B1
ENSG00000127616	-0.38952	0.052785	SMARCA4
ENSG00000100441	0.623035	0.052802	KHNYN
ENSG00000142684	-0.83188	0.052873	ZNF593
ENSG00000144840	-0.44978	0.052977	RABL3
ENSG00000176894	-0.82172	0.052998	PXMP2
ENSG00000214485	-0.63059	0.053013	RPL7P1
ENSG00000241472	-1.17192	0.05303	PTPRG-AS1
ENSG00000109805	-0.54434	0.053155	NCAPG
ENSG00000174276	-0.52784	0.05318	ZNHIT2
ENSG00000166819	2.02556	0.053193	PLIN1
ENSG00000121413	0.800724	0.053231	ZSCAN18
ENSG00000103978	0.53049	0.053239	TMEM87A
ENSG00000113648	-0.4759	0.053241	H2AFY
ENSG00000076043	-0.52598	0.053259	REXO2
ENSG00000137055	-0.38888	0.053286	PLAA
ENSG00000054118	-0.47578	0.0533	THRAP3
ENSG00000109606	-0.41755	0.053343	DHX15
ENSG00000141570	0.46032	0.053355	CBX8
ENSG00000101161	-0.4279	0.053373	PRPF6
ENSG00000037757	-0.47385	0.053374	MRI1
ENSG00000118600	-0.51868	0.053396	RXYLT1
ENSG00000131480	1.234835	0.053407	AOC2
ENSG00000125351	-0.50979	0.053434	UPF3B
ENSG00000275880	1.978053	0.053462	AL139385.1
ENSG00000104980	-0.46323	0.053494	TIMM44
ENSG00000151725	-0.58477	0.053574	CENPU

ENSG00000149100	-0.4796	0.053643	EIF3M
ENSG00000092010	0.646849	0.053777	PSME1
ENSG00000177150	-0.50796	0.053806	FAM210A
ENSG00000257086	0.612978	0.05394	AP001453.4
ENSG00000083454	1.454448	0.053981	P2RX5
ENSG00000196092	-1.57317	0.054003	PAX5
ENSG00000204427	0.459133	0.054039	ABHD16A
ENSG00000261693	1.230096	0.054158	AC134682.1
ENSG00000162032	0.71675	0.054222	SPSB3
ENSG00000279494	1.587206	0.054233	AL117328.2
ENSG00000006611	1.307788	0.054264	USH1C
ENSG00000100744	0.472106	0.054267	GSKIP
ENSG00000226067	0.562838	0.054332	LINC00623
ENSG00000186862	0.670671	0.054416	PDZD7
ENSG00000115020	0.679454	0.054491	PIKFYVE
ENSG00000156162	0.491161	0.054532	DPY19L4
ENSG00000121274	-0.41403	0.054546	PAPD5
ENSG00000178809	1.656714	0.054577	TRIM73
ENSG00000010292	-0.61802	0.054585	NCAPD2
ENSG00000167522	0.665573	0.054674	ANKRD11
ENSG00000032444	0.409556	0.054762	PNPLA6
ENSG00000181045	0.557103	0.05489	SLC26A11
ENSG00000113749	1.90473	0.054906	HRH2
ENSG00000107833	-0.57709	0.054916	NPM3
ENSG00000235912	-1.35337	0.054944	AL031729.1
ENSG00000137038	-0.55598	0.05496	DMAC1
ENSG00000126870	-0.48547	0.054973	WDR60
ENSG00000108823	1.972819	0.054996	SGCA
ENSG00000196116	0.877152	0.055009	TDRD7
ENSG00000121966	1.795283	0.055016	CXCR4
ENSG00000183814	-0.61583	0.055025	LIN9
ENSG00000263847	1.503512	0.055133	AP005899.1
ENSG00000129675	0.889316	0.055162	ARHGEF6
ENSG00000136930	-0.65804	0.055184	PSMB7
ENSG00000140044	1.904883	0.055187	JDP2
ENSG00000108518	-0.66209	0.055207	PFN1
ENSG00000164054	0.771713	0.055213	SHISA5
ENSG00000100714	-0.47405	0.055303	MTHFD1
ENSG00000076067	0.489833	0.055361	RBMS2
ENSG00000143942	-0.80685	0.055379	CHAC2
ENSG00000185238	-0.46023	0.055382	PRMT3

ENSG00000265241	-0.52939	0.055421	RBM8A
ENSG00000188739	-0.61504	0.055438	RBM34
ENSG00000262223	1.595179	0.055487	AC110285.1
ENSG00000241553	-0.54576	0.0555	ARPC4
ENSG00000101049	2.155612	0.055536	SGK2
ENSG00000163655	-0.38556	0.05557	GMPS
ENSG00000018510	-0.41345	0.055597	AGPS
ENSG00000122335	0.52352	0.055627	SERAC1
ENSG00000226853	0.73624	0.055628	AC010894.2
ENSG00000165632	-0.407	0.055628	TAF3
ENSG00000058668	0.551329	0.055741	ATP2B4
ENSG00000080298	0.56917	0.055849	RFX3
ENSG00000169813	-0.44379	0.055851	HNRNPF
ENSG00000142188	0.414588	0.056004	TMEM50B
ENSG00000243147	-0.57395	0.056035	MRPL33
ENSG00000096401	-0.41527	0.056037	CDC5L
ENSG00000175920	1.416494	0.056086	DOK7
ENSG00000163472	-0.581	0.056088	TMEM79
ENSG00000187778	-0.52237	0.056093	MCRS1
ENSG00000203645	-0.44135	0.056111	LINC00501
ENSG00000113391	0.422657	0.05612	FAM172A
ENSG00000248275	-0.55556	0.056188	TRIM52-AS1
ENSG00000102096	-0.49835	0.056232	PIM2
ENSG00000244754	0.534259	0.056408	N4BP2L2
ENSG00000102753	-0.37759	0.056424	KPNA3
ENSG00000177479	-0.39337	0.056442	ARIH2
ENSG00000081870	-0.66194	0.056474	HSPB11
ENSG00000253958	0.769769	0.056504	CLDN23
ENSG00000182004	-0.70331	0.056505	SNRPE
ENSG00000108958	-1.17867	0.056521	AC130689.1
ENSG00000188760	-0.59211	0.056529	TMEM198
ENSG00000023041	-0.65417	0.056573	ZDHHC6
ENSG00000138028	0.568351	0.056638	CGREF1
ENSG00000100629	-0.70921	0.056656	CEP128
ENSG00000177045	0.499736	0.056671	SIX5
ENSG00000142731	-0.65156	0.056674	PLK4
ENSG00000164253	0.525294	0.056683	WDR41
ENSG00000171681	0.530124	0.056751	ATF7IP
ENSG00000183569	-0.63478	0.056828	SERHL2
ENSG00000166788	-0.68298	0.05683	SAAL1
ENSG00000217555	-0.6459	0.056913	CKLF

ENSG00000174238	-0.39346	0.056934	PITPNA
ENSG00000160075	-0.486	0.056993	SSU72
ENSG00000176248	-0.47073	0.057031	ANAPC2
ENSG00000260778	-1.08008	0.057081	AC009065.4
ENSG00000166170	-0.39226	0.057088	BAG5
ENSG00000198554	-0.59302	0.057102	WDHD1
ENSG00000167384	-0.62173	0.057142	ZNF180
ENSG00000104808	0.881419	0.057178	DHDH
ENSG00000177106	0.869835	0.057188	EPS8L2
ENSG00000186594	0.710328	0.057208	MIR22HG
ENSG00000164815	-0.46073	0.057244	ORC5
ENSG00000077312	-0.56101	0.057267	SNRPA
ENSG00000140463	0.474238	0.057307	BBS4
ENSG00000124191	2.029589	0.057311	TOX2
ENSG00000136942	-0.61431	0.057316	RPL35
ENSG00000134046	-0.47648	0.05737	MBD2
ENSG00000159733	1.069027	0.057386	ZFYVE28
ENSG00000176209	0.594969	0.057401	SMIM19
ENSG00000171450	1.000662	0.057401	CDK5R2
ENSG00000213300	-0.77252	0.057452	HNRNPA3P6
ENSG00000261373	-0.49087	0.057547	VPS9D1-AS1
ENSG00000170266	0.659773	0.057669	GLB1
ENSG00000169902	0.452215	0.057683	TPST1
ENSG00000169299	-0.54153	0.05773	PGM2
ENSG00000170579	0.601215	0.05784	DLGAP1
ENSG00000162520	0.922307	0.057899	SYNC
ENSG00000167535	0.575075	0.057918	CACNB3
ENSG00000280374	0.870239	0.05793	AC019080.5
ENSG00000165280	-0.50684	0.057962	VCP
ENSG00000131471	1.261736	0.057964	AOC3
ENSG00000163328	0.657015	0.057969	GPR155
ENSG00000172974	-0.55799	0.058021	AC007318.1
ENSG00000170832	0.524848	0.058024	USP32
ENSG00000178935	-0.63448	0.058068	ZNF552
ENSG00000064102	-0.43093	0.058122	INTS13
ENSG00000064666	-0.47579	0.058161	CNN2
ENSG00000174231	-0.50149	0.058169	PRPF8
ENSG00000188290	1.047064	0.058216	HES4
ENSG00000130182	-2.41388	0.058247	ZSCAN10
ENSG00000146263	-0.56767	0.058251	MMS22L
ENSG00000103275	-0.48768	0.058275	UBE2I

ENSG00000091536	1.158512	0.058451	MYO15A
ENSG00000139618	-0.59021	0.05853	BRCA2
ENSG00000131969	0.914268	0.058602	ABHD12B
ENSG00000165555	1.489653	0.058608	NOXRED1
ENSG00000140350	-0.50315	0.058618	ANP32A
ENSG00000104953	0.576928	0.058636	TLE6
ENSG00000123416	-0.52705	0.058677	TUBA1B
ENSG00000105220	-0.61429	0.058688	GPI
ENSG00000050405	0.579921	0.058724	LIMA1
ENSG00000196656	-0.56843	0.058731	AC004057.1
ENSG00000242173	0.737149	0.05879	ARHGDIG
ENSG00000006607	-0.53121	0.058794	FARP2
ENSG00000134748	-0.43827	0.058829	PRPF38A
ENSG00000267106	0.548829	0.058909	ZNF561-AS1
ENSG00000198189	0.434363	0.058921	HSD17B11
ENSG00000166704	0.485939	0.058966	ZNF606
ENSG00000135912	-0.49526	0.059012	TTLL4
ENSG00000125166	-0.45483	0.059022	GOT2
ENSG00000241506	-0.65369	0.059053	PSMC1P1
ENSG00000229619	-0.6404	0.059058	MBNL1-AS1
ENSG00000079101	1.092342	0.05913	CLUL1
ENSG00000246877	-1.24346	0.059137	DNM1P35
ENSG00000149923	-0.40295	0.059221	PPP4C
ENSG00000223573	1.434359	0.059232	TINCR
ENSG00000273568	-1.2496	0.059272	AC131009.3
ENSG00000206052	0.549801	0.059309	DOK6
ENSG00000157107	0.573557	0.059316	FCHO2
ENSG00000204370	-0.52343	0.059326	SDHD
ENSG00000140284	0.491037	0.059336	SLC27A2
ENSG00000132394	-0.51379	0.059379	EEFSEC
ENSG00000178498	0.406315	0.059383	DTX3
ENSG00000103018	-0.4476	0.05945	CYB5B
ENSG00000204560	-0.43838	0.059463	DHX16
ENSG00000185305	0.476878	0.059523	ARL15.00
ENSG00000234616	-0.54614	0.059571	JRK
ENSG00000160282	2.048091	0.059597	FTCD
ENSG00000018189	0.560953	0.059608	RUFY3
ENSG00000168268	-0.85009	0.059638	NT5DC2
ENSG00000170312	-0.70382	0.059683	CDK1
ENSG00000169976	-0.62429	0.059694	SF3B5
ENSG00000139437	-0.53847	0.05971	TCHP

ENSG00000155256	0.438593	0.059714	ZFYVE27
ENSG00000164346	-0.57154	0.059783	NSA2
ENSG00000149948	0.474042	0.059786	HMGA2
ENSG00000112996	-0.38316	0.05988	MRPS30
ENSG00000178773	-0.47393	0.059943	CPNE7

List of Transcripts in A2780CP20-RBPMSC

ID	log2FoldChange	pvalue	Gene.name
ENSG00000113389	2.783245	3.55E-09	NPR 3.00
ENSG00000023445	1.591552	2.39E-08	BIRC3
ENSG00000153071	7.153801	4.72E-07	DAB2
ENSG00000106546	2.746899	7.91E-07	AHR
ENSG00000172137	6.574845	4.66E-06	CALB2
ENSG00000019186	6.041288	5.67E-06	CYP24A1
ENSG00000112964	2.304923	8.10E-06	GHR
ENSG00000163393	3.586108	1.02E-05	SLC22A15
ENSG00000153253	-4.43726	1.32E-05	SCN3A
ENSG00000154162	3.078959	1.44E-05	CDH12
ENSG00000205765	0.859605	1.65E-05	C5orf51
ENSG00000164187	1.0316	1.95E-05	LMBRD2
ENSG00000172716	3.827804	2.00E-05	SLFN11
ENSG00000169862	6.484328	2.34E-05	CTNND2
ENSG00000145495	1.067094	3.47E-05	6-Mar
ENSG00000164171	1.931533	4.70E-05	ITGA2
ENSG00000164287	3.278587	5.82E-05	CDC20B
ENSG00000137801	2.308267	7.20E-05	THBS1
ENSG00000162545	2.716242	7.39E-05	CAMK2N1
ENSG00000171522	3.770525	0.000133	PTGER4
ENSG00000073282	-2.22616	0.000151	TP63
ENSG00000164089	3.819828	0.000199	ETNPPL
ENSG00000178031	5.367058	0.0002	ADAMTSL1
ENSG00000183783	3.348869	0.000241	KCTD8
ENSG00000271119	1.959753	0.000276	AC026412.3
ENSG00000157551	5.153211	0.000285	KCNJ15
ENSG00000151881	0.761324	0.000291	TMEM267
ENSG00000179406	1.105676	0.000303	LINC00174
ENSG00000151692	-0.82366	0.000313	RNF144A
ENSG00000150457	0.758304	0.000353	LATS2
ENSG00000188818	1.79003	0.000382	ZDHHC11
ENSG00000232615	2.63732	0.000632	AC026412.2

ENSG00000079931	2.120307	0.000651	MOXD1
ENSG00000115616	-2.91411	0.000665	SLC9A2
ENSG00000177685	-1.06978	0.000689	CRACR2B
ENSG00000169126	3.093428	0.000758	ARMC4
ENSG00000145390	1.301715	0.000761	USP53
ENSG00000102038	0.779624	0.000761	SMARCA1
ENSG00000164190	0.894261	0.000884	NIPBL
ENSG00000158966	1.239405	0.001134	CACHD1
ENSG00000151917	1.406978	0.001276	BEND6
ENSG00000145569	1.990233	0.001303	FAM105A
ENSG00000164659	1.828396	0.001303	KIAA1324L
ENSG00000125931	-1.87105	0.001392	CITED1
ENSG00000226287	-1.10586	0.001393	TMEM191A
ENSG00000134871	-3.69041	0.001424	COL4A2
ENSG00000196154	-2.35126	0.001473	S100A4
ENSG00000273142	1.010119	0.001495	AC073335.2
ENSG00000038382	1.142257	0.001537	TRIO
ENSG00000197603	0.971466	0.001572	C5orf42
ENSG00000106069	3.803778	0.001698	CHN2
ENSG00000118523	1.332166	0.001773	CTGF
ENSG00000168542	0.940977	0.001795	COL3A1
ENSG00000173559	1.04206	0.001919	NABP1
ENSG00000182022	1.742452	0.001951	CHST15
ENSG00000087085	1.106222	0.00198	ACHE
ENSG00000135114	1.652627	0.002333	OASL
ENSG00000228486	1.242058	0.00241	C2orf92
ENSG00000165102	0.575522	0.002452	HGSNAT
ENSG00000117600	4.16894	0.002466	PLPPR4
ENSG00000220804	1.430837	0.002556	LINC01881
ENSG00000180178	0.820252	0.002628	FAR2P1
ENSG00000185986	1.107204	0.002814	SDHAP3
ENSG00000138600	0.558895	0.002861	SPPL2A
ENSG00000091844	2.333668	0.003135	RGS17
ENSG00000139278	-2.03729	0.00322	GLIPR1
ENSG00000175793	-3.15224	0.003305	SFN
ENSG00000260708	-0.76873	0.003382	AL118516.1
ENSG00000117598	3.774318	0.00346	PLPPR5
ENSG00000169884	-0.60721	0.003517	WNT10B
ENSG00000187498	-3.56534	0.003824	COL4A1
ENSG00000157168	0.662715	0.003909	NRG1
ENSG00000112378	1.287187	0.003916	PERP

ENSG00000110330	0.519987	0.003961	BIRC2
ENSG00000164841	-5.03697	0.004075	TMEM74
ENSG00000153064	1.10721	0.004086	BANK1
ENSG00000232931	0.839167	0.004185	LINC00342
ENSG00000104447	0.896056	0.004231	TRPS1
ENSG00000251141	1.251071	0.004303	MRPS30-DT
ENSG00000132846	0.714303	0.004304	ZBED3
ENSG00000076716	-4.27033	0.004374	GPC4
ENSG00000134508	-1.11969	0.004811	CABLES1
ENSG00000082196	1.830601	0.004989	C1QTNF3
ENSG00000124275	0.868147	0.004993	MTRR
ENSG00000121879	0.666953	0.004993	PIK3CA
ENSG00000154122	1.12547	0.005092	ANKH
ENSG00000105974	-2.19343	0.005132	CAV1
ENSG00000112333	2.140955	0.005142	NR2E1
ENSG00000215158	0.957167	0.005203	AC138409.2
ENSG00000185813	-0.94543	0.005381	PCYT2
ENSG00000176542	0.629577	0.005481	USF3
ENSG00000153012	4.147914	0.00552	LGI2
ENSG00000187534	-0.81276	0.005576	PRR13P5
ENSG00000188185	0.839943	0.005709	LINC00265
ENSG00000164151	1.018981	0.005783	ICE1
ENSG00000103381	-0.9636	0.005827	CPPED1
ENSG00000142949	1.075365	0.005959	PTPRF
ENSG00000248092	0.552651	0.006085	NNT-AS1
ENSG00000276805	0.675195	0.006318	AL133216.2
ENSG00000128000	0.675602	0.006442	ZNF780B
ENSG00000125148	-0.63554	0.006493	MT2A
ENSG00000186523	-0.66952	0.006547	FAM86B1
ENSG00000112977	0.758885	0.006632	DAP
ENSG00000173376	1.932308	0.006852	NDNF
ENSG00000185621	0.775527	0.00689	LMLN
ENSG00000006062	0.787543	0.00708	MAP3K14
ENSG00000112941	0.836348	0.007151	PAPD7
ENSG00000249915	-0.56377	0.007241	PDCD6
ENSG00000185909	-0.55037	0.007402	KLHDC8B
ENSG00000107130	-0.52302	0.007416	NCS1
ENSG00000215252	0.487726	0.007438	GOLGA8B
ENSG00000167705	-0.54973	0.007531	RILP
ENSG00000188002	0.90293	0.007638	AC026412.1
ENSG00000145545	0.752203	0.007722	SRD5A1

ENSG00000174473	1.299176	0.00776	GALNTL6
ENSG00000164692	-3.93924	0.0079	COL1A2
ENSG00000112379	1.397839	0.0083	ARFGEF3
ENSG00000261236	-0.79553	0.008319	BOP 1.00
ENSG00000152620	0.475755	0.008336	NADK2
ENSG00000196782	2.711723	0.00848	MAML3
ENSG00000188242	-0.61408	0.008605	AC010442.1
ENSG00000175318	3.415685	0.008908	GRAMD2A
ENSG00000154930	2.163568	0.009076	ACSS1
ENSG00000137868	-3.3343	0.009505	STRA6
ENSG00000123119	2.609091	0.009543	NECAB1
ENSG00000142686	-0.5893	0.009739	C1orf216
ENSG00000165272	-1.20973	0.009864	AQP3
ENSG00000282508	0.738745	0.009988	LINC01002
ENSG00000083844	0.630702	0.01004	ZNF264
ENSG00000177738	0.63918	0.010047	AC025171.1
ENSG00000227719	2.538454	0.010126	AC006042.1
ENSG00000146112	-0.53279	0.01018	PPP1R18
ENSG00000175806	-1.00321	0.010264	MSRA
ENSG00000196352	0.70836	0.010269	CD55
ENSG00000178718	-0.66972	0.010405	RPP25
ENSG00000114331	0.638443	0.010547	ACAP2
ENSG00000205220	-0.79603	0.010569	PSMB10
ENSG00000163739	0.776449	0.01057	CXCL1
ENSG00000118162	-0.57844	0.010602	KPTN
ENSG00000197779	0.803177	0.010883	ZNF81
ENSG00000163012	0.650363	0.011086	ZSWIM2
ENSG00000083720	0.508898	0.011273	OXCT1
ENSG00000081014	0.604392	0.011337	AP4E1
ENSG00000163659	0.508817	0.011491	TIPARP
ENSG00000136830	-0.63581	0.011499	FAM129B
ENSG00000263327	1.268851	0.011618	TAPT1-AS1
ENSG00000239887	2.295262	0.01164	C1orf226
ENSG00000198947	0.652443	0.011751	DMD
ENSG00000147155	-0.65757	0.011752	EBP
ENSG00000128309	-0.75205	0.011771	MPST
ENSG00000146674	1.284674	0.011867	IGFBP3
ENSG00000154124	0.811413	0.011887	OTULIN
ENSG00000272556	0.833528	0.01192	GTF2IP13
ENSG00000168724	0.476577	0.012027	DNAJC21
ENSG00000261526	-0.92383	0.012252	AC012615.1

ENSG00000181690	1.176128	0.012861	PLAG1
ENSG00000108852	-0.50478	0.012883	MPP2
ENSG00000272432	-2.11459	0.013223	AL031432.3
ENSG00000264112	0.594207	0.013517	AC015813.1
ENSG00000114127	0.6483	0.013589	XRN1
ENSG00000171621	-0.60442	0.013851	SPSB1
ENSG00000181333	-1.71315	0.01401	HEPHL1
ENSG00000198546	-0.7018	0.014069	ZNF511
ENSG00000196549	-3.02591	0.014079	MME
ENSG00000130511	-0.59144	0.014091	SSBP4
ENSG00000107201	0.580643	0.014136	DDX58
ENSG00000272398	2.861334	0.014143	CD24
ENSG00000112992	0.483052	0.014172	NNT
ENSG00000164237	0.695611	0.014285	CMBL
ENSG00000182050	2.140858	0.014399	MGAT4C
ENSG00000133739	0.447179	0.014454	LRRCC1
ENSG00000237594	-0.93579	0.014529	AP000251.1
ENSG00000110400	-0.84427	0.014639	NECTIN1
ENSG00000189410	-0.45585	0.014659	SH2D5
ENSG00000135164	0.637601	0.014697	DMTF1
ENSG00000188816	-0.70475	0.014799	HMX2
ENSG00000145506	1.041352	0.01484	NKD2
ENSG00000143178	0.84346	0.014996	TBX19
ENSG00000227230	2.041541	0.015128	AL606534.1
ENSG00000196781	-0.48034	0.015147	TLE1
ENSG00000125170	-0.45958	0.015411	DOK4
ENSG00000149968	0.423185	0.015754	MMP3
ENSG00000116691	-0.52653	0.015779	MIIP
ENSG00000282885	1.175127	0.015814	AL627171.2
ENSG00000137825	-0.74331	0.015874	ITPKA
ENSG00000138814	0.672064	0.015887	PPP3CA
ENSG00000179886	-0.67418	0.015953	TIGD5
ENSG00000213445	-0.58378	0.01604	SIPA1
ENSG00000142546	-0.61452	0.016089	NOSIP
ENSG00000169621	1.103196	0.016103	APLF
ENSG00000114646	-0.64435	0.016109	CSPG5
ENSG00000182158	0.570363	0.016271	CREB3L2
ENSG00000155744	0.66843	0.016334	FAM126B
ENSG00000132356	0.549521	0.016416	PRKAA1
ENSG00000266094	-0.78406	0.016817	RASSF5
ENSG00000129911	-0.4815	0.016961	KLF16

ENSG00000281468	-1.09684	0.016998	AC006504.8
ENSG00000099624	-0.71945	0.017172	ATP5F1D
ENSG00000163536	0.560918	0.017205	SERPINI1
ENSG00000262406	1.343361	0.017209	MMP12
ENSG00000005108	2.288368	0.017215	THSD7A
ENSG00000113407	0.436901	0.017308	TARS
ENSG00000102981	-0.84917	0.017311	PARD6A
ENSG00000167011	3.17859	0.017374	NAT16
ENSG00000171004	0.472973	0.01742	HS6ST2
ENSG00000217128	0.545344	0.01747	FNIP1
ENSG00000110318	0.822416	0.017947	CEP126
ENSG00000138735	1.202581	0.018112	PDE5A
ENSG00000198162	0.518479	0.018119	MAN1A2
ENSG00000260924	-0.95168	0.018214	LINC01311
ENSG00000172262	0.495163	0.018274	ZNF131
ENSG00000246089	-0.5729	0.01828	AC016065.1
ENSG00000156381	-0.49665	0.018654	ANKRD9
ENSG00000170892	-0.5696	0.018708	TSEN34
ENSG00000177352	-0.54794	0.018724	CCDC71
ENSG00000157570	1.016116	0.019294	TSPAN18
ENSG00000165233	-0.60833	0.019306	CARD19
ENSG00000155368	-0.67461	0.019419	DBI
ENSG00000203709	1.267492	0.019424	MIR29B2CHG
ENSG00000134202	-0.79113	0.019614	GSTM3
ENSG00000156931	0.410796	0.02025	VPS8
ENSG00000173153	-0.43448	0.020331	ESRRA
ENSG00000168280	0.981058	0.020347	KIF5C
ENSG00000108107	-0.6368	0.020365	RPL28
ENSG00000130054	-0.75177	0.020393	FAM155B
ENSG00000204262	0.643808	0.020573	COL5A2
ENSG00000145348	0.463038	0.020798	TBCK
ENSG00000165795	-0.57412	0.020828	NDRG2
ENSG00000257167	-0.75255	0.020959	TMPO-AS1
ENSG00000165804	-0.50836	0.021144	ZNF219
ENSG00000263002	0.623621	0.021157	ZNF234
ENSG00000167034	1.003816	0.021244	NKX3-1
ENSG00000186472	0.521982	0.021298	PCLO
ENSG00000135441	-0.7261	0.021303	BLOC1S1
ENSG00000280927	1.062099	0.021628	CTBP1-AS
ENSG00000172667	0.6756	0.021935	ZMAT3
ENSG00000168286	-0.46348	0.021996	THAP11

ENSG00000127914	0.708397	0.022002	AKAP9
ENSG00000268030	0.750915	0.022068	AC005253.1
ENSG00000137561	-1.24208	0.022103	TTPA
ENSG00000240204	-0.60436	0.022359	SMKR1
ENSG00000117148	-1.35449	0.022373	ACTL8
ENSG00000080947	1.032293	0.022404	CROCCP3
ENSG00000177427	-0.52863	0.022495	MIEF2
ENSG00000060491	-0.52822	0.022613	OGFR
ENSG00000272645	0.561248	0.022761	GTF2IP20
ENSG00000100029	-0.60861	0.022787	PES 1.00
ENSG00000116863	-0.61042	0.022803	ADPRHL2
ENSG00000174307	-3.5565	0.02282	PHLDA3
ENSG00000186716	-0.45096	0.023285	BCR
ENSG00000197081	0.863157	0.023415	IGF2R
ENSG00000066739	0.536844	0.023544	ATG2B
ENSG00000153048	-0.56922	0.023752	CARHSP1
ENSG00000197977	1.259965	0.023828	ELOVL2
ENSG00000177600	-0.63058	0.023923	RPLP2
ENSG00000142657	-0.54571	0.023979	PGD
ENSG00000034510	-0.82387	0.024006	TMSB10
ENSG00000243364	-0.64676	0.024176	EFNA4
ENSG00000204392	-0.6097	0.024214	LSM 2.00
ENSG00000151150	-2.03168	0.024312	ANK3
ENSG00000173272	-0.64337	0.024379	MZT2A
ENSG00000072954	-0.47001	0.02449	TMEM38A
ENSG00000232653	0.997524	0.024512	GOLGA8N
ENSG00000023902	-0.63458	0.024522	PLEKHO1
ENSG00000113638	0.55108	0.024534	TTC33
ENSG00000145358	1.683285	0.024768	DDIT4L
ENSG00000198919	0.47082	0.024871	DZIP3
ENSG00000186654	-0.63699	0.02489	PRR5
ENSG00000129003	0.558312	0.024987	VPS13C
ENSG00000224066	1.64684	0.025023	AL049795.1
ENSG00000255282	0.710488	0.02531	WTAPP1
ENSG00000168172	0.484129	0.025435	HOOK3
ENSG00000106631	-2.67725	0.025484	MYL7
ENSG00000240024	0.597	0.025528	LINC00888
ENSG00000204237	-0.48951	0.025611	OXLD1
ENSG00000142632	-0.7236	0.025687	ARHGEF19
ENSG00000137818	-0.66253	0.025695	RPLP1
ENSG00000166963	-0.56281	0.025792	MAP1A

ENSG00000131446	-0.37002	0.025897	MGAT1
ENSG00000105649	-0.70204	0.025932	RAB3A
ENSG00000114738	-0.67108	0.025959	MAPKAPK3
ENSG00000147383	-0.47005	0.026057	NSDHL
ENSG00000106066	3.194587	0.026068	CPVL
ENSG00000147257	-0.68528	0.026111	GPC3
ENSG00000203581	1.739141	0.026113	OR1F2P
ENSG00000160113	-0.51003	0.026172	NR2F6
ENSG00000165392	0.598411	0.026303	WRN
ENSG00000158528	0.565981	0.026317	PPP1R9A
ENSG00000222046	2.107791	0.026385	DCDC2B
ENSG00000234684	0.578551	0.026486	SDCBP2-AS1
ENSG00000223760	0.715517	0.02651	MED15P9
ENSG00000172731	-0.52943	0.026686	LRRC20
ENSG00000187164	0.636754	0.026696	SHTN1
ENSG00000148677	0.509399	0.026849	ANKRD1
ENSG00000160999	-0.62095	0.026851	SH2B2
ENSG00000140323	-0.67524	0.026888	DISP2
ENSG00000152240	-0.45752	0.02707	HAUS1
ENSG00000172869	0.513733	0.027172	DMXL1
ENSG00000168386	1.201131	0.027474	FILIP1L
ENSG00000149231	0.524666	0.027503	CCDC82
ENSG00000240291	1.139103	0.027522	AL450384.2
ENSG00000160799	-0.53296	0.027556	CCDC12
ENSG00000164081	-0.5432	0.027578	TEX264
ENSG00000103876	-0.63054	0.027595	FAH
ENSG00000150756	0.771787	0.027715	FAM173B
ENSG00000116667	1.47727	0.02772	C1orf21
ENSG00000167524	0.817835	0.02773	SGK494
ENSG00000152082	-0.66266	0.027736	MZT2B
ENSG00000163960	0.550755	0.028032	UBXN7
ENSG00000180185	-0.55484	0.028065	FAHD1
ENSG00000229119	-1.23826	0.028107	AC026403.1
ENSG00000154102	-0.7904	0.028108	C16orf74
ENSG00000256223	0.538682	0.028144	ZNF10
ENSG00000273604	-0.36029	0.028196	EPOP
ENSG00000126709	-1.92376	0.028212	IFI6
ENSG00000129195	-0.4205	0.028428	PIMREG
ENSG00000139117	0.480564	0.028586	CPNE8
ENSG00000197782	0.435157	0.02861	ZNF780A
ENSG00000247157	1.710835	0.028659	LINC01252

ENSG00000135127	-0.42101	0.028678	BICDL1
ENSG00000073578	-0.46672	0.028744	SDHA
ENSG00000105486	-0.40689	0.02876	LIG1
ENSG00000187984	1.266159	0.028874	ANKRD19P
ENSG00000198915	-0.43432	0.029124	RASGEF1A
ENSG00000154978	-0.46691	0.029341	VOPP1
ENSG00000112183	-0.63237	0.029532	RBM24
ENSG00000014824	0.380114	0.029643	SLC30A9
ENSG00000182575	-0.7535	0.029678	NXPH3
ENSG00000083799	0.508049	0.029727	CYLD
ENSG00000259802	0.805167	0.029915	AC012640.2
ENSG00000008324	-0.57952	0.029932	SS18L2
ENSG00000118985	0.815125	0.029984	ELL2
ENSG00000213222	0.881107	0.030021	AC093724.1
ENSG00000147804	-0.54976	0.030095	SLC39A4
ENSG00000130332	-0.644	0.030257	LSM 7.00
ENSG00000162076	-0.52216	0.030369	FLYWCH2
ENSG00000178662	-2.02078	0.030413	CSRNP3
ENSG00000099364	-0.44146	0.030509	FBXL19
ENSG00000090932	-0.59388	0.030598	DLL3
ENSG00000100347	-0.51659	0.030667	SAMM50
ENSG00000119139	-0.76704	0.030674	TJP2
ENSG00000276045	-0.57228	0.030853	ORAI1
ENSG00000085224	0.507552	0.030888	ATRX
ENSG00000231918	1.221	0.030954	AC007402.1
ENSG00000116685	-0.51283	0.031005	KIAA2013
ENSG00000256673	1.200406	0.031027	AC141557.1
ENSG00000283674	-0.51137	0.031116	AC068587.4
ENSG00000177556	-0.74095	0.031148	ATOX1
ENSG00000139324	0.440003	0.031195	TMTC3
ENSG00000161714	-0.46962	0.031588	PLCD3
ENSG00000274292	1.561795	0.031601	AC084018.2
ENSG00000198718	0.558219	0.031851	TOGARAM1
ENSG00000152582	0.573994	0.031882	SPEF2
ENSG00000204248	0.732405	0.031902	COL11A2
ENSG00000163888	-0.84417	0.031938	CAMK2N2
ENSG00000160326	-0.79923	0.031938	SLC2A6
ENSG00000130193	-0.61936	0.031965	THEM6
ENSG00000075420	0.559256	0.03202	FNDC3B
ENSG00000131018	1.08786	0.032085	SYNE1
ENSG00000149311	0.564339	0.032101	ATM

ENSG00000111669	-0.49153	0.032254	TPI1
ENSG00000115317	-0.53502	0.032325	HTRA2
ENSG00000099977	-0.59719	0.032421	DDT
ENSG00000069998	-0.44644	0.032502	HDHD5
ENSG00000107099	0.991769	0.032542	DOCK8
ENSG00000121989	0.429125	0.032912	ACVR2A
ENSG00000176697	-2.31865	0.032918	BDNF
ENSG00000204356	-0.50267	0.033104	NELFE
ENSG00000065054	-0.62582	0.033361	SLC9A3R2
ENSG00000214022	-0.34271	0.03343	REPIN1
ENSG00000117394	-0.47116	0.033436	SLC2A1
ENSG00000174516	-0.71669	0.033601	PELI3
ENSG00000227212	1.586922	0.033936	PFN1P6
ENSG00000123810	-0.61377	0.033993	B9D2
ENSG00000233461	-0.67771	0.034052	AL445524.1
ENSG00000243056	0.756557	0.034192	EIF4EBP3
ENSG00000248126	1.171661	0.034347	AC091849.1
ENSG00000221869	-0.50028	0.034501	CEBPD
ENSG00000102109	-0.74886	0.034503	PCSK1N
ENSG00000233913	-0.67023	0.034532	RPL10P9
ENSG00000220749	-1.62111	0.034803	RPL21P28
ENSG00000169515	-0.34716	0.034927	CCDC8
ENSG00000146587	0.522051	0.034946	RBAK
ENSG00000271855	-0.9114	0.035091	AC073195.1
ENSG00000225465	0.870308	0.035348	RFPL1S
ENSG00000236914	0.774696	0.035604	LINC01852
ENSG00000204590	-0.37113	0.035609	GNL1
ENSG00000123992	-0.41505	0.03568	DNPEP
ENSG00000107404	-0.38511	0.035724	DVL1
ENSG00000140280	-0.44936	0.035729	LYSMD2
ENSG00000183570	1.207721	0.03581	PCBP3
ENSG00000237125	1.011632	0.035901	HAND2-AS1
ENSG00000174485	0.591483	0.036039	DENND4A
ENSG00000223960	0.504779	0.036052	AC009948.1
ENSG00000161149	-0.84784	0.036185	TUBA3FP
ENSG00000100138	-0.51356	0.036195	SNU13
ENSG00000114631	-0.57732	0.036252	PODXL2
ENSG00000151065	-0.41291	0.036532	DCP1B
ENSG00000106804	0.870556	0.036741	C5
ENSG00000173786	-0.52062	0.03675	CNP
ENSG00000140199	0.570873	0.036887	SLC12A6

ENSG00000258998	-1.91702	0.036925	LINC02302
ENSG00000166171	-0.50232	0.037136	DPCD
ENSG00000092439	0.54133	0.037149	TRPM7
ENSG00000150093	0.590657	0.037394	ITGB1
ENSG00000204410	0.683807	0.037521	MSH5
ENSG00000156103	0.508334	0.037686	MMP16
ENSG00000083097	0.517386	0.037921	DOPEY1
ENSG00000144724	0.453095	0.037943	PTPRG
ENSG00000107672	-0.41723	0.038178	NSMCE4A
ENSG00000263956	0.550797	0.038179	NBPF11
ENSG00000124171	0.456354	0.038251	PARD6B
ENSG00000253741	0.991283	0.038457	AC108002.1
ENSG00000164128	1.837712	0.0385	NPY1R
ENSG00000143469	1.313425	0.038538	SYT14
ENSG00000181284	-0.39253	0.038591	TMEM102
ENSG00000150347	2.775363	0.038664	ARID5B
ENSG00000164620	-0.54039	0.038769	RELL2
ENSG00000244274	-0.4211	0.038823	DBNDD2
ENSG00000237094	1.537881	0.038855	AL732372.2
ENSG00000196712	0.567613	0.038916	NF1
ENSG00000115318	-0.55502	0.038931	LOXL3
ENSG00000170860	-0.60817	0.039001	LSM 3.00
ENSG00000130005	-0.65904	0.039075	GAMT
ENSG00000106268	-0.59231	0.039099	NUDT1
ENSG00000125637	-0.90761	0.039159	PSD4
ENSG00000100300	-0.53303	0.039318	TSPO
ENSG00000186205	-0.64488	0.03933	1-Mar
ENSG00000134184	-0.52313	0.039433	GSTM1
ENSG00000224660	0.566842	0.039569	SH3BP5-AS1
ENSG00000169738	-0.58869	0.03971	DCXR
ENSG00000099385	-0.55949	0.039804	BCL7C
ENSG00000100364	-0.48006	0.039886	KIAA0930
ENSG00000131652	-0.58282	0.040025	THOC6
ENSG00000130787	-0.39353	0.040043	HIP1R
ENSG00000112773	0.528928	0.040108	FAM46A
ENSG00000016391	-0.51875	0.040111	CHDH
ENSG00000110841	0.572977	0.04033	PPFIBP1
ENSG00000164125	1.71252	0.040355	FAM198B
ENSG00000167792	-0.40987	0.040421	NDUFV1
ENSG00000242028	-0.64889	0.040425	HYPK
ENSG00000196696	0.738687	0.040567	AC009022.1

ENSG00000245146	1.036009	0.040699	MALINC1
ENSG00000203993	-0.42509	0.040714	ARRDC1-AS1
ENSG00000125378	-1.95635	0.040731	BMP4
ENSG00000186376	0.467451	0.040853	ZNF75D
ENSG00000119431	-0.44439	0.040963	HDHD3
ENSG00000154760	1.295182	0.040977	SLFN13
ENSG00000173530	0.617966	0.041083	TNFRSF10D
ENSG00000103024	-0.53579	0.041174	NME3
ENSG00000124486	0.523689	0.04119	USP9X
ENSG00000145284	-0.52833	0.041207	SCD5
ENSG00000171858	-0.56163	0.04125	RPS21
ENSG00000083807	-0.47967	0.041331	SLC27A5
ENSG00000149925	-0.5377	0.041348	ALDOA
ENSG00000279035	-1.68679	0.041381	AC022211.4
ENSG00000235823	-0.45058	0.041391	OLMALINC
ENSG00000126952	0.861359	0.041455	NXF5
ENSG00000279312	2.807805	0.041666	AL136164.4
ENSG00000005483	0.543986	0.04179	KMT2E
ENSG00000079215	1.499769	0.041837	SLC1A3
ENSG00000151006	0.640282	0.041854	PRSS53
ENSG00000174021	-0.55087	0.041965	GNG5
ENSG00000147586	-0.4709	0.04198	MRPS28
ENSG00000188763	-0.59955	0.042082	FZD9
ENSG00000261971	0.59311	0.042105	MMP25-AS1
ENSG00000135862	0.458071	0.042163	LAMC1
ENSG00000157764	0.448786	0.042264	BRAF
ENSG00000185803	-0.50785	0.042269	SLC52A2
ENSG00000085788	0.465547	0.042308	DDHD2
ENSG00000184857	-0.46877	0.042369	TMEM186
ENSG00000214837	0.963237	0.042507	LINC01347
ENSG00000122035	-0.74137	0.042532	RASL11A
ENSG00000136717	-0.44133	0.042673	BIN1
ENSG00000240990	1.69626	0.042752	HOXA11-AS
ENSG00000268204	1.567168	0.042888	AC008763.1
ENSG00000283429	-1.33358	0.043031	MIR1244-3
ENSG00000133398	0.628547	0.043052	MED10
ENSG00000272980	1.666086	0.043155	Z94721.2
ENSG00000123505	-0.41074	0.043203	AMD 1.00
ENSG00000178605	-0.50445	0.043305	GTPBP6
ENSG00000188368	-0.76777	0.043359	PRR19
ENSG00000139637	-0.57295	0.043416	C12orf10

ENSG00000280355	0.985603	0.043417	AL132656.4
ENSG00000157741	0.550451	0.043462	UBN2
ENSG00000183155	-0.54908	0.043548	RABIF
ENSG00000151148	0.379103	0.043623	UBE3B
ENSG00000155366	-0.51315	0.043647	RHOC
ENSG00000240972	-0.53733	0.043683	MIF
ENSG00000197483	-0.5457	0.043775	ZNF628
ENSG00000125656	-0.45898	0.043813	CLPP
ENSG00000164066	0.429673	0.043854	INTU
ENSG00000249572	0.73867	0.043854	AC034231.1
ENSG00000197013	0.525616	0.044086	ZNF429
ENSG00000254337	0.578839	0.04421	AC083967.1
ENSG00000129595	0.972929	0.044238	EPB41L4A
ENSG00000204837	0.721992	0.044434	FGF7P3
ENSG00000197016	0.580695	0.044444	ZNF470
ENSG00000138100	-1.88709	0.044452	TRIM54
ENSG00000140650	-0.41083	0.04446	PMM2
ENSG00000134548	1.106537	0.044466	SPX
ENSG00000213139	1.266441	0.044655	CRYGS
ENSG00000100911	-0.53563	0.044661	PSME2
ENSG00000070214	0.370124	0.044727	SLC44A1
ENSG00000172409	-0.50254	0.044858	CLP 1
ENSG00000116544	1.098117	0.044931	DLGAP3
ENSG00000130829	-0.39961	0.045164	DUSP9
ENSG00000123612	2.082726	0.045228	ACVR1C
ENSG00000107872	-0.50776	0.045474	FBXL15
ENSG00000126246	-1.09252	0.045656	IGFLR1
ENSG00000167771	-0.51734	0.045765	RCOR2
ENSG00000124406	0.692318	0.045847	ATP8A1
ENSG00000273036	0.751362	0.045878	AL390726.5
ENSG00000261377	-0.54553	0.045912	PDCD6IPP2
ENSG00000169221	-0.45761	0.045961	TBC1D10B
ENSG00000185220	0.502579	0.045972	PGBD2
ENSG00000257727	-0.61012	0.045985	CNPY2
ENSG00000023287	0.481265	0.046242	RB1CC1
ENSG00000185043	-0.49374	0.046278	CIB1
ENSG00000182872	-0.35569	0.0463	RBM10
ENSG00000261360	1.014125	0.046327	AC010491.1
ENSG00000128294	-0.49397	0.046328	TPST2
ENSG00000160917	-0.35169	0.046336	CPSF4
ENSG00000147642	1.249336	0.046543	SYBU

ENSG00000198466	0.42716	0.046612	ZNF587
ENSG00000250794	-0.88518	0.046624	ALG1L12P
ENSG00000106635	-0.42946	0.046681	BCL7B
ENSG00000121211	-0.48594	0.046735	MND1
ENSG00000198258	-0.53177	0.046797	UBL5
ENSG00000108590	-0.56609	0.046983	MED31
ENSG00000168152	0.532495	0.047174	THAP9
ENSG00000104866	-0.3896	0.047208	PPP1R37
ENSG00000075711	0.390816	0.047518	DLG1
ENSG00000204681	0.494944	0.047622	GABBR1
ENSG00000187187	0.589724	0.047688	ZNF546
ENSG00000089057	0.642723	0.047705	SLC23A2
ENSG00000096093	0.404878	0.047719	EFHC1
ENSG00000173581	-0.47153	0.047785	CCDC106
ENSG00000169836	1.555847	0.047871	TACR3
ENSG00000164114	0.43428	0.047887	MAP9
ENSG00000169604	1.336159	0.047935	ANTXR1
ENSG00000266962	-0.34859	0.04799	AC067852.2
ENSG00000231305	1.042392	0.048055	AC112484.1
ENSG00000230641	-1.35128	0.048081	USP12-AS2
ENSG00000006015	-0.4828	0.048191	REX1BD
ENSG00000178531	-0.68281	0.048314	CTXN1
ENSG00000108479	-0.42101	0.048398	GALK1
ENSG00000065268	-0.48207	0.048403	WDR18
ENSG00000213347	-0.60591	0.048473	MXD3
ENSG00000177283	1.288931	0.048492	FZD8
ENSG00000178449	-0.54879	0.048573	COX14
ENSG00000256436	1.509265	0.048583	TAS2R31
ENSG00000136807	-0.41664	0.048613	CDK9
ENSG00000183828	-0.53558	0.048666	NUDT14
ENSG00000144589	-0.36368	0.048761	STK11IP
ENSG00000145088	-0.56796	0.048794	EAF2
ENSG00000233927	-0.53113	0.048852	RPS28
ENSG00000103274	-0.38198	0.048864	NUBP1
ENSG00000136280	-0.44646	0.048884	CCM2
ENSG00000158246	-0.68675	0.048906	FAM46B
ENSG00000168569	-0.46153	0.048918	TMEM223
ENSG00000135940	-0.50003	0.048952	COX5B
ENSG00000137135	-0.39828	0.049391	ARHGEF39
ENSG00000049618	0.457852	0.049462	ARID1B
ENSG00000127084	-0.49939	0.049492	FGD3

ENSG00000273162	-0.59719	0.049502	AL133215.2
ENSG00000141098	-0.38975	0.04954	GFOD2
ENSG00000230551	0.615557	0.049576	AC021078.1
ENSG00000177990	0.542738	0.049605	DPY19L2
ENSG00000151914	0.545415	0.04961	DST
ENSG00000181817	-0.48611	0.049665	LSM 10.00
ENSG00000100056	-0.49588	0.049694	ESS2
ENSG00000064763	1.124421	0.049702	FAR2
ENSG00000173511	-0.69577	0.049712	VEGFB
ENSG00000188243	-0.54911	0.049827	COMMD6
ENSG00000170689	0.441197	0.050029	HOXB9
ENSG00000182544	-0.46326	0.050119	MFSD5
ENSG00000168884	-0.46979	0.050124	TNIP2
ENSG00000149577	0.352379	0.050248	SIDT2
ENSG00000127824	-0.75247	0.050407	TUBA4A
ENSG00000003987	-1.13755	0.050525	MTMR7
ENSG00000145982	-0.47546	0.050552	FARS2
ENSG00000278200	-1.48268	0.050601	LINC01971
ENSG00000209082	0.462511	0.050726	MT-TL1
ENSG00000232177	0.648329	0.050805	MTND4P24
ENSG00000245848	-0.39506	0.050808	CEBPA
ENSG00000122873	-0.4612	0.050844	CISD1
ENSG00000265749	0.847356	0.05088	AC135178.3
ENSG00000272140	1.179544	0.050905	AC022400.5
ENSG00000067225	-0.41552	0.051028	PKM
ENSG00000166762	0.686199	0.051059	CATSPER2
ENSG00000128656	-0.47531	0.051138	CHN1
ENSG00000169826	0.392512	0.051145	CSGALNACT2
ENSG00000178107	-1.87283	0.051161	AL161668.1
ENSG00000198873	-0.52644	0.051163	GRK5
ENSG00000177105	-0.60443	0.051258	RHOG
ENSG00000154832	-0.45987	0.051312	CXXC1
ENSG00000138036	0.364279	0.051372	DYNC2LI1
ENSG00000145147	0.484422	0.051466	SLIT2
ENSG00000111961	0.612585	0.051616	SASH1
ENSG00000157625	0.436267	0.051904	TAB3
ENSG00000186184	-0.40488	0.051945	POLR1D
ENSG00000244187	-0.47122	0.051954	TMEM141
ENSG00000248334	0.560719	0.052038	WHAMMP2
ENSG00000144677	-0.40691	0.052253	CTDSPL
ENSG00000072778	0.344293	0.052323	ACADVL

ENSG00000203667	-0.54622	0.052352	COX20
ENSG00000100418	-0.44092	0.052408	DESI1
ENSG00000244879	0.577833	0.052555	GABPB1-AS1
ENSG00000221978	0.339034	0.052657	CCNL2
ENSG00000163660	0.37475	0.052672	CCNL1
ENSG00000272853	-0.84503	0.05289	AC069544.1
ENSG00000188986	-0.39599	0.052921	NELFB
ENSG00000116525	-0.45773	0.052943	TRIM62
ENSG00000131127	0.518072	0.053042	ZNF141
ENSG00000135749	0.854127	0.053051	PCNX2
ENSG00000009413	0.477274	0.053065	REV3L
ENSG00000229358	0.599934	0.053322	DPY19L1P1
ENSG00000250138	1.391328	0.053399	AC139495.3
ENSG00000154642	0.535995	0.053419	C21orf91
ENSG00000062370	0.522004	0.053419	ZNF112
ENSG00000130748	-0.59575	0.053514	TMEM160
ENSG00000186908	0.398002	0.05354	ZDHHC17
ENSG00000038219	0.52581	0.053801	BOD1L1
ENSG00000114857	0.451805	0.053854	NKTR
ENSG00000260528	0.915204	0.053861	FAM157C
ENSG00000116871	-0.45138	0.053861	MAP7D1
ENSG00000075826	0.439069	0.053876	SEC31B
ENSG00000238083	0.619602	0.053925	LRRC37A2
ENSG00000184924	-0.48582	0.054069	PTRHD1
ENSG00000186468	-0.42935	0.05429	RPS23
ENSG00000164694	1.830881	0.054503	FNDC1
ENSG00000172403	2.745037	0.054539	SYNPO2
ENSG00000101856	-0.36853	0.054561	PGRMC1
ENSG00000136908	-0.48102	0.05472	DPM2
ENSG00000184508	-0.51552	0.054797	HDDC3
ENSG00000174405	0.50608	0.05499	LIG4
ENSG00000283050	0.741014	0.055056	GTF2IP12
ENSG00000179399	1.366443	0.055193	GPC5
ENSG00000198356	-0.48771	0.055204	ASNA1
ENSG00000256940	-0.88374	0.055268	AP001453.2
ENSG00000119397	0.578353	0.05527	CNTRL
ENSG00000275367	1.620608	0.055383	AC092111.1
ENSG00000135870	0.408884	0.055479	RC3H1
ENSG00000260404	0.692523	0.055483	AC110079.1
ENSG00000163156	-0.39986	0.055485	SCNM1
ENSG00000177954	-0.46167	0.055602	RPS27

ENSG00000111057	-0.46386	0.055607	KRT18
ENSG00000140988	-0.46007	0.05586	RPS2
ENSG00000225439	-0.36269	0.055886	BOLA3-AS1
ENSG00000270728	1.021014	0.055905	AL035413.2
ENSG00000205363	-0.55059	0.055915	C15orf59
ENSG00000166783	0.558638	0.056165	MARF1
ENSG00000181885	1.176785	0.056171	CLDN7
ENSG00000173681	0.473102	0.05621	BCLAF3
ENSG00000170989	0.855282	0.056211	S1PR1
ENSG00000161920	-0.45728	0.056295	MED11
ENSG00000123131	-0.4334	0.05638	PRDX4
ENSG00000243232	1.065039	0.056401	PCDHAC2
ENSG00000153936	0.41294	0.056413	HS2ST1
ENSG00000124172	-0.558	0.056422	ATP5F1E
ENSG00000283312	0.880047	0.056441	AC017104.4
ENSG00000182108	-0.61503	0.056527	DEXI
ENSG00000154537	-0.68978	0.056535	FAM27C
ENSG00000165194	-2.214	0.056587	PCDH19
ENSG00000224837	-1.05846	0.056588	GCSHP5
ENSG00000187608	-0.71475	0.056632	ISG15
ENSG00000100815	0.385594	0.05667	TRIP11
ENSG00000060762	-0.55433	0.05684	MPC1
ENSG00000260589	-1.39849	0.056889	STAM-AS1
ENSG00000095951	0.552127	0.056916	HIVEP1
ENSG00000163125	0.411635	0.057019	RPRD2
ENSG00000259378	1.825347	0.057162	DCAF13P3
ENSG00000243176	0.640449	0.057252	AC092944.1
ENSG00000032219	0.460585	0.057329	ARID4A
ENSG00000087116	1.375646	0.057578	ADAMTS2
ENSG00000173540	-0.53995	0.057585	GMPPB
ENSG00000169100	-0.36294	0.05769	SLC25A6
ENSG00000116176	1.46673	0.05772	TPSG1
ENSG00000151552	-0.47654	0.05799	QDPR
ENSG00000236438	0.589091	0.058011	FAM157A
ENSG00000111058	0.625287	0.058054	ACSS3
ENSG00000259330	-0.40253	0.058102	INAFM2
ENSG00000120519	0.490846	0.0582	SLC10A7
ENSG00000137845	0.384434	0.058259	ADAM10
ENSG00000213903	0.599406	0.058591	LTB4R
ENSG00000167508	-0.50345	0.058803	MVD
ENSG00000113384	0.447681	0.058846	GOLPH3

ENSG00000160753	-0.41907	0.058921	RUSC1
ENSG00000075340	0.795439	0.059148	ADD2
ENSG00000103145	-0.67055	0.059265	HCFC1R1
ENSG00000249626	0.815574	0.05939	AC024560.2
ENSG00000204371	-0.38904	0.059453	EHMT2
ENSG00000107338	-0.56523	0.059456	SHB
ENSG00000144036	0.414796	0.059472	EXOC6B
ENSG00000231784	0.810298	0.059486	DBIL5P
ENSG00000147548	0.334942	0.05954	NSD3
ENSG00000101400	-0.53818	0.059649	SNTA1
ENSG00000171227	-0.96914	0.059786	TMEM37
ENSG00000151876	0.506019	0.059802	FBXO4
ENSG00000274897	-0.51706	0.059935	PANO1
ENSG00000206538	0.56689	0.059944	VGLL3
ENSG00000124588	-0.49105	0.059976	NQO2

List of Shared Transcripts between A2780CP20-RBPMSA and A2780CP20-RBPMSC

ID	log2FoldChange	pvalue	Gene.name
ENSG00000276953	-6.91254142	0.027800278	TRBV12-4
ENSG00000101384	-4.330511817	0.020588056	JAG1
ENSG00000178965	-3.951576843	0.000300472	ERICH3
ENSG00000099250	-3.454159744	0.001731179	NRP1
ENSG00000147481	-3.228723507	0.008223846	SNTG1
ENSG00000196730	-3.221475672	0.004702865	DAPK1
ENSG00000128709	-2.800133712	0.004705564	HOXD9
ENSG00000125046	-2.71336991	0.01549182	SSUH2
ENSG00000106631	-2.677248207	0.025483795	MYL7
ENSG00000175879	-2.593778164	0.015883262	HOXD8
ENSG00000134769	-2.582128781	6.81E-06	DTNA
ENSG00000156113	-2.559606256	0.001963339	KCNMA1
ENSG00000108691	-2.492618661	0.004180812	CCL2
ENSG00000169403	-2.363732454	0.004317176	PTAFR
ENSG00000176697	-2.318649475	0.032918323	BDNF
ENSG00000165194	-2.21400394	0.056586644	PCDH19
ENSG00000229140	-2.170494718	0.004604894	CCDC26
ENSG00000151150	-2.031678566	0.024312339	ANK3
ENSG00000125378	-1.956346285	0.040730812	BMP4
ENSG00000126709	-1.923756964	0.028211854	IFI6
ENSG00000258998	-1.917024488	0.036925242	LINC02302
ENSG00000177098	-1.897216786	0.002776602	SCN4B
ENSG00000196754	-1.747167305	0.000877016	S100A2

ENSG00000164076	-1.745071635	0.002015404	CAMKV
ENSG00000279035	-1.686787075	0.041381165	AC022211.4
ENSG00000185614	-1.530634621	0.011227782	FAM212A
ENSG00000283498	-1.49198065	0.000717745	MIR1244-2
ENSG00000089558	-1.460050653	0.022103622	KCNH4
ENSG00000089101	-1.439892214	0.027860655	CFAP61
ENSG00000260589	-1.398488937	0.056888974	STAM-AS1
ENSG00000230641	-1.351278924	0.048080593	USP12-AS2
ENSG00000283429	-1.333579121	0.043031205	MIR1244-3
ENSG00000276529	-1.328376685	0.001638667	AP001505.1
ENSG00000203724	-1.32159214	0.000723491	C1orf53
ENSG00000263020	-1.269534609	0.011121047	AL662899.2
ENSG00000279528	-1.224019589	0.002973937	AC115618.3
ENSG00000248375	-1.213220241	0.018546004	AC104066.1
ENSG00000265185	-1.166058908	0.011948836	SNORD3B-1
ENSG00000003987	-1.137551525	0.050524826	MTMR7
ENSG00000226950	-1.116833043	0.000800023	DANCR
ENSG00000260018	-1.104655996	0.02520255	AC040169.1
ENSG00000092964	-1.093145219	0.019373151	DPYSL2
ENSG00000126246	-1.092518722	0.04565581	IGFLR1
ENSG00000107859	-1.087496874	0.01455767	PITX3
ENSG00000255198	-1.067834117	0.005761886	SNHG9
ENSG00000272455	-1.064933451	0.001486175	AL391244.3
ENSG00000111424	-1.044136999	0.000469702	VDR
ENSG00000168061	-1.035008668	0.001739821	SAC3D1
ENSG00000175602	-1.025738245	0.003617853	CCDC85B
ENSG00000260442	-1.017804496	0.001338104	ATP2A1-AS1
ENSG00000107262	-1.006786448	0.000690437	BAG1
ENSG00000007376	-1.005266224	0.002377709	RPUSD1
ENSG00000213881	-0.996036108	0.046654148	NPM1P6
ENSG00000254093	-0.993932763	0.001661886	PINX1
ENSG00000260260	-0.978434882	0.002970337	SNHG19
ENSG00000131153	-0.972814099	0.002290589	GINS2
ENSG00000171227	-0.969137418	0.059786461	TMEM37
ENSG00000071282	-0.95023938	0.00274006	LMCD1
ENSG00000213397	-0.931950638	0.013301532	HAUS7
ENSG00000129354	-0.928249251	0.002500347	AP1M2
ENSG00000130489	-0.923704762	0.009983089	SCO2
ENSG00000227496	-0.914374095	0.025488142	AC099066.2
ENSG00000271855	-0.911397536	0.035090616	AC073195.1
ENSG00000125637	-0.907605036	0.039159417	PSD4

ENSG00000167900	-0.907343384	0.003891341	TK1
ENSG00000099849	-0.903681467	0.0085233	RASSF7
ENSG00000182154	-0.903429323	0.003236082	MRPL41
ENSG00000266402	-0.903076218	0.026883102	SNHG25
ENSG00000160345	-0.900931694	0.011819059	C9orf116
ENSG00000184207	-0.889665975	0.001176796	PGP
ENSG00000179958	-0.889068919	0.00374895	DCTPP1
ENSG00000132646	-0.887384487	0.001417506	PCNA
ENSG00000093009	-0.88499003	9.98E-06	CDC45
ENSG00000250479	-0.878027031	0.00878476	CHCHD10
ENSG00000116649	-0.872742505	0.01163949	SRM
ENSG00000233016	-0.870546804	0.002876245	SNHG7
ENSG00000101220	-0.86852835	0.010667523	C20orf27
ENSG00000178821	-0.864450926	0.026007304	TMEM52
ENSG00000101412	-0.862541332	0.002427816	E2F1
ENSG00000183048	-0.861294994	0.005679633	SLC25A10
ENSG00000114767	-0.859169646	0.008907774	RRP9
ENSG00000169683	-0.858633813	0.002907362	LRRC45
ENSG00000169689	-0.857594203	0.014505668	CENPX
ENSG00000115884	-0.855264101	0.003415473	SDC1
ENSG00000125898	-0.852340209	0.008517562	FAM110A
ENSG00000161149	-0.847836581	0.036185	TUBA3FP
ENSG00000272853	-0.845026325	0.052890445	AC069544.1
ENSG00000163888	-0.844166804	0.031937611	CAMK2N2
ENSG00000166803	-0.841476511	0.005276091	PCLAF
ENSG00000173457	-0.841326467	0.018913922	PPP1R14B
ENSG00000135617	-0.839755932	0.013425526	PRADC1
ENSG00000161981	-0.835821045	0.021940762	SNRNP25
ENSG00000065057	-0.83131832	0.004053331	NTHL1
ENSG00000141933	-0.83024483	0.008652408	TPGS1
ENSG00000178896	-0.828633503	0.006859233	EXOSC4
ENSG00000165724	-0.828453823	0.003540719	ZMYND19
ENSG00000184990	-0.824918011	0.0115306	SIVA1
ENSG00000034510	-0.823872776	0.024006232	TMSB10
ENSG00000262814	-0.821019822	0.013768472	MRPL12
ENSG00000278763	-0.820081286	0.04527096	FAM27B
ENSG00000273619	-0.818602162	0.020857792	AL121832.2
ENSG00000162062	-0.818189922	0.008094256	TEDC2
ENSG00000160072	-0.816792118	0.019834765	ATAD3B
ENSG00000158042	-0.816642341	0.000763943	MRPL17
ENSG00000100297	-0.809623779	0.001009722	MCM5

ENSG00000230330	-0.808915188	0.014054058	HMGN2P3
ENSG00000242114	-0.807033075	0.005332288	MTFP1
ENSG00000180822	-0.807016433	0.00364543	PSMG4
ENSG00000167523	-0.801748578	0.011819747	SPATA33
ENSG00000065328	-0.800898175	0.000530781	MCM10
ENSG00000102977	-0.798490853	0.005176254	ACD
ENSG00000181418	-0.797955897	0.000526159	DDN
ENSG00000183527	-0.795522678	0.002359399	PSMG1
ENSG00000130204	-0.795322514	0.019090384	TOMM40
ENSG00000111640	-0.793469197	0.005192934	GAPDH
ENSG00000176058	-0.792581425	0.003065547	TPRN
ENSG00000167513	-0.790312039	0.000834778	CDT1
ENSG00000100228	-0.788288063	0.017531058	RAB36
ENSG00000103260	-0.783472445	0.013906495	METRN
ENSG00000100294	-0.780926487	0.006055518	MCAT
ENSG00000166166	-0.776492056	0.021424732	TRMT61A
ENSG00000169230	-0.775589371	0.006309737	PRELID1
ENSG00000173465	-0.772418112	0.016624319	SSSCA1
ENSG00000188368	-0.76777195	0.043359268	PRR19
ENSG00000119139	-0.767035058	0.030673895	TJP2
ENSG00000128626	-0.762793449	0.028012761	MRPS12
ENSG00000102030	-0.762446963	0.015301241	NAA10
ENSG00000224877	-0.761878403	0.026477148	NDUFAF8
ENSG00000174744	-0.761692111	0.013291585	BRMS1
ENSG00000204922	-0.760776162	0.008872506	UQCC3
ENSG00000148362	-0.759343595	0.02877764	PAXX
ENSG00000168273	-0.758188501	0.023321993	SMIM4
ENSG00000168496	-0.75737519	0.021780472	FEN1
ENSG00000176124	-0.756390108	0.002763899	DLEU1
ENSG00000226944	-0.755207049	0.007989722	AL031847.1
ENSG00000025708	-0.754208754	0.038378278	TYMP
ENSG00000182575	-0.753497059	0.029678473	NXPH3
ENSG00000205138	-0.75251068	0.003098198	SDHAF1
ENSG00000277972	-0.751345439	0.012802709	CISD3
ENSG00000247092	-0.750891638	0.007059235	SNHG10
ENSG00000125520	-0.749224548	0.009865902	SLC2A4RG
ENSG00000102109	-0.748860185	0.034503036	PCSK1N
ENSG00000099795	-0.748130448	0.015359168	NDUFB7
ENSG00000104524	-0.747990998	0.014119677	PYCR3
ENSG00000168393	-0.747801021	0.011817316	DTYMK
ENSG00000105258	-0.744335422	0.018063392	POLR2I

ENSG00000169258	-0.743244306	0.022093308	GPRIN1
ENSG00000122035	-0.741369184	0.042531957	RASL11A
ENSG00000177556	-0.740950191	0.031147748	ATOX1
ENSG00000262919	-0.740570271	0.016159593	CCNQ
ENSG00000051180	-0.740520039	0.000299021	RAD51
ENSG00000175756	-0.740506488	0.010690224	AURKAIP1
ENSG00000148291	-0.740366269	0.032932839	SURF2
ENSG00000112312	-0.738297747	0.009611963	GMNN
ENSG00000102103	-0.738155773	0.019804215	PQBP1
ENSG00000085840	-0.73805831	0.003879154	ORC1
ENSG00000188191	-0.734091759	0.039314212	PRKAR1B
ENSG00000165644	-0.73163664	0.017724112	COMTD1
ENSG00000002330	-0.729214439	0.020036429	BAD
ENSG00000185347	-0.728570611	0.009329757	TEDC1
ENSG00000079462	-0.728311477	0.012919657	PAFAH1B3
ENSG00000180992	-0.728003591	0.012635024	MRPL14
ENSG00000212123	-0.723395856	0.049743673	PRR22
ENSG00000255650	-0.722022435	0.011067284	FAM222A-AS1
ENSG00000174775	-0.721972231	0.03724844	HRAS
ENSG00000114395	-0.71908769	0.018383692	CYB561D2
ENSG00000278619	-0.717377856	0.011310652	MRM1
ENSG00000174516	-0.71668781	0.0336014	PELI3
ENSG00000182809	-0.716389011	0.014314321	CRIP2
ENSG00000174177	-0.716290082	0.012638179	CTU2
ENSG00000187608	-0.714752772	0.056632237	ISG15
ENSG00000115350	-0.713846558	0.012383853	POLE4
ENSG00000130810	-0.711463964	0.003891596	PPAN
ENSG00000112759	-0.711371703	0.017235225	SLC29A1
ENSG00000197785	-0.710980803	0.009578599	ATAD3A
ENSG00000112118	-0.708030204	0.002220026	MCM3
ENSG00000160214	-0.707520821	0.01317259	RRP1
ENSG00000169750	-0.706031701	0.005650357	RAC3
ENSG00000258429	-0.704538166	0.017833184	PDF
ENSG00000184967	-0.703946914	0.016880529	NOC4L
ENSG00000130165	-0.703725373	0.025602076	ELOF1
ENSG00000182173	-0.703370325	0.007107115	TSEN54
ENSG00000174917	-0.70296517	0.022082538	C19orf70
ENSG00000125817	-0.702307831	0.003906632	CENPB
ENSG00000105649	-0.702044102	0.02593174	RAB3A
ENSG00000197345	-0.701331387	0.0156043	MRPL21
ENSG00000161888	-0.699946252	0.002217131	SPC24

ENSG00000167515	-0.699789201	0.016254268	TRAPPC2L
ENSG00000105676	-0.698028153	0.021869791	ARMC6
ENSG00000144354	-0.697269357	0.002109187	CDCA7
ENSG00000267321	-0.695424642	0.004859333	LINC02001
ENSG00000144485	-0.69537958	0.008954231	HES6
ENSG00000214182	-0.694938747	0.016587257	PTMAP5
ENSG00000196976	-0.693879671	0.022586181	LAGE3
ENSG00000103254	-0.690307038	0.030173354	FAM173A
ENSG00000011332	-0.689642932	0.01744827	DPF1
ENSG00000177971	-0.687877196	0.014612754	IMP3
ENSG00000198618	-0.687341866	0.012985039	PPIAP22
ENSG00000183011	-0.685372501	0.027148612	NAA38
ENSG00000147257	-0.685281724	0.026111206	GPC3
ENSG00000073111	-0.684995471	0.010528115	MCM2
ENSG00000239672	-0.680666907	0.024126906	NME1
ENSG00000142634	-0.679928858	0.02377113	EFHD2
ENSG00000069011	-0.675410547	0.023424995	PITX1
ENSG00000140323	-0.675240691	0.026888219	DISP2
ENSG00000007968	-0.674914674	0.000155303	E2F2
ENSG00000128951	-0.674883737	0.008362428	DUT
ENSG00000165502	-0.673549645	0.015164963	RPL36AL
ENSG00000178982	-0.672887059	0.014770406	EIF3K
ENSG00000150779	-0.672865116	0.029717524	TIMM8B
ENSG00000130159	-0.672146773	0.005201174	ECSIT
ENSG00000099256	-0.671841516	0.003508155	PRTFDC1
ENSG00000185340	-0.671165554	0.014065228	GAS2L1
ENSG00000233913	-0.670229921	0.034531794	RPL10P9
ENSG00000186193	-0.668716023	0.013603086	SAPCD2
ENSG00000081692	-0.667586041	0.01144773	JMJD4
ENSG00000126267	-0.667277694	0.025591353	COX6B1
ENSG00000127564	-0.667260092	0.010188913	PKMYT1
ENSG00000117877	-0.66725449	0.032851194	CD3EAP
ENSG00000221983	-0.667172615	0.015058385	UBA52
ENSG00000235173	-0.666407628	0.032783235	HGH1
ENSG00000163584	-0.665859181	0.023341744	RPL22L1
ENSG00000189159	-0.665244402	0.025938021	JPT1
ENSG00000198736	-0.665235473	0.036380493	MSRB1
ENSG00000172009	-0.662816439	0.008932693	THOP1
ENSG00000152082	-0.66266378	0.027736227	MZT2B
ENSG00000137818	-0.662533331	0.02569488	RPLP1
ENSG00000180198	-0.661717869	0.010174793	RCC1

ENSG00000121680	-0.660962392	0.021208238	PEX16
ENSG00000123144	-0.659679914	0.015292051	TRIR
ENSG00000034152	-0.659667907	0.039387746	MAP2K3
ENSG00000130005	-0.659044706	0.039074957	GAMT
ENSG00000148399	-0.658849237	0.011194786	DPH7
ENSG00000117395	-0.657249553	0.025029102	EBNA1BP2
ENSG00000160949	-0.657084217	0.00954031	TONSL
ENSG00000166002	-0.655926076	0.006874825	SMCO4
ENSG00000182512	-0.655774907	0.018067962	GLRX5
ENSG00000105185	-0.65351148	0.027486952	PDCD5
ENSG00000014138	-0.652638684	0.011329931	POLA2
ENSG00000074071	-0.651095618	0.032219012	MRPS34
ENSG00000204315	-0.650621107	0.01211082	FKBPL
ENSG00000161179	-0.649715091	0.021987759	YDJC
ENSG00000176101	-0.647267405	0.023254636	SSNA1
ENSG00000163170	-0.646790199	0.028640413	BOLA3
ENSG00000243364	-0.646755165	0.024176418	EFNA4
ENSG00000111665	-0.644372147	0.01263275	CDCA3
ENSG00000179431	-0.643416322	0.009904062	FJX1
ENSG00000173272	-0.643370636	0.024378931	MZT2A
ENSG00000235919	-0.642877743	0.028804906	ASH1L-AS1
ENSG00000275464	-0.642549773	0.015058829	FP565260.1
ENSG00000106077	-0.642061064	0.029712895	ABHD11
ENSG00000119333	-0.642033055	0.012860247	WDR34
ENSG00000112576	-0.641674995	0.040706181	CCND3
ENSG00000072506	-0.641382528	0.026692786	HSD17B10
ENSG00000109062	-0.639100209	0.009913887	SLC9A3R1
ENSG00000083845	-0.638605055	0.011906134	RPS5
ENSG00000278615	-0.638199013	0.007003597	C11orf98
ENSG00000023902	-0.634580333	0.024521781	PLEKHO1
ENSG00000125901	-0.634266042	0.019187618	MRPS26
ENSG00000160256	-0.63366998	0.025036129	FAM207A
ENSG00000185298	-0.630843174	0.011092991	CCDC137
ENSG00000177600	-0.630577614	0.023922766	RPLP2
ENSG00000103876	-0.630535104	0.027595177	FAH
ENSG00000105248	-0.628091875	0.021004117	CCDC94
ENSG00000106246	-0.628063161	0.012737417	PTCD1
ENSG00000065054	-0.625821913	0.033360977	SLC9A3R2
ENSG00000165244	-0.625172482	0.001245534	ZNF367
ENSG00000157870	-0.624886043	0.019626563	FAM213B
ENSG00000124074	-0.624028945	0.009281075	ENKD1

ENSG00000100413	-0.62365482	0.02235466	POLR3H
ENSG00000242485	-0.622860098	0.038521501	MRPL20
ENSG00000174547	-0.622144082	0.028400278	MRPL11
ENSG00000162910	-0.621441212	0.016205026	MRPL55
ENSG00000184986	-0.62134126	0.040943212	TMEM121
ENSG00000160999	-0.620953217	0.026850634	SH2B2
ENSG00000088727	-0.620849953	0.007729425	KIF9
ENSG00000149806	-0.619928801	0.024478882	FAU
ENSG00000174109	-0.619626671	0.011456431	C16orf91
ENSG00000276043	-0.618150809	0.00940143	UHRF1
ENSG00000004864	-0.617943019	0.023419074	SLC25A13
ENSG00000163528	-0.617593951	0.018576168	CHCHD4
ENSG00000140365	-0.616968313	0.050559473	COMMD4
ENSG00000182108	-0.615026152	0.056526612	DEXI
ENSG00000154328	-0.614597269	0.002875542	NEIL2
ENSG00000112877	-0.613918535	0.003387892	CEP72
ENSG00000049541	-0.613916871	0.00810865	RFC2
ENSG00000123810	-0.613765182	0.03399297	B9D2
ENSG00000152147	-0.613578156	0.039112778	GEMIN6
ENSG00000103266	-0.613111204	0.014286644	STUB1
ENSG00000164045	-0.612832005	0.045291591	CDC25A
ENSG00000197451	-0.612573328	0.034424902	HNRNPAB
ENSG00000105011	-0.612373312	0.016235543	ASF1B
ENSG00000101442	-0.611227621	0.009025796	ACTR5
ENSG00000257727	-0.610115971	0.045985216	CNPY2
ENSG00000239789	-0.608631588	0.019612554	MRPS17
ENSG00000176890	-0.606795146	0.010350355	TYMS
ENSG00000155287	-0.60675903	0.009095384	SLC25A28
ENSG00000111445	-0.604283791	0.012290336	RFC5
ENSG00000142252	-0.603642821	0.024641807	GEMIN7
ENSG00000109084	-0.602481577	0.024066824	TMEM97
ENSG00000110107	-0.601769353	0.029211722	PRPF19
ENSG00000100664	-0.598924978	0.009967778	EIF5
ENSG00000165060	-0.597650348	0.038013194	FXN
ENSG00000073536	-0.597095494	0.022209047	NLE1
ENSG00000160789	-0.596957652	0.007583828	LMNA
ENSG00000135587	-0.596270095	0.021323576	SMPD2
ENSG00000196262	-0.595887326	0.021929592	PPIA
ENSG00000104889	-0.59480288	0.015854458	RNASEH2A
ENSG00000179115	-0.594181137	0.037165707	FARSA
ENSG00000167074	-0.593560192	0.005556437	TEF

ENSG00000136261	-0.593476611	0.01915267	BZW2
ENSG00000083635	-0.593321182	0.006209951	NUFIP1
ENSG00000170779	-0.593207151	0.00734115	CDCA4
ENSG00000103415	-0.593201305	0.021355106	HMOX2
ENSG00000122034	-0.592950173	0.037209407	GTF3A
ENSG00000104529	-0.59155964	0.014113901	EEF1D
ENSG00000111671	-0.590680337	0.020529829	SPSB2
ENSG00000247626	-0.590220514	0.021293654	MARS2
ENSG00000213619	-0.589589517	0.024270618	NDUFS3
ENSG00000204220	-0.589049532	0.031889725	PFDN6
ENSG00000145220	-0.588943674	0.023080609	LYAR
ENSG00000169738	-0.588693787	0.039709938	DCXR
ENSG00000170515	-0.588632591	0.036255566	PA2G4
ENSG00000188976	-0.586825929	0.021119212	NOC2L
ENSG00000076248	-0.586666428	0.019480715	UNG
ENSG00000108826	-0.58622593	0.053297564	MRPL27
ENSG00000122547	-0.585910291	0.009590107	EEPD1
ENSG00000175279	-0.585892573	0.056585183	CENPS
ENSG00000213337	-0.583018437	0.027163395	ANKRD39
ENSG00000164967	-0.58219579	0.023305554	RPP25L
ENSG00000108106	-0.581856551	0.029574446	UBE2S
ENSG00000132661	-0.580175808	0.022866657	NXT1
ENSG00000178307	-0.580142196	0.030024386	TMEM11
ENSG00000008324	-0.579524926	0.02993233	SS18L2
ENSG00000141873	-0.578926694	0.013416971	SLC39A3
ENSG00000114631	-0.577319537	0.036252377	PODXL2
ENSG00000102760	-0.576821221	0.018986069	RGCC
ENSG00000130811	-0.576768574	0.030843791	EIF3G
ENSG00000171848	-0.576112244	0.039126198	RRM2
ENSG00000177380	-0.575318519	0.002228044	PPFIA3
ENSG00000224631	-0.573457932	0.023881658	RPS27AP16
ENSG00000090316	-0.573085752	0.02167792	MAEA
ENSG00000164051	-0.572052067	0.01377723	CCDC51
ENSG00000100726	-0.571157452	0.059997378	TELO2
ENSG00000135245	-0.571035759	0.010350931	HILPDA
ENSG00000143333	-0.570697798	0.021890875	RGS16
ENSG00000104738	-0.568363761	0.042888612	MCM4
ENSG00000123297	-0.568237285	0.016247405	TSFM
ENSG00000133265	-0.568012616	0.023230539	HSPBP1
ENSG00000124541	-0.567818128	0.036482384	RRP36
ENSG00000156928	-0.567762431	0.044870886	MALSU1

ENSG00000122140	-0.566375245	0.0311237	MRPS2
ENSG00000108590	-0.566085101	0.046983032	MED31
ENSG00000157014	-0.566071459	0.047076328	TATDN2
ENSG00000107338	-0.565233218	0.059456384	SHB
ENSG00000134333	-0.564073211	0.014920811	LDHA
ENSG00000105671	-0.564038916	0.034587687	DDX49
ENSG00000151131	-0.563855898	0.036643277	C12orf45
ENSG00000166963	-0.562812424	0.02579161	MAP1A
ENSG00000153406	-0.561971223	0.020014334	NMRAL1
ENSG00000123064	-0.561864927	0.010970108	DDX54
ENSG00000149798	-0.5616471	0.023446893	CDC42EP2
ENSG00000103152	-0.561329453	0.054564433	MPG
ENSG00000099385	-0.559485963	0.039804086	BCL7C
ENSG00000159259	-0.559087153	0.031501833	CHAF1B
ENSG00000122687	-0.557845574	0.024726478	MRM2
ENSG00000163950	-0.55669929	0.021602545	SLBP
ENSG00000101945	-0.556061818	0.026408271	SUV39H1
ENSG00000100479	-0.554944647	0.01331996	POLE2
ENSG00000135723	-0.554782679	0.0329233	FHOD1
ENSG00000060762	-0.554329175	0.056839814	MPC1
ENSG00000175768	-0.553623355	0.036139487	TOMM5
ENSG00000148335	-0.553544742	0.058292412	NTMT1
ENSG00000074800	-0.552854664	0.027050801	ENO1
ENSG00000166189	-0.552106338	0.018664747	HPS6
ENSG00000164405	-0.551948973	0.055257057	UQCRQ
ENSG00000112039	-0.55149303	0.019626638	FANCE
ENSG00000177192	-0.551143079	0.02341411	PUS1
ENSG00000205363	-0.5505867	0.055914983	C15orf59
ENSG00000184281	-0.549810661	0.04078363	TSSC4
ENSG00000147804	-0.549763542	0.030095216	SLC39A4
ENSG00000130475	-0.549749071	0.004221867	FCHO1
ENSG00000176720	-0.549155847	0.02720099	BOK
ENSG00000188243	-0.54910551	0.049827347	COMMD6
ENSG00000178449	-0.548789516	0.048572992	COX14
ENSG00000104522	-0.546954109	0.050127749	TSTA3
ENSG00000170846	-0.546952442	0.015188589	AC093323.1
ENSG00000197483	-0.545703999	0.043774576	ZNF628
ENSG00000184436	-0.545445176	0.019107777	THAP7
ENSG00000189046	-0.545380303	0.028076552	ALKBH2
ENSG00000165912	-0.544848614	0.022163059	PACSIN3
ENSG00000136463	-0.544468402	0.020524249	TACO1

ENSG00000136840	-0.544375484	0.037361751	ST6GALNAC4
ENSG00000160957	-0.544257405	0.049896358	RECQL4
ENSG00000176410	-0.543836042	0.012325983	DNAJC30
ENSG00000164081	-0.543199598	0.027578416	TEX264
ENSG00000105202	-0.541156312	0.014574656	FBL
ENSG00000131148	-0.540552395	0.054654407	EMC8
ENSG00000167114	-0.540460001	0.043930357	SLC27A4
ENSG00000119185	-0.53931524	0.047011643	ITGB1BP1
ENSG00000062582	-0.538677491	0.02511184	MRPS24
ENSG00000115758	-0.538663823	0.058695205	ODC1
ENSG00000101400	-0.538177939	0.059648896	SNTA1
ENSG00000149925	-0.537695154	0.041347541	ALDOA
ENSG00000240972	-0.537326537	0.043683004	MIF
ENSG00000100911	-0.535627636	0.044660952	PSME2
ENSG00000126215	-0.535491995	0.043108583	XRCC3
ENSG00000115317	-0.535020161	0.03232476	HTRA2
ENSG00000131351	-0.534848366	0.016691752	HAUS8
ENSG00000105085	-0.533764925	0.041622053	MED26
ENSG00000132323	-0.533406024	0.044912226	ILKAP
ENSG00000100300	-0.533034695	0.039317994	TSPO
ENSG00000160799	-0.532961715	0.027555537	CCDC12
ENSG00000198258	-0.531768301	0.046796661	UBL5
ENSG00000090971	-0.531606968	0.020944177	NAT14
ENSG00000176014	-0.531167419	0.051593575	TUBB6
ENSG00000137124	-0.530058231	0.031827931	ALDH1B1
ENSG00000167747	-0.52962834	0.021696619	C19orf48
ENSG00000125454	-0.52952329	0.029673245	SLC25A19
ENSG00000172731	-0.529430227	0.026685977	LRRC20
ENSG00000145284	-0.528327675	0.041207468	SCD5
ENSG00000115539	-0.527570376	0.045535754	PDCL3
ENSG00000162783	-0.526660111	0.010771626	IER5
ENSG00000198873	-0.526437962	0.051162811	GRK5
ENSG00000186283	-0.525544349	0.023816411	TOR3A
ENSG00000165916	-0.52503017	0.05470075	PSMC3
ENSG00000114026	-0.524909951	0.034723601	OGG1
ENSG00000217930	-0.524486086	0.029684242	PAM16
ENSG00000130305	-0.524296466	0.034392408	NSUN5
ENSG00000169598	-0.523720627	0.024956382	DFFB
ENSG00000163319	-0.523720482	0.040210801	MRPS18C
ENSG00000162076	-0.522157214	0.030368905	FLYWCH2
ENSG00000173786	-0.520619108	0.036750442	CNP

ENSG00000016391	-0.518749267	0.040111204	CHDH
ENSG00000148187	-0.518588727	0.021543931	MRRF
ENSG00000108010	-0.518562125	0.05953186	GLRX3
ENSG00000092470	-0.518379803	0.002985787	WDR76
ENSG00000274897	-0.517063593	0.059935287	PANO1
ENSG00000100605	-0.516697301	0.014273898	ITPK1
ENSG00000100347	-0.516588407	0.030666718	SAMM50
ENSG00000187514	-0.516261272	0.040259138	PTMA
ENSG00000117748	-0.51543637	0.019933251	RPA2
ENSG00000111361	-0.51491233	0.036244472	EIF2B1
ENSG00000109519	-0.51477873	0.029253331	GRPEL1
ENSG00000141858	-0.514459466	0.055590646	SAMD1
ENSG00000174371	-0.513740724	0.017226749	EXO1
ENSG00000100138	-0.513556348	0.036195065	SNU13
ENSG00000155366	-0.513146181	0.043646979	RHOC
ENSG00000165526	-0.512991243	0.014501888	RPUSD4
ENSG00000272763	-0.512561519	0.025185403	AC103702.2
ENSG00000155189	-0.512099746	0.00722138	AGPAT5
ENSG00000125445	-0.511567007	0.037149733	MRPS7
ENSG00000165609	-0.510493276	0.024759756	NUDT5
ENSG00000183751	-0.510435081	0.04056172	TBL3
ENSG00000160113	-0.510029103	0.026171519	NR2F6
ENSG00000174173	-0.508725125	0.027069902	TRMT10C
ENSG00000185803	-0.50785302	0.042268872	SLC52A2
ENSG00000107872	-0.507761526	0.045473624	FBXL15
ENSG00000164032	-0.507386578	0.034559401	H2AFZ
ENSG00000127554	-0.506451741	0.033160916	GFER
ENSG00000103037	-0.505647527	0.031110453	SETD6
ENSG00000171960	-0.5039846	0.05198966	PPIH
ENSG00000076003	-0.503571362	0.004251833	MCM6
ENSG00000167508	-0.503451578	0.058802998	MVD
ENSG00000145912	-0.502976255	0.038654275	NHP2
ENSG00000204356	-0.502669793	0.03310398	NELFE
ENSG00000172409	-0.502537267	0.044857935	CLP 1
ENSG00000166171	-0.502322567	0.037135848	DPCD
ENSG00000164897	-0.502201113	0.050442353	TMUB1
ENSG00000132434	-0.501205825	0.04214379	LANCL2
ENSG00000152253	-0.501006678	0.016880022	SPC25
ENSG00000135940	-0.500032876	0.04895197	COX5B
ENSG00000126088	-0.499667788	0.030247347	UROD
ENSG00000100401	-0.498384592	0.036340151	RANGAP1

ENSG00000173914	-0.498276699	0.025124256	RBM4B
ENSG00000106009	-0.497833284	0.030704737	BRAT1
ENSG00000164611	-0.497542538	0.022857624	PTTG1
ENSG00000198056	-0.496150294	0.015111984	PRIM1
ENSG00000160972	-0.496127311	0.018411146	PPP1R16A
ENSG00000100056	-0.49588286	0.04969406	ESS2
ENSG00000006744	-0.494720832	0.017534889	ELAC2
ENSG00000176946	-0.494054567	0.041449056	THAP4
ENSG00000128294	-0.493974517	0.046327826	TPST2
ENSG00000181026	-0.493665416	0.030451572	AEN
ENSG00000243678	-0.493200464	0.03380673	NME2
ENSG00000241360	-0.491881627	0.032562363	PDXP
ENSG00000111669	-0.491532148	0.032253739	TPI1
ENSG00000102178	-0.491224254	0.011141253	UBL4A
ENSG00000124588	-0.491050646	0.059976405	NQO2
ENSG00000141076	-0.49067742	0.045347087	UTP4
ENSG00000171861	-0.488483748	0.015876099	MRM3
ENSG00000065427	-0.486247241	0.025353163	KARS
ENSG00000121211	-0.48594216	0.046735219	MND1
ENSG00000184924	-0.485822326	0.054069312	PTRHD1
ENSG00000280789	-0.485818464	0.034112629	PAGR1
ENSG00000105364	-0.484640364	0.058830711	MRPL4
ENSG00000111737	-0.483698218	0.019358766	RAB35
ENSG00000205476	-0.483001362	0.030528457	CCDC85C
ENSG00000166133	-0.482958553	0.054619972	RPUSD2
ENSG00000166851	-0.482945128	0.053429599	PLK1
ENSG00000065268	-0.482069837	0.048403342	WDR18
ENSG00000136908	-0.481019171	0.054720347	DPM2
ENSG00000085999	-0.480224858	0.02339609	RAD54L
ENSG00000100364	-0.480061378	0.039885786	KIAA0930
ENSG00000196372	-0.479130544	0.019965233	ASB13
ENSG00000251669	-0.479118583	0.02873467	FAM86EP
ENSG00000165688	-0.478836756	0.045180128	PMPCA
ENSG00000146109	-0.477208742	0.036373561	ABT1
ENSG00000005022	-0.475459049	0.040392208	SLC25A5
ENSG00000077152	-0.475159094	0.02385373	UBE2T
ENSG00000198805	-0.474167345	0.048381279	PNP
ENSG00000147684	-0.472215145	0.039209249	NDUFB9
ENSG00000173581	-0.471526411	0.0477854	CCDC106
ENSG00000244187	-0.471223864	0.051953703	TMEM141
ENSG00000117394	-0.471159333	0.033435893	SLC2A1

ENSG00000147586	-0.470897764	0.041980163	MRPS28
ENSG00000182541	-0.470337018	0.050598703	LIMK2
ENSG00000168884	-0.46979455	0.050123564	TNIP2
ENSG00000161714	-0.469617692	0.031588375	PLCD3
ENSG00000165283	-0.469610552	0.038989533	STOML2
ENSG00000129255	-0.468945072	0.041204911	MPDU1
ENSG00000184857	-0.468769669	0.042368664	TMEM186
ENSG00000119559	-0.468162724	0.045694684	C19orf25
ENSG00000141698	-0.468100914	0.050068349	NT5C3B
ENSG00000175376	-0.467724268	0.043952594	EIF1AD
ENSG00000154978	-0.466912192	0.029340559	VOPP1
ENSG00000196642	-0.46684808	0.020594778	RABL6
ENSG00000073578	-0.466721851	0.028744262	SDHA
ENSG00000137656	-0.46502709	0.032416314	BUD13
ENSG00000136270	-0.46459973	0.026659046	TBRG4
ENSG00000164087	-0.464545717	0.033667138	POC1A
ENSG00000170855	-0.464128461	0.057052751	TRIAP1
ENSG00000111057	-0.463856828	0.055607189	KRT18
ENSG00000137054	-0.463562461	0.008442949	POLR1E
ENSG00000197562	-0.463396923	0.026727919	RAB40C
ENSG00000100749	-0.462404289	0.055901416	VRK1
ENSG00000126453	-0.461980983	0.045285839	BCL2L12
ENSG00000249353	-0.461809611	0.057479307	NPM1P27
ENSG00000177954	-0.461667613	0.05560185	RPS27
ENSG00000168569	-0.461528717	0.048917965	TMEM223
ENSG00000169592	-0.461378347	0.057179136	INO80E
ENSG00000122873	-0.461196938	0.050844117	CISD1
ENSG00000204209	-0.460957045	0.025097234	DAXX
ENSG00000154832	-0.459871573	0.051312193	CXXC1
ENSG00000090621	-0.459612692	0.010424067	PABPC4
ENSG00000116525	-0.457728983	0.052942673	TRIM62
ENSG00000169221	-0.457612266	0.045960794	TBC1D10B
ENSG00000160439	-0.457578418	0.023669413	RDH13
ENSG00000152240	-0.457518901	0.027070253	HAUS1
ENSG00000132423	-0.456600132	0.057519259	COQ3
ENSG00000165501	-0.454703297	0.046924242	LRR1
ENSG00000171314	-0.454397563	0.032845627	PGAM1
ENSG00000157927	-0.453571132	0.020517044	RADIL
ENSG00000145386	-0.451780889	0.016784269	CCNA2
ENSG00000097021	-0.451686269	0.057514658	ACOT7
ENSG00000116871	-0.451377879	0.05386111	MAP7D1

ENSG00000235823	-0.450582535	0.04139102	OLMALINC
ENSG00000140280	-0.449359297	0.035728738	LYSMD2
ENSG00000167625	-0.449189621	0.050615487	ZNF526
ENSG00000161956	-0.449000206	0.01790284	SENP3
ENSG00000104731	-0.448542163	0.032168038	KLHDC4
ENSG00000198682	-0.448189346	0.059179396	PAPSS2
ENSG00000089685	-0.448050292	0.056072195	BIRC5
ENSG00000108384	-0.447627466	0.052559833	RAD51C
ENSG00000128944	-0.447518904	0.055820802	KNSTRN
ENSG00000136280	-0.44646488	0.04888373	CCM2
ENSG00000069998	-0.446439187	0.032501642	HDHD5
ENSG00000149636	-0.445601277	0.029089335	DSN1
ENSG00000215021	-0.444791981	0.043706718	PHB2
ENSG00000018699	-0.443883627	0.006433328	TTC27
ENSG00000099364	-0.441463803	0.030509361	FBXL19
ENSG00000100418	-0.440918232	0.052407911	DESI1
ENSG00000163931	-0.440642471	0.027314019	TKT
ENSG00000077514	-0.438486882	0.016695382	POLD3
ENSG00000004142	-0.436460856	0.054633989	POLDIP2
ENSG00000127423	-0.435875196	0.045063693	AUNIP
ENSG00000198915	-0.434315767	0.029123517	RASGEF1A
ENSG00000087586	-0.43347264	0.050766095	AURKA
ENSG00000029993	-0.433389032	0.046374128	HMGB3
ENSG00000167112	-0.431005726	0.058236511	TRUB2
ENSG00000169021	-0.430163752	0.05507416	UQCRFS1
ENSG00000122085	-0.427527197	0.049324008	MTERF4
ENSG00000203993	-0.425085809	0.040713926	ARRDC1-AS1
ENSG00000079999	-0.422249783	0.040310717	KEAP1
ENSG00000074266	-0.421793608	0.058446236	EED
ENSG00000176490	-0.421275931	0.037852258	DIRAS1
ENSG00000160753	-0.419074389	0.058920676	RUSC1
ENSG00000141499	-0.418576406	0.053317592	WRAP53
ENSG00000107672	-0.417230902	0.038178378	NSMCE4A
ENSG00000136807	-0.416638462	0.048613282	CDK9
ENSG00000204568	-0.415549064	0.030100716	MRPS18B
ENSG00000067225	-0.415516606	0.051027784	PKM
ENSG00000071655	-0.414887924	0.046770462	MBD3
ENSG00000151065	-0.412912496	0.036531658	DCP1B
ENSG00000124688	-0.412169136	0.051225924	MAD2L1BP
ENSG00000167792	-0.409865183	0.040420627	NDUFV1
ENSG00000177733	-0.409031362	0.022897807	HNRNPA0

ENSG00000141480	-0.406282097	0.034517643	ARRB2
ENSG00000130713	-0.404991013	0.056016203	EXOSC2
ENSG00000205208	-0.404532602	0.054102312	C4orf46
ENSG00000147274	-0.401844913	0.049530244	RBMX
ENSG00000163156	-0.399862147	0.055484673	SCNM1
ENSG00000130829	-0.399613389	0.045163529	DUSP9
ENSG00000182307	-0.399189031	0.035639519	C8orf33
ENSG00000188986	-0.395987938	0.05292132	NELFB
ENSG00000245848	-0.395058672	0.050807582	CEBPA
ENSG00000131470	-0.394301025	0.051278666	PSMC3IP
ENSG00000130787	-0.393530594	0.04004313	HIP1R
ENSG00000101181	-0.391001274	0.038072448	MTG2
ENSG00000143179	-0.390135028	0.019645567	UCK2
ENSG00000141098	-0.389748595	0.049540071	GFOD2
ENSG00000204316	-0.388501043	0.053384741	MRPL38
ENSG00000122783	-0.388287602	0.056590641	C7orf49
ENSG00000178035	-0.387643557	0.051419333	IMPDH2
ENSG00000173674	-0.379246597	0.056032908	EIF1AX
ENSG00000130299	-0.374123666	0.03643089	GTPBP3
ENSG00000204590	-0.371125655	0.035608949	GNL1
ENSG00000101856	-0.368533506	0.054560515	PGRMC1
ENSG00000141560	-0.367970721	0.056947312	FN3KRP
ENSG00000154473	-0.367509518	0.056010169	BUB3
ENSG00000144589	-0.363683189	0.048761111	STK11IP
ENSG00000169100	-0.362941917	0.05768985	SLC25A6
ENSG00000273604	-0.360287907	0.028195617	EPOP
ENSG00000160917	-0.351688395	0.046335822	CPSF4
ENSG00000266962	-0.348591457	0.047989653	AC067852.2
ENSG00000169515	-0.347160566	0.034927327	CCDC8
ENSG00000214022	-0.342713257	0.03343029	REPIN1
ENSG00000147548	0.334941625	0.059540483	NSD3
ENSG00000221978	0.339033577	0.052657146	CCNL2
ENSG00000072778	0.344292865	0.05232331	ACADVL
ENSG00000149577	0.352379381	0.0502476	SIDT2
ENSG00000162298	0.366110125	0.041277629	SYVN1
ENSG00000070214	0.370123996	0.044726892	SLC44A1
ENSG00000163660	0.374749867	0.052671788	CCNL1
ENSG00000151148	0.379102953	0.043623462	UBE3B
ENSG00000014824	0.380114434	0.029642849	SLC30A9
ENSG00000122218	0.382342203	0.058906221	COPA
ENSG00000137845	0.384433906	0.058259324	ADAM10

ENSG00000166532	0.388654959	0.052682227	RIMKLB
ENSG00000169826	0.392512326	0.051144615	CSGALNACT2
ENSG00000096093	0.404877908	0.047719342	EFHC1
ENSG00000135870	0.408883893	0.055478541	RC3H1
ENSG00000164056	0.409410902	0.051532571	SPRY1
ENSG00000163125	0.411635296	0.057019122	RPRD2
ENSG00000153936	0.41293996	0.056413165	HS2ST1
ENSG00000144036	0.414795961	0.059472204	EXOC6B
ENSG00000068912	0.420199415	0.050308194	ERLEC1
ENSG00000025796	0.421567505	0.047866446	SEC63
ENSG00000150630	0.423823095	0.03765834	VEGFC
ENSG00000144115	0.423847625	0.045379093	THNSL2
ENSG00000121989	0.429124834	0.032912138	ACVR2A
ENSG00000164066	0.429673263	0.043853596	INTU
ENSG00000214050	0.433882068	0.046965322	FBXO16
ENSG00000164114	0.43428049	0.047886973	MAP9
ENSG00000157625	0.436266809	0.051903678	TAB3
ENSG00000166435	0.437382103	0.053061626	XRRA1
ENSG00000135596	0.438203133	0.020626008	MICAL1
ENSG00000075826	0.439068856	0.053875956	SEC31B
ENSG00000139324	0.440003293	0.03119533	TMTC3
ENSG00000111897	0.441945769	0.051561884	SERINC1
ENSG00000052841	0.441964775	0.039518591	TTC17
ENSG00000091986	0.442926082	0.053036967	CCDC80
ENSG00000108509	0.44887468	0.054908086	CAMTA2
ENSG00000144724	0.453095058	0.037942842	PTPRG
ENSG00000124171	0.456353512	0.038251254	PARD6B
ENSG00000049618	0.457852451	0.049462117	ARID1B
ENSG00000135862	0.458071013	0.04216287	LAMC1
ENSG00000156140	0.459191387	0.04237787	ADAMTS3
ENSG00000032219	0.460584697	0.057329492	ARID4A
ENSG00000075151	0.462952915	0.046890477	EIF4G3
ENSG00000085788	0.465547103	0.042307893	DDHD2
ENSG00000000971	0.46711537	0.041416647	CFH
ENSG00000135677	0.468971614	0.030662719	GNS
ENSG00000154654	0.469015455	0.043839312	NCAM2
ENSG00000095397	0.469270804	0.019135453	WHRN
ENSG00000164307	0.470328727	0.0229597	ERAP1
ENSG00000160445	0.474105726	0.043734588	ZER1
ENSG00000072135	0.475633108	0.033877164	PTPN18
ENSG00000009413	0.477274229	0.053065297	REV3L

ENSG00000145246	0.478996636	0.03708296	ATP10D
ENSG00000113369	0.479851821	0.019629152	ARRDC3
ENSG00000139117	0.480564042	0.028585741	CPNE8
ENSG00000174749	0.483371907	0.056466537	FAM241A
ENSG00000168172	0.484128873	0.025434913	HOOK3
ENSG00000145147	0.484422229	0.051465793	SLIT2
ENSG00000091136	0.489102297	0.045399806	LAMB1
ENSG00000154265	0.489453045	0.031605515	ABCA5
ENSG00000120519	0.490845669	0.058200295	SLC10A7
ENSG00000166340	0.50006034	0.002752532	TPP1
ENSG00000140398	0.502293705	0.034286659	NEIL1
ENSG00000068305	0.506649496	0.048279303	MEF2A
ENSG00000112246	0.506847457	0.035066894	SIM1
ENSG00000085224	0.507552084	0.030887739	ATRX
ENSG00000083799	0.508048632	0.029726866	CYLD
ENSG00000156103	0.508334003	0.037685637	MMP16
ENSG00000169760	0.509659077	0.018124862	NLGN1
ENSG00000054983	0.512772713	0.059537404	GALC
ENSG00000167785	0.513083245	0.028557667	ZNF558
ENSG00000172869	0.513732615	0.027171931	DMXL1
ENSG00000164603	0.514052097	0.045154831	BMT2
ENSG00000234745	0.517271609	0.003440703	HLA-B
ENSG00000083097	0.51738587	0.037921495	DOPEY1
ENSG00000168772	0.517810887	0.033063498	CXXC4
ENSG00000131374	0.521205884	0.020035981	TBC1D5
ENSG00000146587	0.522051419	0.034945666	RBAK
ENSG00000198380	0.523661422	0.029371436	GFPT1
ENSG00000149231	0.524665742	0.027502657	CCDC82
ENSG00000136021	0.527808048	0.028347983	SCYL2
ENSG00000055609	0.528542492	0.057019001	KMT2C
ENSG00000112773	0.528927948	0.040107503	FAM46A
ENSG00000117228	0.529863925	0.033079157	GBP1
ENSG00000104133	0.531682624	0.015260111	SPG11
ENSG00000168152	0.53249455	0.047173565	THAP9
ENSG00000154642	0.53599453	0.053418549	C21orf91
ENSG00000256223	0.538681837	0.028144445	ZNF10
ENSG00000138834	0.539294411	0.04627229	MAPK8IP3
ENSG00000087074	0.540691521	0.034735885	PPP1R15A
ENSG00000092439	0.541329501	0.037149447	TRPM7
ENSG00000181192	0.545238734	0.042532506	DHTKD1
ENSG00000263956	0.550796935	0.038178792	NBPF11

ENSG00000113638	0.551079894	0.024534257	TTC33
ENSG00000105426	0.551355599	0.0217375	PTPRS
ENSG00000106460	0.552547799	0.017235085	TMEM106B
ENSG00000088340	0.556357453	0.050889553	FER1L4
ENSG00000157796	0.556882589	0.021655764	WDR19
ENSG00000129003	0.558312201	0.024986682	VPS13C
ENSG00000075420	0.559256333	0.032020035	FNDC3B
ENSG00000137103	0.560059024	0.019193816	TMEM8B
ENSG00000115137	0.560373534	0.026398186	DNAJC27
ENSG00000248334	0.560718723	0.05203814	WHAMMP2
ENSG00000256043	0.56233841	0.054054081	CTSO
ENSG00000276141	0.563666045	0.057614313	WHAMMP3
ENSG00000149311	0.564339496	0.032100794	ATM
ENSG00000123636	0.56443286	0.042811455	BAZ2B
ENSG00000274349	0.564563285	0.043004756	ZNF658
ENSG00000158528	0.565981123	0.026317399	PPP1R9A
ENSG00000224660	0.56684227	0.039568896	SH3BP5-AS1
ENSG00000206538	0.566889791	0.059943767	VGLL3
ENSG00000172638	0.567596119	0.002326972	EFEMP2
ENSG00000196712	0.567612907	0.03891584	NF1
ENSG00000188554	0.570162073	0.032634448	NBR1
ENSG00000140199	0.57087321	0.036886798	SLC12A6
ENSG00000124508	0.572196145	0.026939956	BTN2A2
ENSG00000110841	0.572976777	0.040330206	PPFIBP1
ENSG00000152582	0.573993968	0.031881618	SPEF2
ENSG00000128881	0.576252318	0.038094708	TTBK2
ENSG00000179912	0.57638654	0.025684088	R3HDM2
ENSG00000075213	0.57789991	0.024652866	SEMA3A
ENSG00000119397	0.57835339	0.055270072	CNTRL
ENSG00000234684	0.578550616	0.026486111	SDCBP2-AS1
ENSG00000254337	0.578839019	0.044209505	AC083967.1
ENSG00000185650	0.579503636	0.016818684	ZFP36L1
ENSG00000051108	0.579917419	0.002784872	HERPUD1
ENSG00000111653	0.580450729	0.054040604	ING4
ENSG00000186951	0.58113139	0.052684361	PPARA
ENSG00000130751	0.581195024	0.0526768	NPAS1
ENSG00000139318	0.587314556	0.004832973	DUSP6
ENSG00000150093	0.590656876	0.037393642	ITGB1
ENSG00000174485	0.591482684	0.036038604	DENND4A
ENSG00000117139	0.592175162	0.04495651	KDM5B
ENSG00000261971	0.593109761	0.04210545	MMP25-AS1

ENSG00000185761	0.594820923	0.032910576	ADAMTSL5
ENSG00000154237	0.595759712	0.020178928	LRRK1
ENSG00000240024	0.597000352	0.025528365	LINC00888
ENSG00000165392	0.598411075	0.026302866	WRN
ENSG00000213903	0.599405965	0.058590694	LTB4R
ENSG00000229358	0.599933528	0.053322214	DPY19L1P1
ENSG00000141376	0.601912512	0.033723506	BCAS3
ENSG00000116668	0.604163957	0.023388868	SWT1
ENSG00000196967	0.605044354	0.014494335	ZNF585A
ENSG00000166165	0.60626396	0.008442954	CKB
ENSG00000149428	0.606995183	0.011437388	HYOU1
ENSG00000139182	0.612106006	0.024611018	CLSTN3
ENSG00000111961	0.612585482	0.051615834	SASH1
ENSG00000135828	0.612819244	0.013478516	RNASEL
ENSG00000152409	0.613021196	0.038076892	JMY
ENSG00000138468	0.613269118	0.032504037	SENP7
ENSG00000010704	0.615507638	0.030969117	HFE
ENSG00000230551	0.61555699	0.049575883	AC021078.1
ENSG00000114270	0.6185724	0.044224544	COL7A1
ENSG00000238083	0.619602023	0.053924705	LRRC37A2
ENSG00000014123	0.620357687	0.018170809	UFL1
ENSG00000183571	0.620706838	0.044825744	PGPEP1L
ENSG00000019991	0.622115623	0.023585252	HGF
ENSG00000173209	0.623406134	0.016396276	AHSA2P
ENSG00000111058	0.625287183	0.05805407	ACSS3
ENSG00000112972	0.633014256	0.004490273	HMGCS1
ENSG00000112812	0.635468042	0.051434982	PRSS16
ENSG00000187164	0.636753546	0.026696182	SHTN1
ENSG00000214021	0.63709534	0.018464167	TTLL3
ENSG00000114439	0.6393681	0.002961133	BBX
ENSG00000243176	0.64044944	0.05725219	AC092944.1
ENSG00000089057	0.642722739	0.047704698	SLC23A2
ENSG00000026950	0.643838744	0.028972317	BTN3A1
ENSG00000133812	0.64625629	0.031334812	SBF2
ENSG00000177888	0.647839128	0.015293058	ZBTB41
ENSG00000147421	0.64935404	0.005726512	HMBOX1
ENSG00000151320	0.650445014	0.036266194	AKAP6
ENSG00000128342	0.654621469	0.029479829	LIF
ENSG00000179979	0.655036143	0.005361578	NA
ENSG00000189127	0.656542408	0.043960562	ANKRD34B
ENSG00000134243	0.663268086	0.016482728	SORT1

ENSG00000114933	0.664713336	0.019930116	INO80D
ENSG00000123836	0.66529037	0.022508142	PFKFB2
ENSG00000096654	0.665332028	0.035722206	ZNF184
ENSG00000123240	0.667104841	0.007805112	OPTN
ENSG00000096872	0.667900538	0.017494492	IFT74
ENSG00000133110	0.672704648	0.045259269	POSTN
ENSG00000160961	0.674298107	0.028231296	ZNF333
ENSG00000074181	0.674353382	0.008764011	NOTCH3
ENSG00000090530	0.674946003	0.00012468	P3H2
ENSG00000128016	0.675284804	0.018749477	ZFP36
ENSG00000138449	0.678313426	0.006063728	SLC40A1
ENSG00000153214	0.678711882	0.042262701	TMEM87B
ENSG00000134698	0.681321756	0.017793678	AGO4
ENSG00000205517	0.681347799	0.00357781	RGL3
ENSG00000197959	0.683281152	0.017814518	DNM3
ENSG00000204410	0.68380727	0.037521228	MSH5
ENSG00000134294	0.684306227	0.01097861	SLC38A2
ENSG00000065809	0.684532296	0.041169728	FAM107B
ENSG00000064989	0.686116717	0.013890053	CALCRL
ENSG00000166762	0.686198611	0.051059434	CATSPER2
ENSG00000107864	0.686746717	0.048949126	CPEB3
ENSG00000152926	0.687830109	0.022286653	ZNF117
ENSG00000124406	0.692318067	0.045847117	ATP8A1
ENSG00000260404	0.692522505	0.055482738	AC110079.1
ENSG00000204084	0.694950231	0.022532623	INPP5B
ENSG00000173230	0.696141673	0.012223725	GOLGB1
ENSG00000171988	0.696146995	0.021983276	JMJD1C
ENSG00000135298	0.697044218	0.014554371	ADGRB3
ENSG00000267121	0.700434749	0.049047058	AC008105.3
ENSG00000113448	0.702090739	0.012677078	PDE4D
ENSG00000067141	0.70433407	0.033846431	NEO1
ENSG00000219626	0.708438315	0.04872145	FAM228B
ENSG00000255282	0.710488114	0.025310231	WTAPP1
ENSG00000188153	0.714277478	0.001366437	COL4A5
ENSG00000267002	0.714622406	0.005370777	AC060780.1
ENSG00000223760	0.715517094	0.026509883	MED15P9
ENSG00000130150	0.718890243	0.025765244	MOSPD2
ENSG00000153993	0.728821845	0.013804471	SEMA3D
ENSG00000138688	0.729315961	0.022625403	KIAA1109
ENSG00000204248	0.732405414	0.031901653	COL11A2
ENSG00000168671	0.737646313	0.022462029	UGT3A2

ENSG00000249572	0.73866966	0.04385393	AC034231.1
ENSG00000267750	0.741898691	0.02186769	RUNDC3A-AS1
ENSG00000103599	0.743836643	0.016092817	IQCH
ENSG00000178385	0.746172667	0.034803505	PLEKHM3
ENSG00000180318	0.747088317	0.043899475	ALX1
ENSG00000162687	0.747668977	0.013768972	KCNT2
ENSG00000147162	0.749390095	0.015839933	OGT
ENSG00000168917	0.760286003	0.003209441	SLC35G2
ENSG00000143387	0.760334007	0.010885235	CTSK
ENSG00000141068	0.760737404	0.015055692	KSR1
ENSG00000138448	0.764696939	0.013772323	ITGAV
ENSG00000101104	0.765492118	0.007350375	PABPC1L
ENSG00000198398	0.769848821	0.000927041	TMEM207
ENSG00000113916	0.772651768	0.013043381	BCL6
ENSG00000056558	0.772980592	0.05897388	TRAF1
ENSG00000150672	0.773176065	0.00205094	DLG2
ENSG00000221947	0.775019627	0.013576882	XKR9
ENSG00000173575	0.776604195	0.015192364	CHD2
ENSG00000179454	0.778708672	0.008287622	KLHL28
ENSG00000124613	0.7799677	0.031400029	ZNF391
ENSG00000134343	0.781191745	0.013637065	ANO3
ENSG00000198315	0.781857724	0.009393119	ZKSCAN8
ENSG00000155304	0.78324501	0.011839794	HSPA13
ENSG00000133794	0.787093003	0.045229606	ARNTL
ENSG00000108797	0.794165875	0.003725513	CNTNAP1
ENSG00000058063	0.795789907	0.0061462	ATP11B
ENSG00000071537	0.797012898	0.001290337	SEL1L
ENSG00000073605	0.80179946	0.014961862	GSDMB
ENSG00000055732	0.804058814	0.0117467	MCOLN3
ENSG00000167861	0.805288005	0.009501466	HID1
ENSG00000163703	0.814839613	0.005193125	CRELD1
ENSG00000118985	0.815125088	0.029984205	ELL2
ENSG00000167524	0.81783547	0.02772963	SGK494
ENSG00000171551	0.818683852	0.018506275	ECEL1
ENSG00000106261	0.819558193	0.000877249	ZKSCAN1
ENSG00000145476	0.820321572	0.015092748	CYP4V2
ENSG00000143248	0.822116442	0.02693845	RGS5
ENSG00000170381	0.825786543	0.00272721	SEMA3E
ENSG00000137474	0.829301308	0.029765305	MYO7A
ENSG00000144642	0.829734609	0.01414255	RBMS3
ENSG00000164331	0.833732291	0.022835431	ANKRA2

ENSG00000154310	0.834397874	0.024514885	TNIK
ENSG00000167554	0.84208024	0.022017083	ZNF610
ENSG00000162738	0.842139946	0.001300263	VANGL2
ENSG00000230630	0.848128198	0.01302393	DNM3OS
ENSG00000183044	0.849936798	0.048198477	ABAT
ENSG00000164099	0.851292313	0.029392436	PRSS12
ENSG00000135749	0.85412703	0.053051435	PCNX2
ENSG00000170989	0.855281917	0.056211346	S1PR1
ENSG00000164938	0.855781673	0.018026609	TP53INP1
ENSG00000012822	0.856962001	0.015083428	CALCOCO1
ENSG00000146350	0.858268475	0.010222196	TBC1D32
ENSG00000126952	0.861359083	0.041455471	NXF5
ENSG00000204186	0.863306167	0.036871151	ZDBF2
ENSG00000179915	0.864897001	0.019254428	NRXN1
ENSG00000112414	0.866234384	0.003922542	ADGRG6
ENSG00000225465	0.870307543	0.035348331	RFPL1S
ENSG00000106804	0.870555538	0.036740837	C5
ENSG00000186814	0.873500582	0.007226246	ZSCAN30
ENSG00000153822	0.879017068	0.018818771	KCNJ16
ENSG00000215068	0.880314585	0.015733955	AC025171.2
ENSG00000213222	0.881106558	0.03002092	AC093724.1
ENSG00000010310	0.881758952	0.031377186	GIPR
ENSG00000187017	0.882423348	0.05207732	ESPN
ENSG00000197565	0.885338297	0.049159123	COL4A6
ENSG00000168994	0.885528343	0.002635274	PXDC1
ENSG00000132003	0.885747782	0.034988071	ZSWIM4
ENSG00000163430	0.886275195	0.002050308	FSTL1
ENSG00000163975	0.898498424	0.001549747	MELTF
ENSG00000254815	0.898981898	0.022809583	AP006284.1
ENSG00000188338	0.902105917	0.004277834	SLC38A3
ENSG00000158079	0.904338685	0.014544249	PTPDC1
ENSG00000198932	0.90557166	0.05103303	GPRASP1
ENSG00000186301	0.906207437	0.009193867	MST1P2
ENSG00000184925	0.911466898	0.033680167	LCN12
ENSG00000130768	0.912285117	0.04409817	SMPDL3B
ENSG00000230258	0.913163454	0.026841321	AC005208.1
ENSG00000165028	0.914042974	0.041053455	NIPSNAP3B
ENSG00000173531	0.917040065	0.031526618	MST1
ENSG00000182796	0.920672443	0.007466911	TMEM198B
ENSG00000011028	0.922210966	0.009980083	MRC2
ENSG00000251562	0.931013333	0.005211097	MALAT1

ENSG00000088538	0.939565918	0.010464588	DOCK3
ENSG00000142798	0.940120404	0.023929613	HSPG2
ENSG00000260916	0.942358573	0.01273826	CCPG1
ENSG00000020181	0.943587239	0.019639572	ADGRA2
ENSG00000246859	0.944505666	0.030216847	STARD4-AS1
ENSG00000157657	0.944770415	0.011988924	ZNF618
ENSG00000132510	0.945028143	0.01288611	KDM6B
ENSG00000251192	0.946174171	0.045156773	ZNF674
ENSG00000120899	0.947207905	0.01127593	PTK2B
ENSG00000175161	0.951346614	0.006901308	CADM2
ENSG00000049656	0.951538223	0.017523032	CLPTM1L
ENSG00000163431	0.95170649	0.016749241	LMOD1
ENSG00000145012	0.957823169	0.000119916	LPP
ENSG00000104967	0.963616641	0.014088668	NOVA2
ENSG00000130653	0.972672673	0.031245347	PNPLA7
ENSG00000129595	0.972929494	0.044238008	EPB41L4A
ENSG00000102908	0.972949336	0.022501188	NFAT5
ENSG00000144821	0.974486904	0.011350127	MYH15
ENSG00000116962	0.975270005	0.024414721	NID1
ENSG00000214456	0.976285852	0.056026728	PLIN5
ENSG00000056487	0.980250373	0.000764624	PHF21B
ENSG00000188177	0.982774725	0.034166072	ZC3H6
ENSG00000273033	0.983237686	0.031935115	LINC02035
ENSG00000280355	0.985602738	0.043416577	AL132656.4
ENSG00000198939	0.988979679	0.039406678	ZFP2
ENSG00000253741	0.991283344	0.038457176	AC108002.1
ENSG00000107099	0.991768618	0.032542021	DOCK8
ENSG00000099365	0.995344683	0.015602655	STX1B
ENSG00000138434	0.999500641	0.006363184	SSFA2
ENSG00000239467	1.010288846	0.022829112	AC007405.3
ENSG00000164342	1.011497222	0.004671047	TLR3
ENSG00000237125	1.011632413	0.035901002	HAND2-AS1
ENSG00000170345	1.012154918	0.008032985	FOS
ENSG00000261360	1.014125347	0.046326727	AC010491.1
ENSG00000130147	1.018669562	0.021279387	SH3BP4
ENSG00000181804	1.018919104	0.007100628	SLC9A9
ENSG00000270728	1.02101433	0.055904674	AL035413.2
ENSG00000117525	1.021753202	0.038788134	F3
ENSG00000245532	1.02874106	0.014808961	NEAT1
ENSG00000197892	1.031785798	0.002723254	KIF13B
ENSG00000204789	1.04221806	0.007020524	ZNF204P

ENSG00000105856	1.042382081	0.013820449	HBP1
ENSG00000049239	1.043348496	0.013016197	H6PD
ENSG00000230724	1.045692066	0.013677626	LINC01001
ENSG00000142173	1.053815393	9.60E-05	COL6A2
ENSG00000226696	1.055568689	0.049248355	LENG8-AS1
ENSG00000166432	1.060777387	0.005919788	ZMAT1
ENSG00000135439	1.062407328	0.020140011	AGAP2
ENSG00000141505	1.063361439	0.008229012	ASGR1
ENSG00000250091	1.072609358	0.034325747	DNAH10OS
ENSG00000225764	1.072869811	0.015891751	P3H2-AS1
ENSG00000028310	1.075552112	0.003208527	BRD9
ENSG00000251026	1.07573683	0.033535367	LINC02163
ENSG00000105696	1.083445607	0.000799053	TMEM59L
ENSG00000131018	1.087860384	0.032084538	SYNE1
ENSG00000182257	1.088714075	0.050607317	PRR34
ENSG00000049192	1.08882399	0.053412334	ADAMTS6
ENSG00000175197	1.089877111	0.004451921	DDIT3
ENSG00000116544	1.098117187	0.044930656	DLGAP3
ENSG00000153157	1.100321017	0.021508132	SYCP2L
ENSG00000006459	1.10083023	0.008870138	KDM7A
ENSG00000178947	1.102645864	0.045224727	SMIM10L2A
ENSG00000134548	1.106536585	0.044466376	SPX
ENSG00000176244	1.10818141	0.042696584	ACBD7
ENSG00000141497	1.108601703	0.033594587	ZMYND15
ENSG00000132702	1.116408685	0.011316123	HAPLN2
ENSG00000204257	1.116483092	0.030259316	HLA-DMA
ENSG00000274750	1.117693683	0.011737323	HIST1H3E
ENSG00000258768	1.123214814	0.003881051	AL356019.2
ENSG00000064763	1.124420769	0.049701924	FAR2
ENSG00000074370	1.128927261	0.007342375	ATP2A3
ENSG00000167608	1.130094353	0.01466995	TMC4
ENSG00000259065	1.141480043	0.033161055	AC005520.2
ENSG00000104419	1.14226916	0.049726278	NDRG1
ENSG00000275395	1.146336267	0.00266357	FCGBP
ENSG00000251136	1.151076682	0.003917247	AF117829.1
ENSG00000166323	1.152209772	0.013375057	C11orf65
ENSG00000248126	1.171661003	0.034346847	AC091849.1
ENSG00000163346	1.173609615	0.01099122	PBXIP1
ENSG00000181885	1.176784704	0.056170719	CLDN7
ENSG00000272140	1.179544097	0.050904724	AC022400.5
ENSG00000123384	1.184872196	0.006350287	LRP1

ENSG00000159208	1.187414212	0.020853302	CIART
ENSG00000256673	1.200405738	0.031027204	AC141557.1
ENSG00000243224	1.202396246	0.045012313	AC006252.1
ENSG00000169894	1.203829212	0.024578805	MUC3A
ENSG00000123870	1.206591614	0.025228389	ZNF137P
ENSG00000115935	1.208549038	0.006685987	WIPF1
ENSG00000012171	1.213119934	0.015327328	SEMA3B
ENSG00000076770	1.214678522	0.019767031	MBNL3
ENSG00000164088	1.219118297	0.014268903	PPM1M
ENSG00000164327	1.222255892	2.08E-06	RICTOR
ENSG00000167103	1.225558734	0.049270259	PIP5KL1
ENSG00000196083	1.235493256	2.01E-06	IL1RAP
ENSG00000231551	1.237613134	0.030682044	AC245100.4
ENSG00000147642	1.249335729	0.046543299	SYBU
ENSG00000135525	1.253501605	0.020805143	MAP7
ENSG00000133134	1.254386314	0.016229545	BEX2
ENSG00000246982	1.255814155	0.058580874	Z84485.1
ENSG00000174469	1.257621815	0.002969786	CNTNAP2
ENSG00000187984	1.266158529	0.028874354	ANKRD19P
ENSG00000258334	1.278051481	0.038269367	AC125611.4
ENSG00000073331	1.283348547	0.017558763	ALPK1
ENSG00000226985	1.28949876	0.000613272	LINC01203
ENSG00000114796	1.293069522	0.004038015	KLHL24
ENSG00000119681	1.294598064	0.008072641	LTBP2
ENSG00000154760	1.295181966	0.040977128	SLFN13
ENSG00000164463	1.296171878	0.003937891	CREBRF
ENSG00000175274	1.299944661	8.53E-06	TP53I11
ENSG00000163347	1.30647872	3.06E-06	CLDN1
ENSG00000268812	1.306515008	0.012563673	AC004264.1
ENSG00000179855	1.307831325	0.004971011	GIPC3
ENSG00000253305	1.311403814	0.034936667	PCDHGB6
ENSG00000143469	1.313425098	0.038537503	SYT14
ENSG00000116191	1.316633348	0.000288062	RALGPS2
ENSG00000273333	1.320625508	0.053177843	AL662884.1
ENSG00000090539	1.321341376	0.015962343	CHRD
ENSG00000170153	1.32502913	0.010021978	RNF150
ENSG00000113946	1.325209375	3.03E-07	CLDN16
ENSG00000266714	1.325375392	0.013883868	MYO15B
ENSG00000104848	1.333908095	0.021590947	KCNA7
ENSG00000105289	1.335340223	0.016958328	TJP3
ENSG00000102401	1.343422967	0.016948767	ARMCX3

ENSG00000170485	1.352937485	0.001808015	NPAS2
ENSG00000071242	1.354709406	0.014679859	RPS6KA2
ENSG00000139269	1.356328306	0.018677235	INHBE
ENSG00000258183	1.363794306	0.011105074	LINC02392
ENSG00000179399	1.366442644	0.055193068	GPC5
ENSG00000177694	1.368977553	0.004966248	NAALADL2
ENSG00000087116	1.375646413	0.057578161	ADAMTS2
ENSG00000175155	1.393846458	0.012865719	YPEL2
ENSG00000105499	1.394129023	0.002128476	PLA2G4C
ENSG00000196668	1.402389114	0.049182341	LINC00173
ENSG00000161381	1.402741799	0.045258128	PLXDC1
ENSG00000179388	1.412684385	0.00332184	EGR3
ENSG00000129757	1.412724332	0.010126247	CDKN1C
ENSG00000189184	1.416556783	0.01127008	PCDH18
ENSG00000208024	1.420363599	0.032321482	MIR199A2
ENSG00000174567	1.420793789	0.020242725	GOLT1A
ENSG00000236516	1.421121358	0.022461461	KLF2P4
ENSG00000210077	1.431655631	2.57E-05	MT-TV
ENSG00000210049	1.435961947	0.000406744	MT-TF
ENSG00000225783	1.441228011	0.016232926	MIAT
ENSG00000235703	1.445673724	0.016501703	LINC00894
ENSG00000268575	1.45890285	0.000561586	AL031282.2
ENSG00000187260	1.462617634	0.016180061	WDR86
ENSG00000116176	1.466730388	0.057719753	TPSG1
ENSG00000185291	1.467703274	0.042328003	IL3RA
ENSG00000197594	1.468894718	0.011998192	ENPP1
ENSG00000166046	1.473206895	0.053352313	TCP11L2
ENSG00000116667	1.477270165	0.02772031	C1orf21
ENSG00000231196	1.489357627	0.015422114	NA
ENSG00000010810	1.490321396	0.031167925	FYN
ENSG00000136404	1.504275723	0.009199782	TM6SF1
ENSG00000226434	1.505904064	8.73E-05	AC135371.1
ENSG00000226314	1.509093909	0.008492128	ZNF192P1
ENSG00000237094	1.537881479	0.038854678	AL732372.2
ENSG00000113504	1.546961033	3.88E-05	SLC12A7
ENSG00000169836	1.55584733	0.047870673	TACR3
ENSG00000129946	1.56173328	0.010951352	SHC2
ENSG00000274292	1.561795051	0.03160132	AC084018.2
ENSG00000268204	1.567167631	0.042888355	AC008763.1
ENSG00000157601	1.578964338	0.00920965	MX1
ENSG00000227212	1.58692156	0.033935739	PFN1P6

ENSG00000231216	1.598055073	0.045037519	AC004674.1
ENSG00000169885	1.615371961	0.023561864	CALML6
ENSG00000178977	1.626364552	0.018140063	LINC00324
ENSG00000133246	1.626774608	0.023641088	PRAM1
ENSG00000135919	1.64557312	0.002543453	SERPINE2
ENSG00000224066	1.646839592	0.025022905	AL049795.1
ENSG00000254064	1.665016976	0.048143699	AC105206.2
ENSG00000272980	1.666085666	0.043155126	Z94721.2
ENSG00000172264	1.685531958	0.005228293	MACROD2
ENSG00000240990	1.696259864	0.042751663	HOXA11-AS
ENSG00000071539	1.699022377	0.025868565	TRIP13
ENSG00000165731	1.702170844	0.030383657	RET
ENSG00000224081	1.736454122	0.030113673	SLC44A3-AS1
ENSG00000262583	1.73807073	0.03049653	AC009163.5
ENSG00000246763	1.73891829	0.000251863	RGMB-AS1
ENSG00000203581	1.739140751	0.026112735	OR1F2P
ENSG00000120327	1.766638996	0.003025222	PCDHB14
ENSG00000147003	1.766782496	0.000847594	CLTRN
ENSG00000275778	1.767440294	0.04243603	AC018630.2
ENSG00000273018	1.798494062	0.044864317	AC107983.2
ENSG00000214279	1.803856886	0.004504476	SCART1
ENSG00000275832	1.825407498	0.026239918	ARHGAP23
ENSG00000164694	1.830880726	0.054503085	FNDC1
ENSG00000077264	1.855963981	0.014898748	PAK3
ENSG00000005187	1.872952928	0.030699239	ACSM3
ENSG00000170006	1.910131425	0.039088976	TMEM154
ENSG00000172232	1.927742275	0.01403867	AZU1
ENSG00000271755	1.936372319	0.009894464	AL031118.1
ENSG00000139515	1.959797571	0.007547559	PDX1
ENSG00000137285	1.962581914	0.007396532	TUBB2B
ENSG00000111981	1.973097898	0.003771393	ULBP1
ENSG00000213999	1.974580236	0.024787379	MEF2B
ENSG00000228626	1.976301475	0.01228753	AC245100.3
ENSG00000133401	1.984796775	0.000299548	PDZD2
ENSG00000197558	2.023012736	0.005029939	SSPO
ENSG00000126733	2.049385406	1.22E-05	DACH2
ENSG00000123612	2.082726114	0.045228053	ACVR1C
ENSG00000196139	2.104002764	0.017476926	AKR1C3
ENSG00000222046	2.107791463	0.026384601	DCDC2B
ENSG00000115339	2.109736621	0.011231217	GALNT3
ENSG00000106688	2.13669733	5.75E-07	SLC1A1

ENSG00000182179	2.138134275	0.006129274	UBA7
ENSG00000277406	2.155976053	0.024609354	AC245407.1
ENSG00000266824	2.165014587	0.020678312	AC129492.4
ENSG00000188848	2.166448085	3.46E-11	BEND4
ENSG00000231105	2.207867104	0.034400282	AL031728.1
ENSG00000138622	2.21078486	0.014122142	HCN4
ENSG00000130518	2.227089775	0.01815248	IQCN
ENSG00000225148	2.234147338	0.011629325	AL050338.1
ENSG00000270935	2.297484553	0.020385229	AL021808.1
ENSG00000122574	2.37130455	6.02E-07	WIPF3
ENSG00000053747	2.375107264	0.000762034	LAMA3
ENSG00000162344	2.425191007	0.049283565	FGF19
ENSG00000117226	2.433432366	5.05E-05	GBP3
ENSG00000205890	2.517193079	0.026716282	AC108134.1
ENSG00000124126	2.538878694	8.10E-13	PREX1
ENSG00000145287	2.591642493	0.000124368	PLAC8
ENSG00000146592	2.633842496	0.01375421	CREB5
ENSG00000112175	2.713897228	0.000640323	BMP5
ENSG00000064042	2.733476906	1.99E-13	LIMCH1
ENSG00000172403	2.745036698	0.054539439	SYNPO2
ENSG00000139910	2.757956951	4.46E-08	NOVA1
ENSG00000113594	2.762157244	1.40E-07	LIFR
ENSG00000115232	2.773697717	0.005151233	ITGA4
ENSG00000150347	2.775363372	0.038663534	ARID5B
ENSG00000279312	2.807805452	0.041666214	AL136164.4
ENSG00000154118	2.887139234	7.40E-07	JPH3
ENSG00000085276	2.916175167	0.000347763	MECOM
ENSG00000174640	3.051499285	5.08E-05	SLCO2A1
ENSG00000135116	3.081023117	0.008801698	HRK
ENSG00000268869	3.087006691	0.029321578	ESPNP
ENSG00000113361	3.421265843	3.55E-06	CDH6
ENSG00000185008	3.448549593	0.000544494	ROBO2
ENSG00000131196	3.620469318	0.000673515	NFATC1
ENSG00000230798	3.654548595	5.57E-05	FOXD3-AS1
ENSG00000151834	3.844344607	0.011552663	GABRA2
ENSG00000114279	3.920423579	0.000203465	FGF12
ENSG00000150722	4.253043369	7.15E-05	PPP1R1C
ENSG00000164236	4.556503793	9.70E-15	ANKRD33B
ENSG00000157110	4.920050075	1.54E-27	RBPMS
ENSG00000178162	5.29742507	9.62E-05	FAR2P2

Appendix D

Top canonical pathways generated with the unique and common deregulated RNAs in A2780CP20- RBPMSA and A2780CP20-RBPMSC.

Canonical Pathways for A2780CP20-RBPMSA			
Ingenuity Canonical Pathways	***log10 (p-Value)***	***Number of Genes***	***Genes***
Cancer, Cardiovascular System Development and Function Organismal Development	1.24×10^{-03}	31	ADAM17, ANXA3, ARHGDIB, ATP5MC1, AXL, C3, CDH2, CLDN7, CXCL8, DDR2, E2F3, EGFR, GAS6, IFI44, IRF1, ITGB1, LGALS3, LOXL2, MMP1, MMP2, MMP9, MRPL36, NCOA7, PHGDH, PRSS8, PTGS2, SNAI1, SPINT1, TIMP2, TWIST1, UBE2L2
Cell Cycle, Cellular Development, Cellular Growth, and Proliferation	4.30×10^{-03}	25	ARID1A, BMI1, BTG2, CAMKK2, CCND1, CCNE1, CCNE2, CDK2, CDK4, CDK6, CDKN1A, CDKN18, COL6A1, CYFIP2, DHRS3, GDF15, GGT7, HDAC5, ITGB4, PTPRR, RB1, SALL2, SIN3A, TERT, TP53
Antimicrobial Response, Inflammatory Response, and Organismal Injury and Abnormality	3.54×10^{-02}	35	BBC3, CASP1, CCL26, CD70, CD83, CHIT1, COLEC12, DDX58, DLX4, DUSP4, EPAS1, FGF2, HLA-A, ICAM1, IFI27, IFI35, IFIH1, IFIT1, IFIT2, IL18, IL23A, IRAK2, IRF7, ISG20, MAVS, NOS2, PMAIP1, RELB, SERPING1, STING1, THBS1, TNFRSF11B, TP73, TXNIP, VEGFA
Cell Cycle, Gene expression, Cellular Growth, and Proliferation	4.64×10^{-02}	18	ATF3, BRCA1, CCNG2, CLSPN, CPM, ETV6, FOS, FOXL2, FOXO3, GNRHR, HERC2, JUN, JUNB, MAFF, NODAL, RAF1, SMAD4, SOX4
Cellular Function and Maintenance	4.64×10^{-02}	4	AR, MAP2K6, MYOF, PGK1
Canonical Pathways for A2780CP20-RBPMSC			
Ingenuity Canonical Pathways	***log10 (p-Value)***	***Number of Genes***	***Genes***
Cardiovascular System Development and Function, Cell to Cell Signaling and Interaction, Cellular Movement	6.64×10^{-03}	2	CCN2, CLDN7
Organ Morphology, Reproductive System Development and Function, Tissue Development	4.56×10^{-02}	3	CAV1, EGFR, ITGA2
Antimicrobial Response, Cell Cycle and Survival	3.15×10^{-02}	2	BIRC3, PPKAR2B
Cancer, Cellular Movement, Organismal Injury and Abnormality	2.68×10^{-03}	2	BDNF, TUG1
Cell Morphology, Cell to Cell Signaling and Interaction, Cellular Development	2.68×10^{-03}	2	AKT1, TP63
Common *Canonical Pathways Between RBPMSA and RBPMSC*			
Ingenuity Canonical Pathways	***log10 (p-Value)***	***Number of Genes***	***Genes***
Cancer, Cardiovascular Disease Hematological System Development and Function	4.67×10^{-03}	2	CLDN7, F3
Cell to Cell Signaling and Interaction, Cellular Development, Cellular growth, and Proliferation	4.38×10^{-03}	2	FOS, MECOM
Cancer, Cellular Movement, Organismal Injury and Abnormality	3.44×10^{-02}	2	BDNF, TUG1
Cell Death and Survival, Molecular Transport, Protein Trafficking	2.82×10^{-02}	2	ANKRD1, DDIT3
Cancer, Cell to Cell Signaling and Interaction, Dermatological Disease and Conditions	1.73×10^{-03}	2	LRP1, PTPRR

Appendix E

Proteins identified by IP/MS assay in A2780CP20-RBPMSA

Gene Symbol	Ensembl Gene ID	Description
ACTB	ENSG00000075624	Actin, cytoplasmic 1 [OS=Homo sapiens]
HSPA8	ENSG00000109971	Heat shock cognate 71 kDa protein [OS=Homo sapiens]
HSPA1B	ENSG00000204388;	Heat shock 70 kDa protein 1B [OS=Homo sapiens]
ALDOA	ENSG00000149925	Fructose-bisphosphate aldolase A [OS=Homo sapiens]
MDH2	ENSG00000146701	Malate dehydrogenase, mitochondrial [OS=Homo sapiens]
TPI1	ENSG00000111669	Triosephosphate isomerase [OS=Homo sapiens]
GAPDH	ENSG00000111640	Glyceraldehyde-3-phosphate dehydrogenase [OS=Homo sapiens]
ENO1	ENSG00000074800	Alpha-enolase [OS=Homo sapiens]
YWHAZ	ENSG00000164924	14-3-3 protein zeta/delta [OS=Homo sapiens]
PRDX2	ENSG00000167815	Peroxiredoxin-2 [OS=Homo sapiens]
EEF1A1	ENSG00000156508	Elongation factor 1-alpha 1 [OS=Homo sapiens]
HSPD1	ENSG00000144381	60 kDa heat shock protein, mitochondrial [OS=Homo sapiens]
TKT	ENSG00000163931	Transketolase [OS=Homo sapiens]
HSPA5	ENSG00000044574	Endoplasmic reticulum chaperone BiP [OS=Homo sapiens]
RBPMS	ENSG00000157110	RNA-binding protein with multiple splicing [OS=Homo sapiens]
PRDX1	ENSG00000117450	Peroxiredoxin-1 [OS=Homo sapiens]
PKM	ENSG00000067225	Pyruvate kinase PKM [OS=Homo sapiens]
PGAM1	ENSG00000171314	Phosphoglycerate mutase 1 [OS=Homo sapiens]
ASS1	ENSG00000130707	Argininosuccinate synthase [OS=Homo sapiens]
FBP1	ENSG00000165140	Fructose-1,6-bisphosphatase 1 [OS=Homo sapiens]
HSPA9	ENSG00000113013	Stress-70 protein, mitochondrial [OS=Homo sapiens]
PPIB	ENSG00000166794	Peptidyl-prolyl cis-trans isomerase B [OS=Homo sapiens]
ANXA2	ENSG00000182718	Annexin A2 [OS=Homo sapiens]
P4HB	ENSG00000185624	Protein disulfide-isomerase [OS=Homo sapiens]
PDIA4	ENSG00000155660	Protein disulfide-isomerase A4 [OS=Homo sapiens]
RPSA	ENSG00000168028	40S ribosomal protein SA [OS=Homo sapiens]
NCL	ENSG00000115053	Nucleolin [OS=Homo sapiens]
PDIA6	ENSG00000143870	Protein disulfide-isomerase A6 [OS=Homo sapiens]
NME1	ENSG00000239672	Nucleoside diphosphate kinase A [OS=Homo sapiens]
HRNR	ENSG00000197915	Hornerin [OS=Homo sapiens]
HMGB1	ENSG00000189403	High mobility group protein B1 [OS=Homo sapiens]
IGKV2-29	ENSG00000075624	Immunoglobulin kappa variable 2-29 [OS=Homo sapiens]
MYH9	ENSG00000100345	Myosin-9 [OS=Homo sapiens]
GAPDH	ENSG00000111640	Glyceraldehyde-3-phosphate dehydrogenase [OS=Homo sapiens]
ALDOA	ENSG00000149925	Fructose-bisphosphate aldolase A [OS=Homo sapiens]

Proteins identified by IP/MS assay in A2780CP20-RBPMSC

Gene Symbol	Ensembl Gene ID	Description
ACTB	ENSG00000075624	Actin, cytoplasmic 1 [OS=Homo sapiens]
HSPA8	ENSG00000109971	Heat shock cognate 71 kDa protein [OS=Homo sapiens]
HSPA1B	ENSG00000204388;	Heat shock 70 kDa protein 1B [OS=Homo sapiens]
ALDOA	ENSG00000149925	Fructose-bisphosphate aldolase A [OS=Homo sapiens]
TPI1	ENSG00000111669	Triosephosphate isomerase [OS=Homo sapiens]
GAPDH	ENSG00000111640	Glyceraldehyde-3-phosphate dehydrogenase [OS=Homo sapiens]
MDH2	ENSG00000146701	Malate dehydrogenase, mitochondrial [OS=Homo sapiens]
ENO1	ENSG00000074800	Alpha-enolase [OS=Homo sapiens]
HSPD1	ENSG00000144381	60 kDa heat shock protein, mitochondrial [OS=Homo sapiens]
TKT	ENSG00000163931	Transketolase [OS=Homo sapiens]
PRDX2	ENSG00000167815	Peroxiredoxin-2 [OS=Homo sapiens]
NME1	ENSG00000239672	Nucleoside diphosphate kinase A [OS=Homo sapiens]
EEF1A2	ENSG00000101210	Elongation factor 1-alpha 2 [OS=Homo sapiens]
PGAM1	ENSG00000171314	Phosphoglycerate mutase 1 [OS=Homo sapiens]
PKM	ENSG00000067225	Pyruvate kinase PKM [OS=Homo sapiens]
HSPA5	ENSG00000044574	Endoplasmic reticulum chaperone BiP [OS=Homo sapiens]
YWHAZ	ENSG00000164924	14-3-3 protein zeta/delta [OS=Homo sapiens]
ACTN1	ENSG00000072110	Alpha-actinin-1 [OS=Homo sapiens]
NCL	ENSG00000115053	Nucleolin [OS=Homo sapiens]
EFHD2	ENSG00000142634	EF-hand domain-containing protein D2 [OS=Homo sapiens]
GANAB	ENSG00000089597	Neutral alpha-glucosidase AB [OS=Homo sapiens]
CFL1	ENSG00000172757	Cofilin-1 [OS=Homo sapiens]
HRNR	ENSG00000197915	Hornerin [OS=Homo sapiens]
CALR	ENSG00000179218	Calreticulin [OS=Homo sapiens]
ACTA1	ENSG00000143632	Actin, alpha skeletal muscle [OS=Homo sapiens]
MYH9	ENSG00000100345	Myosin-9 [OS=Homo sapiens]
IGKV2-40	ENSG00000273962	Immunoglobulin kappa variable 2-40 [OS=Homo sapiens]
MYH10	ENSG00000133026	Myosin-10 [OS=Homo sapiens]

Proteins identified by IP/MS assay in A2780CP20-RBPMS-EV

Gene Symbol	Ensembl Gene ID	Description
ACTB	ENSG00000075624	Actin, cytoplasmic 1 [OS=Homo sapiens]
ACTA1	ENSG00000143632	Actin, alpha skeletal muscle [OS=Homo sapiens]
HSPA1B	ENSG00000204388;	Heat shock 70 kDa protein 1B [OS=Homo sapiens]
HSPA8	ENSG00000109971	Heat shock cognate 71 kDa protein [OS=Homo sapiens]
ENO1	ENSG00000074800	Alpha-enolase [OS=Homo sapiens]
MDH2	ENSG00000146701	Malate dehydrogenase, mitochondrial [OS=Homo sapiens]
ALDOA	ENSG00000149925	Fructose-bisphosphate aldolase A [OS=Homo sapiens]
TPI1	ENSG00000111669	Triosephosphate isomerase [OS=Homo sapiens]
GAPDH	ENSG00000111640	Glyceraldehyde-3-phosphate dehydrogenase [OS=Homo sapiens]
HSPD1	ENSG00000144381	60 kDa heat shock protein, mitochondrial [OS=Homo sapiens]
PKM	ENSG00000067225	Pyruvate kinase PKM [OS=Homo sapiens]
TKT	ENSG00000163931	Transketolase [OS=Homo sapiens]
EEF1A1	ENSG00000156508	Elongation factor 1-alpha 1 [OS=Homo sapiens]
ACTN4	ENSG00000130402; ENSG00000282844	Alpha-actinin-4 [OS=Homo sapiens]
HSPA5	ENSG00000044574	Endoplasmic reticulum chaperone BiP [OS=Homo sapiens]
EEF1A2	ENSG00000101210	Elongation factor 1-alpha 2 [OS=Homo sapiens]
YWHAZ	ENSG00000164924	14-3-3 protein zeta/delta [OS=Homo sapiens]
PRDX2	ENSG00000167815	Peroxiredoxin-2 [OS=Homo sapiens]
ASS1	ENSG00000130707	Argininosuccinate synthase [OS=Homo sapiens]
ACTN1	ENSG00000072110	Alpha-actinin-1 [OS=Homo sapiens]
ATP5F1B	ENSG00000110955	ATP synthase subunit beta, mitochondrial [OS=Homo sapiens]
HSPA9	ENSG00000113013	Stress-70 protein, mitochondrial [OS=Homo sapiens]
NCL	ENSG00000115053	Nucleolin [OS=Homo sapiens]
RPSA	ENSG00000168028	40S ribosomal protein SA [OS=Homo sapiens]
HMGB1	ENSG00000189403	High mobility group protein B1 [OS=Homo sapiens]
FBP1	ENSG00000165140	Fructose-1,6-bisphosphatase 1 [OS=Homo sapiens]
PRDX1	ENSG00000117450	Peroxiredoxin-1 [OS=Homo sapiens]
PDIA6	ENSG00000143870	Protein disulfide-isomerase A6 [OS=Homo sapiens]
ANXA2	ENSG00000182718	Annexin A2 [OS=Homo sapiens]
PGK1	ENSG00000102144	Phosphoglycerate kinase 1 [OS=Homo sapiens]
NME2	ENSG00000243678	Nucleoside diphosphate kinase B [OS=Homo sapiens]
PGAM1	ENSG00000171314	Phosphoglycerate mutase 1 [OS=Homo sapiens]
HNRNPA2B1	ENSG00000122566	Heterogeneous nuclear ribonucleoproteins A2/B1 [OS=Homo sapiens]
PPIB	ENSG00000166794	Peptidyl-prolyl cis-trans isomerase B [OS=Homo sapiens]
CFL1	ENSG00000172757	Cofilin-1 [OS=Homo sapiens]
PDIA4	ENSG00000155660	Protein disulfide-isomerase A4 [OS=Homo sapiens]
PFN1	ENSG00000108518	Profilin-1 [OS=Homo sapiens]
P4HB	ENSG00000185624	Protein disulfide-isomerase [OS=Homo sapiens]
GANAB	ENSG00000089597	Neutral alpha-glucosidase AB [OS=Homo sapiens]
AHCY	ENSG00000101444	Adenosylhomocysteinase [OS=Homo sapiens]

LCP1	ENSG00000136167	Plastin-2 [OS=Homo sapiens]
NPM1	ENSG00000181163	Nucleophosmin [OS=Homo sapiens]
PLS3	ENSG00000102024	Plastin-3 [OS=Homo sapiens]
PEBP1	ENSG00000089220	Phosphatidylethanolamine-binding protein 1 [OS=Homo sapiens]
ECHS1	ENSG00000127884	Enoyl-CoA hydratase, mitochondrial [OS=Homo sapiens]
SFPQ	ENSG00000116560	Splicing factor, proline- and glutamine-rich [OS=Homo sapiens]
PAICS	ENSG00000128050	Multifunctional protein ADE2 [OS=Homo sapiens]
HRNR	ENSG00000197915	Hornerin [OS=Homo sapiens]
ANXA5	ENSG00000164111	Annexin A5 [OS=Homo sapiens]
EFHD2	ENSG00000142634	EF-hand domain-containing protein D2 [OS=Homo sapiens]
LDHA	ENSG00000134333; ENSG00000288299	L-lactate dehydrogenase A chain [OS=Homo sapiens]
PLS1	ENSG00000120756	Plastin-1 [OS=Homo sapiens]
TALDO1	ENSG00000177156	Transaldolase [OS=Homo sapiens]
PDIA3	ENSG00000167004	Protein disulfide-isomerase A3 [OS=Homo sapiens]
DLD	ENSG00000091140	Dihydrolipoyl dehydrogenase, mitochondrial [OS=Homo sapiens]
EIF5A	ENSG00000132507; ENSG00000288145	Eukaryotic translation initiation factor 5A-1 [OS=Homo sapiens]
IMPDH2	ENSG00000178035	Inosine-5'-monophosphate dehydrogenase 2 [OS=Homo sapiens]
EEF2	ENSG00000167658	Elongation factor 2 [OS=Homo sapiens]
BLVRB	ENSG00000090013	Flavin reductase (NADPH) [OS=Homo sapiens]
GOT2	ENSG00000125166	Aspartate aminotransferase, mitochondrial [OS=Homo sapiens]
PA2G4	ENSG00000170515	Proliferation-associated protein 2G4 [OS=Homo sapiens]
PRDX6	ENSG00000117592	Peroxiredoxin-6 [OS=Homo sapiens]
CALR	ENSG00000179218	Calreticulin [OS=Homo sapiens]
FLNA	ENSG00000196924	Filamin-A [OS=Homo sapiens]
ACTB	ENSG00000075624	Actin, cytoplasmic 1 [OS=Homo sapiens]
ACTA1	ENSG00000143632	Actin, alpha skeletal muscle [OS=Homo sapiens]
HSPA1B	ENSG00000204388;	Heat shock 70 kDa protein 1B [OS=Homo sapiens]
HSPA8	ENSG00000109971	Heat shock cognate 71 kDa protein [OS=Homo sapiens]
ENO1	ENSG00000074800	Alpha-enolase [OS=Homo sapiens]
MDH2	ENSG00000146701	Malate dehydrogenase, mitochondrial [OS=Homo sapiens]
ALDOA	ENSG00000149925	Fructose-bisphosphate aldolase A [OS=Homo sapiens]
TPI1	ENSG00000111669	Triosephosphate isomerase [OS=Homo sapiens]
GAPDH	ENSG00000111640	Glyceraldehyde-3-phosphate dehydrogenase [OS=Homo sapiens]
HSPD1	ENSG00000144381	60 kDa heat shock protein, mitochondrial [OS=Homo sapiens]
PKM	ENSG00000067225	Pyruvate kinase PKM [OS=Homo sapiens]
TKT	ENSG00000163931	Transketolase [OS=Homo sapiens]
EEF1A1	ENSG00000156508	Elongation factor 1-alpha 1 [OS=Homo sapiens]
ACTN4	ENSG00000130402; ENSG00000282844	Alpha-actinin-4 [OS=Homo sapiens]

HSPA5	ENSG00000044574	Endoplasmic reticulum chaperone BiP [OS=Homo sapiens]
EEF1A2	ENSG00000101210	Elongation factor 1-alpha 2 [OS=Homo sapiens]
YWHAZ	ENSG00000164924	14-3-3 protein zeta/delta [OS=Homo sapiens]
PRDX2	ENSG00000167815	Peroxiredoxin-2 [OS=Homo sapiens]
ASS1	ENSG00000130707	Argininosuccinate synthase [OS=Homo sapiens]
ACTN1	ENSG00000072110	Alpha-actinin-1 [OS=Homo sapiens]
ATP5F1B	ENSG00000110955	ATP synthase subunit beta, mitochondrial [OS=Homo sapiens]
HSPA9	ENSG00000113013	Stress-70 protein, mitochondrial [OS=Homo sapiens]
NCL	ENSG00000115053	Nucleolin [OS=Homo sapiens]
RPSA	ENSG00000168028	40S ribosomal protein SA [OS=Homo sapiens]
HMGB1	ENSG00000189403	High mobility group protein B1 [OS=Homo sapiens]
FBP1	ENSG00000165140	Fructose-1,6-bisphosphatase 1 [OS=Homo sapiens]
PRDX1	ENSG00000117450	Peroxiredoxin-1 [OS=Homo sapiens]
PDIA6	ENSG00000143870	Protein disulfide-isomerase A6 [OS=Homo sapiens]
ANXA2	ENSG00000182718	Annexin A2 [OS=Homo sapiens]
PGK1	ENSG00000102144	Phosphoglycerate kinase 1 [OS=Homo sapiens]
NME2	ENSG00000243678	Nucleoside diphosphate kinase B [OS=Homo sapiens]
PGAM1	ENSG00000171314	Phosphoglycerate mutase 1 [OS=Homo sapiens]
HNRNPA2B1	ENSG00000122566	Heterogeneous nuclear ribonucleoproteins A2/B1 [OS=Homo sapiens]
PPIB	ENSG00000166794	Peptidyl-prolyl cis-trans isomerase B [OS=Homo sapiens]
CFL1	ENSG00000172757	Cofilin-1 [OS=Homo sapiens]
PDIA4	ENSG00000155660	Protein disulfide-isomerase A4 [OS=Homo sapiens]
PFN1	ENSG00000108518	Profilin-1 [OS=Homo sapiens]
P4HB	ENSG00000185624	Protein disulfide-isomerase [OS=Homo sapiens]
GANAB	ENSG00000089597	Neutral alpha-glucosidase AB [OS=Homo sapiens]
AHCY	ENSG00000101444	Adenosylhomocysteinase [OS=Homo sapiens]
LCP1	ENSG00000136167	Plastin-2 [OS=Homo sapiens]
NPM1	ENSG00000181163	Nucleophosmin [OS=Homo sapiens]
PLS3	ENSG00000102024	Plastin-3 [OS=Homo sapiens]
PEBP1	ENSG00000089220	Phosphatidylethanolamine-binding protein 1 [OS=Homo sapiens]
ECHS1	ENSG00000127884	Enoyl-CoA hydratase, mitochondrial [OS=Homo sapiens]
SFPQ	ENSG00000116560	Splicing factor, proline- and glutamine-rich [OS=Homo sapiens]
PAICS	ENSG00000128050	Multifunctional protein ADE2 [OS=Homo sapiens]
HRNR	ENSG00000197915	Hornerin [OS=Homo sapiens]
ANXA5	ENSG00000164111	Annexin A5 [OS=Homo sapiens]
EFHD2	ENSG00000142634	EF-hand domain-containing protein D2 [OS=Homo sapiens]
LDHA	ENSG00000134333	L-lactate dehydrogenase A chain [OS=Homo sapiens]
PLS1	ENSG00000120756	Plastin-1 [OS=Homo sapiens]
TALDO1	ENSG00000177156	Transaldolase [OS=Homo sapiens]
PDIA3	ENSG00000167004	Protein disulfide-isomerase A3 [OS=Homo sapiens]
DLD	ENSG00000091140	Dihydrolipoyl dehydrogenase, mitochondrial [OS=Homo sapiens]
EIF5A	ENSG00000132507; ENSG00000288145	Eukaryotic translation initiation factor 5A-1 [OS=Homo sapiens]
IMPDH2	ENSG00000178035	Inosine-5'-monophosphate dehydrogenase 2 [OS=Homo sapiens]

EEF2	ENSG00000167658	Elongation factor 2 [OS=Homo sapiens]
BLVRB	ENSG00000090013	Flavin reductase (NADPH) [OS=Homo sapiens]
GOT2	ENSG00000125166	Aspartate aminotransferase, mitochondrial [OS=Homo sapiens]
PA2G4	ENSG00000170515	Proliferation-associated protein 2G4 [OS=Homo sapiens]
PRDX6	ENSG00000117592	Peroxiredoxin-6 [OS=Homo sapiens]
CALR	ENSG00000179218	Calreticulin [OS=Homo sapiens]
FLNA	ENSG00000196924	Filamin-A [OS=Homo sapiens]
ACTA2	ENSG00000107796	Actin, aortic smooth muscle [OS=Homo sapiens]
MYH4	ENSG00000264424	Myosin-4 [OS=Homo sapiens]
MYH1	ENSG00000109061	Myosin-1 [OS=Homo sapiens]
IGKV2-40	ENSG00000273962	Immunoglobulin kappa variable 2-40 [OS=Homo sapiens]
MYH6	ENSG00000197616	Myosin-6 [OS=Homo sapiens]

Appendix F

Appendix G

References

1. Torre, L.A., et al., *Global Cancer Incidence and Mortality Rates and Trends--An Update.* Cancer Epidemiol Biomarkers Prev, 2016. **25**(1): p. 16-27.
2. Siegel, R.L., et al., *Cancer statistics, 2022.* CA Cancer J Clin, 2022. **72**(1): p. 7-33.
3. Dutta, D.K. and I. Dutta, *Origin of ovarian cancer: molecular profiling.* J Obstet Gynaecol India, 2013. **63**(3): p. 152-7.
4. Kurman, R.J. and M. Shih Ie, *The Dualistic Model of Ovarian Carcinogenesis: Revisited, Revised, and Expanded.* Am J Pathol, 2016. **186**(4): p. 733-47.
5. Prat, J., *Ovarian carcinomas: five distinct diseases with different origins, genetic alterations, and clinicopathological features.* Virchows Arch, 2012. **460**(3): p. 237-49.
6. van der Burg, M.E., *Advanced ovarian cancer.* Curr Treat Options Oncol, 2001. **2**(2): p. 109-18.
7. Jemal, A., et al., *Global cancer statistics.* CA Cancer J Clin, 2011. **61**(2): p. 69-90.
8. team, T.A.C.S.m.a.e.c., *Cancer Facts & Figures 2022.* American Cancer Society , 2022.
9. Matulonis, U.A., et al., *Ovarian cancer.* Nat Rev Dis Primers, 2016. **2**: p. 16061.
10. Torre, L.A., et al., *Ovarian cancer statistics, 2018.* CA Cancer J Clin, 2018. **68**(4): p. 284-296.
11. Institute, N.c., *SEER statistics fact sheets: ovarian cancer.* 2016.
12. Karst, A.M. and R. Drapkin, *Ovarian cancer pathogenesis: a model in evolution.* J Oncol, 2010. **2010**: p. 932371.
13. Pearce, C.L., et al., *Combined and interactive effects of environmental and GWAS-identified risk factors in ovarian cancer.* Cancer Epidemiol Biomarkers Prev, 2013. **22**(5): p. 880-90.
14. Oswald, A.J. and C. Gourley, *Low-grade epithelial ovarian cancer: a number of distinct clinical entities?* Curr Opin Oncol, 2015. **27**(5): p. 412-9.
15. Marchini, S., et al., *Analysis of gene expression in early-stage ovarian cancer.* Clin Cancer Res, 2008. **14**(23): p. 7850-60.
16. Hart, W.R. and H.J. Norris, *Borderline and malignant mucinous tumors of the ovary. Histologic criteria and clinical behavior.* Cancer, 1973. **31**(5): p. 1031-45.
17. Lack, E.E., R.H. Young, and R.E. Scully, *Pathology of ovarian neoplasms in childhood and adolescence.* Pathol Annu, 1992. **27 Pt 2**: p. 281-356.
18. Seidman, J.D., et al., *The histologic type and stage distribution of ovarian carcinomas of surface epithelial origin.* Int J Gynecol Pathol, 2004. **23**(1): p. 41-4.
19. Tonin, P.N., et al., *A review of histopathological subtypes of ovarian cancer in BRCA-related French Canadian cancer families.* Fam Cancer, 2007. **6**(4): p. 491-7.
20. Mok, S.C., et al., *Mutation of K-ras protooncogene in human ovarian epithelial tumors of borderline malignancy.* Cancer Res, 1993. **53**(7): p. 1489-92.
21. Schuijer, M. and E.M. Berns, *TP53 and ovarian cancer.* Hum Mutat, 2003. **21**(3): p. 285-91.
22. Olawaiye, A.B., et al., *Utility of pre-operative serum CA-125 in the management of uterine papillary serous carcinoma.* Gynecol Oncol, 2008. **110**(3): p. 293-8.
23. O'Brien, M.E., et al., *Clear cell epithelial ovarian cancer (mesonephroid): bad prognosis only in early stages.* Gynecol Oncol, 1993. **49**(2): p. 250-4.

24. Jenison, E.L., et al., *Clear cell adenocarcinoma of the ovary: a clinical analysis and comparison with serous carcinoma.* Gynecol Oncol, 1989. **32**(1): p. 65-71.
25. Kennedy, A.W., et al., *Survival probability in ovarian clear cell adenocarcinoma.* Gynecol Oncol, 1999. **74**(1): p. 108-14.
26. Ohkawa, K., et al., *Clear cell carcinoma of the ovary: light and electron microscopic studies.* Cancer, 1977. **40**(6): p. 3019-29.
27. Recio, F.O., et al., *Lack of improved survival plus increase in thromboembolic complications in patients with clear cell carcinoma of the ovary treated with platinum versus nonplatinum-based chemotherapy.* Cancer, 1996. **78**(10): p. 2157-63.
28. Zorn, K.K., et al., *Gene expression profiles of serous, endometrioid, and clear cell subtypes of ovarian and endometrial cancer.* Clin Cancer Res, 2005. **11**(18): p. 6422-30.
29. Fadare, O., et al., *Precursors of endometrial clear cell carcinoma.* Am J Surg Pathol, 2006. **30**(12): p. 1519-30.
30. Creasman, W.T., et al., *Prognosis of papillary serous, clear cell, and grade 3 stage I carcinoma of the endometrium.* Gynecol Oncol, 2004. **95**(3): p. 593-6.
31. Jones, M.R., et al., *Genetic epidemiology of ovarian cancer and prospects for polygenic risk prediction.* Gynecol Oncol, 2017. **147**(3): p. 705-713.
32. Lauby-Secretan, B., et al., *Body Fatness and Cancer--Viewpoint of the IARC Working Group.* N Engl J Med, 2016. **375**(8): p. 794-8.
33. Frezza, M., et al., *Novel metals and metal complexes as platforms for cancer therapy.* Curr Pharm Des, 2010. **16**(16): p. 1813-25.
34. Rosenberg, B., et al., *Platinum compounds: a new class of potent antitumour agents.* Nature, 1969. **222**(5191): p. 385-6.
35. Kelland, L., *The resurgence of platinum-based cancer chemotherapy.* Nat Rev Cancer, 2007. **7**(8): p. 573-84.
36. Shen, Y., et al., *Mitochondrial localization of P-glycoprotein in the human breast cancer cell line MCF-7/ADM and its functional characterization.* Oncol Rep, 2012. **27**(5): p. 1535-40.
37. Lee, J., et al., *Biochemical characterization of the human copper transporter Ctr1.* J Biol Chem, 2002. **277**(6): p. 4380-7.
38. Holzer, A.K., G.H. Manorek, and S.B. Howell, *Contribution of the major copper influx transporter CTR1 to the cellular accumulation of cisplatin, carboplatin, and oxaliplatin.* Mol Pharmacol, 2006. **70**(4): p. 1390-4.
39. Dasari, S. and P.B. Tchounwou, *Cisplatin in cancer therapy: molecular mechanisms of action.* Eur J Pharmacol, 2014. **740**: p. 364-78.
40. Ober, M. and S.J. Lippard, *A 1,2-d(GpG) cisplatin intrastrand cross-link influences the rotational and translational setting of DNA in nucleosomes.* J Am Chem Soc, 2008. **130**(9): p. 2851-61.
41. Kunkel, T.A. and D.A. Erie, *DNA mismatch repair.* Annu Rev Biochem, 2005. **74**: p. 681-710.
42. Vitale, I., et al., *Mitotic catastrophe: a mechanism for avoiding genomic instability.* Nat Rev Mol Cell Biol, 2011. **12**(6): p. 385-92.
43. Damia, G., et al., *Cisplatinum and taxol induce different patterns of p53 phosphorylation.* Neoplasia, 2001. **3**(1): p. 10-6.
44. Galluzzi, L., et al., *Mitochondrial liaisons of p53.* Antioxid Redox Signal, 2011. **15**(6): p. 1691-714.

45. Yeh, P.Y., et al., *Increase of the resistance of human cervical carcinoma cells to cisplatin by inhibition of the MEK to ERK signaling pathway partly via enhancement of anticancer drug-induced NF kappa B activation.* Biochem Pharmacol, 2002. **63**(8): p. 1423-30.
46. Wang, J., et al., *Caspase-mediated cleavage of ATM during cisplatin-induced tubular cell apoptosis: inactivation of its kinase activity toward p53.* Am J Physiol Renal Physiol, 2006. **291**(6): p. F1300-7.
47. Pabla, N., et al., *ATR-Chk2 signaling in p53 activation and DNA damage response during cisplatin-induced apoptosis.* J Biol Chem, 2008. **283**(10): p. 6572-83.
48. Meads, M.B., R.A. Gatenby, and W.S. Dalton, *Environment-mediated drug resistance: a major contributor to minimal residual disease.* Nat Rev Cancer, 2009. **9**(9): p. 665-74.
49. Lippert, T.H., H.J. Ruoff, and M. Volm, *Current status of methods to assess cancer drug resistance.* Int J Med Sci, 2011. **8**(3): p. 245-53.
50. O'Connor, D., et al., *Infection-related mortality in children with acute lymphoblastic leukemia: an analysis of infectious deaths on UKALL2003.* Blood, 2014. **124**(7): p. 1056-61.
51. Dingemans, A.M., H.M. Pinedo, and G. Giaccone, *Clinical resistance to topoisomerase-targeted drugs.* Biochim Biophys Acta, 1998. **1400**(1-3): p. 275-88.
52. Ellis, L.M. and D.J. Hicklin, *Resistance to Targeted Therapies: Refining Anticancer Therapy in the Era of Molecular Oncology.* Clin Cancer Res, 2009. **15**(24): p. 7471-7478.
53. Mansoori, B., et al., *The Different Mechanisms of Cancer Drug Resistance: A Brief Review.* Adv Pharm Bull, 2017. **7**(3): p. 339-348.
54. Kumar, M.S., et al., *The GATA2 transcriptional network is requisite for RAS oncogene-driven non-small cell lung cancer.* Cell, 2012. **149**(3): p. 642-55.
55. Rosell, R., et al., *Screening for epidermal growth factor receptor mutations in lung cancer.* N Engl J Med, 2009. **361**(10): p. 958-67.
56. Yun, C.H., et al., *The T790M mutation in EGFR kinase causes drug resistance by increasing the affinity for ATP.* Proc Natl Acad Sci U S A, 2008. **105**(6): p. 2070-5.
57. Sasaki, T., et al., *A novel ALK secondary mutation and EGFR signaling cause resistance to ALK kinase inhibitors.* Cancer Res, 2011. **71**(18): p. 6051-60.
58. Engelman, J.A., et al., *MET amplification leads to gefitinib resistance in lung cancer by activating ERBB3 signaling.* Science, 2007. **316**(5827): p. 1039-43.
59. Sos, M.L., et al., *PTEN loss contributes to erlotinib resistance in EGFR-mutant lung cancer by activation of Akt and EGFR.* Cancer Res, 2009. **69**(8): p. 3256-61.
60. Chang, J.H., et al., *The impact of a multidisciplinary breast cancer center on recommendations for patient management: the University of Pennsylvania experience.* Cancer, 2001. **91**(7): p. 1231-7.
61. Szakacs, G., et al., *Predicting drug sensitivity and resistance: profiling ABC transporter genes in cancer cells.* Cancer Cell, 2004. **6**(2): p. 129-37.
62. Gottesman, M.M., T. Fojo, and S.E. Bates, *Multidrug resistance in cancer: role of ATP-dependent transporters.* Nat Rev Cancer, 2002. **2**(1): p. 48-58.
63. Longley, D.B. and P.G. Johnston, *Molecular mechanisms of drug resistance.* J Pathol, 2005. **205**(2): p. 275-92.
64. Dean, M., A. Rzhetsky, and R. Allikmets, *The human ATP-binding cassette (ABC) transporter superfamily.* Genome Res, 2001. **11**(7): p. 1156-66.
65. Yu, T., et al., *MetaLnc9 Facilitates Lung Cancer Metastasis via a PGK1-Activated AKT/mTOR Pathway.* Cancer Res, 2017. **77**(21): p. 5782-5794.

66. Goldsmith, D.F., R.P. Ruble, and C.O. Klein, *Comparative cancer potency for silica from extrapolations of human and animal findings.* Scand J Work Environ Health, 1995. **21 Suppl 2**: p. 104-7.
67. Seelig, A., *P-Glycoprotein: One Mechanism, Many Tasks and the Consequences for Pharmacotherapy of Cancers.* Front Oncol, 2020. **10**: p. 576559.
68. Man, R.J., et al., *A patent review of RAF kinase inhibitors (2010-2018).* Expert Opin Ther Pat, 2019. **29**(9): p. 675-688.
69. Schinkel, A.H., *P-Glycoprotein, a gatekeeper in the blood-brain barrier.* Adv Drug Deliv Rev, 1999. **36**(2-3): p. 179-194.
70. Ferreira, L.M. and M.A. Mostajo-Radji, *How induced pluripotent stem cells are redefining personalized medicine.* Gene, 2013. **520**(1): p. 1-6.
71. Kuhn, E., R.J. Kurman, and I.M. Shih, *Ovarian Cancer Is an Imported Disease: Fact or Fiction?* Curr Obstet Gynecol Rep, 2012. **1**(1): p. 1-9.
72. Kuhn, E., et al., *Ovarian Brenner tumour: a morphologic and immunohistochemical analysis suggesting an origin from fallopian tube epithelium.* Eur J Cancer, 2013. **49**(18): p. 3839-49.
73. Domcke, S., et al., *Evaluating cell lines as tumour models by comparison of genomic profiles.* Nat Commun, 2013. **4**: p. 2126.
74. Indraccolo, S., et al., *Establishment and characterization of xenografts and cancer cell cultures derived from BRCA1 -/- epithelial ovarian cancers.* Eur J Cancer, 2006. **42**(10): p. 1475-83.
75. Barretina, J., et al., *The Cancer Cell Line Encyclopedia enables predictive modelling of anticancer drug sensitivity.* Nature, 2012. **483**(7391): p. 603-7.
76. Abaan, O.D., et al., *The exomes of the NCI-60 panel: a genomic resource for cancer biology and systems pharmacology.* Cancer Res, 2013. **73**(14): p. 4372-82.
77. Shepherd, T.G., et al., *Primary culture of ovarian surface epithelial cells and ascites-derived ovarian cancer cells from patients.* Nat Protoc, 2006. **1**(6): p. 2643-9.
78. Theriault, B.L., et al., *Establishment of primary cultures from ovarian tumor tissue and ascites fluid.* Methods Mol Biol, 2013. **1049**: p. 323-36.
79. Barua, A., et al., *Histopathology of ovarian tumors in laying hens: a preclinical model of human ovarian cancer.* Int J Gynecol Cancer, 2009. **19**(4): p. 531-9.
80. Tillmann, T., K. Kamino, and U. Mohr, *Incidence and spectrum of spontaneous neoplasms in male and female CBA/J mice.* Exp Toxicol Pathol, 2000. **52**(3): p. 221-5.
81. Cooper, T.K. and K.L. Gabrielson, *Spontaneous lesions in the reproductive tract and mammary gland of female non-human primates.* Birth Defects Res B Dev Reprod Toxicol, 2007. **80**(2): p. 149-70.
82. Walsh, K.M. and J. Poteracki, *Spontaneous neoplasms in control Wistar rats.* Fundam Appl Toxicol, 1994. **22**(1): p. 65-72.
83. Perets, R., et al., *Transformation of the fallopian tube secretory epithelium leads to high-grade serous ovarian cancer in Brca;Tp53;Pten models.* Cancer Cell, 2013. **24**(6): p. 751-65.
84. Sherman-Baust, C.A., et al., *A genetically engineered ovarian cancer mouse model based on fallopian tube transformation mimics human high-grade serous carcinoma development.* J Pathol, 2014. **233**(3): p. 228-37.
85. Kim, J., et al., *High-grade serous ovarian cancer arises from fallopian tube in a mouse model.* Proc Natl Acad Sci U S A, 2012. **109**(10): p. 3921-6.

86. Kuhn, E., et al., *Current preclinical models of ovarian cancer.* J Carcinog Mutagen, 2015. **6**(2): p. 220.
87. Connolly, D.C. and H.H. Hensley, *Xenograft and Transgenic Mouse Models of Epithelial Ovarian Cancer and Non Invasive Imaging Modalities to Monitor Ovarian Tumor Growth In situ -Applications in Evaluating Novel Therapeutic Agents.* Curr Protoc Pharmacol, 2009. **45**: p. 14 12 1-14 12 26.
88. Fu, X. and R.M. Hoffman, *Human ovarian carcinoma metastatic models constructed in nude mice by orthotopic transplantation of histologically-intact patient specimens.* Anticancer Res, 1993. **13**(2): p. 283-6.
89. Verschraegen, C.F., et al., *Establishment and characterization of cancer cell cultures and xenografts derived from primary or metastatic Mullerian cancers.* Clin Cancer Res, 2003. **9**(2): p. 845-52.
90. Burger, R.A., et al., *Phase II trial of bevacizumab in persistent or recurrent epithelial ovarian cancer or primary peritoneal cancer: a Gynecologic Oncology Group Study.* J Clin Oncol, 2007. **25**(33): p. 5165-71.
91. Shaw, T.J., et al., *Characterization of intraperitoneal, orthotopic, and metastatic xenograft models of human ovarian cancer.* Mol Ther, 2004. **10**(6): p. 1032-42.
92. Chen, K., Y.H. Huang, and J.L. Chen, *Understanding and targeting cancer stem cells: therapeutic implications and challenges.* Acta Pharmacol Sin, 2013. **34**(6): p. 732-40.
93. Garcia, A.A., et al., *Phase II clinical trial of bevacizumab and low-dose metronomic oral cyclophosphamide in recurrent ovarian cancer: a trial of the California, Chicago, and Princess Margaret Hospital phase II consortia.* J Clin Oncol, 2008. **26**(1): p. 76-82.
94. Hirte, H., et al., *A phase 2 study of cediranib in recurrent or persistent ovarian, peritoneal or fallopian tube cancer: a trial of the Princess Margaret, Chicago and California Phase II Consortia.* Gynecol Oncol, 2015. **138**(1): p. 55-61.
95. Matulonis, U.A., et al., *Cediranib, an oral inhibitor of vascular endothelial growth factor receptor kinases, is an active drug in recurrent epithelial ovarian, fallopian tube, and peritoneal cancer.* J Clin Oncol, 2009. **27**(33): p. 5601-6.
96. Ciardiello, F., *Epidermal growth factor receptor inhibitors in cancer treatment.* Future Oncol, 2005. **1**(2): p. 221-34.
97. Salomon, D.S., et al., *Epidermal growth factor-related peptides and their receptors in human malignancies.* Crit Rev Oncol Hematol, 1995. **19**(3): p. 183-232.
98. Gordon, A.N., et al., *Efficacy and safety of erlotinib HCl, an epidermal growth factor receptor (HER1/EGFR) tyrosine kinase inhibitor, in patients with advanced ovarian carcinoma: results from a phase II multicenter study.* Int J Gynecol Cancer, 2005. **15**(5): p. 785-92.
99. Schilder, R.J., et al., *Phase II study of gefitinib in patients with relapsed or persistent ovarian or primary peritoneal carcinoma and evaluation of epidermal growth factor receptor mutations and immunohistochemical expression: a Gynecologic Oncology Group Study.* Clin Cancer Res, 2005. **11**(15): p. 5539-48.
100. Konner, J., et al., *A phase II study of cetuximab/paclitaxel/carboplatin for the initial treatment of advanced-stage ovarian, primary peritoneal, or fallopian tube cancer.* Gynecol Oncol, 2008. **110**(2): p. 140-5.
101. McPhillips, F., et al., *Raf-1 is the predominant Raf isoform that mediates growth factor-stimulated growth in ovarian cancer cells.* Carcinogenesis, 2006. **27**(4): p. 729-39.

102. Han, E.S., P. Lin, and M. Wakabayashi, *Current status on biologic therapies in the treatment of epithelial ovarian cancer.* Curr Treat Options Oncol, 2009. **10**(1-2): p. 54-66.
103. Altomare, D.A., et al., *AKT and mTOR phosphorylation is frequently detected in ovarian cancer and can be targeted to disrupt ovarian tumor cell growth.* Oncogene, 2004. **23**(34): p. 5853-7.
104. Huang, S., et al., *Blockade of nuclear factor-kappaB signaling inhibits angiogenesis and tumorigenicity of human ovarian cancer cells by suppressing expression of vascular endothelial growth factor and interleukin 8.* Cancer Res, 2000. **60**(19): p. 5334-9.
105. Mabuchi, S., et al., *Inhibition of inhibitor of nuclear factor-kappaB phosphorylation increases the efficacy of paclitaxel in in vitro and in vivo ovarian cancer models.* Clin Cancer Res, 2004. **10**(22): p. 7645-54.
106. Liu, G.H., et al., *Inhibition of nuclear factor-kappaB by an antioxidant enhances paclitaxel sensitivity in ovarian carcinoma cell line.* Int J Gynecol Cancer, 2006. **16**(5): p. 1777-82.
107. Glisovic, T., et al., *RNA-binding proteins and post-transcriptional gene regulation.* FEBS Lett, 2008. **582**(14): p. 1977-86.
108. Hogan, D.J., et al., *Diverse RNA-binding proteins interact with functionally related sets of RNAs, suggesting an extensive regulatory system.* PLoS Biol, 2008. **6**(10): p. e255.
109. Pereira, B., M. Billaud, and R. Almeida, *RNA-Binding Proteins in Cancer: Old Players and New Actors.* Trends Cancer, 2017. **3**(7): p. 506-528.
110. Lee, M.H. and T. Schedl, *RNA-binding proteins.* WormBook, 2006: p. 1-13.
111. Stefl, R., L. Skrisovska, and F.H. Allain, *RNA sequence- and shape-dependent recognition by proteins in the ribonucleoprotein particle.* EMBO Rep, 2005. **6**(1): p. 33-8.
112. Hafner, M., et al., *Transcriptome-wide identification of RNA-binding protein and microRNA target sites by PAR-CLIP.* Cell, 2010. **141**(1): p. 129-41.
113. Jolma, A., et al., *Binding specificities of human RNA-binding proteins toward structured and linear RNA sequences.* Genome Res, 2020. **30**(7): p. 962-973.
114. Urnov, F.D., et al., *Genome editing with engineered zinc finger nucleases.* Nat Rev Genet, 2010. **11**(9): p. 636-46.
115. Nakashima, K., et al., *The novel zinc finger-containing transcription factor osterix is required for osteoblast differentiation and bone formation.* Cell, 2002. **108**(1): p. 17-29.
116. Burd, C.G. and G. Dreyfuss, *Conserved structures and diversity of functions of RNA-binding proteins.* Science, 1994. **265**(5172): p. 615-21.
117. Appasani, K., *RNA interference a technology platform for target validation, drug discovery and therapeutic development.* Drug Discovery World, 2003: p. 61-68.
118. Bandziulis, R.J., M.S. Swanson, and G. Dreyfuss, *RNA-binding proteins as developmental regulators.* Genes Dev, 1989. **3**(4): p. 431-7.
119. Wang, Z.L., et al., *Comprehensive Genomic Characterization of RNA-Binding Proteins across Human Cancers.* Cell Rep, 2018. **22**(1): p. 286-298.
120. Frisone, P., et al., *SAM68: Signal Transduction and RNA Metabolism in Human Cancer.* Biomed Res Int, 2015. **2015**: p. 528954.
121. Wang, J., et al., *Multiple functions of the RNA-binding protein HuR in cancer progression, treatment responses and prognosis.* Int J Mol Sci, 2013. **14**(5): p. 10015-41.

122. Qian, J., et al., *The RNA binding protein FXR1 is a new driver in the 3q26-29 amplicon and predicts poor prognosis in human cancers.* Proc Natl Acad Sci U S A, 2015. **112**(11): p. 3469-74.
123. Clower, C.V., et al., *The alternative splicing repressors hnRNP A1/A2 and PTB influence pyruvate kinase isoform expression and cell metabolism.* Proc Natl Acad Sci U S A, 2010. **107**(5): p. 1894-9.
124. David, C.J., et al., *HnRNP proteins controlled by c-Myc deregulate pyruvate kinase mRNA splicing in cancer.* Nature, 2010. **463**(7279): p. 364-8.
125. Kang, M.J., et al., *NF-kappaB activates transcription of the RNA-binding factor HuR, via PI3K-AKT signaling, to promote gastric tumorigenesis.* Gastroenterology, 2008. **135**(6): p. 2030-42, 2042 e1-3.
126. Larsen, J.E., et al., *ZEB1 drives epithelial-to-mesenchymal transition in lung cancer.* J Clin Invest, 2016. **126**(9): p. 3219-35.
127. Preca, B.T., et al., *A self-enforcing CD44s/ZEB1 feedback loop maintains EMT and stemness properties in cancer cells.* Int J Cancer, 2015. **137**(11): p. 2566-77.
128. Zhang, J., et al., *Mice deficient in Rbm38, a target of the p53 family, are susceptible to accelerated aging and spontaneous tumors.* Proc Natl Acad Sci U S A, 2014. **111**(52): p. 18637-42.
129. Shu, L., W. Yan, and X. Chen, *RNPC1, an RNA-binding protein and a target of the p53 family, is required for maintaining the stability of the basal and stress-induced p21 transcript.* Genes Dev, 2006. **20**(21): p. 2961-72.
130. Fu, J., et al., *The RNA-binding protein RBPMS1 represses AP-1 signaling and regulates breast cancer cell proliferation and migration.* Biochim Biophys Acta, 2015. **1853**(1): p. 1-13.
131. Wilmore, H.P., et al., *Expression profile of the RNA-binding protein gene hermes during chicken embryonic development.* Dev Dyn, 2005. **233**(3): p. 1045-51.
132. Kwong, J.M., J. Caprioli, and N. Piri, *RNA binding protein with multiple splicing: a new marker for retinal ganglion cells.* Invest Ophthalmol Vis Sci, 2010. **51**(2): p. 1052-8.
133. Farazi, T.A., et al., *Identification of the RNA recognition element of the RBPMS family of RNA-binding proteins and their transcriptome-wide mRNA targets.* RNA, 2014. **20**(7): p. 1090-102.
134. Gerber, W.V., et al., *A role for the RNA-binding protein, hermes, in the regulation of heart development.* Dev Biol, 2002. **247**(1): p. 116-26.
135. Rodriguez, A.R., L.P. de Sevilla Muller, and N.C. Brecha, *The RNA binding protein RBPMS is a selective marker of ganglion cells in the mammalian retina.* J Comp Neurol, 2014. **522**(6): p. 1411-43.
136. Rambout, X., et al., *The transcription factor ERG recruits CCR4-NOT to control mRNA decay and mitotic progression.* Nat Struct Mol Biol, 2016. **23**(7): p. 663-72.
137. Hornberg, H., et al., *RNA-binding protein Hermes/RBPMS inversely affects synapse density and axon arbor formation in retinal ganglion cells in vivo.* J Neurosci, 2013. **33**(25): p. 10384-95.
138. Notarnicola, C., et al., *The RNA-binding protein RBPMS2 regulates development of gastrointestinal smooth muscle.* Gastroenterology, 2012. **143**(3): p. 687-697 e9.
139. Hapkova, I., et al., *High expression of the RNA-binding protein RBPMS2 in gastrointestinal stromal tumors.* Exp Mol Pathol, 2013. **94**(2): p. 314-21.

140. Shimamoto, A., et al., *A unique human gene that spans over 230 kb in the human chromosome 8p11-12 and codes multiple family proteins sharing RNA-binding motifs.* Proc Natl Acad Sci U S A, 1996. **93**(20): p. 10913-7.
141. Maris, C., C. Dominguez, and F.H. Allain, *The RNA recognition motif, a plastic RNA-binding platform to regulate post-transcriptional gene expression.* FEBS J, 2005. **272**(9): p. 2118-31.
142. Teplova, M., et al., *Structural basis underlying CAC RNA recognition by the RRM domain of dimeric RNA-binding protein RBPMS.* Q Rev Biophys, 2016. **49**: p. e1.
143. Sagnol, S., et al., *Homodimerization of RBPMS2 through a new RRM-interaction motif is necessary to control smooth muscle plasticity.* Nucleic Acids Res, 2014. **42**(15): p. 10173-84.
144. Skawran, B., et al., *Loss of 13q is associated with genes involved in cell cycle and proliferation in dedifferentiated hepatocellular carcinoma.* Mod Pathol, 2008. **21**(12): p. 1479-89.
145. Zearfoss, N.R., et al., *Hermes is a localized factor regulating cleavage of vegetal blastomeres in Xenopus laevis.* Dev Biol, 2004. **267**(1): p. 60-71.
146. Zearfoss, N.R., et al., *Identification of new Xlsirt family members in the Xenopus laevis oocyte.* Mech Dev, 2003. **120**(4): p. 503-9.
147. Rabelo-Fernandez, R.J., et al., *Reduced RBPMS Levels Promote Cell Proliferation and Decrease Cisplatin Sensitivity in Ovarian Cancer Cells.* Int J Mol Sci, 2022. **23**(1).
148. Nakagaki-Silva, E.E., et al., *Identification of RBPMS as a mammalian smooth muscle master splicing regulator via proximity of its gene with super-enhancers.* Elife, 2019. **8**.
149. Shanmugaapriya, S., et al., *Expression of TGF-beta Signaling Regulator RBPMS (RNA-Binding Protein With Multiple Splicing) Is Regulated by IL-1beta and TGF-beta Superfamily Members, and Decreased in Aged and Osteoarthritic Cartilage.* Cartilage, 2016. **7**(4): p. 333-45.
150. Aguero, T., et al., *Hermes (Rbpms) is a Critical Component of RNP Complexes that Sequester Germline RNAs during Oogenesis.* J Dev Biol, 2016. **4**(1).
151. Akerberg, A.A., C.E. Burns, and C.G. Burns, *Exploring the Activities of RBPMS Proteins in Myocardial Biology.* Pediatr Cardiol, 2019. **40**(7): p. 1410-1418.
152. Fisher, S.A., *Vascular smooth muscle phenotypic diversity and function.* Physiol Genomics, 2010. **42A**(3): p. 169-87.
153. Nakagaki-Silva, E.E., et al., *Identification of RBPMS as a mammalian smooth muscle master splicing regulator via proximity of its gene with super-enhancers.* Elife, 2019. **8**.
154. Gan, P., et al., *RBPMS is an RNA-binding protein that mediates cardiomyocyte binucleation and cardiovascular development.* Dev Cell, 2022. **57**(8): p. 959-973 e7.
155. Ye, L., et al., *RNA-binding protein Rbpms is represented in human retinas by isoforms A and C and its transcriptional regulation involves Sp1-binding site.* Mol Genet Genomics, 2018. **293**(4): p. 819-830.
156. Song, H.W., et al., *Hermes RNA-binding protein targets RNAs-encoding proteins involved in meiotic maturation, early cleavage, and germline development.* Differentiation, 2007. **75**(6): p. 519-28.
157. Nijjar, S. and H.R. Woodland, *Localisation of RNAs into the germ plasm of vitellogenic Xenopus oocytes.* PLoS One, 2013. **8**(4): p. e61847.
158. Miller, B.G. and J.A. Stamatoyannopoulos, *Integrative meta-analysis of differential gene expression in acute myeloid leukemia.* PLoS One, 2010. **5**(3): p. e9466.

159. Rastgoo, N., et al., *Dysregulation of EZH2/miR-138 axis contributes to drug resistance in multiple myeloma by downregulating RBPMS.* Leukemia, 2018. **32**(11): p. 2471-2482.
160. Drozdov, I., et al., *Functional and topological properties in hepatocellular carcinoma transcriptome.* PLoS One, 2012. **7**(4): p. e35510.
161. Yang, C., et al., *Circular RNA RBPMS inhibits bladder cancer progression via miR-330-3p/RAI2 regulation.* Mol Ther Nucleic Acids, 2021. **23**: p. 872-886.
162. Baez-Vega, P.M., et al., *Targeting miR-21-3p inhibits proliferation and invasion of ovarian cancer cells.* Oncotarget, 2016. **7**(24): p. 36321-36337.
163. Wang, X., et al., *Prediction of candidate RNA signatures for recurrent ovarian cancer prognosis by the construction of an integrated competing endogenous RNA network.* Oncol Rep, 2018. **40**(5): p. 2659-2673.
164. Jiao, W., et al., *Different miR-21-3p isoforms and their different features in colorectal cancer.* Int J Cancer, 2017. **141**(10): p. 2103-2111.
165. Fortner, R.T., et al., *Ovarian cancer risk factors by tumor aggressiveness: An analysis from the Ovarian Cancer Cohort Consortium.* Int J Cancer, 2019. **145**(1): p. 58-69.
166. Pokhriyal, R., et al., *Chemotherapy Resistance in Advanced Ovarian Cancer Patients.* Biomark Cancer, 2019. **11**: p. 1179299X19860815.
167. Zhang, C., et al., *Platinum-based drugs for cancer therapy and anti-tumor strategies.* Theranostics, 2022. **12**(5): p. 2115-2132.
168. Echevarria-Vargas, I.M., F. Valiyeva, and P.E. Vivas-Mejia, *Upregulation of miR-21 in cisplatin resistant ovarian cancer via JNK-1/c-Jun pathway.* PLoS One, 2014. **9**(5): p. e97094.
169. Wang, F., et al., *MiR-214 reduces cell survival and enhances cisplatin-induced cytotoxicity via down-regulation of Bcl2l2 in cervical cancer cells.* FEBS Lett, 2013. **587**(5): p. 488-95.
170. Reyes-Gonzalez, J.M., et al., *Downstream Effectors of ILK in Cisplatin-Resistant Ovarian Cancer.* Cancers (Basel), 2020. **12**(4).
171. Vivas-Mejia, P.E., et al., *Silencing survivin splice variant 2B leads to antitumor activity in taxane--resistant ovarian cancer.* Clin Cancer Res, 2011. **17**(11): p. 3716-26.
172. Reyes-Gonzalez, J.M. and P.E. Vivas-Mejia, *c-MYC and Epithelial Ovarian Cancer.* Front Oncol, 2021. **11**: p. 601512.
173. Quinones-Diaz, B.I., et al., *MicroRNA-18a-5p Suppresses Tumor Growth via Targeting Matrix Metalloproteinase-3 in Cisplatin-Resistant Ovarian Cancer.* Front Oncol, 2020. **10**: p. 602670.
174. Santana-Rivera, Y., et al., *Reduced expression of enolase-1 correlates with high intracellular glucose levels and increased senescence in cisplatin-resistant ovarian cancer cells.* Am J Transl Res, 2020. **12**(4): p. 1275-1292.
175. Bahar, E. and H. Yoon, *Modeling and Predicting the Cell Migration Properties from Scratch Wound Healing Assay on Cisplatin-Resistant Ovarian Cancer Cell Lines Using Artificial Neural Network.* Healthcare (Basel), 2021. **9**(7).
176. Chan, P.P. and T.M. Lowe, *GtRNAdb 2.0: an expanded database of transfer RNA genes identified in complete and draft genomes.* Nucleic Acids Res, 2016. **44**(D1): p. D184-9.
177. Langmead, B. and S.L. Salzberg, *Fast gapped-read alignment with Bowtie 2.* Nat Methods, 2012. **9**(4): p. 357-9.
178. Dobin, A., et al., *STAR: ultrafast universal RNA-seq aligner.* Bioinformatics, 2013. **29**(1): p. 15-21.

179. Love, M.I., W. Huber, and S. Anders, *Moderated estimation of fold change and dispersion for RNA-seq data with DESeq2.* Genome Biol, 2014. **15**(12): p. 550.
180. Gerace, E. and D. Moazed, *Affinity Pull-Down of Proteins Using Anti-FLAG M2 Agarose Beads.* Methods Enzymol, 2015. **559**: p. 99-110.
181. Chen, J., et al., *ToppGene Suite for gene list enrichment analysis and candidate gene prioritization.* Nucleic Acids Res, 2009. **37**(Web Server issue): p. W305-11.
182. Zhou, Y., et al., *Metascape provides a biologist-oriented resource for the analysis of systems-level datasets.* Nat Commun, 2019. **10**(1): p. 1523.
183. Gyorffy, B., *Survival analysis across the entire transcriptome identifies biomarkers with the highest prognostic power in breast cancer.* Comput Struct Biotechnol J, 2021. **19**: p. 4101-4109.
184. Xu, J.H., et al., *Tumor suppressor genes and their underlying interactions in paclitaxel resistance in cancer therapy.* Cancer Cell Int, 2016. **16**: p. 13.
185. Huang, J., et al., *XAF1 as a prognostic biomarker and therapeutic target in pancreatic cancer.* Cancer Sci, 2010. **101**(2): p. 559-67.
186. Chowdhury, U.R., et al., *Emerging role of nuclear protein 1 (NUPR1) in cancer biology.* Cancer Metastasis Rev, 2009. **28**(1-2): p. 225-32.
187. Flores, E.R., *The roles of p63 in cancer.* Cell Cycle, 2007. **6**(3): p. 300-4.
188. Hallen, L.C., et al., *Antiproliferative activity of the human IFN-alpha-inducible protein IFI44.* J Interferon Cytokine Res, 2007. **27**(8): p. 675-80.
189. Pan, H., et al., *Interferon-Induced Protein 44 Correlated With Immune Infiltration Serves as a Potential Prognostic Indicator in Head and Neck Squamous Cell Carcinoma.* Front Oncol, 2020. **10**: p. 557157.
190. Kramer, A., et al., *Causal analysis approaches in Ingenuity Pathway Analysis.* Bioinformatics, 2014. **30**(4): p. 523-30.
191. Langevin, S.M., et al., *Comprehensive mapping of the methylation landscape of 16 CpG-dense regions in oral and pharyngeal squamous cell carcinoma.* Epigenomics, 2019. **11**(9): p. 987-1002.
192. Zhang, X., et al., *RAD51 is a potential marker for prognosis and regulates cell proliferation in pancreatic cancer.* Cancer Cell Int, 2019. **19**: p. 356.
193. Huang, W.C., et al., *IFI44L is a novel tumor suppressor in human hepatocellular carcinoma affecting cancer stemness, metastasis, and drug resistance via regulating met/Src signaling pathway.* BMC Cancer, 2018. **18**(1): p. 609.
194. Wang, Q., et al., *Distinct prognostic value of mRNA expression of guanylate-binding protein genes in skin cutaneous melanoma.* Oncol Lett, 2018. **15**(5): p. 7914-7922.
195. Song, F., et al., *Regulation and biological role of the peptide/histidine transporter SLC15A3 in Toll-like receptor-mediated inflammatory responses in macrophage.* Cell Death Dis, 2018. **9**(7): p. 770.
196. Chen, R., et al., *Systematic Transcriptome Analysis Reveals the Inhibitory Function of Cinnamaldehyde in Non-Small Cell Lung Cancer.* Front Pharmacol, 2020. **11**: p. 611060.
197. Mukai, S., et al., *Overexpression of Transmembrane Protein BST2 is Associated with Poor Survival of Patients with Esophageal, Gastric, or Colorectal Cancer.* Ann Surg Oncol, 2017. **24**(2): p. 594-602.
198. Dai, H., et al., *FGF21 facilitates autophagy in prostate cancer cells by inhibiting the PI3K-Akt-mTOR signaling pathway.* Cell Death Dis, 2021. **12**(4): p. 303.

199. Herrin, B.R., A.L. Groeger, and L.B. Justement, *The adaptor protein HSH2 attenuates apoptosis in response to ligation of the B cell antigen receptor complex on the B lymphoma cell line, WEHI-231.* J Biol Chem, 2005. **280**(5): p. 3507-15.
200. Masuda, T., et al., *Overexpression of the S100A2 protein as a prognostic marker for patients with stage II and III colorectal cancer.* Int J Oncol, 2016. **48**(3): p. 975-82.
201. Zou, A., et al., *Distribution and functional properties of human KCNH8 (Elk1) potassium channels.* Am J Physiol Cell Physiol, 2003. **285**(6): p. C1356-66.
202. Dieci, G., M. Preti, and B. Montanini, *Eukaryotic snoRNAs: a paradigm for gene expression flexibility.* Genomics, 2009. **94**(2): p. 83-8.
203. Voss, F.K., et al., *Identification of LRRC8 heteromers as an essential component of the volume-regulated anion channel VRAC.* Science, 2014. **344**(6184): p. 634-8.
204. Suzuki, N., K. Nara, and T. Suzuki, *Skewed Th1 responses caused by excessive expression of Txk, a member of the Tec family of tyrosine kinases, in patients with Behcet's disease.* Clin Med Res, 2006. **4**(2): p. 147-51.
205. Piovani, G., et al., *De novo 1Mb interstitial deletion of 8p22 in a patient with slight mental retardation and speech delay.* Mol Cytogenet, 2014. **7**: p. 25.
206. Li, X., et al., *Identification of a histone family gene signature for predicting the prognosis of cervical cancer patients.* Sci Rep, 2017. **7**(1): p. 16495.
207. Li, Y., et al., *Bioinformatics analysis identified MMP14 and COL12A1 as immune-related biomarkers associated with pancreatic adenocarcinoma prognosis.* Math Biosci Eng, 2021. **18**(5): p. 5921-5942.
208. Yang, M.H., et al., *Somatic mutations of PREX2 gene in patients with hepatocellular carcinoma.* Sci Rep, 2019. **9**(1): p. 2552.
209. Craig, M.J. and R.D. Loberg, *CCL2 (Monocyte Chemoattractant Protein-1) in cancer bone metastases.* Cancer Metastasis Rev, 2006. **25**(4): p. 611-9.
210. Xie, Y., et al., *Disabled homolog 2 is required for migration and invasion of prostate cancer cells.* Front Med, 2015. **9**(3): p. 312-21.
211. Stevenson, L., et al., *Calbindin 2 (CALB2) regulates 5-fluorouracil sensitivity in colorectal cancer by modulating the intrinsic apoptotic pathway.* PLoS One, 2011. **6**(5): p. e20276.
212. Wang, T., et al., *Increased nucleotide polymorphic changes in the 5'-untranslated region of delta-catenin (CTNND2) gene in prostate cancer.* Oncogene, 2009. **28**(4): p. 555-64.
213. Sakaki, T., et al., *CYP24A1 as a potential target for cancer therapy.* Anticancer Agents Med Chem, 2014. **14**(1): p. 97-108.
214. Brandenberger, R., et al., *Transcriptome characterization elucidates signaling networks that control human ES cell growth and differentiation.* Nat Biotechnol, 2004. **22**(6): p. 707-16.
215. Liu, L., et al., *MicroRNA-182 targets protein phosphatase 1 regulatory inhibitor subunit 1C in glioblastoma.* Oncotarget, 2017. **8**(70): p. 114677-114684.
216. Luan, J., et al., *SLFN11 is a general target for enhancing the sensitivity of cancer to chemotherapy (DNA-damaging agents).* J Drug Target, 2020. **28**(1): p. 33-40.
217. Murn, J., et al., *Prostaglandin E2 regulates B cell proliferation through a candidate tumor suppressor, Ptger4.* J Exp Med, 2008. **205**(13): p. 3091-103.
218. Wan, N., et al., *FOXD3-AS1 Contributes to the Progression of Melanoma Via miR-127-3p/FJX1 Axis.* Cancer Biother Radiopharm, 2020. **35**(8): p. 596-604.

219. Requena, T., et al., *Identification of two novel mutations in FAM136A and DTNA genes in autosomal-dominant familial Meniere's disease.* Hum Mol Genet, 2015. **24**(4): p. 1119-26.
220. Tan, N.N., et al., *Epigenetic Downregulation of Scn3a Expression by Valproate: a Possible Role in Its Anticonvulsant Activity.* Mol Neurobiol, 2017. **54**(4): p. 2831-2842.
221. Sanuki, R., et al., *Panky, a novel photoreceptor-specific ankyrin repeat protein, is a transcriptional cofactor that suppresses CRX-regulated photoreceptor genes.* FEBS Lett, 2010. **584**(4): p. 753-8.
222. Bhushan, A., et al., *Identification and Validation of Fibroblast Growth Factor 12 Gene as a Novel Potential Biomarker in Esophageal Cancer Using Cancer Genomic Datasets.* OMICS, 2017. **21**(10): p. 616-631.
223. Yan, L., et al., *Distinct diagnostic and prognostic values of gamma-aminobutyric acid type A receptor family genes in patients with colon adenocarcinoma.* Oncol Lett, 2020. **20**(1): p. 275-291.
224. Guan, Y., et al., *lncRNA FOXD3-AS1 is associated with clinical progression and regulates cell migration and invasion in breast cancer.* Cell Biochem Funct, 2019. **37**(4): p. 239-244.
225. Northrop, J.P., et al., *NF-AT components define a family of transcription factors targeted in T-cell activation.* Nature, 1994. **369**(6480): p. 497-502.
226. Dickinson, R.E., M. Myers, and W.C. Duncan, *Novel regulated expression of the SLIT/ROBO pathway in the ovary: possible role during luteolysis in women.* Endocrinology, 2008. **149**(10): p. 5024-34.
227. Shimoyama, Y., et al., *Isolation and sequence analysis of human cadherin-6 complementary DNA for the full coding sequence and its expression in human carcinoma cells.* Cancer Res, 1995. **55**(10): p. 2206-11.
228. Zhang, Y., et al., *HOXD8 inhibits the proliferation and migration of triple-negative breast cancer cells and induces apoptosis in them through regulation of AKT/mTOR pathway.* Reprod Biol, 2021. **21**(4): p. 100544.
229. Rudnicki, M.A., et al., *Actin and myosin expression during development of cardiac muscle from cultured embryonal carcinoma cells.* Dev Biol, 1990. **138**(2): p. 348-58.
230. Niwa, R., et al., *Control of actin reorganization by Slingshot, a family of phosphatases that dephosphorylate ADF/cofilin.* Cell, 2002. **108**(2): p. 233-46.
231. Liu, D.B., et al., *Immunocytochemical detection of HoxD9 and Pbx1 homeodomain protein expression in Chinese esophageal squamous cell carcinomas.* World J Gastroenterol, 2005. **11**(10): p. 1562-6.
232. Lee, Y.R., et al., *The Cullin 3 substrate adaptor KLHL20 mediates DAPK ubiquitination to control interferon responses.* EMBO J, 2010. **29**(10): p. 1748-61.
233. Hogan, A., et al., *Interaction of gamma 1-syntrophin with diacylglycerol kinase-zeta. Regulation of nuclear localization by PDZ interactions.* J Biol Chem, 2001. **276**(28): p. 26526-33.
234. Gagnon, M.L., et al., *Identification of a natural soluble neuropilin-1 that binds vascular endothelial growth factor: In vivo expression and antitumor activity.* Proc Natl Acad Sci U S A, 2000. **97**(6): p. 2573-8.
235. Liu, D., et al., *ERICH3: vesicular association and antidepressant treatment response.* Mol Psychiatry, 2021. **26**(6): p. 2415-2428.

236. Liu, Z., et al., *GATA1-regulated JAG1 promotes ovarian cancer progression by activating Notch signal pathway.* Protoplasma, 2020. **257**(3): p. 901-910.
237. Rossjohn, J., et al., *T cell antigen receptor recognition of antigen-presenting molecules.* Annu Rev Immunol, 2015. **33**: p. 169-200.
238. Lanczky, A. and B. Gyorffy, *Web-Based Survival Analysis Tool Tailored for Medical Research (KMplot): Development and Implementation.* J Med Internet Res, 2021. **23**(7): p. e27633.
239. Sun, Y., et al., *Potentiation of Smad-mediated transcriptional activation by the RNA-binding protein RBPMS.* Nucleic Acids Res, 2006. **34**(21): p. 6314-26.
240. Gordon, R.R. and P.S. Nelson, *Cellular senescence and cancer chemotherapy resistance.* Drug Resist Updat, 2012. **15**(1-2): p. 123-31.
241. Guo, X., et al., *Increased p38-MAPK is responsible for chemotherapy resistance in human gastric cancer cells.* BMC Cancer, 2008. **8**: p. 375.
242. Guillon, J., et al., *Chemotherapy-induced senescence, an adaptive mechanism driving resistance and tumor heterogeneity.* Cell Cycle, 2019. **18**(19): p. 2385-2397.
243. Bavik, C., et al., *The gene expression program of prostate fibroblast senescence modulates neoplastic epithelial cell proliferation through paracrine mechanisms.* Cancer Res, 2006. **66**(2): p. 794-802.
244. Krtolica, A., et al., *Senescent fibroblasts promote epithelial cell growth and tumorigenesis: a link between cancer and aging.* Proc Natl Acad Sci U S A, 2001. **98**(21): p. 12072-7.
245. Coppe, J.P., et al., *Senescence-associated secretory phenotypes reveal cell-nonautonomous functions of oncogenic RAS and the p53 tumor suppressor.* PLoS Biol, 2008. **6**(12): p. 2853-68.
246. McConkey, D.J., et al., *Role of epithelial-to-mesenchymal transition (EMT) in drug sensitivity and metastasis in bladder cancer.* Cancer Metastasis Rev, 2009. **28**(3-4): p. 335-44.
247. Sundqvist, A., et al., *TGFβ and EGF signaling orchestrates the AP-1- and p63 transcriptional regulation of breast cancer invasiveness.* Oncogene, 2020. **39**(22): p. 4436-4449.
248. Wong, C., et al., *Smad3-Smad4 and AP-1 complexes synergize in transcriptional activation of the c-Jun promoter by transforming growth factor beta.* Mol Cell Biol, 1999. **19**(3): p. 1821-30.
249. Selcuklu, S.D., M.T. Donoghue, and C. Spillane, *miR-21 as a key regulator of oncogenic processes.* Biochem Soc Trans, 2009. **37**(Pt 4): p. 918-25.
250. Asangani, I.A., et al., *MicroRNA-21 (miR-21) post-transcriptionally downregulates tumor suppressor Pdcd4 and stimulates invasion, intravasation and metastasis in colorectal cancer.* Oncogene, 2008. **27**(15): p. 2128-36.
251. Qu, K., et al., *Extracellular miRNA-21 as a novel biomarker in glioma: Evidence from meta-analysis, clinical validation and experimental investigations.* Oncotarget, 2016. **7**(23): p. 33994-4010.
252. Medimegh, I., et al., *MicroRNAs expression in triple negative vs non triple negative breast cancer in Tunisia: interaction with clinical outcome.* PLoS One, 2014. **9**(11): p. e111877.
253. Zhao, W., et al., *Serum miR-21 level: a potential diagnostic and prognostic biomarker for non-small cell lung cancer.* Int J Clin Exp Med, 2015. **8**(9): p. 14759-63.

254. Jackson, B.L., A. Grabowska, and H.L. Ratan, *MicroRNA in prostate cancer: functional importance and potential as circulating biomarkers.* BMC Cancer, 2014. **14**: p. 930.
255. Del Mar Diaz-Gonzalez, S., et al., *Transregulation of microRNA miR-21 promoter by AP-1 transcription factor in cervical cancer cells.* Cancer Cell Int, 2019. **19**: p. 214.
256. Jiang, W.G., et al., *Com-1/p8 acts as a putative tumour suppressor in prostate cancer.* Int J Mol Med, 2006. **18**(5): p. 981-6.
257. Zhou, H.H., et al., *Smad3 Sensitizes Hepatocelluar Carcinoma Cells to Cisplatin by Repressing Phosphorylation of AKT.* Int J Mol Sci, 2016. **17**(4).
258. Clark, D.W., et al., *NUPR1 interacts with p53, transcriptionally regulates p21 and rescues breast epithelial cells from doxorubicin-induced genotoxic stress.* Curr Cancer Drug Targets, 2008. **8**(5): p. 421-30.
259. Jiang, W.G., et al., *Expression of Com-1/P8 in human breast cancer and its relevance to clinical outcome and ER status.* Int J Cancer, 2005. **117**(5): p. 730-7.
260. Huang, T.C., et al., *Cinnamaldehyde enhances Nrf2 nuclear translocation to upregulate phase II detoxifying enzyme expression in HepG2 cells.* J Agric Food Chem, 2011. **59**(9): p. 5164-71.
261. Lan, T., et al., *Long non-coding RNA small nucleolar RNA host gene 12 (SNHG12) promotes tumorigenesis and metastasis by targeting miR-199a/b-5p in hepatocellular carcinoma.* J Exp Clin Cancer Res, 2017. **36**(1): p. 11.
262. Jia, Y., et al., *Death associated protein 1 is correlated with the clinical outcome of patients with colorectal cancer and has a role in the regulation of cell death.* Oncol Rep, 2014. **31**(1): p. 175-82.
263. Winkler, C., et al., *SLFN11 informs on standard of care and novel treatments in a wide range of cancer models.* Br J Cancer, 2021. **124**(5): p. 951-962.
264. Tseng, C.P., et al., *The role of DOC-2/DAB2 protein phosphorylation in the inhibition of AP-1 activity. An underlying mechanism of its tumor-suppressive function in prostate cancer.* J Biol Chem, 1999. **274**(45): p. 31981-6.
265. Melino, G., *p63 is a suppressor of tumorigenesis and metastasis interacting with mutant p53.* Cell Death & Differentiation, 2011. **18**(9): p. 1487-1499.
266. Lau, C.P., et al., *p63 regulates cell proliferation and cell cycle progressionassociated genes in stromal cells of giant cell tumor of the bone.* Int J Oncol, 2013. **42**(2): p. 437-43.
267. Senoo, M., et al., *p63 Is essential for the proliferative potential of stem cells in stratified epithelia.* Cell, 2007. **129**(3): p. 523-36.
268. He, Z. and M. Tessier-Lavigne, *Neuropilin is a receptor for the axonal chemorepellent Semaphorin III.* Cell, 1997. **90**(4): p. 739-51.
269. Soker, S., et al., *Neuropilin-1 is expressed by endothelial and tumor cells as an isoform-specific receptor for vascular endothelial growth factor.* Cell, 1998. **92**(6): p. 735-45.
270. Yi, C., et al., *Association study between CYP24A1 gene polymorphisms and cancer risk.* Pathol Res Pract, 2020. **216**(1): p. 152735.
271. Lodillinsky, C., et al., *Metastasis-suppressor NME1 controls the invasive switch of breast cancer by regulating MT1-MMP surface clearance.* Oncogene, 2021. **40**(23): p. 4019-4032.
272. Shi, X., et al., *Association between NME1 polymorphisms and cancer susceptibility: A meta-analysis based on 1644 cases and 2038 controls.* Pathol Res Pract, 2018. **214**(4): p. 467-474.

273. Yang, S.B., et al., *Immunoglobulin kappa and immunoglobulin lambda are required for expression of the anti-apoptotic molecule Bcl-xL in human colorectal cancer tissue.* Scand J Gastroenterol, 2009. **44**(12): p. 1443-51.
274. You, G.R., et al., *MYH9 Facilitates Cell Invasion and Radioresistance in Head and Neck Cancer via Modulation of Cellular ROS Levels by Activating the MAPK-Nrf2-GCLC Pathway.* Cells, 2022. **11**(18).
275. Wang, Y., et al., *Myosin Heavy Chain 10 (MYH10) Gene Silencing Reduces Cell Migration and Invasion in the Glioma Cell Lines U251, T98G, and SHG44 by Inhibiting the Wnt/beta-Catenin Pathway.* Med Sci Monit, 2018. **24**: p. 9110-9119.
276. McCorkle, J.R., et al., *The metastasis suppressor NME1 regulates expression of genes linked to metastasis and patient outcome in melanoma and breast carcinoma.* Cancer Genomics Proteomics, 2014. **11**(4): p. 175-94.
277. Postel, E.H., et al., *Human c-myc transcription factor PuF identified as nm23-H2 nucleoside diphosphate kinase, a candidate suppressor of tumor metastasis.* Science, 1993. **261**(5120): p. 478-80.
278. Cervoni, L., et al., *DNA sequences acting as binding sites for NM23/NDPK proteins in melanoma M14 cells.* J Cell Biochem, 2006. **98**(2): p. 421-8.
279. Ma, D., et al., *Autocrine platelet-derived growth factor-dependent gene expression in glioblastoma cells is mediated largely by activation of the transcription factor sterol regulatory element binding protein and is associated with altered genotype and patient survival in human brain tumors.* Cancer Res, 2005. **65**(13): p. 5523-34.
280. Manoharan, A., et al., *De novo DNA Methyltransferases Dnmt3a and Dnmt3b regulate the onset of Igkappa light chain rearrangement during early B-cell development.* Eur J Immunol, 2015. **45**(8): p. 2343-55.
281. Consortium, A.P.G., *AACR Project GENIE: Powering Precision Medicine through an International Consortium.* Cancer Discov, 2017. **7**(8): p. 818-831.
282. Betapudi, V., *Myosin II motor proteins with different functions determine the fate of lamellipodia extension during cell spreading.* PLoS One, 2010. **5**(1): p. e8560.
283. Kacsoh, D.B., et al., *Tumor Resident, B-Cell Receptor Chemical Characteristics Associated with Better Overall Survival for Neuroblastoma.* J Mol Neurosci, 2022. **72**(9): p. 2011-2019.
284. Kai, J.D., et al., *MYH9 is a novel cancer stem cell marker and prognostic indicator in esophageal cancer that promotes oncogenesis through the PI3K/AKT/mTOR axis.* Cell Biol Int, 2022. **46**(12): p. 2085-2094.